Doctoral Dissertation

Proposal for the design of reinforced concrete columns that carry high axial force developing ductile behavior

靭性性状を示す高軸力をうける鉄筋コンクリート柱の規準に関する提案

Juan Pablo HIDALGO TOXQUI

A dissertation submitted in partial fulfillment of the

requirements for the degree of

Doctor of Philosophy in Engineering

Graduate School of Engineering
Yokohama National University

2016 – 3

This page intentionally left blank

ABSTRACT

Large earthquakes are predicted to occur in Japan within the next decades. The many constructions that were designed with previous guidelines will probably be demanded with greater force than for which they were designed. Especially, high axial force may be acting during an earthquake for the columns that are located at the corners of lower floors of buildings.

Regarding to the previous, the objective of this dissertation is to propose a criterion for the structural design of RC columns carrying high axial force that are able to develop large ductility in flexural failure mode.

At the beginning, the current criterion of design proposed by Ministry of Land, Infrastructure, Transport, and Tourism (MLITT) and the Architectural Institute of Japan (AIJ) were studied as a part of the background of the research. In the case of the AIJ normative, an evaluation was carried out.

At the end, three points are proposed as a guide in the design of RC columns carrying high axial force; these are the index to avoid shear failure and the shear stress index and additional requirements.

The proposal was based not only done in experimental and analytical results of the tested columns but also was done using the results of previous experiments since 1979 until 2015 published by the Japanese Concrete Institute (JCI) and the AIJ, this is a column database that gather more than 1800 experiment results.

This study is limited to columns with the next characteristics: reinforced concrete columns with square cross section, square stirrups with 4 sub-bands of hoops as a lateral reinforcement, normal strength materials, flexural failure mode, and focused in columns with high axial force tests.

ACKNOWLEDGMENT

Gratitude to my academic supervisor AKIRA TASAI, in the Yokohama National University for accepted me in his research group as a PhD student, for the though lessons.

Associate Professor SUGIMOTO KUNIYOSHI from the Yokohama National University for his valuable suggestions, constructive criticism, friendly discussions and patient supervision, which were indispensable for completion of this dissertation.

Associate Professor KOICHI KUSUNOKI from the Earthquake Research Institute of Japan for his enthusiastic guidance, constructive criticism and friendly company.

Gratitude to Professor TOSHIMI KABEYASAWA from the Earthquake Research Institute for accepted me as a research student in The Tokyo University, sharing his knowledge with me.

Gratitude to MONBUKAGAKUSHO scholarship to provide financial support in the PhD course.

Gratitude to classmates, Friends and new relatives in this life in Japan Ana, Juan Carlos, Gustavo, Jagana, Moheko, Fernando, William, Valeria, Ayeon, Yoriko, Bota, Kato, Kimi, Deng, Bui, Tanzil, Thomas, Miguel, Mohamed, Ning, Hatanaka, Hinata, Takto, Yamada, Mika, Saoud and Sola for your unconditional friendship, for all the moments that we share together, for give me the most important understandings from Japan.

Gratitude to each people that in one way or another participated in the realization of this dissertation.

LIST OF CONTENTS

CHAPTER 1. INTRODUCTION

1.1. General background

Earthquakes affect many areas in the world reaching all over 5000, 000 detectable earthquakes every year, from these, 706 events have been classified as big disasters from 1980 to 2008. These catastrophes affect an average of 4,700 000 people per year and estimated economic damage of 350 trillion dollars. The further effects of the earthquakes, like tsunamis, volcano eruptions and fires, cause even more damage [1-1].

Japan is located in the most earthquake prone area. The landmass of Japan is over the volcanic zone of the "Ring of Fire," the tectonic plate movement all around the Pacific Ocean, what is the origin of the earthquakes in several other countries like Unite States, Indonesia, New Zealand and Mexico. Figure 1-1 shows the major tectonic plates in the earth. The earthquakes in Japan are originated by the movement of four juncture plates, Eurasian, North American continental, Pacific and Philippine oceanic, the position of Japan has been marked in Figure 1-1 [1-2].

There are many historical records of earthquakes in Japan; one of the first record is the called Yamato earthquake in the prefecture of Nara in the year 416AC [1-3]. In 1899 the Catalogue of Historical Data on Japanese Earthquakes was published by the Imperial Earthquake Investigation Committee, now days, the Earthquake Research Institute. Recently, T. Usami [1-4] published the most complete and detailed version of historic earthquakes in Japan.

Between the most important earthquakes, it can be mentioned the next ones [1-4]: The Great Kanto earthquake in 1923, this disaster caused around 140,000 casualties. Its magnitude was M= 7.9. Nankai earthquake in 1946, just after the end of the World War II, 1362 people died in this event, its magnitude was M=8.0. Tokachi earthquake (or Aomori earthquake) in 1968 had a magnitude of M=8.2, caused several damage in the southern part of Hokkaido, 52 people died during this disaster. Moreover, the most recently great event Tohoku earthquake in 2011, where a confirmed 14 941 deaths and 9 882 missed; this event has been the largest magnitude ever recorded in Japan with Mw= 9.0; its subsequent tsunami recorded the maximum height of 7.3m; the economic damage was estimated in 305 billon dollars [1-5].

Between the further effects of the earthquakes, it can be mentioned the liquefaction of soils, landslides, tsunamis, and evidently, the shaking of the ground causes the damage to the structures, such as, houses, dams, bridges and buildings. When building collapse, they produce large number of casualties, and the number of fatalities has increased in recently years. In Japan, the number of fatalities produced by the collapse of structures has been considerable negligible before the Kobe earthquake in 1995, but during that event more than 5000 people perished for the collapse of some structure. Moreover, other example is the earthquakes of Loma Prieta (1989) and Northridge (1994) in United States where most of the casualties were due to the collapse of some structure [1-6].

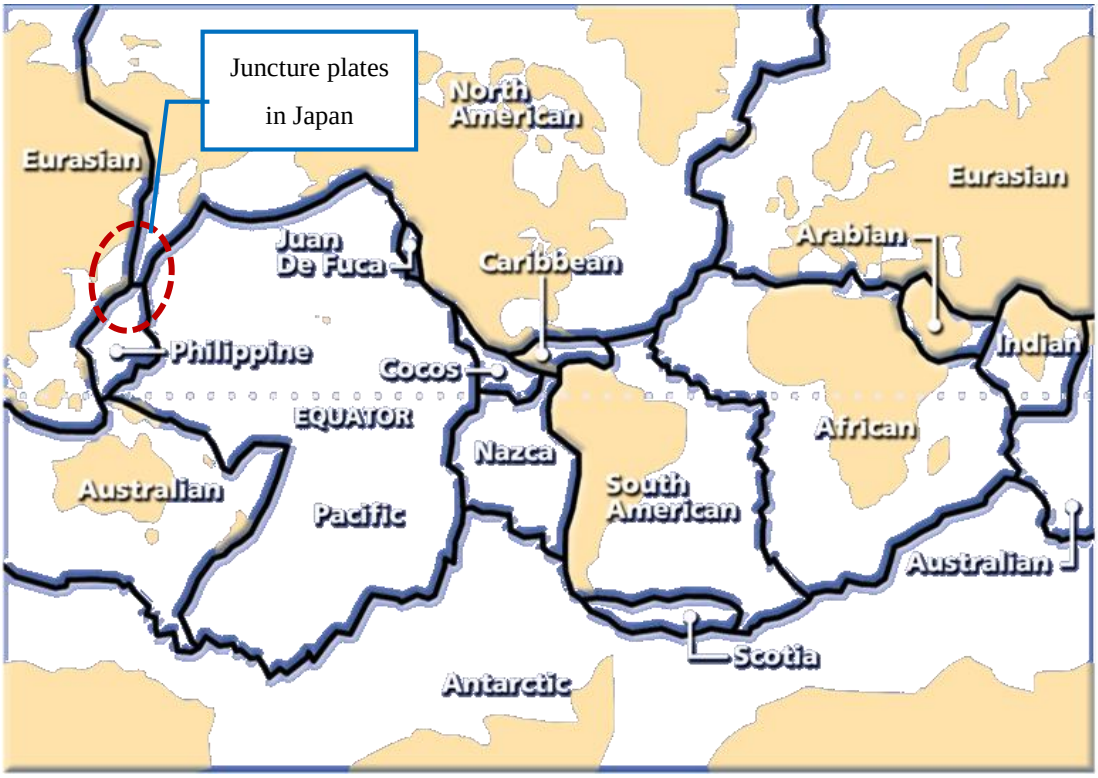

Figure 1-1 Earth's major tectonic plates

Earthquakes can affect a building in several ways; the damage produced by the shaking on the structures deepens on several factors, between the main reasons, it can be mentioned the next:

The strength shaking

The distance of the epicenter to the building is important due to the mitigation or the enlarger of the shaking waves. For mention and example, the waves at the distance of 30 miles could be 16 times stronger than that located to a distance of 50 miles from the epicenter, but this depends of several other factors.

Length of the shaking

The quantity of damage in the buildings is directly related to the duration of the earthquakes. The longer is the building shakes, the greater the damage.

Type of soil

There is an appropriated foundation for the building in every type of soil. In stiffness soils, the short to medium high structures are the most affected buildings. In soft soils where the shaking waves can be enlarged, the most affected buildings are the tall ones.

Type of buildings

Depending of the type of structure, buildings could be affected or nor by specific earthquake. The materials, height, structural configuration and other factors define the seismic response of the building to the earthquakes.

Summarizing, combining waves shake the structures damaging them in different ways depending of the strength and length of the earthquakes. The shaking is different in each area, it depends of the variation of the fault slippage and rock characteristics. Additionally, the different characteristics of the building will determine its response, as it is, the size, age, configuration and structural systems, construction materials, and quality of the construction [1-7].

It is important to research about the damage on buildings to prevent casualties. Several reports and studies have been issued for the damage produced by earthquakes on buildings in Japan [1-8][1-9][1-10][1-11][1-12]. Some comments about the type of damages than can be observed in reinforced concrete (RC) buildings after large earthquakes are mentioned in the next:

Foundation and soil

Due to the shaking of the soil and the interaction soil-structure of the surrounding area and the foundation, the building can present the next damage: liquefaction of the ground, inclination of the building, damage to the service pipes, and damage of the accessory facilities. Figure 1-2 shows some imagines of this type of damages in buildings foundation and surrounding soil.

The structural and nonstructural members in the building may present damages, in a general view; the damages can be resume as:

Structural walls and slaps

The damage in the slaps is characterized by cracks that fissure the floor. Vertical wall, as spandrel wall over or under beams, commonly present shear failure. It is common that side walls attached to vertical structural elements, as columns, also present this type of failure. Another typically shear failure in walls happens in the openings, as doors or windows. Figure 1-3 shows some illustration of damage in walls and slaps.

Joints node between columns and beams

This type of damage is more likely difficult to be discover due to the fact that crack close when the seismic event finish. However, damage in the joints have been observed in concrete buildings, the loss of stiffness in the joints is a factor of collapse. Some imagens of this type of damage can be observed in Figure 1-4.

Short span beams

In this type of elements, the damage by shear failure is common due to the concentration of force. These elements have higher stiffness that attract more seismic force during an earthquake than other elements. Figure 1-5 shows pictures of this type of damage.

Beams

Shear failure is the most common failure in these elements. However, mayor damage in the beams has not been reported, in contrast, some cases where the column and shear walls had collapsed but the beams remains with minor damage. Shear failure is also present in beams with spandrel or drop walls. Some pictures of shear failure are presented in Figure 1-6.

Figure 1-2 Common damage in foundation and soil [1-9]

From left to right: Liquefaction of soil, damage of foundation and leaning of building

Figure 1-3 Common damage in Structural walls and slaps [1-9]

From left to right: cracked slap, spandrel wall, and shear wall

Figure 1-4 Common damage in beam-column joints [1-9]

From left to right: L shaped joint, joint with spandrel wall, joint with transverse beam

Figure 1-5 Shear cracks in short span beams [1-9]

Figure 1-6 Damage in beams [1-9]

From left to right: slit between spandrel wall and column, and shear failure cracks

Columns

All the elements that compound the structure are important, whereas, columns are of mayor significance. The failure of a column in the structure may conduct to the collapse of the entire buildings; on the other hand, total failure of a beam element not always carries the structure to the whole collapse. The damage in columns should be well controlled to secure the stability of the building.

There are several types of failure mode in columns [1-13]; but they can be generalized in four type of damages; Shear damage, this failure in general happens when the flexural strength in the column is larger than the shear strength, due to the fact that the lateral reinforcement is insufficient for the acting force. It is characterized by cracks at 45◦ of inclination. The second type is by Flexural damage, when the flexural strength in the column is large than the shear strength. Example of these two types of failure are shown in Figure 1-7. The next type is bond failure damage; it is characterized by the separation of the rebar from the concrete core of the column due to the fact of excessive quantity of main reinforcement in the farthest fiber to the neutral axis of the cross section.

Moreover, compressive failure of columns is another kind of damage observed in building after severe earthquakes. The failure of concrete lead in the buckling of the rebar and collapse of the member due to the high axial force induced by the earthquake. Compressive failure is not exclusive of columns, many other cases have been reported with this kind of damage in walls [1-10]. Figure 1-8 shows examples of this failure.

Figure 1-7 Damage in columns [1-9]
From left to right: Shear failure and Flexural cracks

Figure 1-8 Compressive failure
From left to right and from up to down: compressive failure in wall [1-10], column designed with the standard low of Japan of 1968, 1974, and 1966 respectively [1-9].

Large earthquakes are predicted to occur within the next decades in Japan, for example the called Tokay earthquake pointed by the Coordinating Committee for Earthquake Prediction [1-14]. The many constructions that were designed with previous guidelines will probably be demanded with greater force than for which they were designed. Higher axial force may be applied on these buildings; consequently, a larger capacity will be needed on the columns.

It can be summarized that, in fact, earthquakes are one of the natural disasters that affect most the humanity, and more work need to be done in the research area of mitigating its damage and prevent its occurrence, especially in the area of prevention of collapse of structures.

1.2. Problem statement

In the structural design of reinforced concrete buildings, it is important to consider the failure mode. It is needed to prevent the collapse of structures and, the most important, provide ductile behavior of its components, in order to ensure that human lives will be protected.

In the previous paragraphs, it was talked about different type of failures that structural elements may have. This research is focused in columns but, especially, in the case of this type of elements that presented compressive failure due to the incremented axial force by the earthquake effects. This problem can be explained briefly through one of the most famous building that was damaged with this type of failure, the Imperial County Service Building, California USA [1-15].

The Imperial County Service Building was a special study case because this building was one of the three buildings which instruments recorded damage during strong ground motion in a working period of 40 years [1-16]. Thirteen accelerometers provided information about the translation torsion and in plane bending response.

In October 15 of 1979 an earthquake of magnitude 6.5 took place in the Imperial Valley at the southern part of California, USA, near to the border with Mexico, a total of 9 people was injured, the seismic event produced an estimated infrastructure damage of 30 million dollars, the most affected building was the Imperial County Service Building.

Figure 1-9 Imperial County Service Building

Photo by C. Rojahn. Figure 243, U.S. Geological Survey Professional

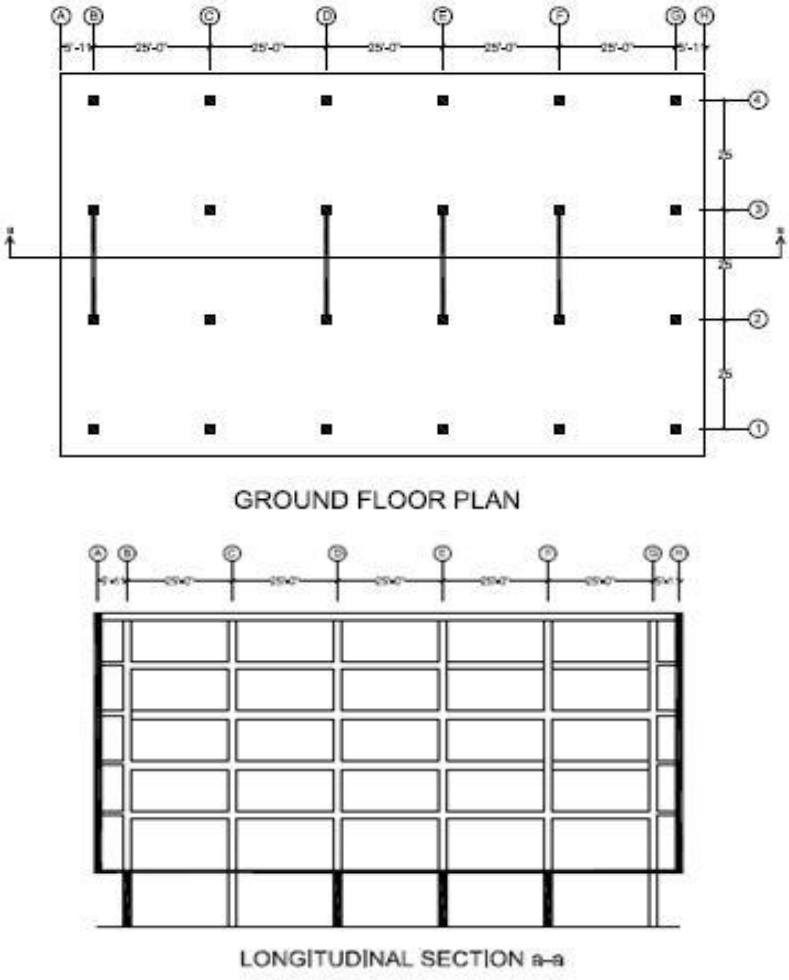

Figure 1-10 Floor plant and raised view [1-17]

The Imperial County Service Building was a RC building of six stories, the footprint was rectangular with 41.7m by 26m, its bay was regular distance of 7.6m in both directions, and the ground story height was 4.4m, the rest of the stories 4.1m but 4.0m for the upper story height.

The lateral force resistance system of the building was provided by moment frames parallel to the largest direction of the floor plant. In the perpendicular frames to the largest direction of the floor plant, 4 of 6 axes contained shear walls [1-17]. This can be observed in the floor plant of the Figure 1-10.

The observed damage was widespread in the building but the most significant damage was the failure of the four reinforced concrete columns in the first floor over the axis G of the Figure 1-10, the axe in the verge where no shear-wall was constructed. The concrete in the base of these columns was spalled per complete, the rebar buckled, and the building dropping down around 30cm in this axis when the earthquake finished.

Many researchers conducted analyses to study the seismic behavior of this building. The analyzing provided information about the probability to develop the recorded failure in the building, improving the knowledge about the elastic response to dynamic load. Additionally, the analysis pointed which columns were expected to fail when experience large bending and high axial load due to the overturning moment of the building [1-17].

Figure 1-11 depicts the collapse mechanism of the building, two different moments acting simultaneously in the corned column. This effect increased drastically the axial force in the element leading it to the collapse (World Housing Encyclopedia's property [1-18]). As result of the damage, the building was demolished in the following years.

The design of the columns in the ground floor was inadequate in this building, the columns did not developed a desirable ductility. This is not an isolated case; this problem is common in the structural engineering. Non-ductile RC columns failing by compressive mode have been observed in other structures damaged by earthquakes.

Figure 1-12 shows two cases of non-ductile columns with compressive failure, from left to right, these are from the Bhuj of the India earthquake in 2001 and the Canterbury Earthquakes from New Zealand in 2010. In both pictures, it can be seen that the rebar bending and the compressive failure of the concrete (the pictures belong to the C.V.R. Murty EERI Reconnaissance Team, and to Hyland Consultants respectively).

It can be summarized that, the increment of the axial force and the lack of ductility capacity can lead in the collapse of the structure, here, cases where the structures did not collapse were presented, and however, many causes of collapse remain unknown.

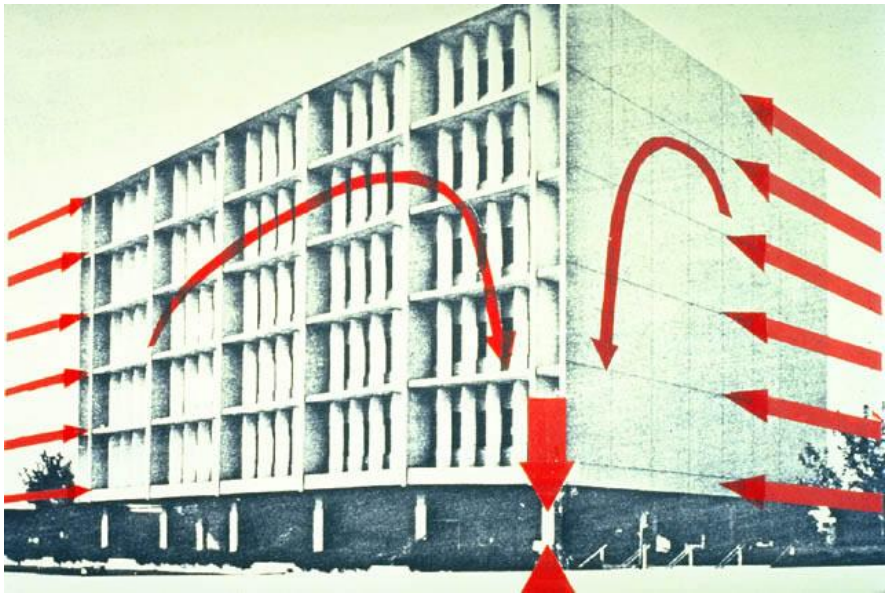

Figure 1-11 Collapse mechanism [1-18]

Figure 1-12 Non-ductile RC column failure

1.3. Objective and scope

Given the fact that, the increment of axial force produced by earthquakes on RC buildings may lead to the collapse of the structure, the main objective of this research is to propose a criteria to the design RC columns carrying high axial force that are able to develop satisfactory ductility.

Part of this study was carried out by a large RC columns database provided by TasaiLab. This database contains the results and characteristics of a huge number on squared cross sectional concrete columns tested since 1979 until now days.

The selection was limited to columns that have rectangular cross section and were built with materials that meet with the following:

- Effective compressive strength of concrete $\sigma_B \leq 60$MPa
- Yielding strength of longitudinal reinforcement $\sigma_y \leq 600$MPa
- Yielding strength of lateral reinforcement $\sigma_{wy} \leq 600$MPa

The analyses were conducted with the actual strength of materials. The limit of the strength of the materials is due to the ductile behavior. It was intended to avoid materials that present brittle failure. Additionally, all the reinforcing bars were deformed bars. For lateral reinforcement, more than four hoops and ties were arranged in the cross section. All available axial force ratios (η) as well as the aspect relationships were included. The aspect relationship is defined as h_0/D, where h_0 is the height of the column and D is the depth of the cross section. The failure mode was the mode that was originally report in the reference documents.

The research was based not only on experimental and analytical results of the tested in the TasaiLab column database but also on the experimental results of RC columns designed and tested during this work.

At the end of the dissertation, it will be provided a recommendation useful and practical to help in the design of squared sectional columns built with normal strength reinforcement and normal strength of concrete that can develop a minimum of 2.0% of lateral drift angle in the last stage.

Additionally, factors to estimate the actual strength of materials were develop as a complement of the proses of design of the testes columns.

Bibliography of Chapter 1

[1-1] Statistic Brain Research Institute: Earthquakes Statistics, 2005. http://www.statisticbrain.com/earthquake-statistics/

[1-2] Barnes, Gina L.: Origins of the Japanese Islands: The New "Big Picture," University of Durham, Retrieved, August 11, 2003.

[1-3] Ishibashi, K.: Status of historical seismology in Japan, Earthquake catalogue 47, Historical seismology; Annals of Geophysics, 2004

[1-4] Usami T.: Historical earthquakes in Japan, International Geophysics, Academic Press, International Handbook of Earthquake and Engineering Seismology, pp. 799–802, Volume 81, Part 1, 2002

[1-5] Japan International Cooperation Agency: Project Study on the Effective Countermeasures against Earthquake and Tsunami Disasters, Bulletin (No. 2), May 20, 2011

[1-6] Yamazaki F., Nishimura A., Ueno Y.: Estimation of human casualties due to urban earthquakes, Eleventh World Conference on Earthquake Engineering 11WCEE, paper No. 443, Mexico, 1996

[1-7] Federal Emergency Management Agency: FEMA 454 Designing for Earthquakes, Chapter 4, pp. 4-1 to 4-27, USA, December 2006

[1-8] 日本建築学会: 阪神･淡路大震災調査報告, 鉄筋コンクリート造建物建築編-1、阪神･淡路大震災調査報告編集委員会、1997 年

[1-9] 日本建築学会等: 東日本大震災合同調査報告、鉄筋コンクリート造建物建築編-1、第 4 章 被害形態、pp。107-160、東日本大震災合同調査報書編集委員会、2015 年 5 月 30 日

[1-10] 日本建築学会: 2010 年チリ*マワル地震、 建築物被害査報会、災害委員会、2010 年 9 月

[1-11] 日本建築学会: 2011 年東北地方太平洋沖地震、2011 年 7 月

[1-12] National Research Institute for Earth Science and Disaster Prevention & Pacific earthquake Research Center: The second NEES/E-Defense workshop on collapse of reinforced concrete building structure, March 2007

[1-13] California Department of Transportation: Visual catalog of reinforcement concrete bridge damage, USA, 2006

[1-14] K. Mogi: Two grave issues concerning the expected Tokai Earthquake, Earth Planes Space, 56, li-lxvi, 2004.

[1-15] Science for a changing world USGS: Earthquake hazard program http://quake.usgs.gov/prepare/future/

[1-16] Coakley C.: Imperial County Services Building Collapse, Wikispaces Classroom, 2013, https://failures.wikispaces.com/Imperial+County+Services+Building+Collapse

[1-17] Kreger, M. and Sozen, M.: Seismic Response of Imperial Country Services Building in 1979, Journal of Structural Engineering Division, ASCE, Vol. 115, Issue 12. USA, 1989

[1-18] Earthquake Engineering Research Institute: World Housing Encyclopedia, USa, web page, 2014, http://db.world-housing.net/

CHAPTER 2. LITERATURE REVIEW

2.1. Introduction

In this chapter, the current literature about the design of RC columns that can develop high ductility carrying large axial force is presented and commented.

Three references from Japan were studied. The first belongs to the Ministry of Land, Infrastructure, Transport, and Tourism (MLITT) [2.1] it is the Technical standard manual concerned to the structure of buildings. The second one belongs to the Architectural Institute of Japan (AIJ) the document "Calculation standard for horizontal load-carrying of reinforced concrete structure and comments (For public comments)" available on internet [2.2]. In addition, the last one is a huge collection of database of Reinforced Concrete Columns experiments where the experimental results of the behavior of columns were achieved (TasaiLab) [2.3].

Some comments about the differences between these bibliographies were drawn, and the major problems about them were pointed in the conclusion of this section.

2.2. Technical standard manual concerned to the structure of buildings

This reference was published in the year 2007 and did not considered the design of RC columns that can develop large ductility when high axial force is applied. Table 2-1 shows the recommendation of the Technical standard manual concerned to the structure of buildings [2.1], where, the requirements for the aforementioned classification FD corresponds to the least ductile (brittle) column. Following the recommendation of the mentioned reference [2.2], columns classified as FD in Table 2-1 can be classified as the most ductile columns (FA).

The maximum axial force ratio (η) for columns that develop large ductility is 0.35. Where: $\eta = \sigma_0/Fc;$ σ_0: axial stress in the column σ_0=N/bD (MPa), N : axial force (N), b: width of the cross section (mm), D: deep of the cross section (mm), F_c: specific compressive strength of concrete (MPa).

This recommendation is widely conservative in compare with the second bibliography [2.2]; it is just in the case of columns with brittle failure (FD) that axial forces ratio larger than 0.55 were allowed.

Other requirements for the columns that are expected to develop large ductility in this recommendation are: the quantity of axial force reinforcement p_g < 0.80%, and the shear concrete stress ratio should be lower than 0.1, the aspect ratio (height of the column to the deep of the cross section h_0/D) should be larger than 2.5.

Table 2-1 Toughness classification of columns

h_0 / D	σ_0 / F_c	p_t %	τ_u / F_c	*Type*
> 2.5	< 0.35	< 0.80	< 0.100	FA
> 2.0	< 0.45	< 1.0	< 0.125	FB
--	< 0.55	--	< 0.15	FC
Another values				FD

p_g: ratio of total reinforcement (%)

τ_u / F_c shear concrete stress ratio

τ_u: ultimate shear stress (MPa)

2.3. AIJ proposal

Recently, The Architectural Institute of Japan has shown the recommendation of "Calculation Standard for Horizontal Load-Carrying of Reinforced Concrete Structure" [2.2], where columns built with non-high strength materials can develop ductility up to the drift angle of 2.5% under high axial force.

Table 2-2 Requirements for FA Columns 2015

σ_0 / F_c	*SRI*	h_0 / D	p_g *(%)*	τ_u / F_c	*Notes*
≤ 0.45	Eq. 2-1	≥ 2.0	--	≤ 0.20	--
≤ 0.67		≥ 3.0	≥ 1.6		*

* Two or more sub-ties should be placed in each face of the column for each direction of the cross section. Four or more longitudinal reinforcement bars should be arranged. The spacing of the transverse reinforcement should be less than 100mm and less than six times of the smallest diameter of the longitudinal bars.

Shear reinforcement index (SRI) is determined as:

$$\frac{p_w \, \sigma_{we} \, / \, \upsilon_0 F_c}{0.30(\eta)^2 + 0.10} \geq 1.0 \qquad (2\text{-}1)$$

Where:

p_w: shear reinforcement ratio

σ_{we}: effective strength of shear reinforcement ($\leq 85\sqrt{F_C}$) (MPa)

υ_0: effective strength coefficient of concrete ($=1.7F_C^{-0.333}$)

$$\frac{Q_{su}}{Q_{mu}} \geq 1.1 \qquad (2\text{-}2)$$

Where:

Q_{su}: ultimate shear strength (N)

Q_{mu}: ultimate flexural strength (N)

$$Q_{mu} = \frac{M_u}{M/Q} \qquad (2\text{-}3)$$

Where:

M_u: ultimate bending moment (N•mm)

M/Q: shear span (mm)

The ultimate bending moment M_u is determined according to the axial force as follows:

If $N_{min} \leq N \leq 0$

$$M_u = \frac{1}{2} a_g \sigma_y g_1 D + \frac{1}{2} N D g_1$$

If $0 \leq N \leq N_b$

$$M_u = \frac{1}{2} a_g \sigma_y g_1 D + \frac{1}{2} N D \left(1 - \frac{N}{bDF_c}\right) \qquad (2\text{-}4)$$

If $N_b \leq N \leq M_{max}$

$$M_u = \left\{\frac{1}{2} a_g \sigma_y g_1 D + 0.024(1 + g_1)(3.6 - g_1) b D^2 F_c\right\} \left(\frac{N_{max} - N}{N_{max} - N_b}\right)$$

Where:

$N_{min} = -a_g \sigma_y$ (N)

a_g: total area of longitudinal reinforcement (mm)

σ_y: yield stress of longitudinal reinforcement (MPa)

g_1: d''/D

d'' : distance between the center of gravity of longitudinal bars in tension and the center of gravity of longitudinal bars in compression (mm).

$N_{max} = bdF_c + a_g \sigma_y$

$N_b = 0.22(1 + g_1)bDF_c$

Ultimate shear strength Q_{su}:

$$Q_{su} = \left\{ \frac{0.068 p_t^{0.23}(F_c + 18)}{\frac{M}{Qd} + 0.12} + 0.85\sqrt{P_w \sigma_{wy}} + 0.1\sigma_0 \right\} bj \qquad (2\text{-}5)$$

From this proposal of AIJ, some comments are drown:

From this new proposal, more columns are allowed to be designed as ductile columns FA up to axial force ratio of 0.67, this is a great step in comparison with the previous recommendation [2.1]. For this case of axial force ratio, the quantity of axial force reinforcement should not by lower than 1.6%, this is point of particular attention since the fact that, mayor p_g value will produce larger flexural strength and as a consequence, less probability to fail in flexural mode.

For all cases of axial force ratio, the value of the shear concrete stress ratio (τ_u / F_c) was increased up to 0.2. It is also important that the relationship of h_0 / D decrease down to 2.0 for columns that are designed with axial force ratio of 0.45 in compare with the previous reference, columns that use axial force ratio up to 0.65 should have h_0 / D larger than 3.0.

This recommendation mentions that, this recommendation can be employed as far as the designer can ensure that the column will fail in flexural failure. However, the recommendation is not very clear in the way to que ensure this will happen, but, the conventional idea of used the index to avoid shear failure of Q_{su}/Q_{mu} larger than 1.1 is adopted [2.4].

2.4. TasaiLab Database

TasaiLab database is an RC element database [2.3], Tasai Laboratory has been collected experimental data issued by many researchers in order to have a reliable database. This database contains documents published by the Architectural Institute of Japan (AIJ) and the Japan Concrete Institute (JCI) since 1979 to the present. It includes two kinds of structural members, RC columns and beams. Although many parameters were collected, the skeleton curve of the relationship of the shear force and the available lateral drift angle from the papers was not yet collected.

A comparison of the information on the database was carried out. For the whole information, it is just 6 cases which match the requirements of the AIJ reference [2.2], this experiment are listed in the Table 2-3 and plotted in Figure 2-1.

These experiments were the only ones that developed flexural failure with ultimate lateral drift angle *(Ru)* larger than 2.5%. (The information of *Ru* is presented in Appendix 1 which will be explained in Chapter 4). However, all these cases presented a problem, none of them was close to the minimum limit of the requirements of section 2.3. Figure 2-1 shows the Shear reinforcement index of the mentioned columns and the tendency of equation 2-1, no column is close to the tendency of equation 2-1.

This situation is a problem because the accuracy of the AIJ proposal for the minimum limits cannot be shown with the data found in the TasaiLab database. For this research is needed to determine if the structural design in the boundary limits of AIJ proposal work properly.

Table 2-3 Characteristics of the columns in the database

Number	*Name*	*Fc*	σ_y	σ_{wy}	η	p_g	p_w
		MPa	MPa	MPa		%	%
17	CSUS2	36	314	369	0.50	2.15	1.19
18	CSUS3	36	326	404	0.50	2.15	1.19
36	18	23	423	396	0.60	2.14	1.07
40	22	27	423	396	0.60	2.14	1.60
68	No.11	23	423	396	0.61	2.14	1.06
73	No.16	27	423	396	0.65	2.14	1.58

Continuation

Number	*Name*	Q_{su} / Q_{mu}	*SRI*	τ_u/F_c	S/ϕ	h_0/D
17	CSUS2	1.1	1.3	0.15	3.16	3.0
18	CSUS3	1.1	1.5	0.16	3.16	3.0
36	18	1.1	1.5	0.19	6.00	3.0
40	22	1.2	2.0	0.20	4.00	3.0
68	No.11	1.1	1.4	0.19	6.00	3.0
73	No.16	1.2	1.8	0.18	4.00	3.0

Note: The references of the above columns are listed in Appendix 1.

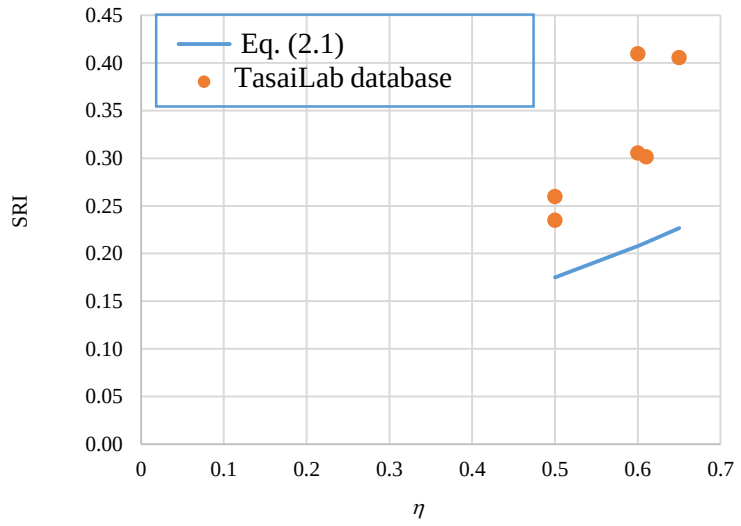

Figure 2-1 Shear reinforcement index – axial force ratio relationship

Additionally, it was found during the study of TasaiLab database that certain kinds of columns developed high ductility despite the fact that their standard assumption index to avoid shear failure was pessimistic, it means that the relationship Q_{su}/Q_{mu} was lower than 1.0. In the next Chapters, it will attempt to explain how columns with this characteristic can develop satisfactory large ductility.

2.5. Conclusions of Chapter 2

After the revision of the literature in this chapter, it can be mentioned that the new proposal from AIJ [2.2] allow more columns to be classify as high ductile columns FA in comparison with the classification recommended by the Transport and Tourism: Technical Standard Manual Concerned to the Structure of Buildings document [2.1].

From the information in database, it is just the case of 6 test results that match the requirements of the reference and none of them was close to the minimum limit of the requirements of section 2.3. It is need to know about the boundary limits of AIJ proposal.

For this reason in the next chapter, an evaluation of the AIJ proposal [2.2] was conducted.

Bibliography of Chapter 2

[2.1] Ministry of Land, Infrastructure, Transport and Tourism: Technical Standard Manual Concerned to the Structure of Buildings (2007)

[2.2] Architectural Institute of Japan: Calculation standard for horizontal load-carrying of reinforced concrete structure and comments (Public comments), 2014.12.
http://www.aij.or.jp/jpn/symposium/2014/public_20141215.html

[2.3] Tasai A.: TasaiLab Reinforced Concrete Elements Database (Columns section), Institute of Urban Innovation, Yokohama National University, Japan, 2011, Personal communication.

[2.4] The Japan Building Disaster Prevention Association: Seismic Evaluation and Retrofit (English version), translated by BRI, 2005.

CHAPTER 3. EVALUATION OF AIJ PROPOSAL

3.1. Introduction

This chapter presents the evaluation carried out for the AIJ proposal [3-1] over the design of reinforced concrete columns carrying high axial force. The influence of the axial force was considered in the study of this type of columns given the fact that the influence of the variation of the axial force is still uncertain [3-2] . For this purpose, four columns were designed and static loading tests were conducted.

The design of the columns match the minimum recommendations required by the AIJ proposal [3-1] to classify as ductile columns FA in flexural failure for the two categories of axial force ratio described in Table 2-2 of Chapter 2.

3.2. Design of specimens

3.2.1. Outline of the specimens

The first specimen, named as No.1, was designed to agree all the requirements of section 2.3 of Chapter 2 for axial force ratio of $\eta \leq 0.45$. The rest of the specimens were named as No.2-A, No.2-B, and No.3 respectively, they were designed to match all the requirements of $0.45 \leq \eta \leq 0.67$. The second and third specimens were physically identical, the difference is the variation of the maximum axial force applied during the test, specimen No.2-A was loaded with axial force ratio of the design (0.65) and No.2-B with a lower one (0.4).

3.2.2. Materials

The standard strengths of the materials (*SS*) were: Fc=21MPa for concrete, 345MPa for hoops SD345 diameter 6mm, 390MPa for rebar SD390 diameter 13mm and, 490MPa for rebar SD490 diameter 16mm.The actual strength of these materials (*AS*) obtained from material tests are shown in Table 3-1.

Table 3-1 Materials properties

Name	F_C (MPa)	σ_y (MPa)		σ_{wy} (MPa)
		D13	D16	D6
1	30	419	537	340
2-A	31			
2-B	31			
3	30			

It is important to remark that concrete compressive strength increased but the strength of the lateral reinforcement did not increase. This will affect the original design criteria of match the minimum values of Q_{su}/Q_{mu} and *SRI*.

Concrete

The Figure 3-1 presents the experimental results for the compressive test carried on the concrete employed for the experiments. It is important to mention that the expected value of the concrete was 21MPa in the original design. This value increased up to 30MPa, and 31MPa depending of the specimen. *SRI* reduced for columns No.1, No.2-A and No.3 because the increment of *Fc* made the numerator smaller in the *SRI* equation.

Reinforcing Steel

Figure 3-2 shows the experimental result of the material test of the reinforcement steel. It is notable to be mention that SD345 diameter 6mm had no clear yielding point in graphic of the stress-strain relationship, whereas, this value was modeled as elastoplastic model with σ_{wy} = 340MPa in the further analyses.

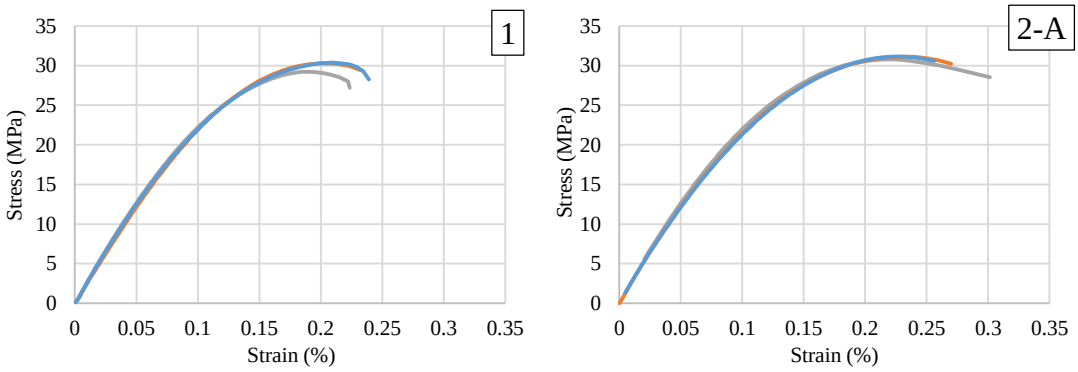

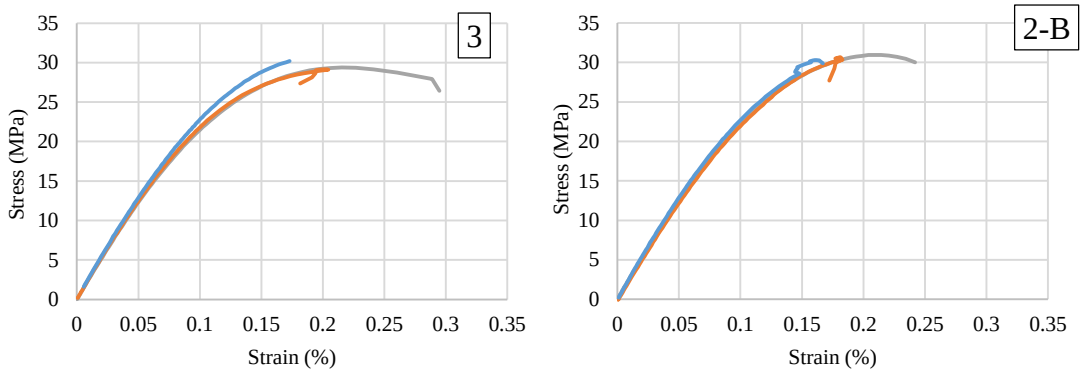

Figure 3-1 Stress – Strain relationship for concrete

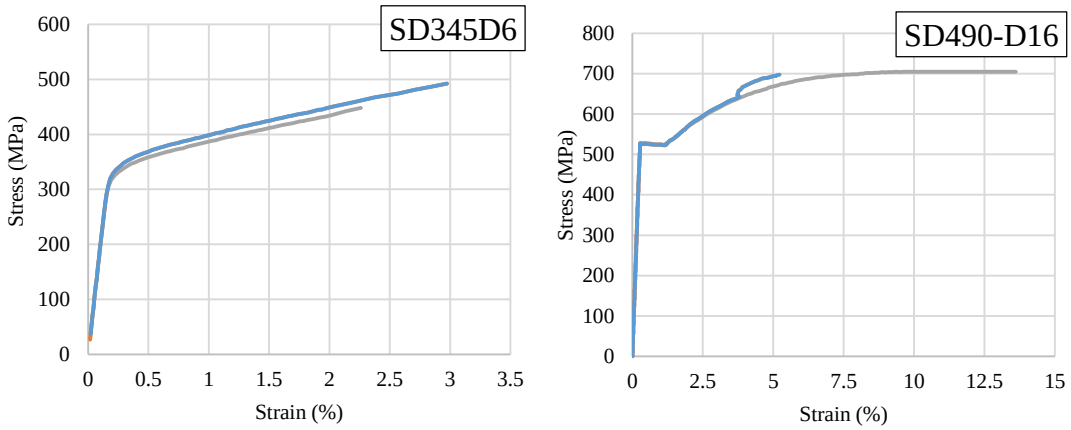

Figure 3-2 Stress – Strain relationship for steel reinforcement

The dimensions and arrangement of the reinforcing bars of the cross section of all columns are shown from Figure 3-3, Figure 3-4 and Figure 3-5.

It was attempted to design the columns so that satisfy the minimum limits of the SRI of Eq. 2-1 and Q_{su}/Q_{mu} relationship of Eq. 2-2 for the actual strength of materials. However, due to the increment in the strength of the materials, it was impossible.

The values of Q_{su}/Q_{mu} reduced for columns No.1 and No.2-B, but remained practically constant for columns No.2-A and No.3.

SRI reduced for columns No.1, No.2-A and No.3 because the increment of Fc made the numerator smaller in Eq. 2-1, in contrast, the reduction of η in No.2-B made the denominator of Eq. 2-1 much smaller than the numerator, as a consequence, SRI got increased. For No.2-B, the value of SRI increased up to 1.20 but Q_{su}/Q_{mu} decreased down to 0.80 what suggest that this specimen can present shear failure.

Table 3-3 shows the characteristics of the columns. The values were calculated by using the nominal and actual strength of materials with the before mentioned equations in section 2.3.

.

Table 3-2 Specimens outline

Name	b mm	D mm	h_0 mm	Reinforcement Rebar	Hoops
1	350	350	1100	8-D13	2-D6@30
2-A	325		975	4-D16 + 8-D13	4-D6@45
2-B					
3			1100	12-D16	

Table 3-3 Characteristics of the columns

Col.	p_g %	p_t %	p_w %	σ_0 / F_c SS	σ_0 / F_c AS	Q_{su} (kN)	Q_{mu} (kN)	* 2007
1	0.83	0.31	0.60	0.45	0.45	365	368	FB
2-A	1.71	0.86	0.87	0.66	0.65	323	288	FD
2-B				0.66	0.40	319	401	
3	2.26	1.13		0.66	0.62	303	323	

* Respective toughness classification 2007 [3-3]

SS Standard strength of materials, AS Actual strength of materials

Continuation

Col.	*SRI* SS	*SRI* AS	Q_{su} / Q_{mu} SS	Q_{su} / Q_{mu} AS	τ_u / F_c SS	τ_u / F_c AS
1	1.0	0.75	1.10	1.0	0.12	0.10
2-A	1.0	0.77	1.17	1.12	0.12	0.12
2-B	1.0	1.20	1.17	0.80	0.12	0.13
3	1.0	0.84	1.00	0.94	0.12	0.14

3.2.3. Instrumentation

The specimens were instrumented internally and externally to record the strain and deformations during the test. Internally, sets of pair strain gauges were pasted in strategically points over the transversal and longitudinal reinforcement, the strain of each of these points was taken as the average of the strain recorded for both gauges. The placement of the strain gauges in the columns is shown in Figure 3-6 through Figure 3-8.

Externally, the columns were divided into six rectangular portions to place a set of transducers for the calculation of shear and axial deformation. The placed transducers for the columns are shown in Figure 3-9 through Figure 3-11.

3.2.4. Test setup

Figure 3-12 shows the test setup of the specimens in the laboratory. Two hydraulic oil jacks of 1000kN were used to apply the axial force and to keep the top and bottom stubs of the specimens in parallel during the test. Two hydraulic oil jacks of 500kN were used to apply lateral force to the specimens. Load cells were placed in the hydraulic jacks to measure the acting force.

3.2.5. Load history

Lateral and axial loads were simultaneously controlled during the test to simulate the seismic effect on columns. The direction of the lateral and axial load is illustrated in Figure 3-12.

Lateral load history

Figure 3-13 shows the applied lateral load history for each specimen. In the first two cycles, the lateral load was applied with force control and constant compressive axial force, which were, the cycles of ±50% and ±100% of the shear cracking strength given by Eq. 3-1 [3-1]. For the rest of the cycles of Figure 3-13, the lateral force was controlled by displacement and the axial force was controlled according to the acting shear force at each step.

$$Q_{cr} = \left(1 + \frac{\sigma_0}{14.7}\right)\left\{\frac{0.061(\sigma_0 + 49)}{\frac{M}{Qd} + 1.7}\right\} bj \qquad (3\text{-}1)$$

Where:

$\frac{M}{Qd}$: shear span ratio ($1 \leq \frac{M}{Qd} \leq 3$).

The value of Q_{cr} for the cycles of ±50% and ±100% of the shear cracking strength for the specimens was: 200kN for column 1, 210kN for column 2−A, 143kN for column 2−B and 177kN for column 3.

Control of axial force ratio

The axial force was applied in terms of axial force ratio (η). For the cycles of ±50% and ±100% of Q_{cr}, constant compressive axial force ratio (η_i) was applied. For column No.1, η_i was 0.15 and 0.25 for the rest of the specimens. For the rest of the lateral load cycles, the axial force was controlled according to the measured shear force applied during the test by Eq. 3-2.

$$\eta_{applied} = \eta_i + \frac{Q}{Q_{Su}} \Delta_\eta \tag{3-2}$$

Where:

η_i: constant compressive axial force ratio

Δ_η : increment of the axial force ratio

Q_{Su}: shear strength calculated by Eq. 2-5. (N)

Q: measured shear force in each step during the test (N)

Δ_η was equal to 0.3 for column No.1, 0.40 for column No.2-A, 0.15 for column No.2-B, and 0.37 for column No.3. During the test, the applied axial force ratio was limited to the maximum value of $\eta_i + \Delta_\eta$ and minimum value of $\eta_i - \Delta_\eta$ for all column.

The maximum axial force ratio was applied at the same time when the positive lateral load was applied, and the minimum axial force ratio was applied at the same time when the negative lateral load was applied.

Figure 3-14 shows the relationship between the axial force ratio and the lateral force, the computed values of Q_{su} and Q_{mu} were plotted with the axial force ratio in terms of η. In this figure, it can be observed that for column No.2-B the shear force reaches the shear strength before the flexural strength.

3.2.6. Drawings

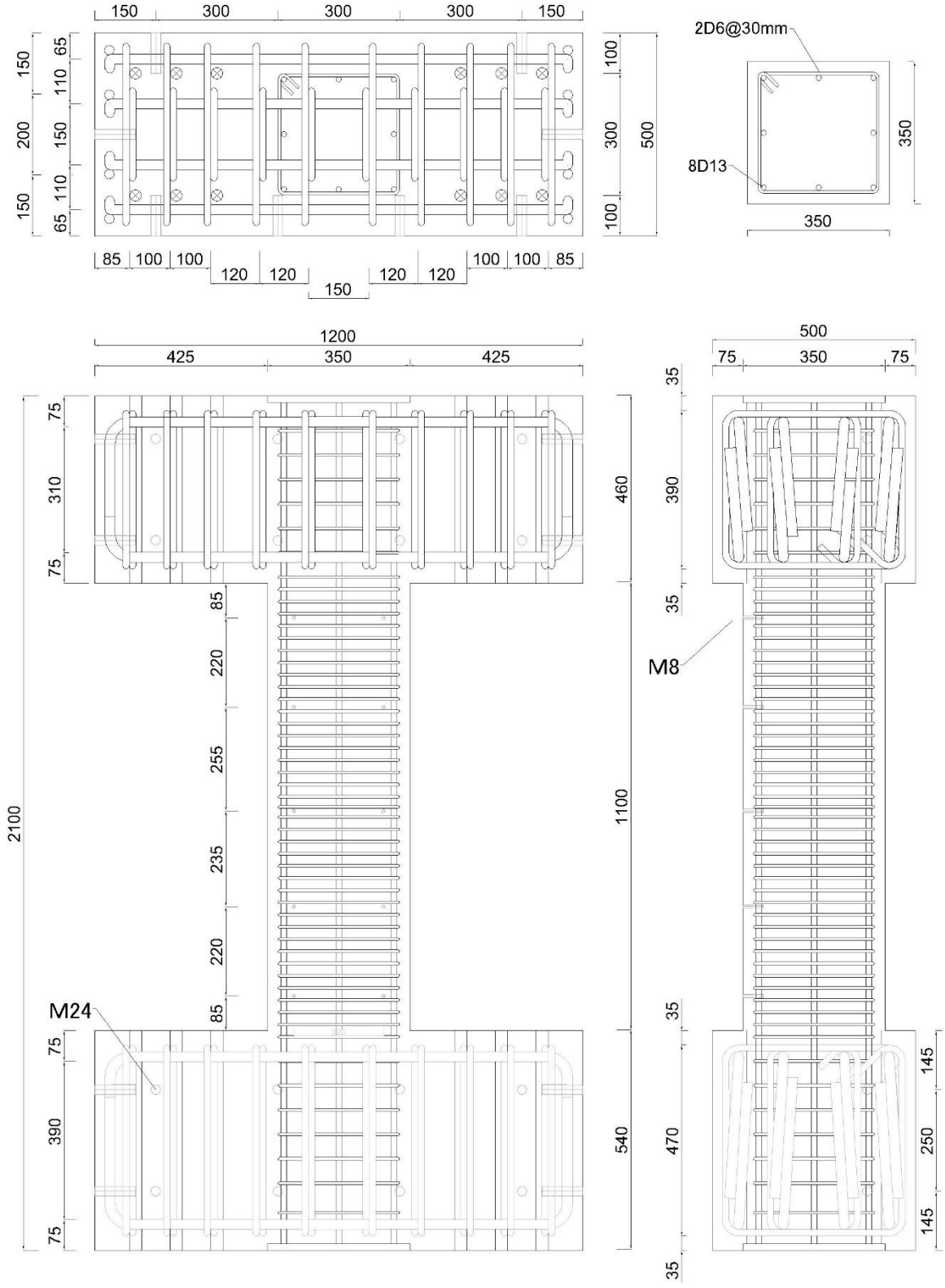

Figure 3-3 Reinforcement details of the specimen 1

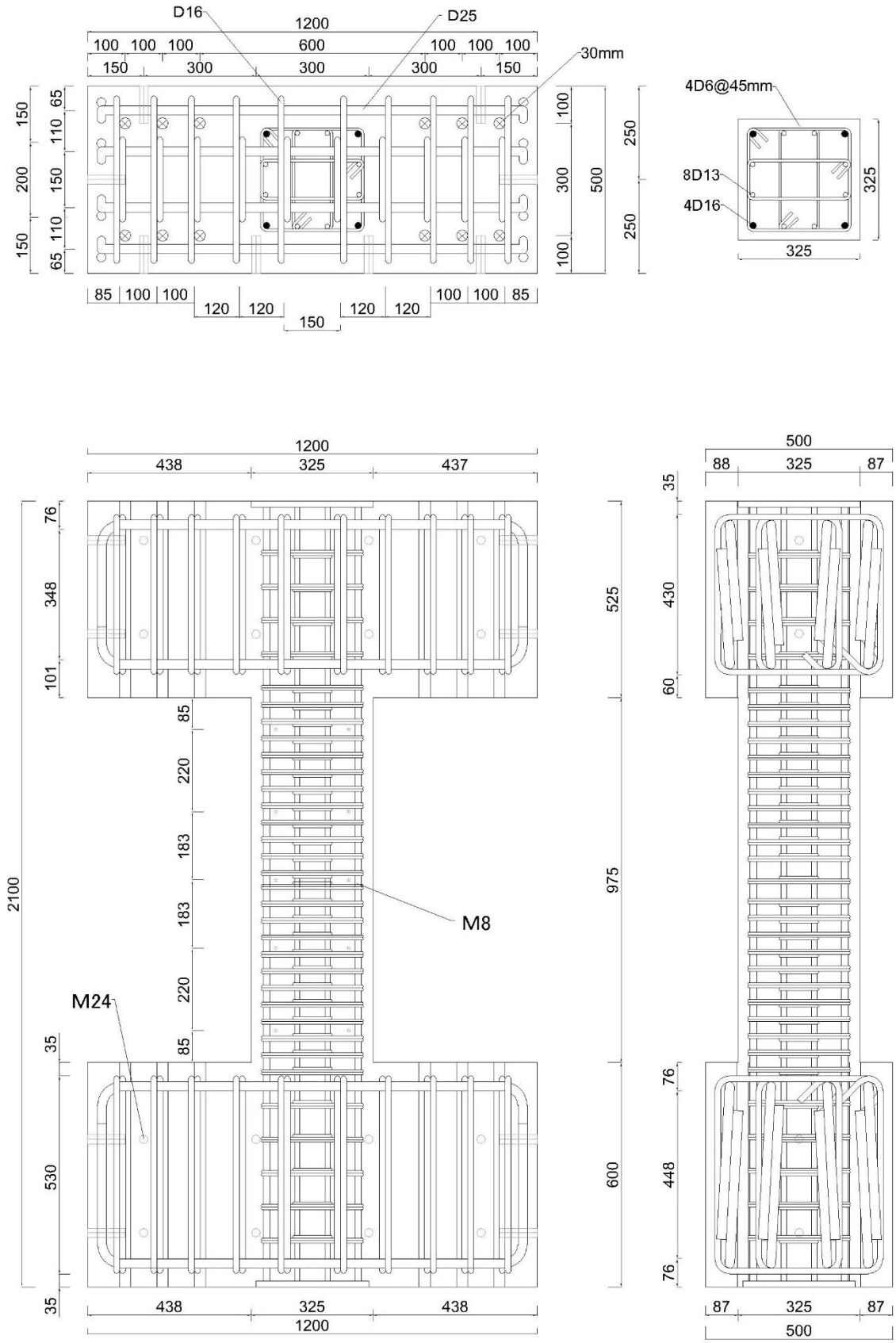

Figure 3-4　Reinforcement details of the specimens 2-A and 2-B

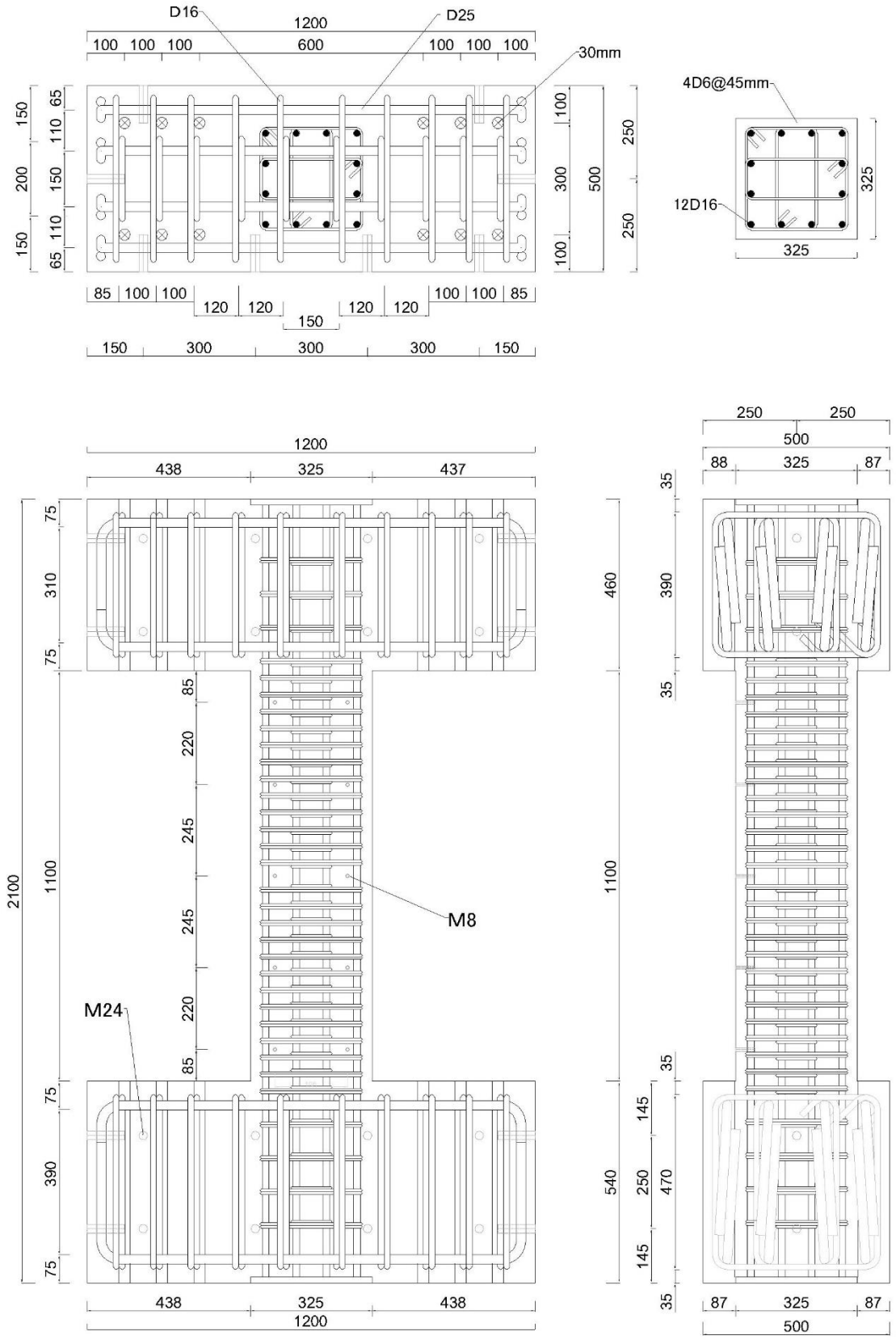

Figure 3-5 Reinforcement details of the specimen 3

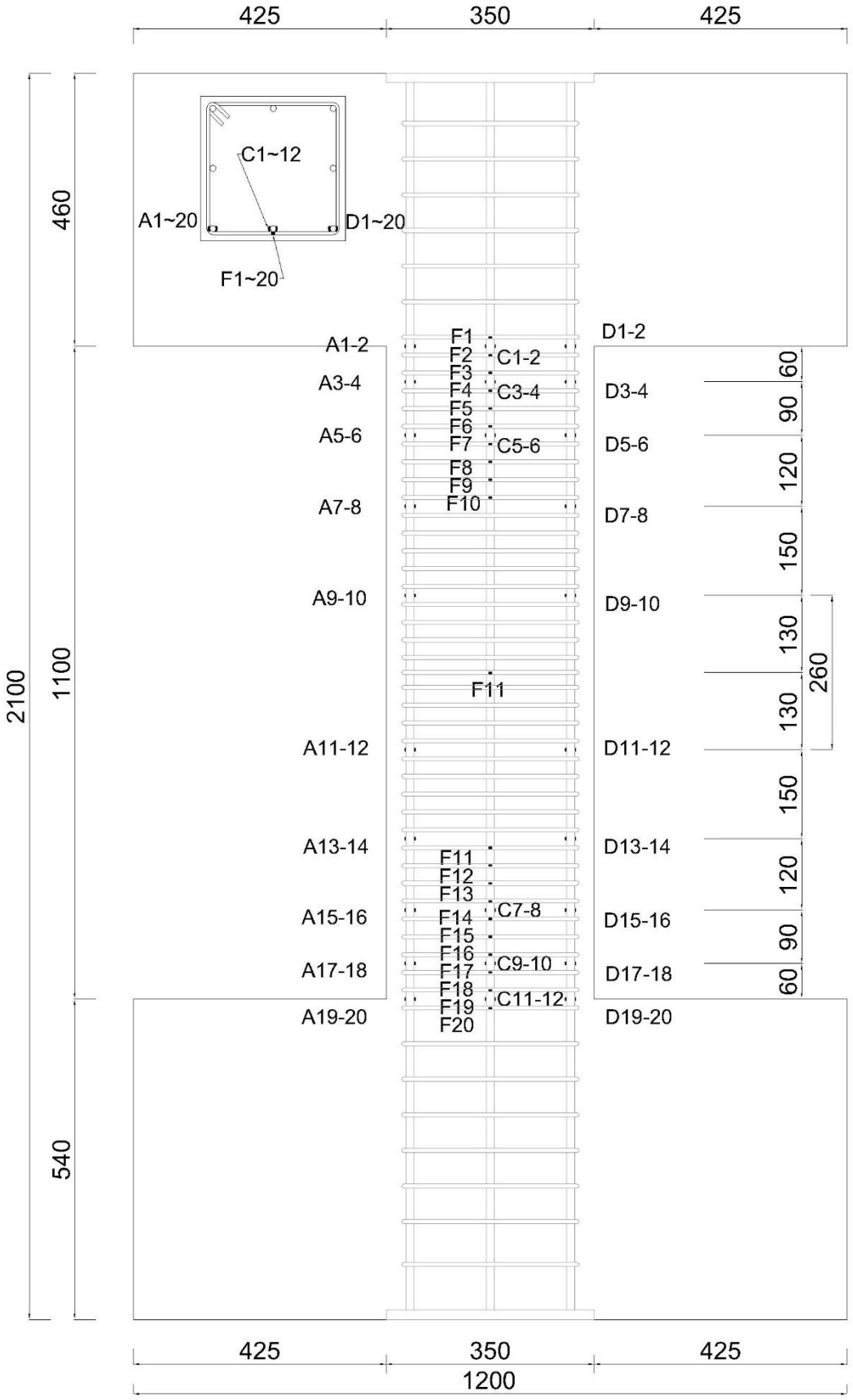

Figure 3-6 Placement of strain gauges of the specimen 1

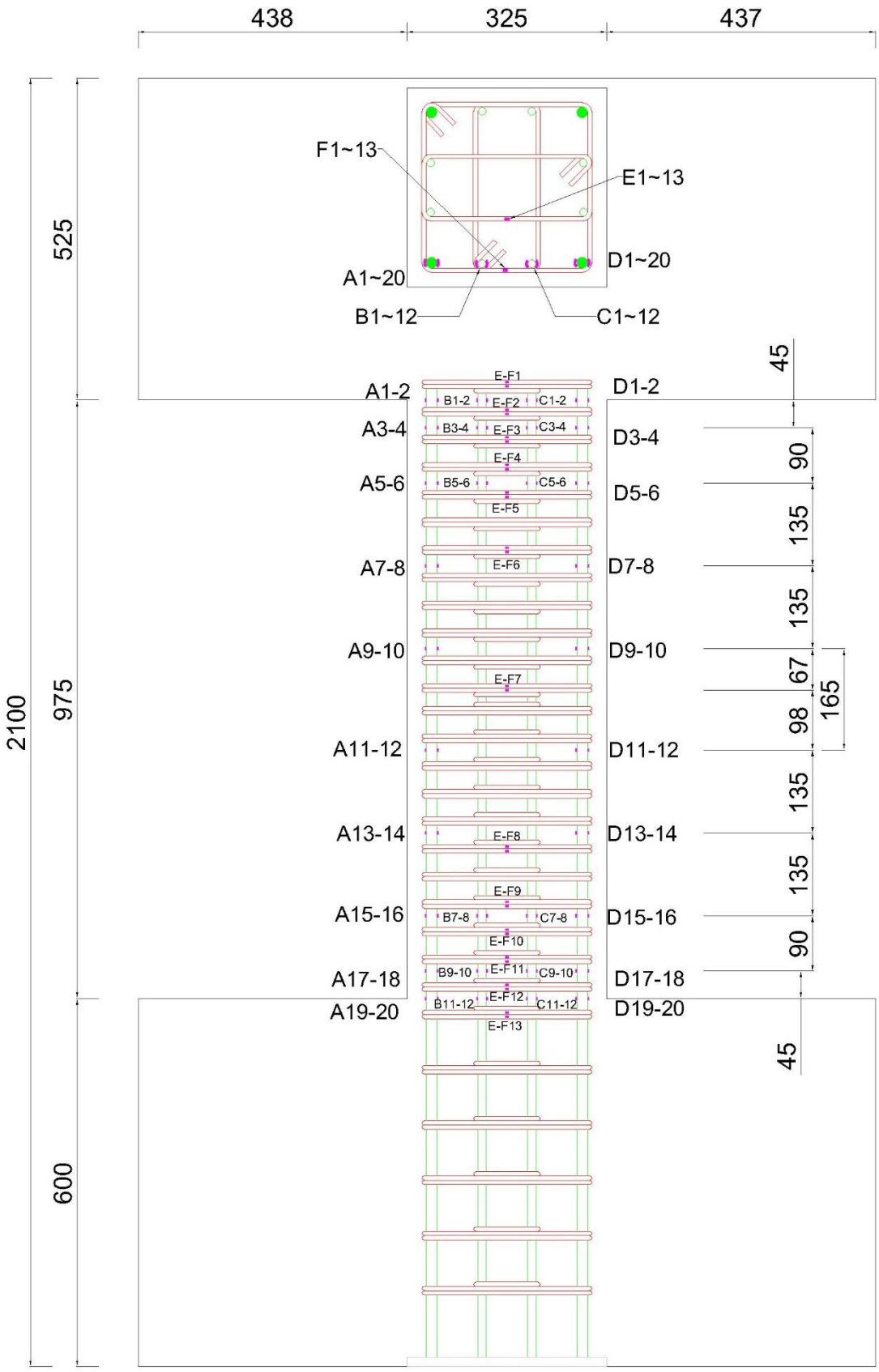

Figure 3-7　Placement of strain gauges of the specimens 2-A and 2-B

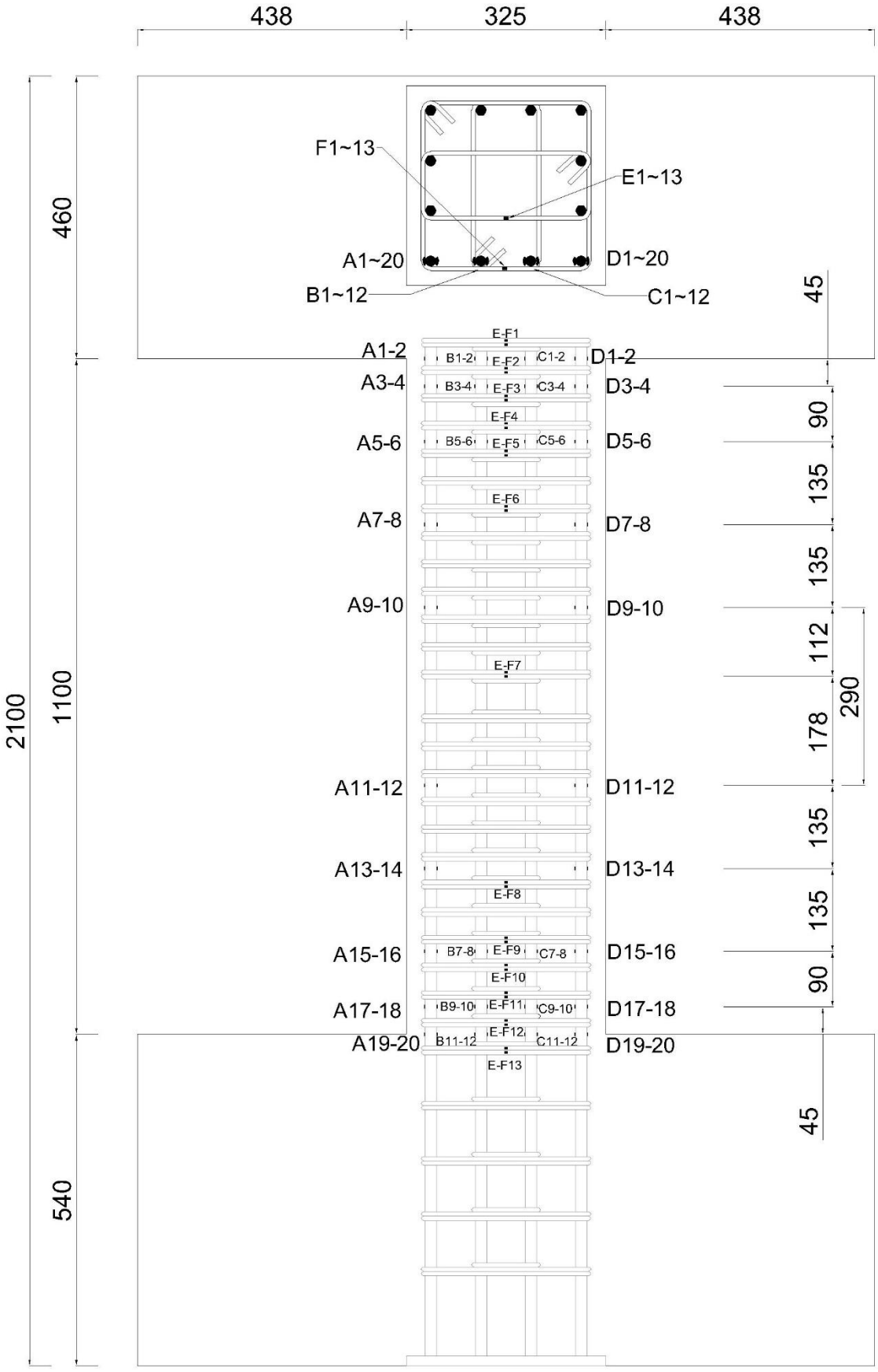

Figure 3-8 Placement of strain gauges of the specimen 3

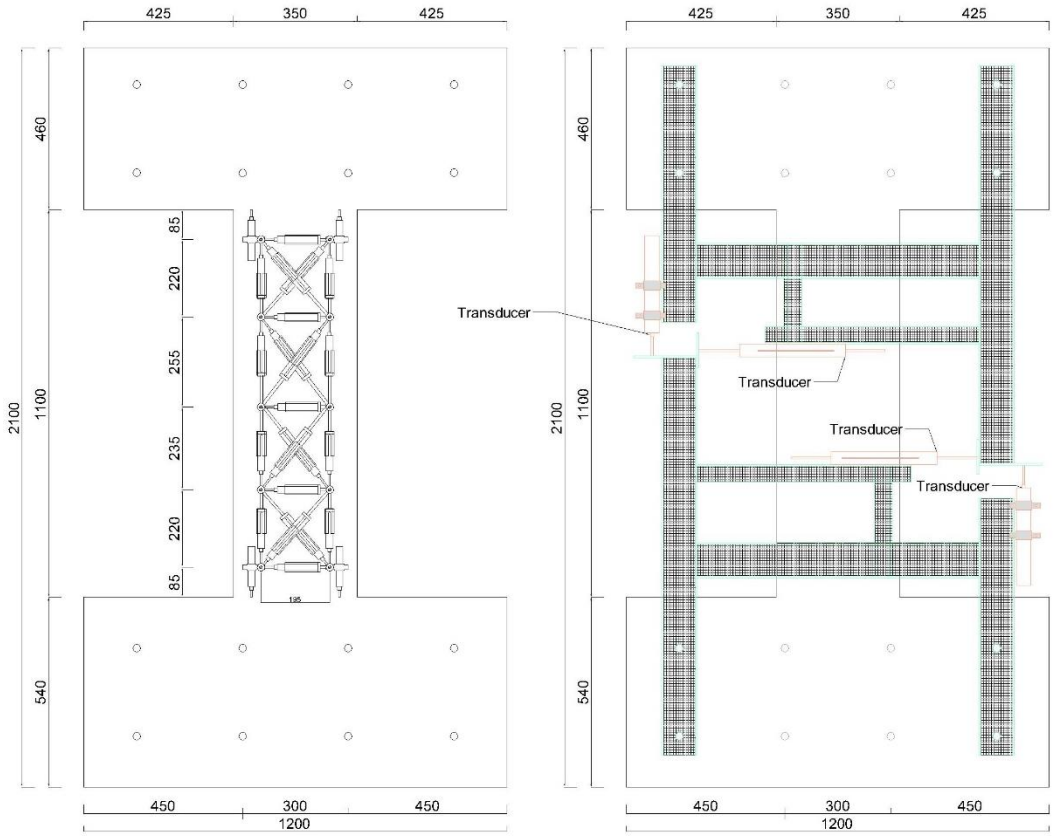

Figure 3-9 Placement of transducers of the specimen 1

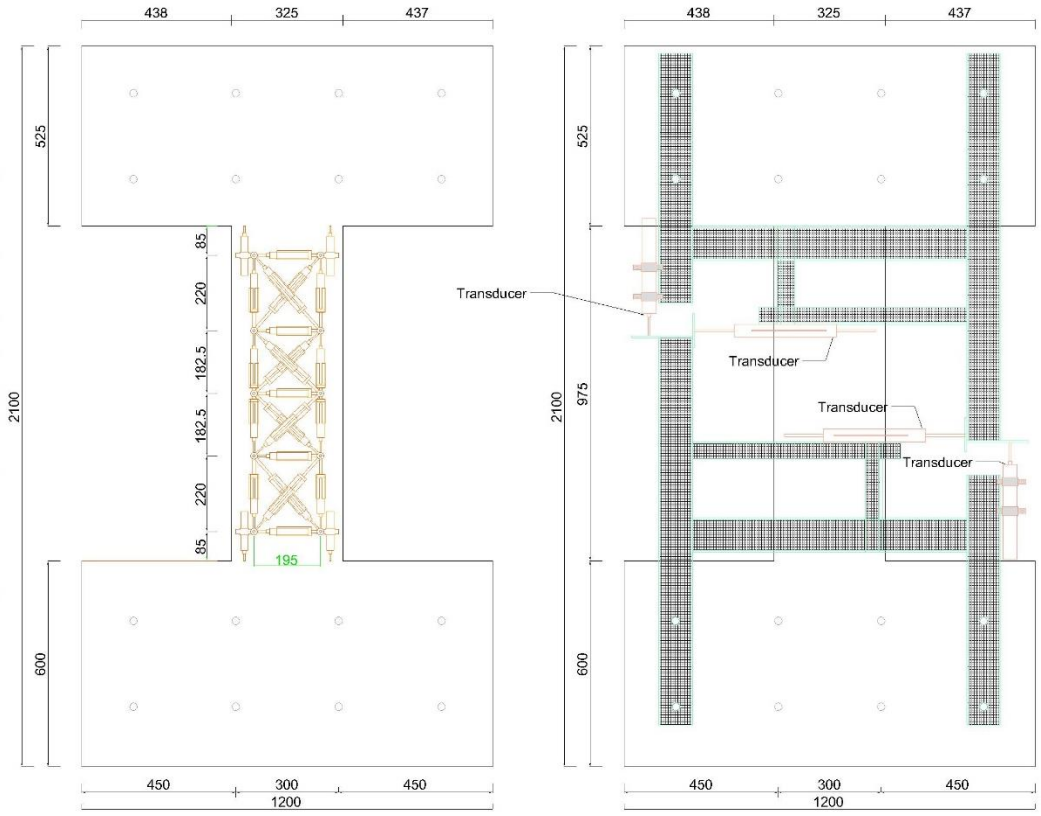

Figure 3-10 Placement of transducers of the specimens 2-A and 2-B

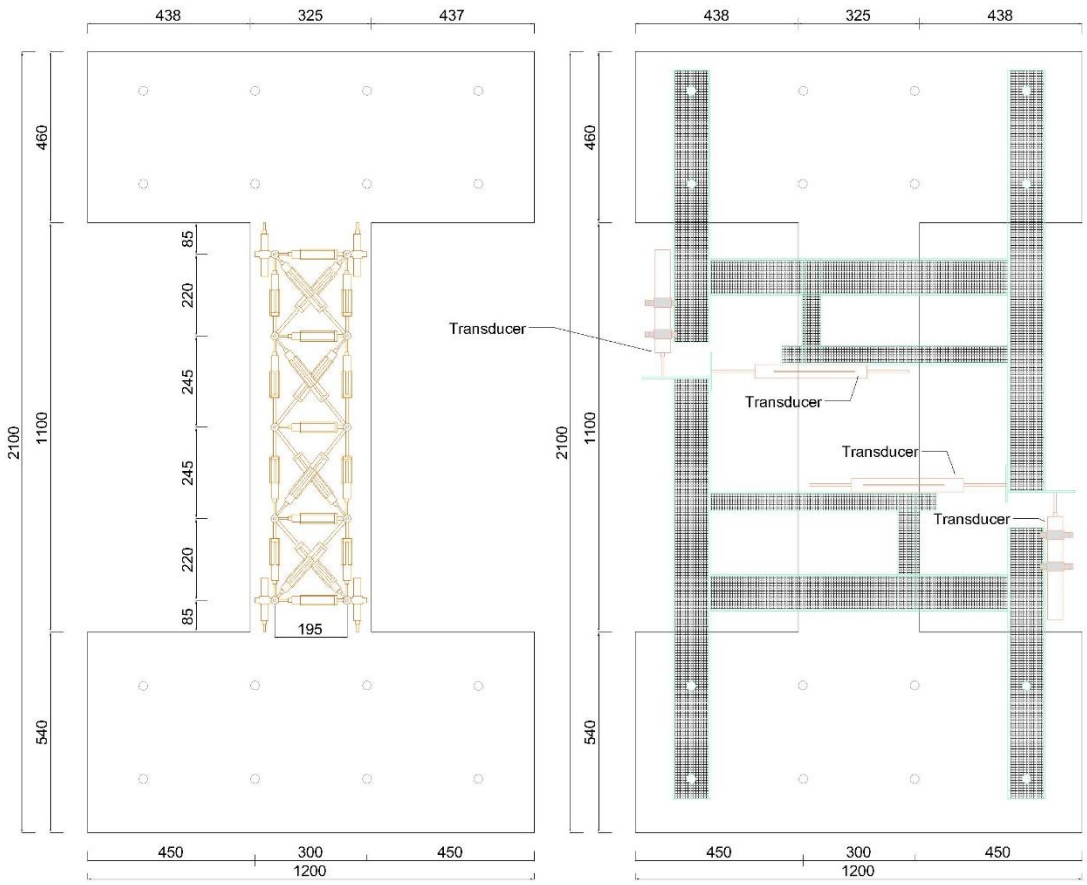

Figure 3-11 Placement of transducers of the specimen 3

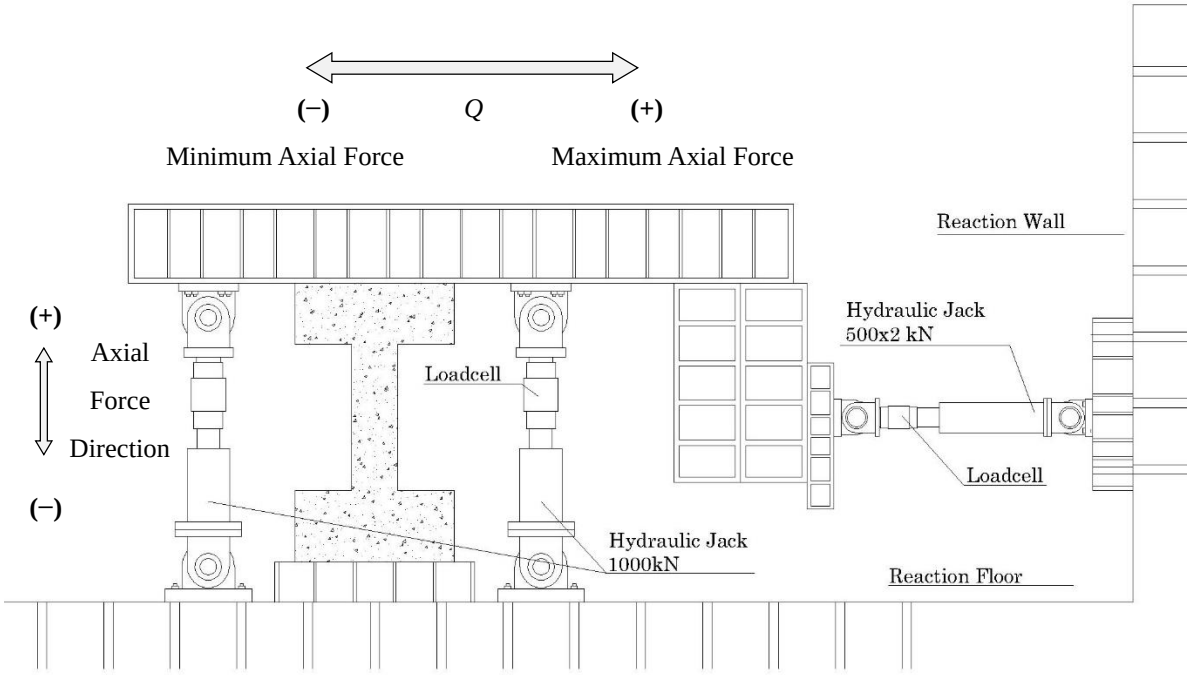

Figure 3-12 General test setup of specimens

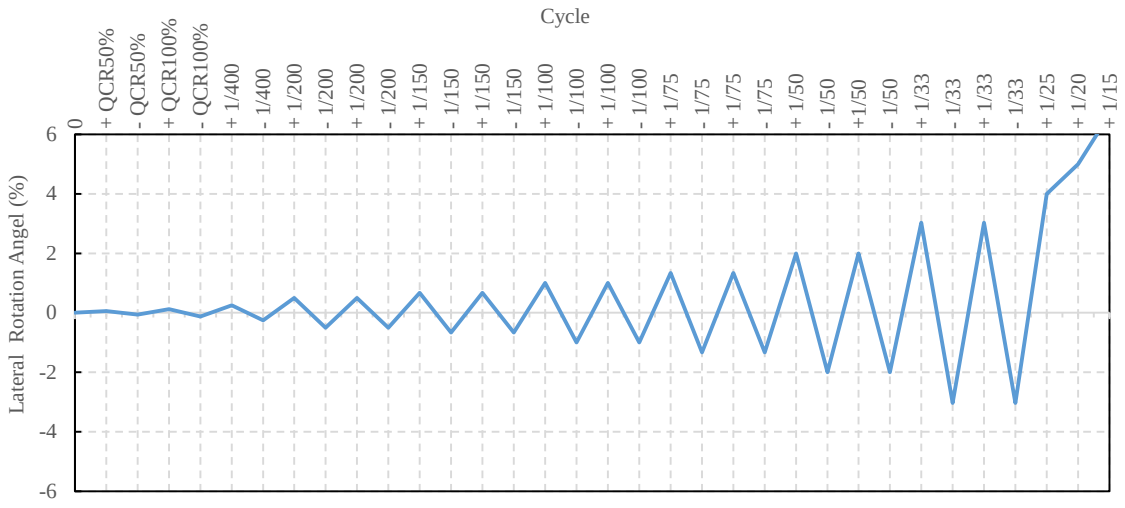

Figure 3-13 Lateral Load History

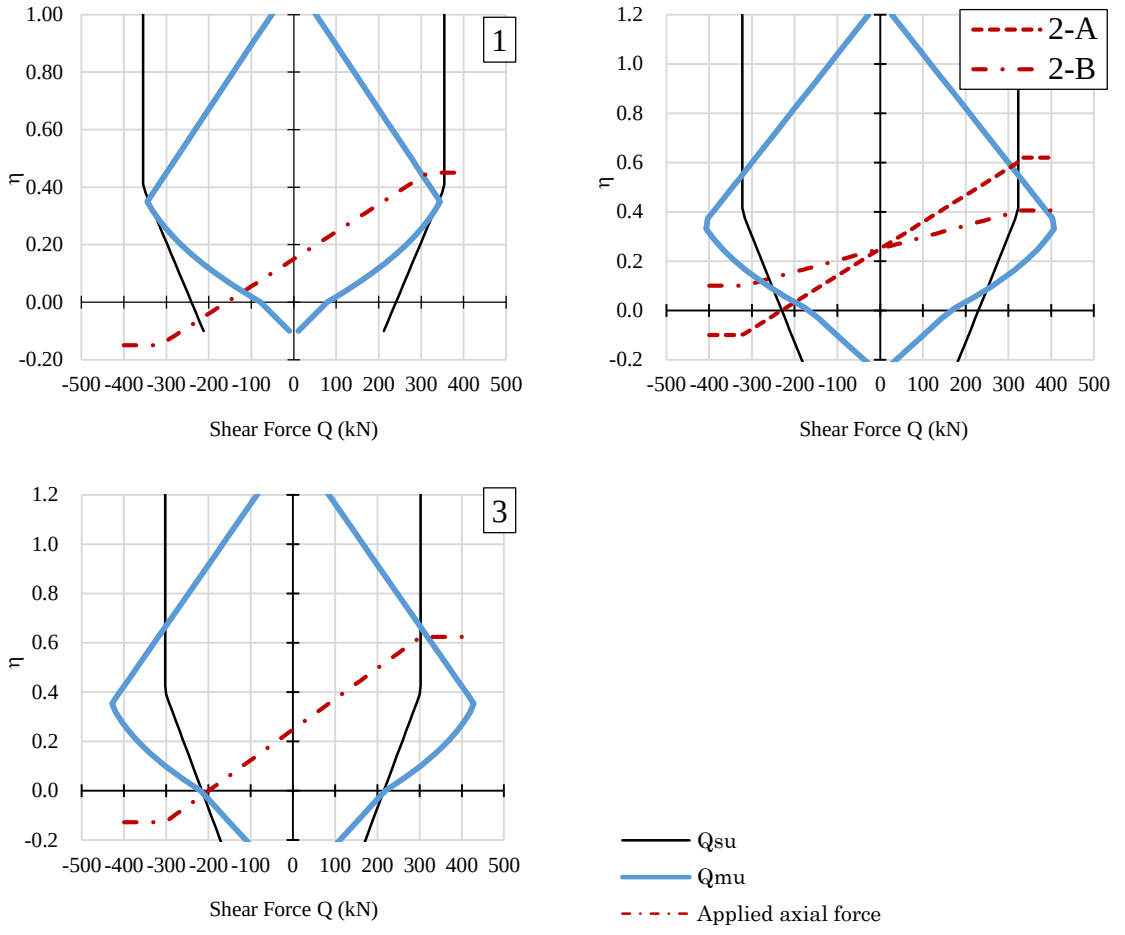

Figure 3-14 Applied Axial Force Ratio and Shear Force Relationship

3.3. Test results

3.3.1. Cracking of Concrete

Flexural cracks appeared before than shear cracks in all specimens. Figure 3-15 (from *a* to *i*) shows the cracks panther for each cycle of load history. Combined shear and flexural cracks appeared in all columns after the cycle of +1/200. Figure 3-15-*i* shows the cracking pattern of all columns at the final stage of the test. Figure 3-16 shows pictures of the final stage of the specimens at the end of the test. For columns 2-A and 2-B, indicial flexural cracks indicated that the reduction of axial force ratio from 0.65 to 0.40 did not affect the planned failure mode at the beginning of the test. However, in the columns with lower axial force ratio concrete cracked earlier. It can be said that Eq. **3-1** prognosticated conservatively the shear force when concrete cracked even the fact that this equation does not consider explicitly the axial force ratio or the quantity of lateral and longitudinal reinforcement.

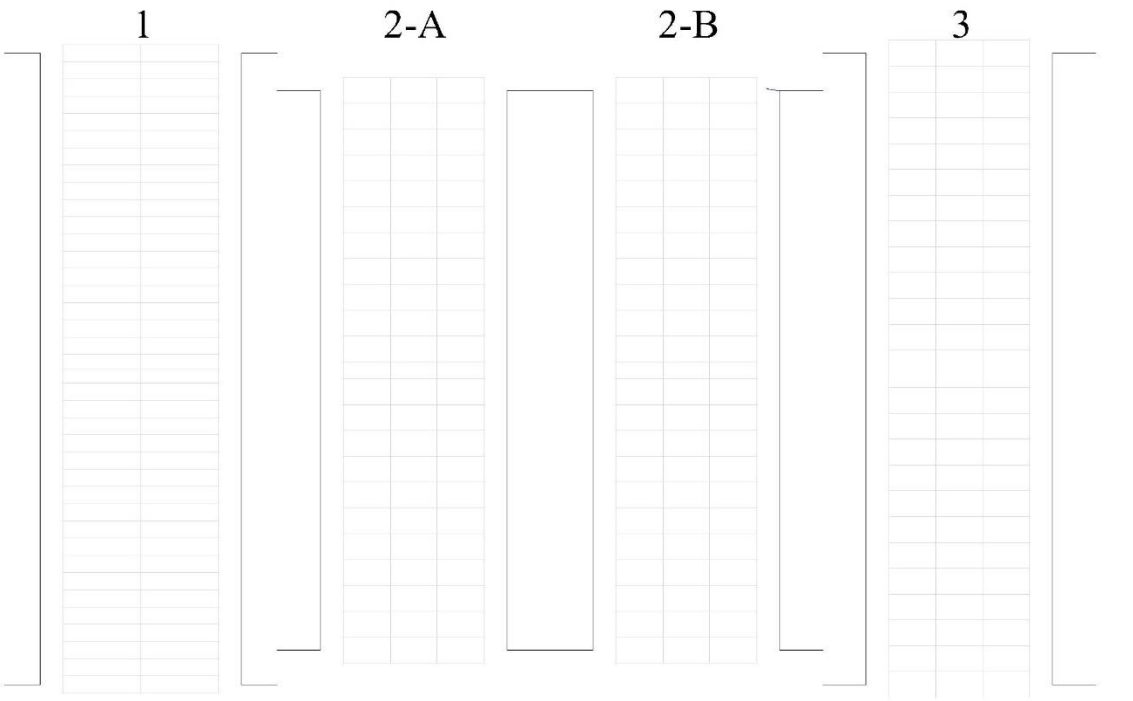

a) At the end of the Q_{cr} cylices

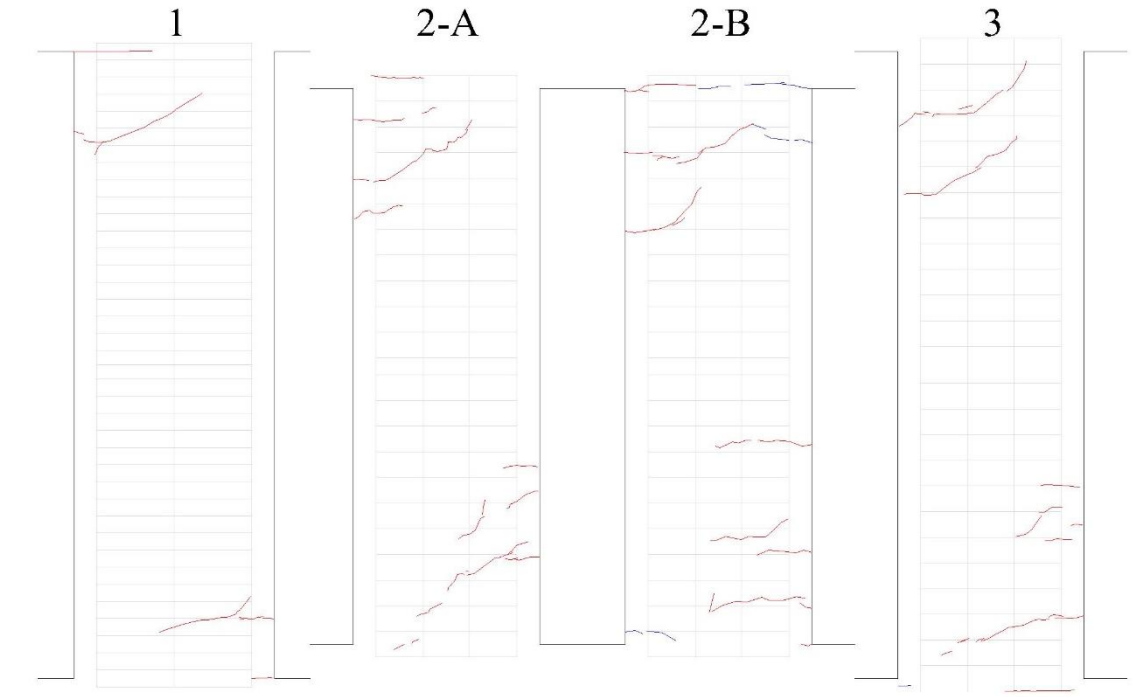

b) At the end of the 1/400 cylices

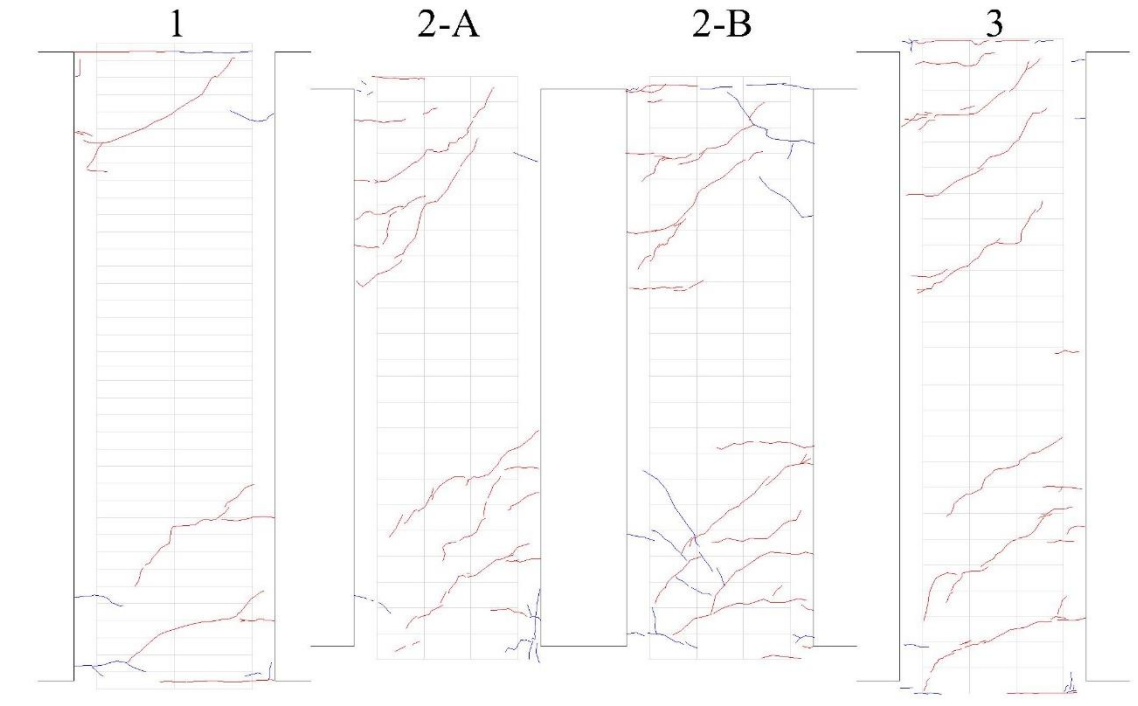

c) At the end of the 1/200 cylices

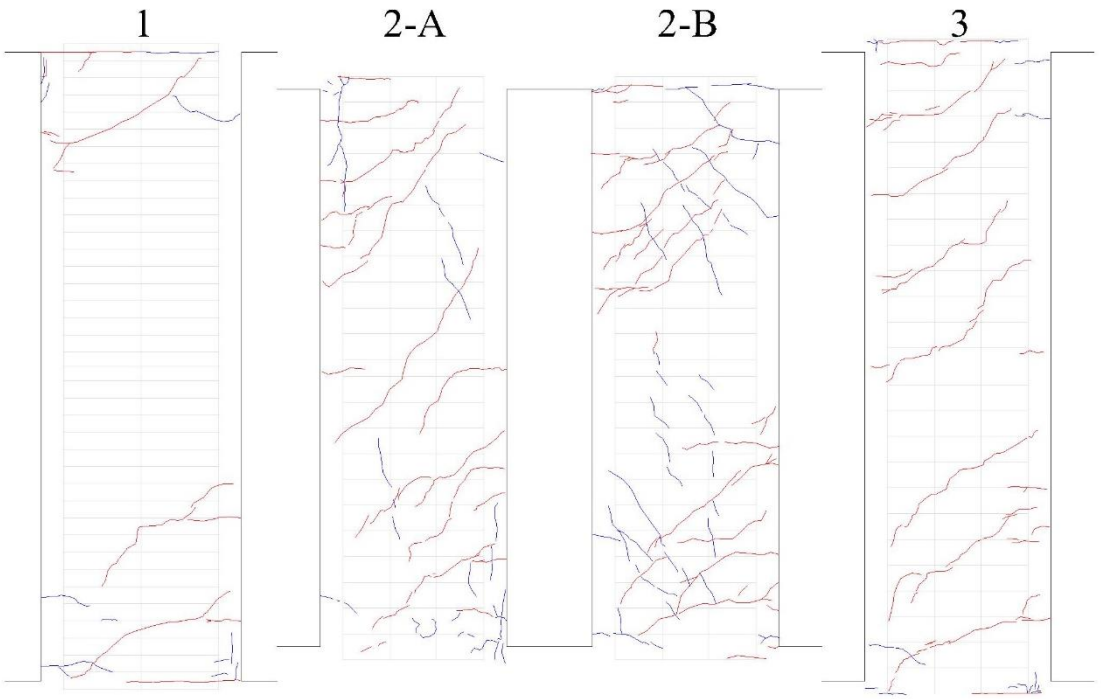

d) At the end of the 1/150 cylices

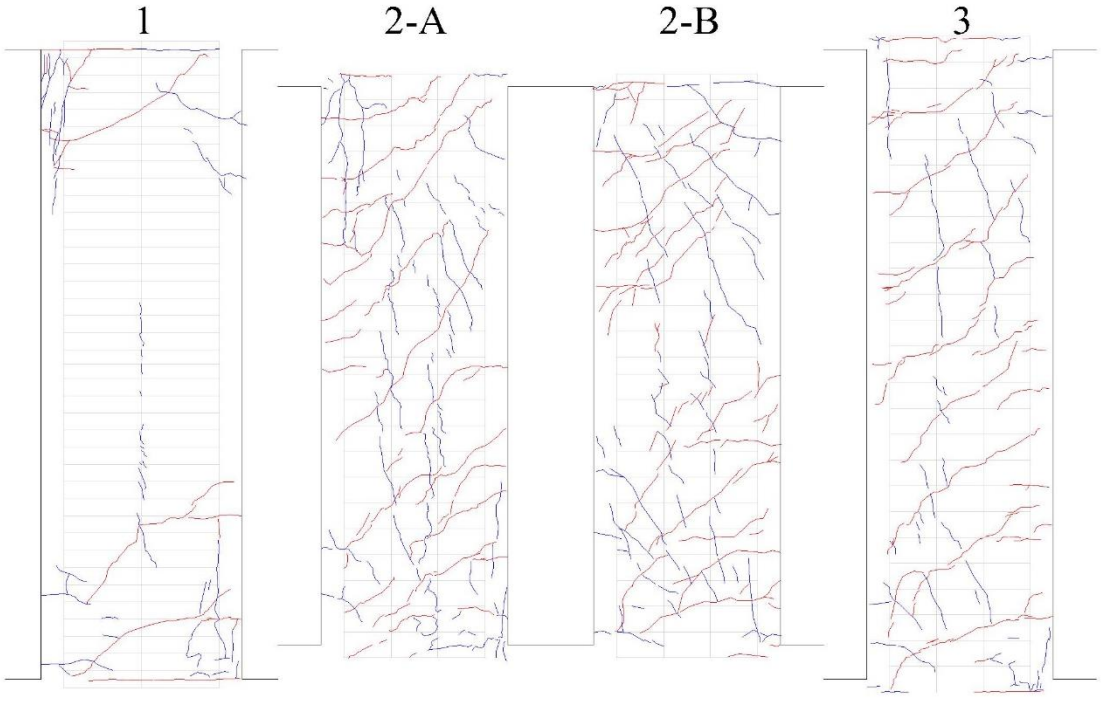

e) At the end of the 1/100 cylices

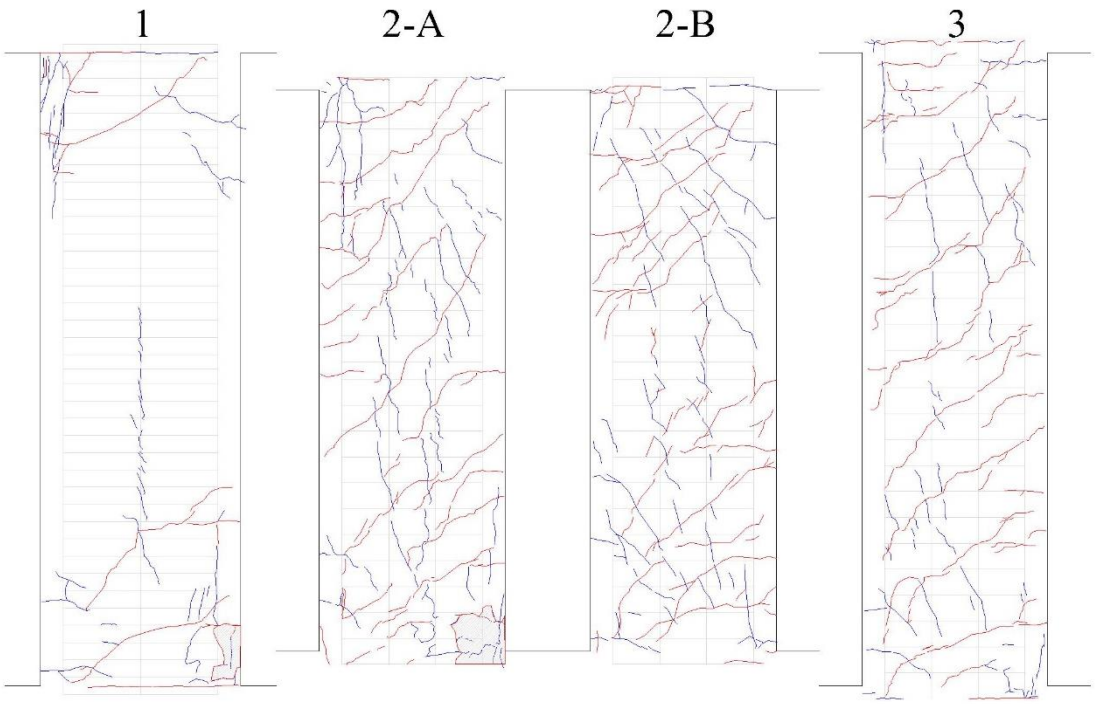

f) At the end of the 1/75 cylices

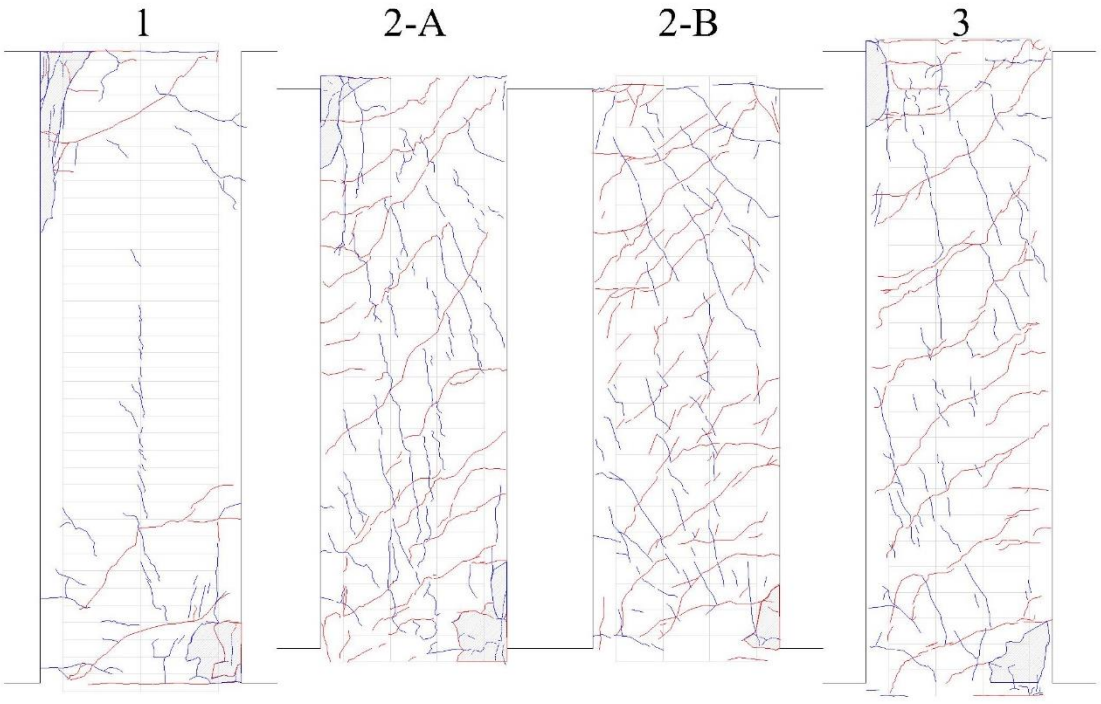

g) At the end of the 1/50 cylices

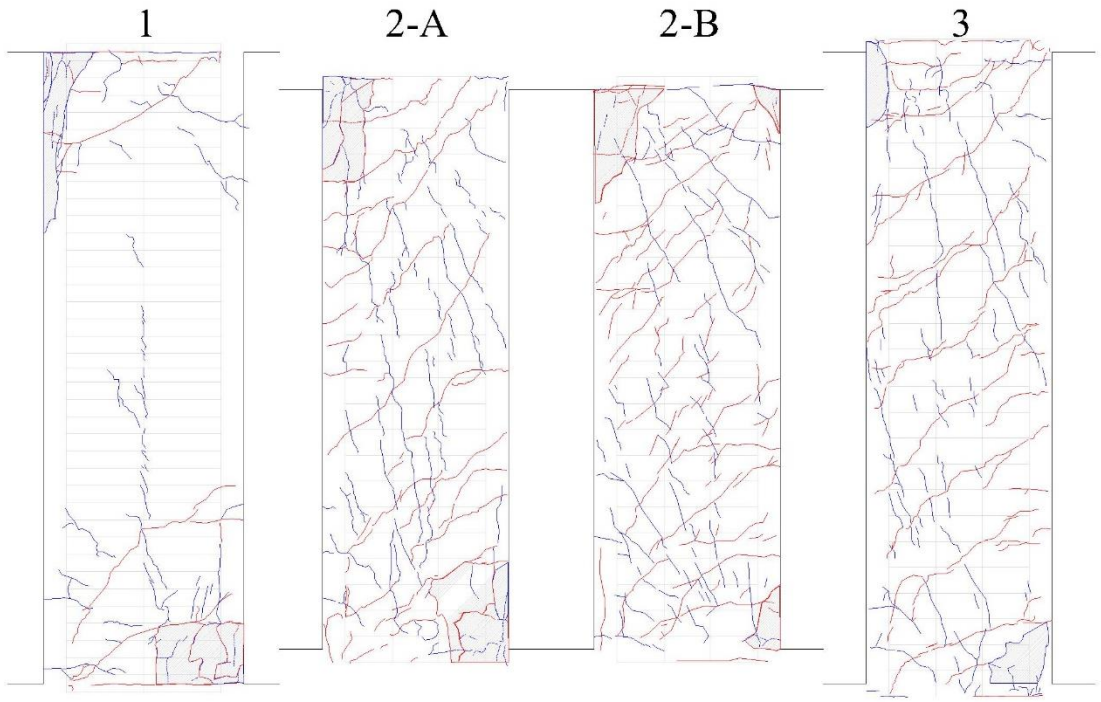

h) At the end of the 1/33 cylices

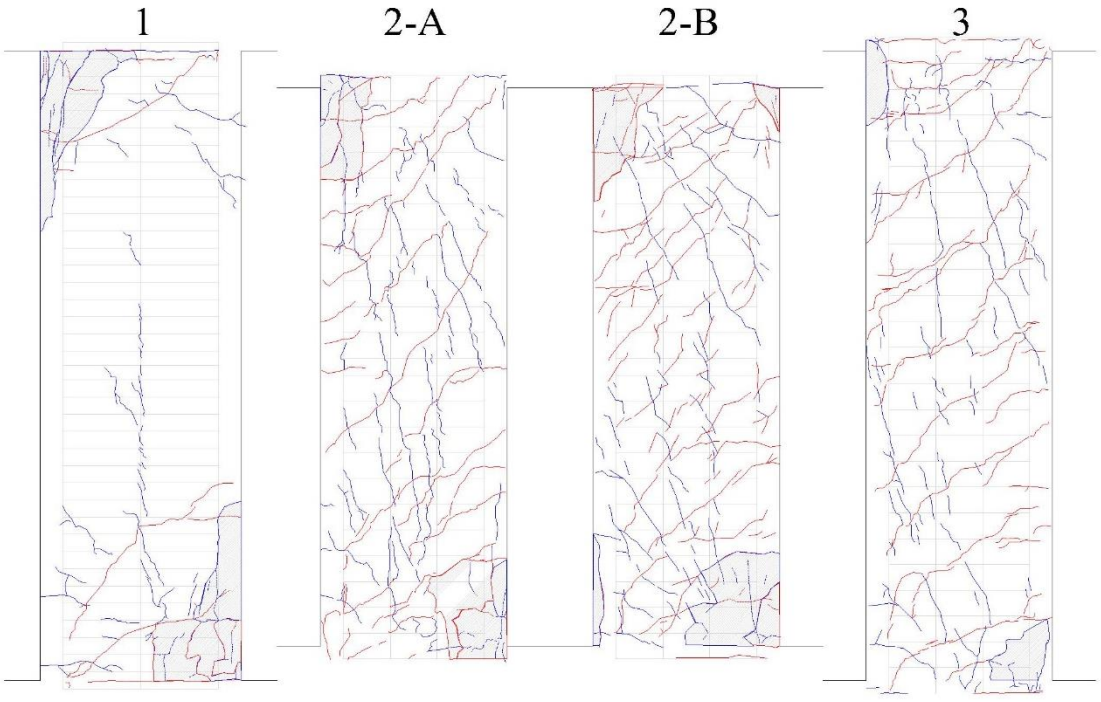

i) At the end of the 1/33 cylices

Figure 3-15 Cracking of specimens

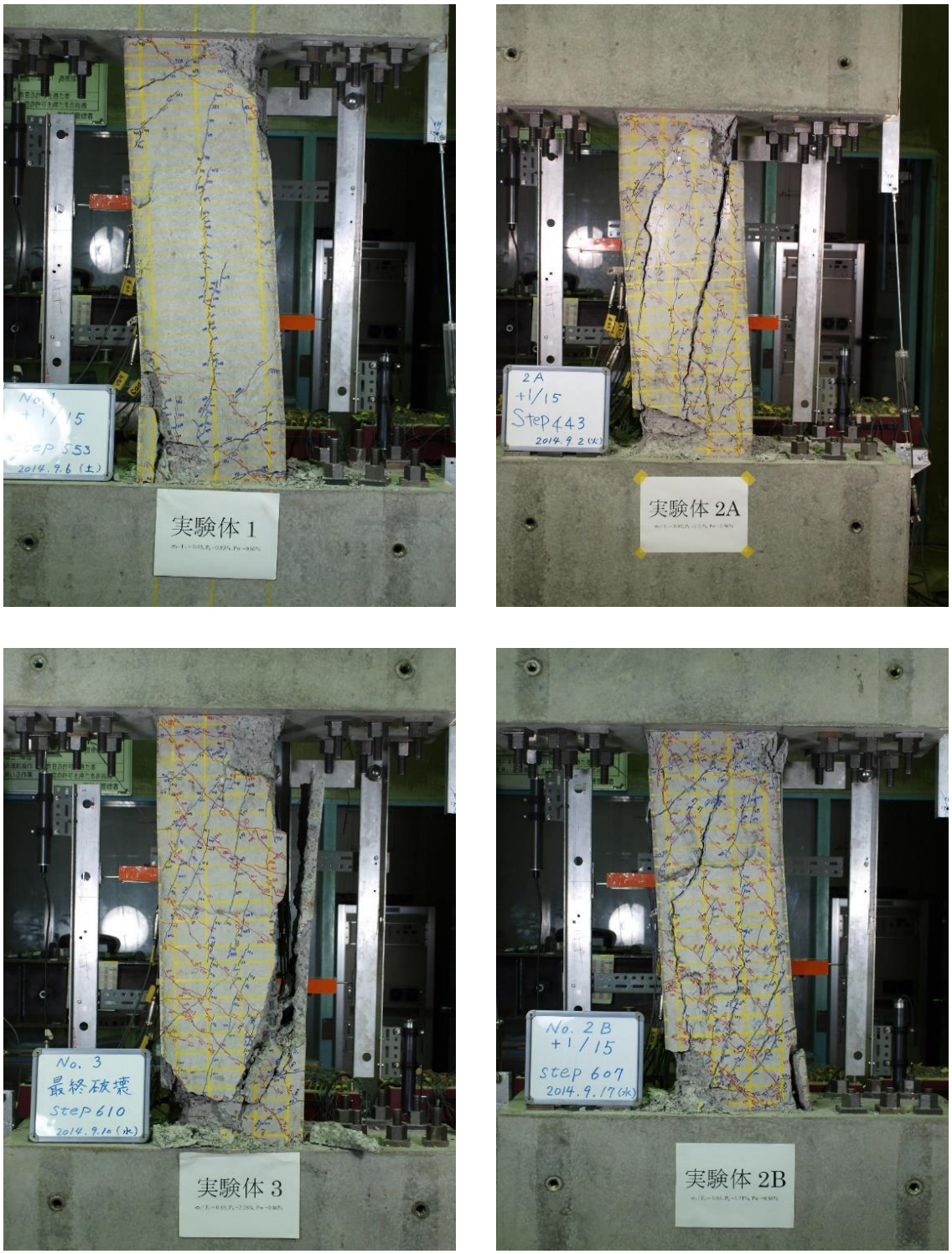

Figure 3-16　Final stage of specimens

3.3.2. Hysteresis characteristics

In Figure 3-17, the hysteresis characteristics of the columns are shown as the relationship between shear force and the lateral drift angle. In specimen number 1, the initial constant axial compressive force of 551kN was applied for the cycles of concrete cracking, the axial force was increased and decreased proportional up to σ_0/Fc of Eq. 3-2. After the cracking cycles, the maximum applied axial force was 1665kN and tensile force of 65kN. Cracks were visible until $+2.5x10^{-3}$rad (+1/400 cycle). When the load cycle reach $-5\ x10^{-3}$rad (-1/200) rebar yielded in tension when a lateral force was equal to -143kN, at this point hoops working at 8% of its yielding capacity. The yielding of the rebar in compression started at $+10x10^{-3}$rad (+1/100) with shear force equal to 370kN, the hoops works at 5% of its capacity, from this point the column started to reduce its strength, when the hoops reach 100% of its capacity then failure occurred at $+91x10^{-3}$rad, at this step the lateral force was 148kN. It is known by the information acquired by sensors that hoops in the middle of the span of the column work more than that located in the extremes of the column, however, it was in the bottom of the column where concrete failure took place.

In the same Figure 3-17, it can be seen that the longitudinal reinforcement of column 2-B yielded at the drift angle of 0.64%, later than that of the column 2-A that yielded at 0.5%; however, in both columns the longitudinal reinforcement yielded at almost the same lateral force of 370kN. On the other hand, hoops yielded at the lateral drift angle of 1.82% with the lateral force of +423kN for column 2-B, and lateral drift angle of 2.01% with the lateral force of +394kN for column 2-A. It can be said that the reduction of the maximum axial force ratio from 0.65 to 0.40 practically had no effect on the strength of these columns, but it reduced the lateral drift angel when the lateral reinforcement yield. This effect was attributed to the redistribution of stress in the column with low axial force ratio.

Flexural behavior dominated the failure mode of column 2-B even the fact that the analytical value of Q_{su}/Q_{mu} suggested shear failure. It can be implied that Eq. 2 is not prognosticating a proper failure mode in this column. However, column 2-B collapsed at lateral drift angle of +6.6%, whereas at the same lateral drift angle, no failure was observed in column 2-A.

In specimen number 3, the constant axial compressive force was 784kN, and later increased until 2009kN and decreased until tensile force equal to 251kN. The compressive

yielding of rebar took place at +13.33 x10^{-3}rad when shear force was equal to +392kN and hoops where working at 14% of its capacity. No tensile yielding of rebar was registered in that specimen, the maximum work develop by the rebar in tensile was 50%. The column increased its strength until a maximum of +423kN at rotation equal to +20x10^{-3}rad then it decreased. Hoops reached 100% of its capacity at +33.3x10^{-3}rad and Q = +363kN, the failure was reached at +46x10^{-3}rad.

It is well known that the longitudinal reinforcement bars buckle when large axial loads are applied [3-6]. For column 1, local buckling was observed in the longitudinal reinforcement. After the rebar yielded, the column lost strength quickly compared with the rest of the columns. On the contrary, no local buckling was observed in the rest of the columns during the test. It can be implied that the longitudinal reinforcement was properly restricted against buckling for the columns 2-A, 2-B and 3. It is recommended that, as much as possible, columns that carry high axial force of η = 0.45 also use the subtie configuration given for the columns design with columns $0.45 \leq \eta \leq 0.65$.

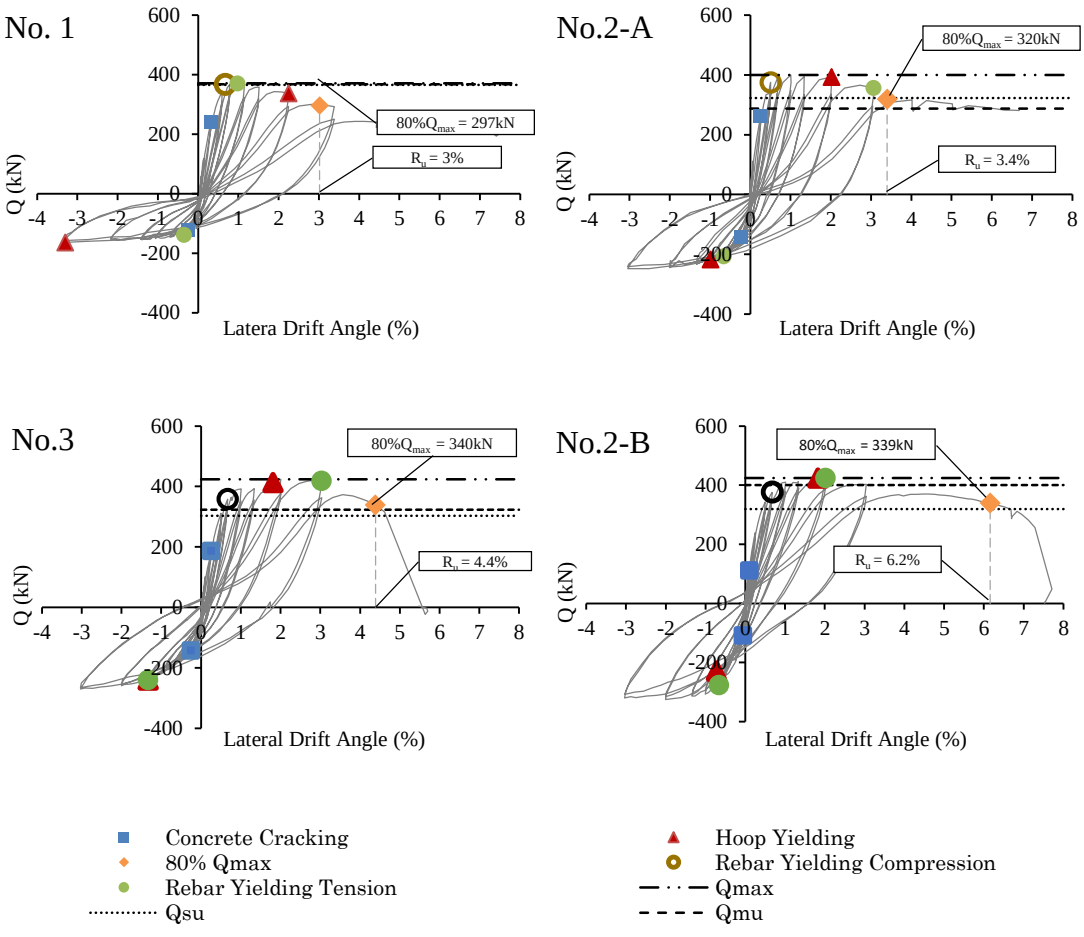

Figure 3-17 Shear force – Lateral Drift Angle Relationship

3.3.3. Flexural Deformation

The relationships of the flexural deformation (δ_f) and the lateral drift angle are shown in Figure 3-18. The flexural deformation was calculated for 6 different portions in each column as follow:

For portions in the edge of the column, portion 1 and 6, the deformation was:

$$\delta_i = \varphi_i \frac{h_i^2}{2} \tag{3-3}$$

For portions in the middle span of the column, portions from 2 to 5, flexural deformation was:

$$\delta_i = \varphi_i \frac{h_i^2}{2} \ (\varphi_{i-1} h_{i-1} h_i) \tag{3-4}$$

The total flexural deformation was the summation of all portion deformations from 1 to 6.

$$\delta_F = \sum_{i=1}^{n} \delta_i \tag{3-5}$$

Where φ_i is the curvature:

$$\varphi_i = \frac{\delta_{ai} - \delta_{bi}}{h_i D_x} \tag{3-6}$$

δ_{ai}: measured displacement with the transducer a_i (mm)

δ_{bi}: measured displacement with the transducer b_i (mm)

i = 6 (portion at bottom of the column). The location of δ_{ai} and δ_{bi} are shown in the detail of Figure 3-19.

Figure 3-19 shows the columns were divided by portions and it respective numbering.

In Figure 3-18 can be observed that, the flexural deformation increased in both positive and negative loading for all columns from the lateral drift angle of -3% to 2%.

After lateral drift angle of 2%, flexural deformation of column 2-A increased more than that of column 2-B. Flexural deformations were 19.5mm and 15.7mm for column 2-A and 2-B respectively at the lateral drift angle of 4%. It can be said that, the reduction of the axial force produced fewer flexural deformation. Flexural deformations was 14.9mm for column 3 at the lateral drift angle of 4%; then, the increment of the flexural strength between column 2-A and 3 had the same effect in the flexural deformation as reducing the axial force ratio.

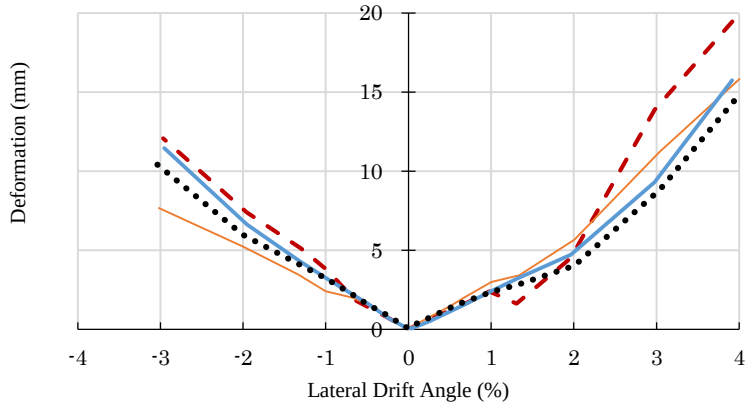

Figure 3-18 Flexural deformation-lateral drift angle relationship

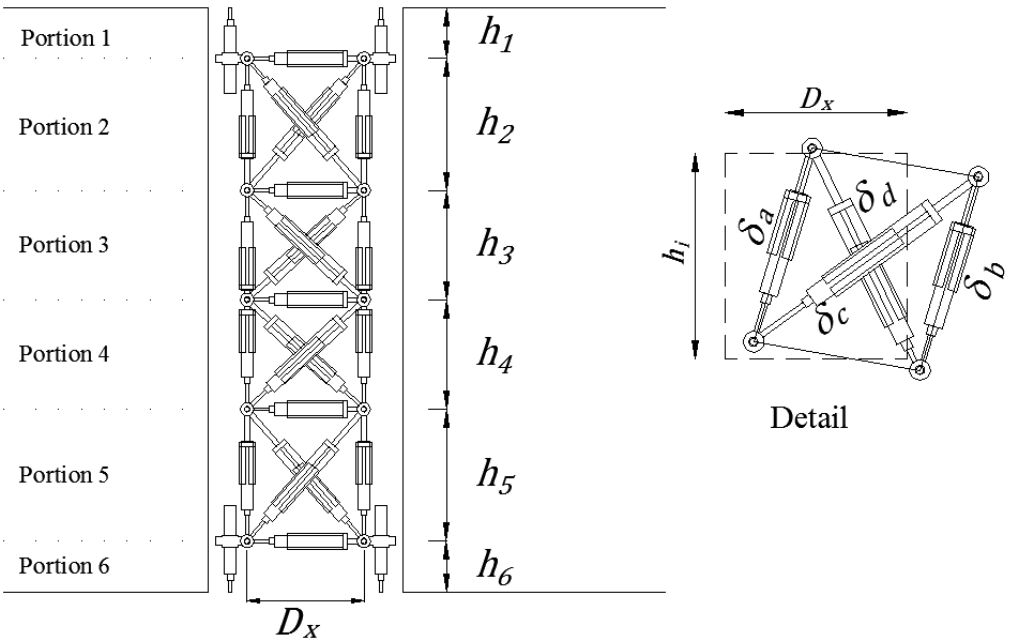

Figure 3-19 Setup of portions for the specimens

3.3.4. Shear Deformation

The relationship of the shear deformation (δ_S) and the lateral drift angle is shown in Figure 3-20. The shear deformation was calculated with the measured displacements by the transducers placed in the columns for all portions according to Eq. 3-7

$$\delta_S = \sum_{i=1}^{n}\left[\frac{\sqrt{D_x^2 + h_i^2}}{2D_x}(\delta_{ci} + \delta_{di})\right] \tag{3-7}$$

Where:

δ_{ci} and δ_{di}: the measured displacement in the portion i (mm).

D_x is the width of the portion

h_i the height of the portion.

In Figure 3-20 can be observed that, the shear deformation was approximately the same for columns 2-A, 2-B and 3 from the lateral drift angle of −3% to 1.5%. For lateral drift angle of 4%, the shear deformation of column 2−A was 7.1mm, smaller than that of column 2-B and 3 of 10.3mm and 11mm respectively. It can be said that, the reduction of the higher axial force increased the shear deformation in the column as well as in the case of increment of flexural strength in these cases.

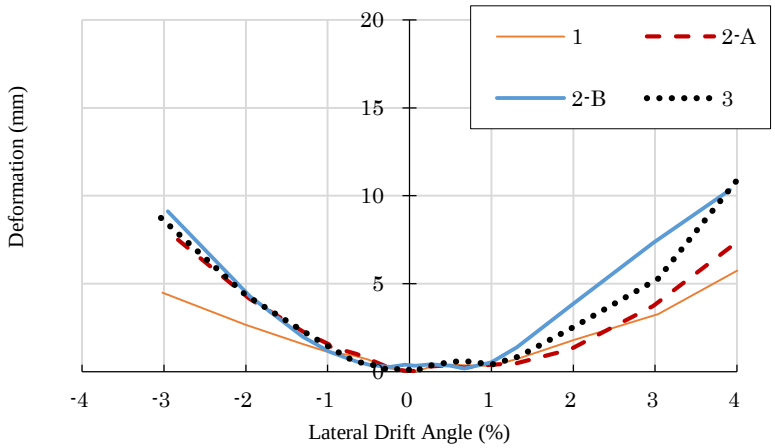

Figure 3-20 Flexural deformation-lateral drift angle relationship

3.3.5. Curvature

Figure 3-21 shows the moment-curvature relationship of the test and analytical results. This relationship was computed for the cross section at the bottom of the columns. The numerical analysis was done with fiber analysis and the curvature (φ_i) was calculated in function of the displacement recorded by vertical transducers of Figure 3-19 with the equation 3-6.

In Figure 3-21, it can be observed that column 2-B and column 3 developed more curvature than that in columns 1 and 2-A. Columns 2-B and 2-A had almost the same flexural moment, but column 3 developed 20% more than both of them. Reducing the maximum axial force ratio from 0.65 to 0.4 allow to the column to develop more curvature. In the case of increasing flexural strength, the curvature increased as well as the flexural moment at the bottom of the column.

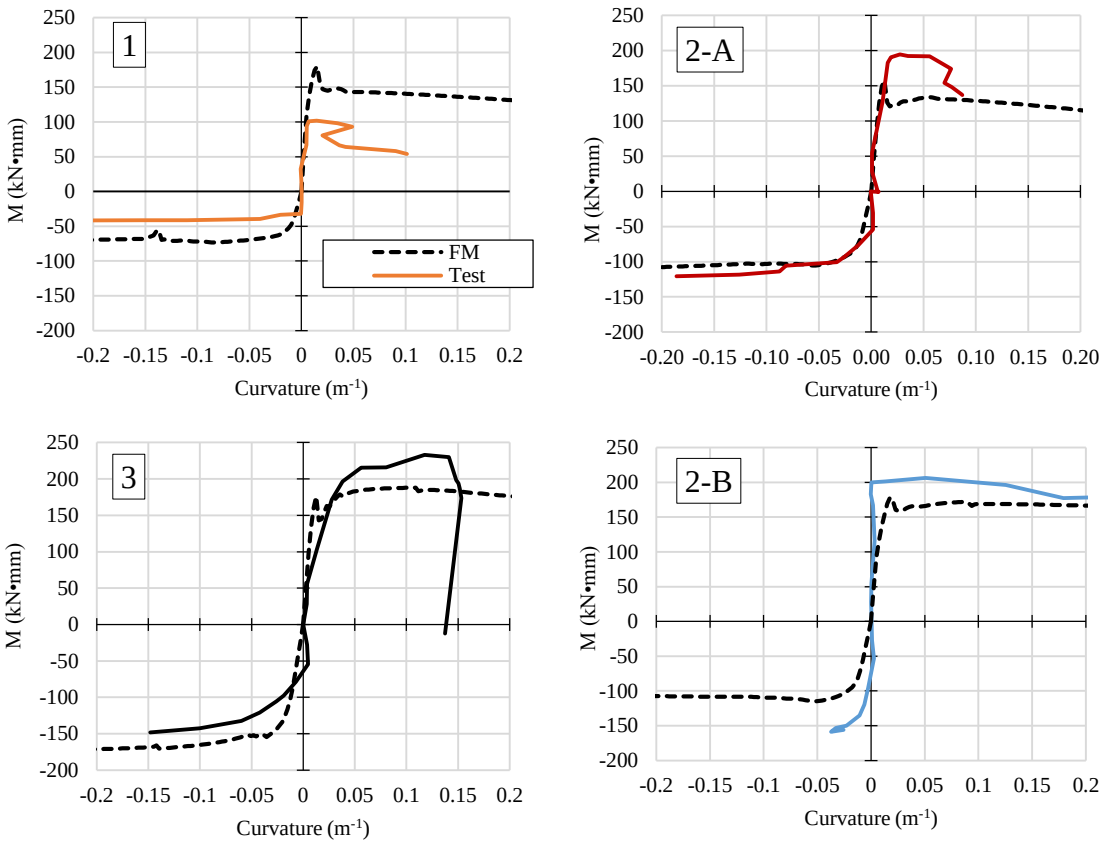

Figure 3-21 Moment-Curvature relationship

3.3.6. Energy Dissipation Capacity

Figure 3-22 shows the relationship of the energy dissipation capacity and the lateral drift angle up to +6.5%. The energy dissipation capacity (E_x) was calculated as the area under the hysteresis curve using equation 3-8.

$$E_x = \int Q\, \delta_x \tag{3-8}$$

When columns 2-A, 2-B and 3 reached lateral drift angle of +2.5%, the dissipated energy had no difference between them. At the lateral drift angle of +6.5%, the maximum difference of the energy dissipation capacity was 5%, the specimen 2-B dissipated 58.3kJ and column 2-A dissipated 55.4kJ, respectively. It can be said that, when the maximum axial force ratio was reduced from 0.65 to 0.40, no significant difference took place in the energy dissipation capacity. The same happened with the column with larger flexural strength, this is due the fact that more energy was dissipated by axial deformation in the column with higher axial force ratio (2-A).

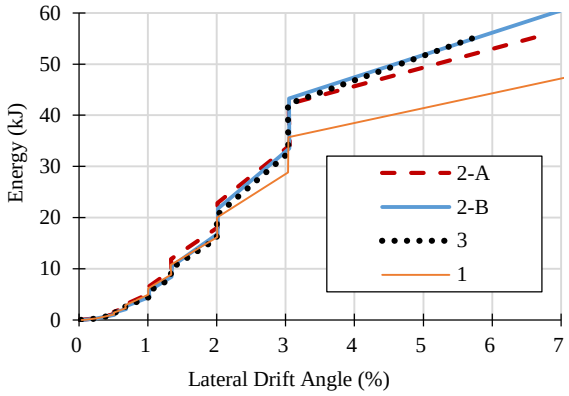

Figure 3-22 Energy Dissipation-Lateral Drift Angle Relationship

3.3.7. Deformation behavior in each portion

In order to explain the failure behavior of the specimens, four types of data related to the deformations are presented. The first data corresponds to the global axial deformation (δ_{aG}) obtained according to equation 3-9 which data were recorded by two transducers placed between the upper and lower concrete stubs of the specimens. These transducers are shown from Figure 3-9 to Figure 3-11 . The global axial deformation is presented in Figure 3-23 as a continuous line.

$$\delta_{aG} = \frac{\bar{\delta}}{h_0} \tag{3-9}$$

Where $\bar{\delta}$ is the average axial displacement recorded by the vertical transducers

On the second type, the axial deformation was obtained according to equation 3-10 from 12 vertical transducers (δ_{aP}). The position of the transducers on the column is presented on Figure 3-19.

$$\delta_{aP} = \frac{1}{h_0}\sum_{i}^{n}\frac{\delta_a + \delta_b}{2} \tag{3-10}$$

Where:

δ_a and δ_b correspond to the vertical transducers shown in the detail of Figure 3-19. These axial deformations are shown in Figure 3-23 with a dashed line.

On third type of data, the axial deformation per each portion (δap_i) is presented to equation 3-11.

$$\delta_{ap} = \frac{\delta_a + \delta_b}{2}\frac{1}{h_i} \tag{3-11}$$

Where: h_i is the height of each portion

The fourth data is the shear deformation obtained from the diagonal set of eight transducers from portion 2 to portion 5 according to the equation 3-12.

$$\delta_V = \frac{1}{4h_i D_x}(\delta_d - \delta_c)(2l_\alpha + \delta_d + \delta_c) \tag{3-12}$$

Where:

δ_d and δ_c are the diagonal transducers shown in detail on Figure 3-19.

The comparison of the global axial deformation (δ_{aG}) and the axial deformation obtained from portions (δ_{aP}) shows a similar tendency on the behavior of the axial deformation of all specimens. For that reason, it is considered that the addition of axial deformations for all portion in equation 3-10 in general represent the global behavior of the axial capacity.

In the following paragraphs, the behavior and deformation are described by the displacement peaks of the lateral load history. From now on, just the positive direction of lateral force, where the lateral drift angle is positive and the applied axial force was high compression will be discussed. The direction of the forces can be observed in Figure 3-12. Column 2-A was deeply study, for that reason more information is provided.

Specimen No. 1

For specimen No 1, the increment of the axial deformation is linear up to the lateral drift angle R_u =0.68%. After this point, it had considerably constant average value of -0.14% up to the lateral drift angle of 8.8% where the specimen presented suddenly loss of axial capacity, this can be observed in Figure 3-24.

Flexural and compressive cracks were observed during the test (Figure 3-15) at the lateral drift angle of 0.67% (1/150rad),. Rebar started yielding in compression at these same portions and started yielding in tension at the lateral drift angle of 1%. The balance between positive and negative axial deformation in each portion produce the average constant axial deformation in the specimen. The shear deformation observed in Figure 3-25 is softly reduced.

The loss of the concrete cover at the bottom of the column observed during the test at lateral drift angle of 2% is accompanied by the reduction in the axial deformation of portion 6 and the increasing of shear deformation of portion 5 as it is shown in Figure 3-24 and Figure 3-25 respectively. At this step, axial deformation of portion 6 was equal to -0.48% larger than the last compressive deformation of concrete ε = 0.24% found in the material test.

At the lateral drift angle of 8.9% (1/11rad), bending was observed in rebar during the last stage of the test, but no failure of lateral or transversal reinforcement per tension was observed at the final inspection of this specimen. Shear deformation is comparatively small with the rest of the specimens in Figure 3-25. The axial capacity decrease drastically at this lateral drift angle (Figure 3-23).

Specimen No. 2-A

At the lateral drift angle of 0.50% (1/200rad), compressive and flexural cracks appeared in the specimen (Figure 3-15) as well as the rebar yielded in compression, these

data were registered by the strain gauges A43 and D17-20 pasted in the specimen (Figure 3-7), and the axial deformation behaved linear increasing constantly as the lateral drift angle increased (Figure 3-24).

At the lateral drift angle of 0.67% (1/150rad), vertical cracks appeared in the specimen (Figure 3-15). The data recorded in gauges D17-18 (Figure 3-7) shows that the deformation started to increase in compression, the same took place in A56 gauges. The axial deformation of portion 1and 6 started to increment more than the rest given the fact that there was more deformation in compression than in tension in extremes of the portion (Figure 3-24). Hoops increased deformation too, and shear deformation increased lightly as it is shown in Figure 3-25.

At the lateral drift angle of 1.0% (1/100ad), bond cracks and vertical crack spread in the specimen (Figure 3-15). Axial deformations continued increasing (Figure 3-23). The axial deformation of portion 1and 6 started to increment more than the rest given the fact that there was more deformation in compression than in tension (Figure 3-24). Rebar continued increasing and B1-6 and also C1-6 increased its deformation. Shear deformation increased lightly (Figure 3-25).

At the lateral drift angle of 1.3% (1/75ad), vertical crack continued spreading. Axial deformations continued incrementing (Figure 3-23). Lateral deformation started to incrementing deformation faster in all portions. Axial deformation in portions 1 and 6 increased lightly, portion 2 and 5 started to increase fast, global axial deformation continued increasing (Figure 3-23). Data from B1-6 and C1-6 kept constant its strain but others bars (D15-20, A1-6) kept increasing.

At the lateral drift angle of 2.0% (1/50rad), vertical crack spread and concrete cover split (Figure 3-15). Axial deformations continued incrementing (Figure 3-23). Hoops started yielding. Lateral deformation increased for all portions but in the middle span. Absolute axial deformation continued increasing for portions 2 and 5, portions in the edges, 1 and 6, seemed constant. Strain data from rebar in points A5-6 and D15-16 showed bending, D17-20, C78, B56, kept increasing, the rest kept constant. Shear deformation increased lightly in Figure 3-25.

At the lateral drift angle of 3.0% (1/33rad), vertical cracks spread and concrete cover split. Rebar yielded in tension. Axial deformations continued incrementing. All the lateral deformations increased at the same speed. Absolute axial deformation continued

increasing for all portions but portions in the edges (Figure 3-23), 1 and 6 seemed constant. Central portions increased in tension deformation, portions 2 and 5 increased in compression deformation and edge portion 6 seemed constant, portion 1 increased lightly in compression. Strain gauges A5-6, A7-8 and D15-16 continued showing bending, D17-20, C78, B56, kept increasing, the rest kept constant. (Given the loss of lateral strength η reduced down to 0.6). Shear deformation increased faster in portion 5 (Figure 3-25).

At the lateral drift angle of 4.0% (1/25rad), cracks kept growing and showed a truss mechanism shape. Axial deformations continued incrementing (Figure 3-23). In absolutely axial deformation, portion 2, 3 and 5 kept growing deformation, the rest kept constant. Shear deformation increased faster in all portions (Figure 3-25). Lateral deformation in LD4 (transducers of Figure 3-10) increased more than the rest. Hoops kept incrementing its deformation. This tendency continued for the rest of the test, it is the case of portion 5 that axial deformation increased larger, no collapse was registered up to the final stage of the test.

However, there is a gap between the global axial deformation and the total axial deformation by portions in Figure 3-23. One possible reason could be that the distribution of shear and axial deformation in each portion. Compressive axial deformation per portion was distributed in bout edges of the column for columns No.2-A. (Portions 1, 2, 5, 6). Shear deformation was also better distributed in this column in the portions (2, 3, 4, 5 of Figure 10) in comparison with the rest of the specimens.

Specimen No. 2-B

Flexural cracks were visible at 100% of Q_{cr}, where shear force was +111kN and drift angle equal to 1/1.2rad. The axial deformation increased linear up to the lateral drift angle R_u =0.50%. After this point, it had considerably constant average value of -0.11% up to the lateral drift angle of 6.0%, after this step, the specimen presented gradually loss of axial capacity until collapse at 7.28%, this can be observed in Figure 3-24.

At the lateral drift angle of 1.3% (1/75rad), rebar yielded in compression, the acting shear force in that step was -314kN and hoops were working at 15% of its yielding capacity. The axial deformation of Figure 3-24 remained constant due to the equilibrium between the positive and negative axial deformations of the portions. The shear deformation of Figure 3-25 increased softly up to the value of 0.31%.

At the lateral drift angle of 2.0% (1/50rad), hoops started to yielding, from this point the column lateral strength started to decrease. The global axial deformation still was in average 0.11%. In Figure 3-25, the shear deformation the portion 2 started to increase its deformation larger than the rest of them.

At the lateral drift angle of 3.0% (1/33rad), rebar yielded in tension. The axial deformation of portion 6 had increased larger than the rest, and portion 2 from Figure 3-25 continued increasing its shear deformation, and in the case of shear deformation, portion 2 had increased up to the value of 1%.

At the lateral drift angle of 5.0% (1/20rad), the deformations suddenly increased its values. Axial deformation of portion 2 increased suggesting the buckling of the rebar at this step (Figure 3-24), in contrast, portion 5 reduced its axial deformation up to negative values at lateral drift angle of 7.3%. On the other hand, shear deformation of portion 5 showed a drastic increment (Figure 3-25) but portion 2 still possessed the larger strain.

At the lateral drift angle of 7.3% (1/13.7rad), axial capacity was lost (Figure 3-23). Axil deformation of portion 5 showed large values that indicates failure in the portion (Figure 3-24), this portion also showed a large shear deformation in Figure 3-25. The column failed at this lateral drift angle.

Specimen No. 3

For specimen No 3, axial deformation had linear behavior up to the lateral drift angle of 0.5%. From lateral drift angle of 0.5 to 3%, the axial deformation reduced its increasing tendency compared with the previous part.

At lateral drift angle of 0.5%, Figure 3-23 shows that the axial deformation was approximately -0.4% in portions 1 and 6, this means that concrete had passed its maximum deformation capacity of 0.21%. This was confirmed by the compressive cracks that appeared at the bottom of the specimen during the test (Figure 3-15). The softening of the concrete started and triggered the yielding in compression of the rebar located at portions 1, 5, and 6. Shear deformation increased softly in all portions (Figure 3-25).

At the lateral drift angle of 1%, concrete cover split in portions 1 and 6 (Figure 3-15). These portions mostly carried the axial deformation in compression due to the concentration of compressive stress in this portions, this can be seen in Figure 3-24. At

this lateral drift angle, potion 5 started to develop larger shear deformation compared with the rest of the portions as it is shown in Figure 3-25. In addition, the rebar in this section started to develop large compressive deformation as it can be seen in Figure 3-24. At this point, it can be said that portion 5 presented a state of crushing.

At the lateral drift angle of 3%, axial deformation increased its tendency as it is shown in Figure 3-24. Rebar in compression of portion 5 started to bending due to the concentrated deformation near to the zone where strain gauges D15 and D16 (Figure 3-8) were placed, this can be observed in the same figure.

At the lateral drift angle of 4.5%, the column suffered of suddenly loss of axial capacity, portion 6 had larger deformation compared with the rest, this is shown in Figure 3-23. In Figure 3-25 is shown that portion 5 presented large shear deformation as positive axial deformation, therefore, seemingly that the confined concrete in portion 5 loss its strength capacity.

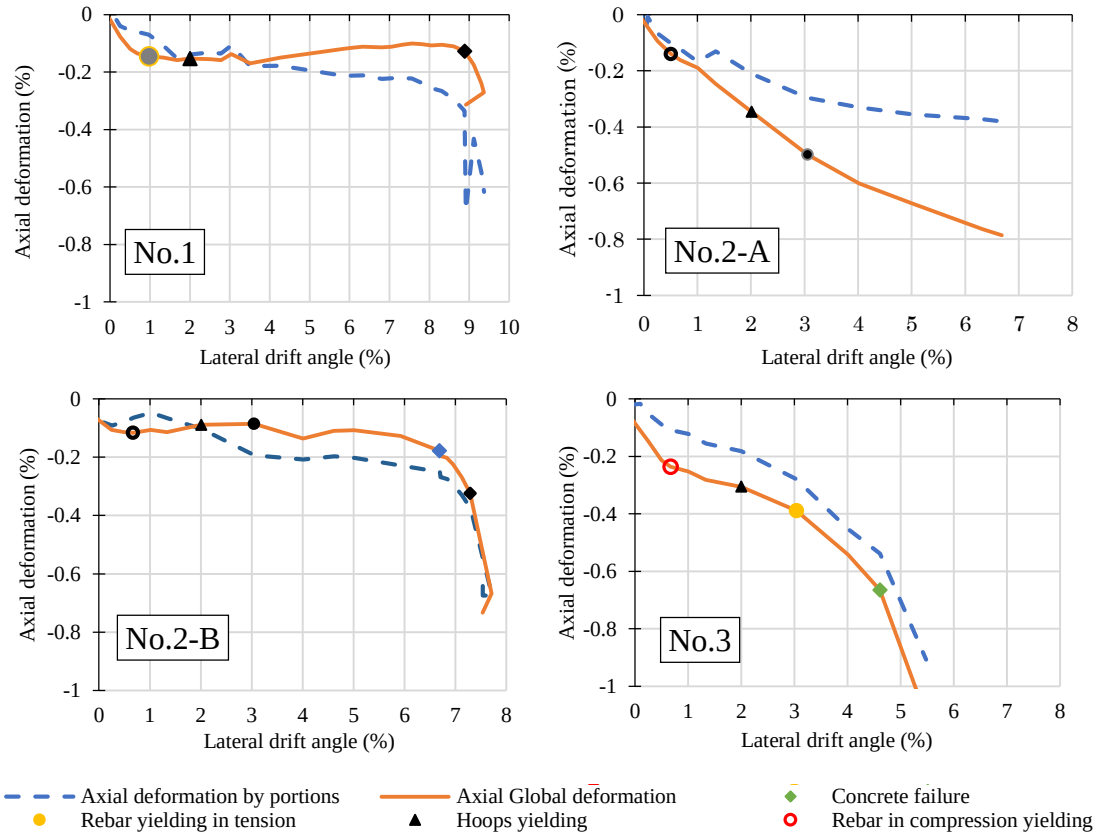

Figure 3-23 Axial deformation – lateral drift angle relationship

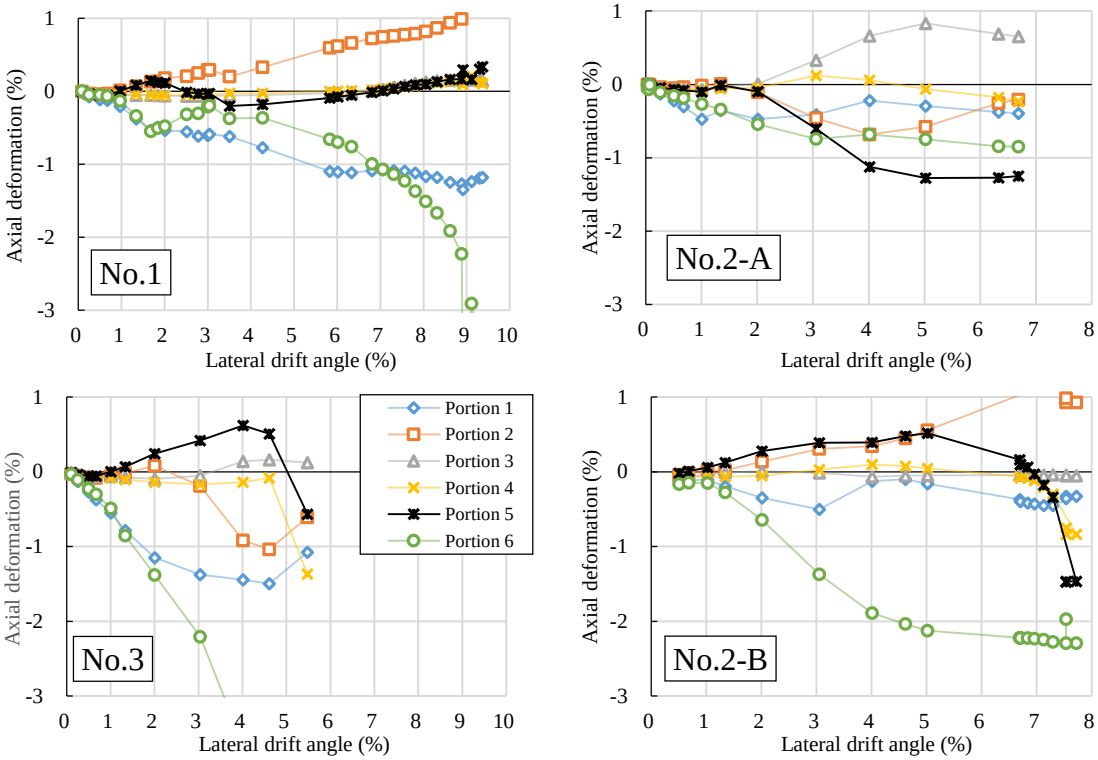

Figure 3-24 Axial deformation – lateral drift angle relationship by portions

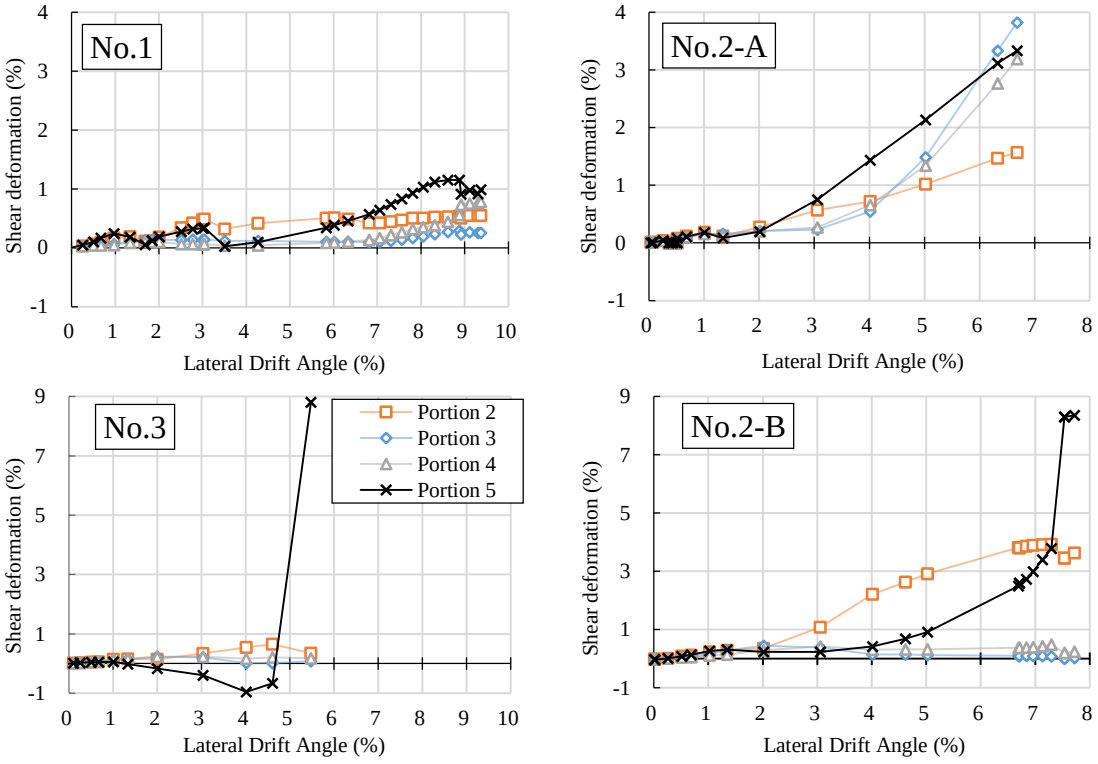

Figure 3-25 Shear deformation per portion

The axial deformation behavior of the columns described in the previous paragraphs can be summarized by figures as follows:

Figure 3-23 showed the total axial deformation derived from Eq. 3-9 and 3-10. For all the specimens, the total axial deformation was linear approximately up to the lateral drift angle of 0.6% (=1/150). Beyond this point, the different behaviors of axial deformation were shown depending on the applied axial force ratio. For specimens No.1 and No.2-B, on which a lower axial force ratio was applied, the total axial deformation remained almost constant before a sudden drop was observed at R=9% or 7% respectively. For specimens No.2-A and No.3, on which a higher axial force ratio was applied, the axial deformation became larger as the lateral drift angle increased. For specimen No.3, a sudden drop was observed when the lateral drift angle reached 4.5%, whereas the axial deformation of specimen No.2-A was not observed to drop at any time as it did on the others.

Figure 3-24 showed the axial deformation in compression of each portion. These figures indicate that, compressive deformation at the portions 5 or 6 was dominant to the failure except for specimen No.2-A due to the fact that, the total deformation shown in Figure 3-24 was smaller than the directly measured data δ_{aG}. The increasing tendency of the axial deformation was similar in each specimen. The figure corresponding to No.2-A showed that the drastic failure did not occur on any portion.

Figure 3-25 showed the shear deformation of each portion. For specimens No.1 and No.2-A, the shear deformation was smaller as compared to the other columns, it can be stated that the failure of specimen No.1 was not caused by shear behavior, and for specimen No.2-A no failure was registered during the test. For specimens No.2-B and No.3, shear deformation on portion 5, which was hinge region, increased drastically at R=7% and 5% respectively. In conjunction with the behavior shown in Figure 3-25, specimens No.2-B and No.3 failed by shear force at the hinge region at a further lateral drift angle than that of the yielding of hoop of R=2%. The ultimate deformation of specimen No.2-B was larger than that of specimen No.3, because the applied axial force of No.2-B was smaller than that of No.3.

3.4. Conclusions of Chapter 3

This chapter presented an evaluation on the failure mode and shear strength deterioration of four RC columns designed with the requirements of AJI [3-1]. The columns were designed to have flexural failure at the beginning of the test. High axial force and cyclic lateral displacement were employed to recreate the seismic effect during the test. At the end of the study, the following conclusions were achieved.

Specimen No.1 suffered of axial collapse, given the fact that shear deformation was not dominant as shown in Figure 3-25.

Specimen No.2-A did not collapse up to the lateral drift angle of 6.7% when the test was finished. However, shear deformation on all portions and axial deformation of member edge (or hinge region) continued increasing as it is shown in Figure 3-24 and Figure 3-25 respectively. At the hinge region, especially portion 5, deformation seemed to be concentrated (from Figure 3-24 and Figure 3-25). It is implied that, if lateral loading continues further, portion 5 may be failed by shear manner at the last stage.

No.2-B and No.3 presented shear failure with axial collapse. The difference on the axial deformation between these columns was due to the applied axial force ratio. The axial deformation reduced in the same way that the axial force reduced. In addition, because of the same reason, deformation capacity of No.3 was smaller than that of No.2-B.

All specimens presented a large deformation capacity. The selected specimens developed desirable deformation capacity, with lateral drift angle larger than 2.5%. However, the specimens loaded with lower axial force ratio, No.1 and No.2-B, collapsed drastically. For the specimens loaded with high axial force ratio, No.3 collapsed drastically and the other, No.2-A, did not collapse but large axial deformation was observed. These characteristics cannot be said to be safe enough.

Bibliography of Chapter 3

[3-1] Architectural Institute of Japan: Calculation standard for horizontal load-carrying of reinforced concrete structure and comments (For public comments), 2014.12.
http://www.aij.or.jp/jpn/symposium/2014/public_20141215.html.

[3-2] D.P. Abrams: Influence of axial force variations on flexural behavior of reinforced concrete columns, ACI Structural Journal, Title no. 84-S26, pp.246-254, 1987.5-7.

[3-3] Ministry of Land, Infrastructure, Transport, and Tourism: Technical standard manual concerned to the structure of buildings (2007), 2007.8.

[3-4] Architectural Institute of Japan: Design guidelines for earthquake resistant reinforced concrete building based on inelastic displacement concept, 1999.

[3-5] Tasai and A. Watanabe: Residual axial capacity of reinforced concrete columns during shear deterioration, Japan concrete Institute annual meeting, 2000.

[3-6] D.C. Kent and R. Park: Flexural member with confined concrete, journal of the structural division, ASCE, Vol. 97 ST7, pp. 1969-1990, 1979.7.

[3-7] H. Ousalem, T. Kabeyasawa, A. Tasai, Y. Ohsugi: Experimental study on seismic behavior of reinforced concrete columns under constant and variable axial loading, Japan Concrete Institute, Vol. 24, No. 2, pp.229-234, 2002.

[3-8] T. Okanishi, K. Katori, S. Hayashi, S. Kokusho: Deformability of reinforced concrete column subjected to high axial force, Journal of Structural and Construction Engineering, AIJ, No. 461, pp.65-74, 1994.7.

[3-9] Y. Ishikawa, H. Kimura: Study on displacement at maximum strength of high strength r/c columns under high axial compression, Structural Engineering Papers, AIJ, No. 51B, pp.441-447, 2005.3.

CHAPTER 4. DATABASE OF DUCTILITY BEHAVIOR OF RC COLUMNS

4.1. Introduction

Much research has been carried out to find out about the lateral deformation capacity of RC structural members subjected to axial force. Experimental data, issued by many researchers, have been collected in order to have a reliable database. This database (Called here Tasai-Lab Database) contains documents published by the Architectural Institute of Japan (AIJ) and the Japan Concrete Institute (JCI) since 1979 to 2011. It includes two kinds of structural members, RC columns, and beams. Besides other parameters, the geometrical characteristics, material properties, and resistant strength of the members have been inputted in the database but between all this information, the ultimate drift angle was collected in few cases.

The ultimate lateral drift angle is the most accepted parameter to evaluate the ductile behavior of earthquake resistance reinforced concrete columns, the lack of this information represents an obstacle to determine if the structural design of the tested columns in the TasaiLab database is adequate.

It is matter of major importance to recognize which structural designs from the experimental data succeed developing the minimum expected values. The data achieved in this chapter is essential for the analysis carried out in the next chapter.

In order to determinate the ultimate lateral drift angle and others behavior characteristic of the lateral load response of the members achieved in the TasaiLab database, the skeleton curve of the hysteresis relationship of the shear force and the lateral drift angle available from the bibliography was collected in a digital file. This will be called from now on Ductility Behavior of RC Columns Database or simply Behavior Database.

Synthetizing, Tasai-Lab database contains all the characteristics of the RC columns and the Behavior Database contains only the curve of the ductile behavior of the columns. In this chapter, the process to get the digital version of the skeleton curve of the shear force – lateral drift angle relationship will be explain, subsequently, the ductility of the RC columns will be evaluated by some ductility performance criteria found in the

literature. At the end of this chapter, the characteristics of the RC columns that develop large ductility will be listed.

Additionally, a study over the strength of the materials was carried out. The purpose of this additional study is to provide coefficient factors to estimate the actual strength of reinforcement steel and to show statistics about the employed materials in the tests.

4.2. Process of data compilation

The database RC Columns Database (Tasai-Lab) contains 1859 test results for RC columns failing in both, shear and flexural mode, the strength of materials are wide varied as well as others characteristic. From that database, the entire experimental tests that employ high axial force were chosen to be accomplished with the digital version of the shear force – lateral drift angle (in the Behavior Database of this Chapter). The selected columns are listed at the Appendix 1 (from Ref. [4.1] to Ref. [4.89]), the selection contains 376 experimental test and the graphics are plotted in Appendix 2.

At the beginning of the data compilation of the Behavior Database, the collection of information was randomly, for that motive the characteristics of the RC columns present variation between shear and flexural failure, materials with high strength and normal strength, different lengths of shear span, different quantity of reinforcement, and different quantity of applied axial force. It means that, the CR columns in the Behavior Database also contains wide variation of characteristics but, it is important to remake that all the experimental test that employ high axial force were achieved as mention before.

In order to collect the shear force – lateral drift angle (or rotation angle) relationship, some of the journal papers were downloaded from the web page CiNii [4.90], where the experimental data is divulgated. Next, the lateral force – lateral drift angle figure was capture in screen as *.JPG imagen from the original journal papers, this imagen was pasted in AutoCAD where it was scaled to fix in the horizontal axis with lateral drift angle in radians and in vertical axis to match in units of kiloNewtons (kN). Point by point, the hysteretic curve or skeleton curve of the shear force –lateral drift angle was drawn by the "*spline fit*" function under the layer called "*plot*" after this, the coordinates of each point that form the drawn curve was exported to a excel worksheet to be plot. Figure **4-1** shows an example of the worksheets employed compilation process of the experimental test 49 from the list of Appendix 1.

The analysis to evaluate the ductility were done in the excel worksheet. In order to make easier to read the units of the horizontal axis, the units of the lateral drift angle was changed from radians to percentage (%) in this worksheet.

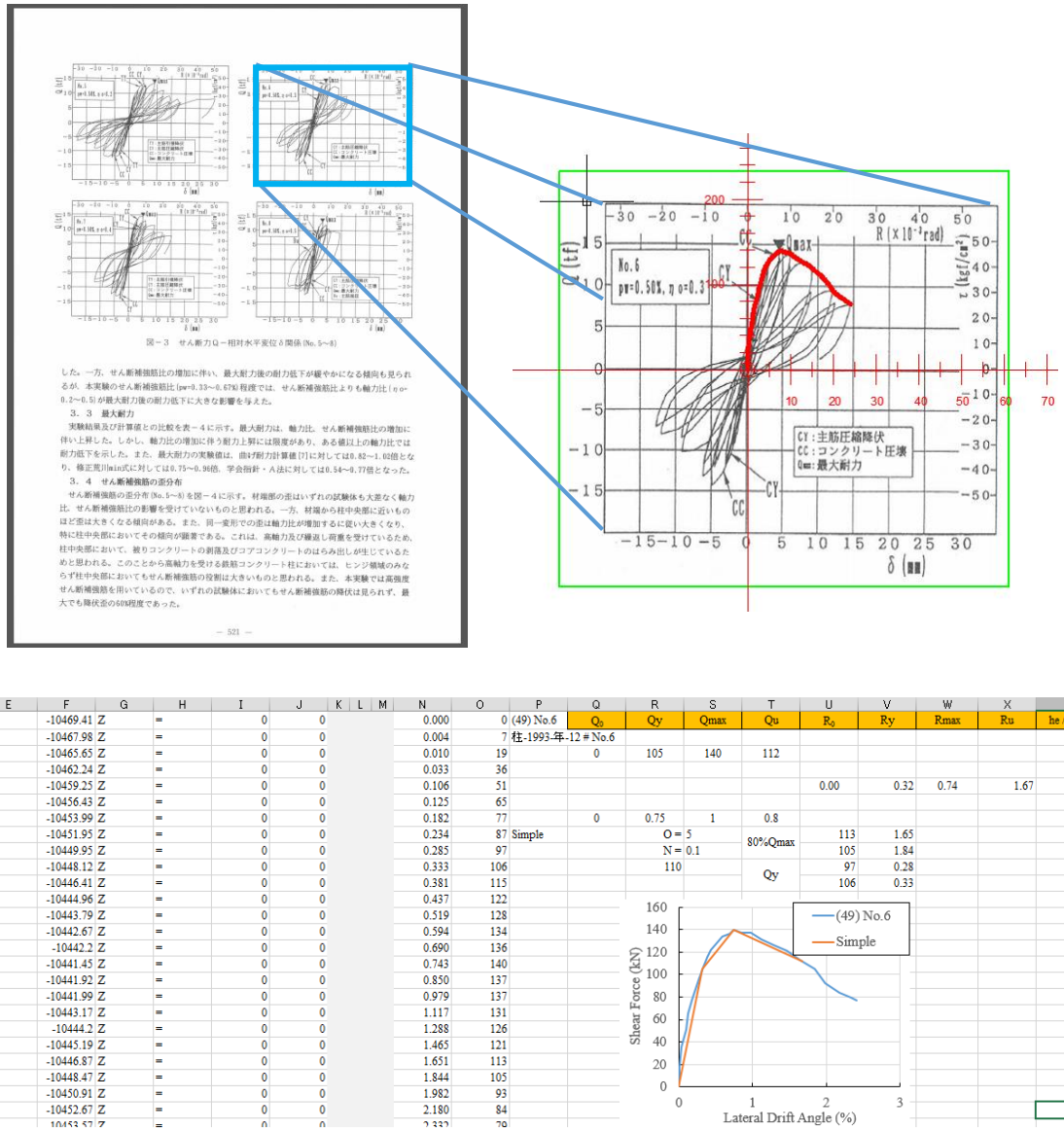

E	F	G	H	I	J	K	L	M	N	O	P	Q	R	S	T	U	V	W	X	Y
=	-10469.41	Z	=	0	0				0.000	0	(49) No.6	Q_0	Qy	Qmax	Qu	R_0	Ry	Rmax	Ru	he / Qmax
=	-10467.98	Z	=	0	0				0.004	7	柱-1993-年-12＃No.6									
=	-10465.65	Z	=	0	0				0.010	19		0	105	140	112					
=	-10462.24	Z	=	0	0				0.033	36										
=	-10459.25	Z	=	0	0				0.106	51						0.00	0.32	0.74	1.67	1.6
=	-10456.43	Z	=	0	0				0.125	65										
=	-10453.99	Z	=	0	0				0.182	77		0	0.75	1	0.8					
=	-10451.95	Z	=	0	0				0.234	87	Simple		O = 5		80%Qmax	113	1.65			
=	-10449.95	Z	=	0	0				0.285	97			N = 0.1			105	1.84			
=	-10448.12	Z	=	0	0				0.333	106			110		Qy	97	0.28			
=	-10446.41	Z	=	0	0				0.381	115						106	0.33			
=	-10444.96	Z	=	0	0				0.437	122										
=	-10443.79	Z	=	0	0				0.519	128										
=	-10442.67	Z	=	0	0				0.594	134										
=	-10442.2	Z	=	0	0				0.690	136										
=	-10441.45	Z	=	0	0				0.743	140										
=	-10441.92	Z	=	0	0				0.850	137										
=	-10441.99	Z	=	0	0				0.979	137										
=	-10443.17	Z	=	0	0				1.117	131										
=	-10444.2	Z	=	0	0				1.288	126										
=	-10445.19	Z	=	0	0				1.465	121										
=	-10446.87	Z	=	0	0				1.651	113										
=	-10448.47	Z	=	0	0				1.844	105										
=	-10450.91	Z	=	0	0				1.982	93										
=	-10452.67	Z	=	0	0				2.180	84										
=	-10453.57	Z	=	0	0				2.332	79										

Figure 4-1 Collection of data

4.2.1. Characteristics of the columns

Most of the cross sections of the columns in the Behavior Database are square sections, this can be observed in the Figure 4-2a) where 96% of the specimens had relationship of width (b) to depth (D) of the cross-section equal to 1.0. There is just 2% of specimens that have b/D relationship equal to 0.25 and 2% for b/D= 1.75.

For the arrangement of the main bars in the cross section, the relationship of the effective depth of the cross section *(d)* to the nominal height (*D*) equal to 0.80 is the dominant with 42% of the total. The ratio of *d/D* for the whole data varies from 0.76 to 0.90, this can be observed in the Figure 4-2b) where no values are for $d/D < 0.7$ and $d/D > 0.96$. The importance of this value will be reflected in the determination of the flexural moment of equation 2-3, given the fact that this value is mostly constant to 0.80 the influence of the arrangement of main bars could be neglected in this study.

In Figure 4-2c) can be seen that, the value of the shear span ratio (h_0/D) of the specimens in the Behavior Database 3.0 accumulated the 56% of the total, followed by h_0/D=2.0 with 13%. In the rest, the frequency is spread in other values where just 1% is lower than 2.0 and 14% is larger than 3.0%. It can be consider that, the shear span ratio is dominantly 3.0 but also, there are columns under this value which can be considered as short columns.

The dominant axial force ratio is shared by η between 0.20 and 0.30 with the 53% of the total of the specimens. Only 28% of the total the columns that were tested with axial for ratio larger than 0.30. The average frequency of the axial force ratio from 0.4 to 0.7 is approximately constant to 5%. The rest 18% is spread in other values of η. This can be observed in the Figure 4-2d). It can be said that more experimental work should be done in columns where high axial force is applied due to the reduced number of test results.

The employed axial reinforcement ratio (p_g) in the experimental tests of RC columns is between 2 and 4%, this can be observed in the Figure 4-2e) where this range of values accumulated the 91% of the total data. This also indicates that probably the result of the proposal in this work may be limited for columns with p_g values into the limit of this range.

For the range of lateral reinforcement (p_w), the frequency in the specimens is uniformly spread for values from 0.1% to 1.2%, this can be observed in the Figure 4-2f). This condition is ideal for the research given the case that this parameter will be evaluated in the next chapters.

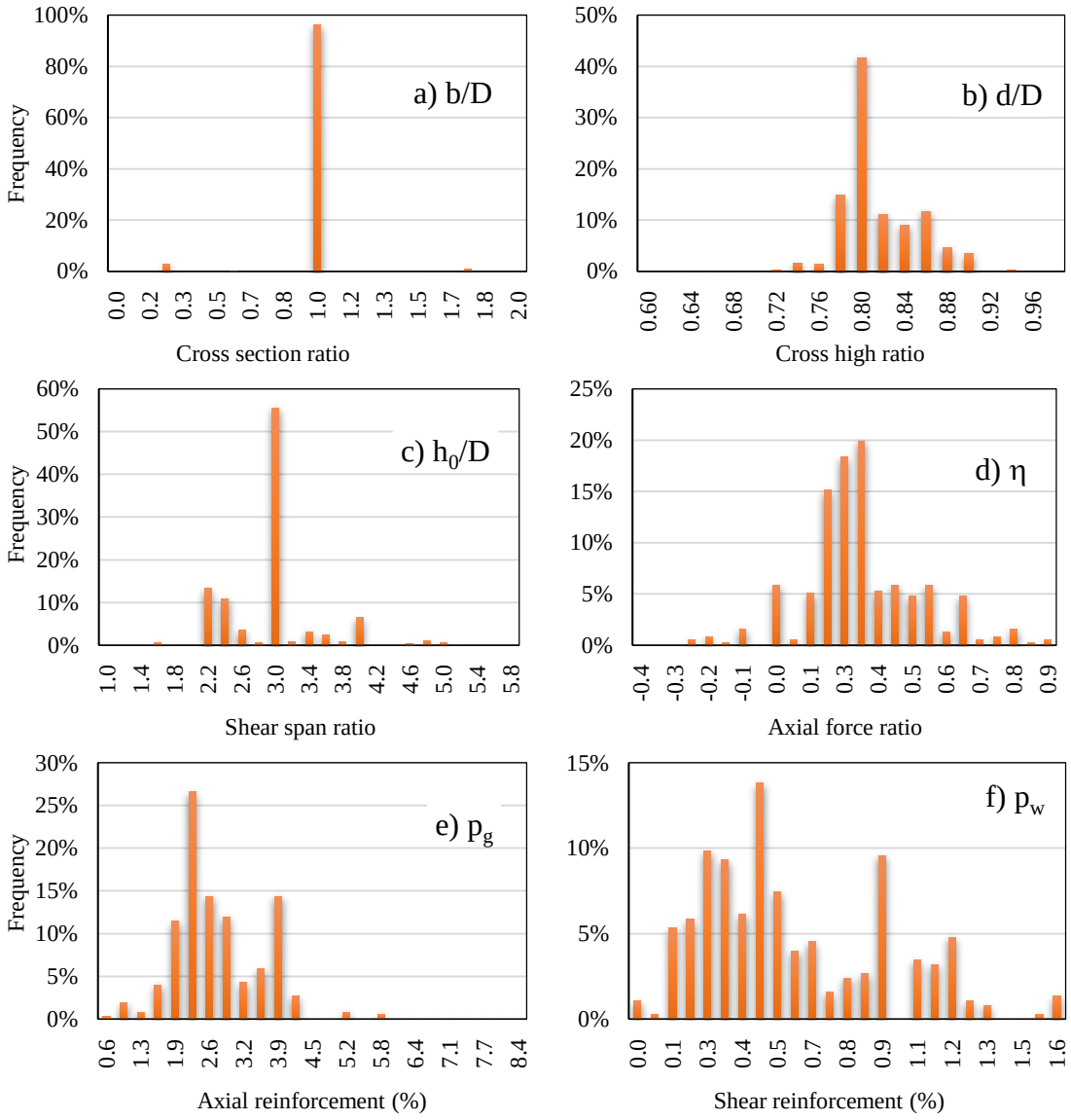

Figure 4-2 Characteristics of the columns of the behavior database

It can be concluded from the previous paragraphs that the characteristics of the specimens in the behavior database are the next:

The cross section of the specimens are dominantly squared sections, it means that the length of the base of the section is equal to the height in the cross section. The relationship of the effective height to the height in the cross section is in average 0.8. The shear span ratio is mostly equal to 3.0, the axial reinforcement ratio is limited to the range of 2% to 4%, and the frequency of the lateral reinforcement ratio p_w is conveniently well spread.

4.2.2. Materials

In the Figure 4-3, the actual strength of materials frequencies of the Behavior Database are shown. In Figure 4-3a) can be seen that the most employed concrete strength in the experimental tests was 30MPa with a frequency of 19%, the compressive strength of 20, 40, 45, 60 and 77MPa have an average employed frequency of 5%. For compressive strength from 85 to 120MPa the average employed frequency was 0.7%.

It can be concluded that the results of this research will be influenced by the strength of the concrete, which is dominantly 30MPa, and more important is that a proposal for high strength of concrete cannot be set.

Figure 4-3b) shows the frequency on which specific strength of the main reinforcement was employed. It can be seen that dominant values are between 344 and 462MPa, which accumulated 71% from the total data and an average frequency equal to 14%. The second dominant value was between 700 and 760MPa, this range accumulated the 13% of the total data and an average of 4%.

That means that the results of this research may be employed for columns on which the strength of the main reinforcement should be lower than 500MPa approximately. It will be shown in the following chapters that the employed analysis to get the flexural moment also limited the strength of the main reinforcement.

For the strength of the lateral reinforcement steel, Figure 4-3b) shows three well defined groups. The first group corresponds to the average strength of 400MPa, which accumulated frequency is 57%. This group has great advantage over the rest of the groups, it seems logical that the results of the research will be also affected by this information. The proposal of this research work may be applied preferably to strength of lateral reinforcement lower than 500MPa.

The second group corresponds to the average strength of 900MPa with 23% of the employed frequency in the experimental tests. With this group, it will be attempted to make a proposal for design RC columns with high axial force using this second group.

The third group is located around the strength of 1400MPa with frequency equal to 12% from the total. It is clear that, it could not be possible to use these data for the final proposal of this study and more research is needed for the design of columns with high axial force that employ really high strength in lateral reinforcement.

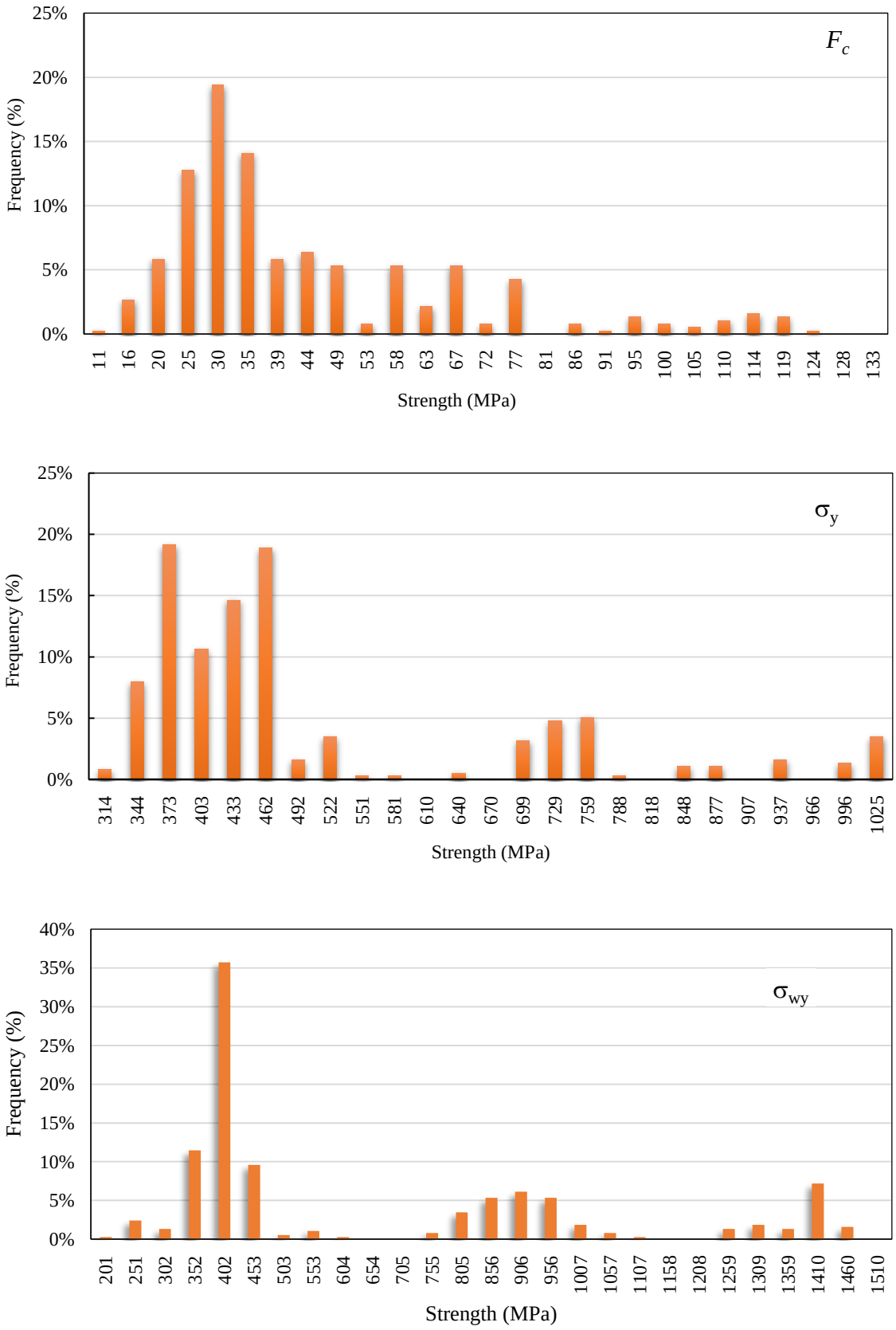

Figure 4-3 Materials strength in database

In this section, it is concluded that the useful range of effective strength of materials for the proposal may be the next:

- Compressive strength of concrete may be in the range of 20 to 50MPa.
- Strength yielding of main reinforcement may be in the range of 340 to 500MPa.
- Strength yielding of lateral reinforcement may be in the range of 350 to 460MPa.

This information is provisional, the final values will depend on the results of the following analysis. The final range will be presented in Chapter 6.

4.2.3. Factors to estimate the actual strength of reinforcement bars

During the planning of the experiments, it was important to estimate the actual strength of materials for a well-controlled test, especially when the cost of specimens is high and the unexpected variation of strength of materials can affect the conditions of the of the tests.

Considering the above, this section research about the factor needed to estimate the actual strength of the reinforcement bars. This factor is applied to the nominal strength of the bars. The employed data was obtained not only from the RC columns Tasai-Lab database *Fc* but also from that achieved form the RC beams database [4.91].

This section is complementary for the research. These factors were obtained as the average of the actual values of the strength of the main and lateral reinforcement according to the modulus of elasticity. The data was classified according to the nominal value published in the bibliography but given the fact that no all authors published the nominal and actual value of strength and modulus of elasticity of the reinforcement, this data was drastically reduced to 915 useful samples.

From Table 4-1 to Table 4-5, the useful data for the reinforcement bars are presented, in the respective order for deformed bars of SD295, SD345, SD390, SD490, and SD685(MPa). Each table presents in the upper part the actual strength according to the modulus of elasticity (MPa), in the vertical column the data is classify by the nominal diameter (mm). In the last column, the average value per diameter is shown, for this value, the influence of the modulus of elasticity is not considered. In the last row, the average

value in function of the modulus of elasticity is shown. In the lower part of the Tables, the factor is presented as the ratio of the actual strength divided by the nominal strength. This value was larger than 1.0 in most of the cases.

The average value per modulus of elasticity is more reliable than that by diameter but given the fact that the modulus of elasticity was also uncertain during the planning of experiments, the employed value for estimating the actual strength of the reinforcement steel was that in the rightmost column.

In the tables, it can be observed the lack of information for different diameters and modulus of elasticity, it is essential that the nominal, actual and modulus of elasticity should issued in every publication.

Figure 4-4 shows the frequency in percentage of the modulus of elasticity (*E*) employed data in this section. In this figure, it is worthy to note that the mean of the modulus of elasticity is 191MPa and the media is 192MPa, the standard deviation is 28MPa. This means that there is a large probability that the modulus of elasticity of the reinforced bars will be around 190MPa.

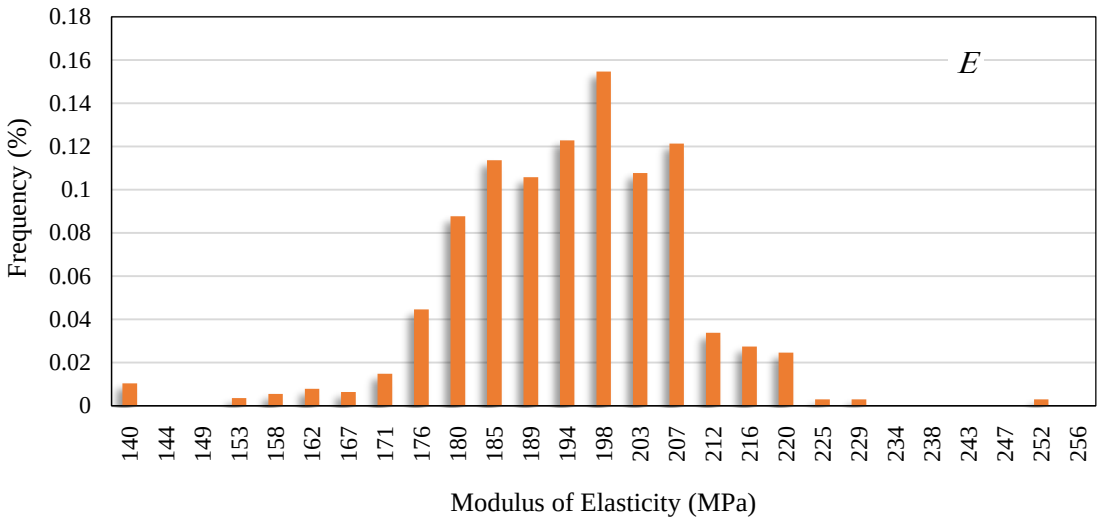

Figure 4-4 Elasticity modulus of the reinforcement steel study

Table 4-1 SD295

Strength (MPa)											
Diam.	Elasticity Modulus (MPa)										
mm	160	170	175	180	185	190	195	200	205	210	Avg.
D4											
D5			370								370
D6				380				440			410
D8											
D10	340	340		380		350	365				355
D13	325		360	360	330		345				344
D16	350				330						340
D19									340		340
D22						388					
D25						345		400			373
Avg.					330	361	355	420			360

Factor											
Diam.	Elasticity Modulus (MPa)										
D	160	170	175	180	185	190	195	200	205	210	Avg.
D4											
D5											
D6				1.29				1.49			1.39
D8											
D10	1.15	1.15		1.29		1.19	1.24				1.20
D13	1.10		1.22	1.22	1.12		1.17				1.17
D16	1.19										1.19
D19									1.15		1.15
D22						1.32					
D25						1.17		1.36			1.26
Avg.	1.15	1.15	1.22	1.27	1.12	1.22	1.20	1.42	1.15		1.22

Table 4-2 SD345

Strength (MPa)											
Diam.	Elasticity Modulus (MPa)										
D	160	170	175	180	185	190	195	200	210	220	Avg.
D4		365									365
D5											
D6		360	395		370		341	410		375	375
D8											
D10				390			422	405			406
D13			365	373	370						369
D16	400		360	380		405		370			383
D19		380				400					390
D22			405					395	370		390
D25							385				385
D29											
D32	368					380	380				376
Avg.	384	368	381	381	370	395	382	395	370	375	382

Factor											
Diam.	Elasticity Modulus (MPa)										
D	160	170	175	180	185	190	195	200	210	220	Avg.
D4		1.06									1.06
D5											
D6		1.04	1.14		1.07			1.19		1.09	1.11
D8											
D10				1.13			1.22	1.17			1.18
D13			1.06	1.08	1.07						1.07
D16	1.16		1.04	1.1		1.17		1.07			1.11
D19		1.1				1.16					1.13
D22			1.17					1.14	1.07		1.13
D25							1.12				1.12
D29											
D32	1.07					1.1	1.1				1.09
Avg.	1.11	1.07	1.11	1.1	1.07	1.14	1.15	1.14	1.07	1.09	1.12

Table 4-3 SD390

Strength (MPa)											
Diam.	Elasticity Modulus (MPa)										
D	160	170	175	180	185	190	195	200	210	220	Avg.
D4											
D5											
D6								420			420
D8											
D10											
D13					435				535		485
D16					415		440		470		442
D19						460	490				475
D22						465		460			463
D25											
Avg.					425	462	465	440	503		459

Factor											
Diam.	Elasticity Modulus (MPa)										
D	160	170	175	180	185	190	195	200	210	220	Avg.
D4											
D5											
D6								1.08			1.08
D8											
D10											
D13					1.12				1.37		1.24
D16					1.06		1.13		1.21		1.13
D19						1.18	1.26				1.22
D22						1.19		1.18			1.19
D25											
Avg.					1.09	1.19	1.19	1.13	1.29		1.18

Table 4-4 SD490

Strength (MPa)											
Diam.	Elasticity Modulus (MPa)										
D	160	170	175	180	185	190	195	200	210	215	Avg.
D4											
D5											
D6											
D8											
D10											
D13					480	570	550				533
D16			615		540		565				573
D19					545	530	525	545		615	552
D22							525				525
D25											
D29											
D32											
Avg.			615		522	550	541	545		615	550

Factor											
Diam.	Elasticity Modulus (MPa)										
D	160	170	175	180	185	190	195	200	210	220	Avg.
D4											
D5											
D6											
D8											
D10											
D13					0.98	1.16	1.12				1.09
D16			1.26		1.10		1.15				1.17
D19					1.11	1.08	1.07	1.11		1.26	1.13
D22							1.07				1.07
D25											
D29											
D32											
Avg.			1.26		1.06	1.12	1.10	1.11		1.26	1.12

Table 4-5 SD685

Strength (MPa)											
Diam.	Elasticity Modulus (MPa)										
D	170	175	180	185	190	195	200	205	210	220	Avg.
D4											
D5											
D6					740						740
D8											
D10										885	885
D13					717	725		795			746
D16				713	730	747	723	687			720
D19					785	710	750	722			742
D22											
D25							690				690
D29							693				693
D32											
Avg.				713	743	727	714	735		885	738

Factor											
Diam.	Elasticity Modulus (MPa)										
D	160	170	175	180	185	190	195	200	210	220	Avg.
D4											
D5											
D6					1.08						1.08
D8											
D10										1.29	1.29
D13					1.05	1.06		1.16			1.09
D16				1.04	1.07	1.09	1.06	1.00			1.05
D19					1.15	1.04	1.09	1.05			1.08
D22											
D25							1.01				1.01
D29							1.01				1.01
D32											
Avg.				1.04	1.08	1.06	1.04	1.07		1.29	1.08

Figure 4-5 presents the summary of the factor useful to estimate the actual strength of reinforcement steel.

In the material denominated SD295 had the most unstable strength, the largest value of the factor to obtain the actual strength is for diameter 6mm (1.39) compared with the rest of the factors. For the rest of the diameters, the factor is in average 1.19.

In this figure, it can be observed that the denominated SD345 material had the most complete information per diameter, the average factor to obtain the actual strength is 1.1, it is just for the case of the smallest diameter (4mm) that this value can overestimate the actual strength, for this case, it is recommendable to use the factor of 1.06.

The denominated reinforcement SD390 presents similar behavior than in the previous case, for the small diameter (6mm) this factor is low and equal to 1.08, but for the rest of the case the factor to estimate the actual strength of materials is 1.19.

The factor to obtain the actual strength for the case of SD490 is in average 1.11 for diameter between 13mm and 22mm; for other diameter no information is available so far.

It is the case of SD685, which presents the most unfavorable case, for diameters larger than 13mm the factor is lower than 1.1 what results in a dangerous condition from the point of view of the structural design, for the rest of the cases the actual strength is over the nominal strength.

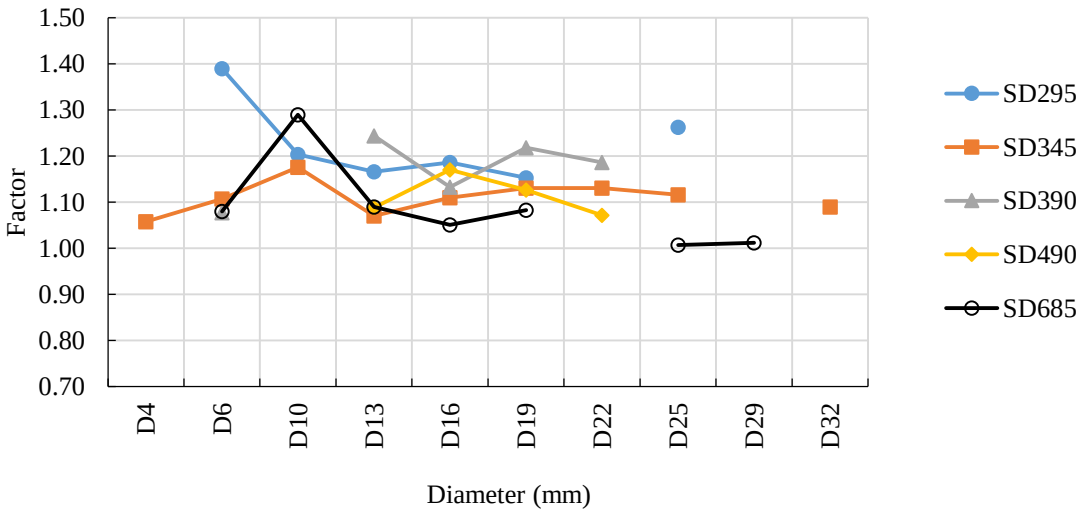

Figure 4-5 Factor to estimate actual strength in the steel reinforcement

Summarizing, the factor to estimate the actual strength of the reinforcement steel can be obtained by Table 4-6 where, the factor is classified by nominal strength and nominal diameter.

These factors are exclusively for research purpose and do not to be used in the structural design. Additionally, its functionality should be confirmed by the user, this information is purely statistically and strongly depends of the source data. It is recommended to increase this information in order to get more accuracy.

Table 4-6 Factor to estimate the actual strength

	SD295	SD345	SD390	SD490	SD685
D4		1.06			
D6	1.39	1.11	1.08		1.08
D10	1.20	1.18			1.29
D13	1.17	1.07	1.24	1.09	1.09
D16	1.19	1.11	1.13	1.17	1.05
D19	1.15	1.13	1.22	1.13	1.08
D22		1.13	1.19	1.07	
D25	1.26	1.12			1.01
D29					1.01
D32		1.09			

4.3. Evaluation of the ductility

The curves that show the relationship between the shear force and the lateral drift angle of the Behavior Database were simplified as trilinear models. The main points for the shear force are: the maximum strength (Q_{max}), the yielding shear force (Q_y), and the ultimate shear force (Q_μ). R_y, R_{max} and R_u are the lateral drift angles corresponding to these main points of Q_y, Q_{max} and Q_μ respectively. The yielding shear force (Q_y) was defined as the corresponding preliminary force equal to 75% of Q_{max} (based in a work of Ref. [4.92]), and the ultimate shear force (Q_μ) was defined as the corresponding closing force equal to 80% of Q_{max} [4.93].

As an example, Figure 4-6 shows the outline of the simplified as trilinear model of the skeleton curve of the Q-R_u relationship for column number 65 from Appendix 1.

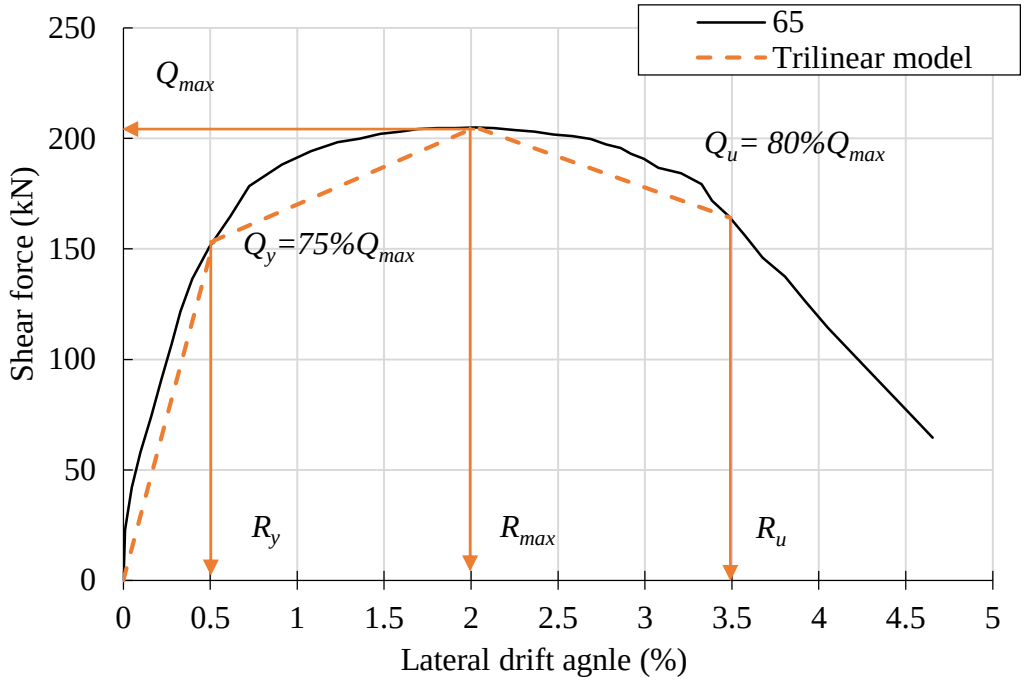

Figure 4-6 Simplified trilinear model

Ductility performance

On this research, the ductility performance of the columns was evaluated with three criteria; these are, the deflection ductility index (μ_y), the degradation index (μ_d) and the ultimate drift angle (R_u).

The deflection ductility index, described by Woods and others [4.94], reflects the relationship between the yielding strength and the ultimate strength in the columns:

$$\mu_y = \frac{R_u}{R_y} \tag{4-1}$$

The degradation index is the coefficient of the ultimate lateral drift angle and the lateral drift angle corresponding to the maximum shear force (Equation **4-2**.). Woods and others [4.94] found that brittle failure occurs when the degradation index tends to 1.0 due to the lack of confinement in the column.

$$\mu_d = \frac{R_u}{R_{max}} \tag{4-2}$$

For the ultimate drift angle, the ductility performance of the column is considered satisfactory when R_u is larger than 2.5% [4.95].

Results

The values of R_u, μ_y and μ_d calculated for the columns are presented from the Figure 4-7 until Figure 4-9. The data are presented in function of the calculated value of SRI of equation **2-1** and the value of Q_{su}/Q_{mu}.

In Figure 4-7, the data are presented according to the developed R_u in three ranges, larger than 2.5%, lower than 2.0% and between both values (from 2.0 to 2.5%), and by the failure mode, flexural or shear. In this figure, it can be seen that there is not a clearly division between columns that develop R_u lower than 2.5% but of the columns placed in SRI larger than 1.5 and Q_{su}/Q_{mu} larger than 0.8 developed the desirable R_u. Then, it can be said that SRI larger than 1.0 and Q_{su}/Q_{mu} larger than 1.0 do not represent a clear division for classify RC columns as ductile performances.

The deflection ductility index shown in Figure 4-8 is divided in three categories, lower than 5.0, from 5.0 up to 11.0% and larger than 11.0%. This figure shows that there are columns that develop μ_y lower than 5.0 even the fact that the calculate values of SRI and Q_{su}/Q_{mu} larger than 1.0 and 1.1 respectively. The intermediate values of μ_y from 4.0 up to 11.0% are uniformly spread all over the figure. It can be said that any division cannot be fixed to define which columns can develop large deflection ductility index.

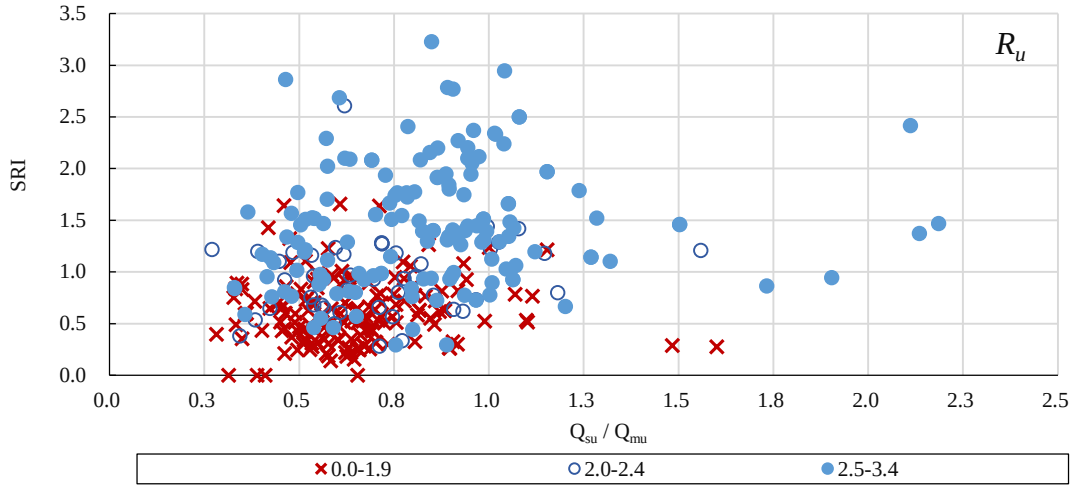

Figure 4-7　Ultimate drift angle R_u

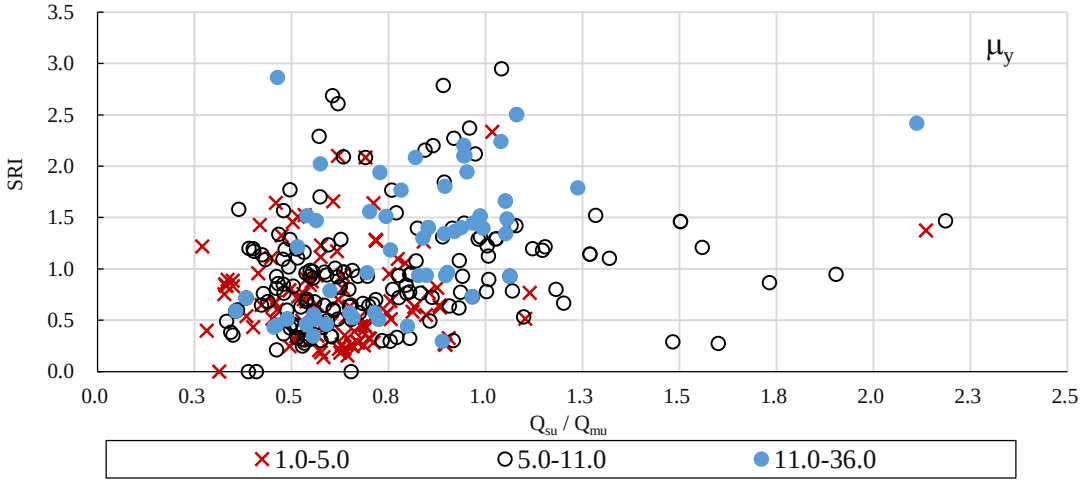

Figure 4-8　Deflection ductility index μ_y

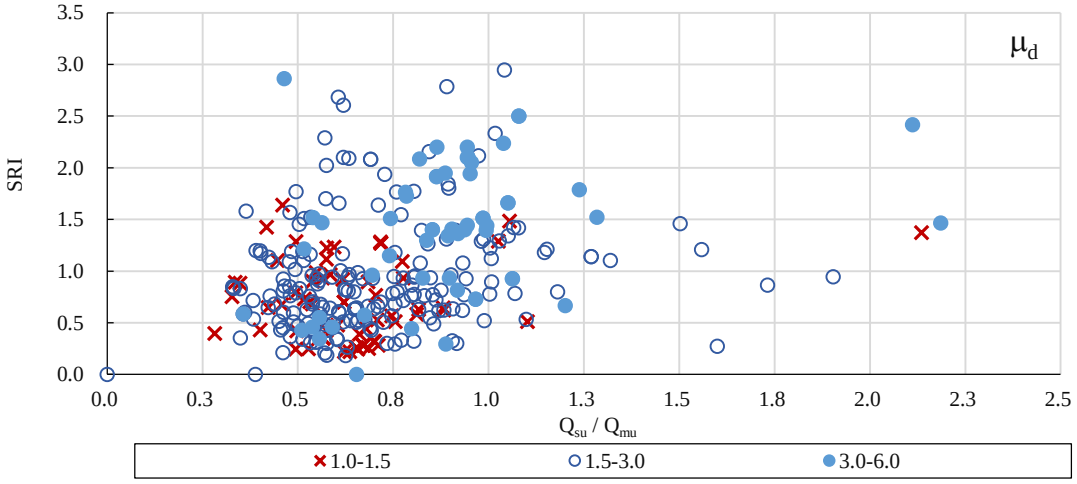

Figure 4-9　Degradation index μ_d

The degradation index is shown in three categories in Figure 4-9, the first corresponds to μ_d lower than 1.5, in this group columns with brittle failure are included. The second groups corresponds to values between 1.5 and 3.0, and the third group for values between 3.0and 6.0. In this figure, it is important to remark that there are columns that develop short μ_d even the value of SRI is larger than the minimum stablished by AIJ proposal [4.96].

Additionally, the failure mode has been plot in Figure 4-10, the figure was divided in columns that fail in shear, flexural and other mode. Most of the columns that present flexural failure are placed in values of SRI large than 1.0 and Q_{su}/Q_{mu} larger than 0.75 (Section 4 marked in the figure). There are few cases of columns with shear failure presented in that section, these are the special cases of: columns 358, 362, 363 and 364 which were built with high strength materials and smooth lateral reinforcement bars. These characteristics can be observed in the table of calculation in Appendix 1.

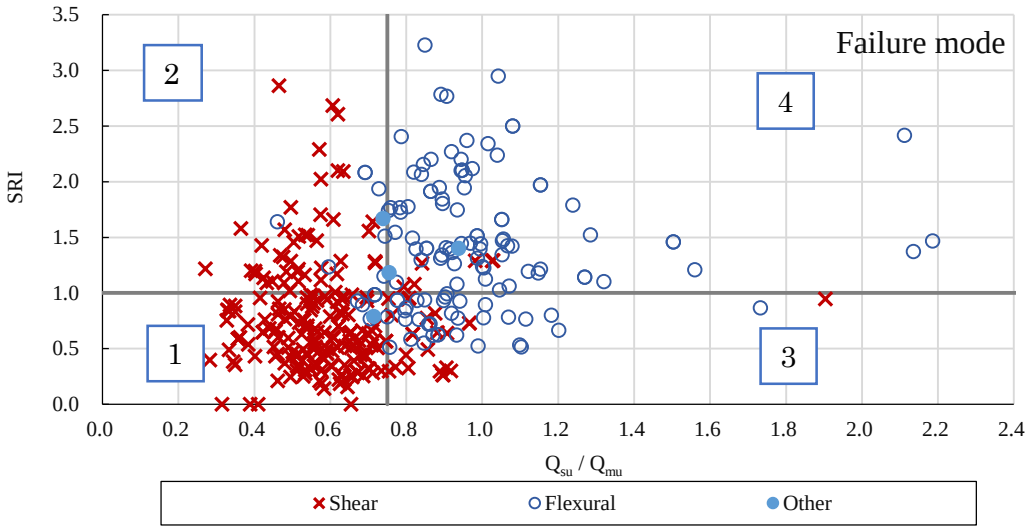

Figure 4-10 Failure mode

Comparing Figure 4-10, with the previously mentioned figures the next comments can be drown:

In section 1 of Figure 4-10, the columns with values of SRI lower than 1.0 and Q_{su}/Q_{mu} lower than 0.75 corresponds in general to columns with shear failure. The

ultimate lateral drift angle developed was lower than 1.9%, the value of μ_y is completely arbitrary, but the lowest values of μ_d are present in this section. It can be said that this is the most unfavorable developed ductility, it means, the lower toughness columns.

In section 2 of Figure 4-10 is transition. The columns with values of SRI larger than 1.0 and Q_{su}/Q_{mu} lower than 0.75 presented shear failure but, most of them developed desirable lateral drift angle larger than 2.5%, and in few cases, μ_d is lower than 1.5. This can be considered as an area where columns can be developed large R_u in shear failure.

For columns SRI lower than 1.0 and Q_{su}/Q_{mu} larger than 1.0, section 3 of Figure 4-10 is another transition area where no clear behavior is shown, whereas, it happens the opposite than in section 2, more columns developed flexural behavior but they don't develop large ductility.

Section 4 of Figure 4-10 is an area where the tested columns presented desirable behavior. Most of the columns presented flexural failure and large lateral drift angle. In the same way, most of the columns have μ_y larger than 5.0 and μ_d larger than 1.5. The columns contained in this section can be considered as desirable ductile behavior. Then, the structural design should be focused in this area.

Observing Figure 4-10, it can be said that the index of Q_{su}/Q_{mu} is useful to separate the tested columns by failure mode. In this case, Most of the cases of Q_{su}/Q_{mu} lower than 0.75 presented shear failure and, most of the cases of Q_{su}/Q_{mu} larger than 0.75 presented flexural failure. On the other hand, the quantity of shear reinforcement resulted in a viable factor to separate columns by ductility, the acceptable value of R_u plotted in Figure 4-7 separate satisfactorily columns with large ductility from that with low ductility.

For this reason, two index should be used to get a good classification of the columns that could develop high ductility. However, Q_{su}/Q_{mu} larger than 0.75 is not viable given the fact that it opposes the common theory of index to avoid shear failure, then a new proposal that works better should be set.

Even the fact that the SRI worked satisfactorily, this research work will propose an improved version of this index in the next chapter, its objective will be to set the minimum value for the lateral reinforcement necessary to develop desirable ultimate lateral drift angle.

4.3.1. Current design philosophy area

The current philosophy of design consists mainly in meeting the requirements of SRI of Eq. 2-1 (besides other additional requirements [4.96]) and the standard assumption to avoid shear failure [4.97]. Figure 4-7 shows the current philosophy area of design where SRI>1.0 and Q_{su}/Q_{mu} >1.10.

It was found during the study of the Tasai-Lab database that certain kinds of columns developed high ductility despite the fact that their standard assumption to avoid shear failure was pessimistic, it means that the relationship Q_{su}/Q_{mu} is lower than 1.1. This is shown in Figure 4-7 where they have been marked in the missing area.

In Figure 4-7, it can be seen that most of the selected columns which presented flexural fail mode have SRI>1.0. But in this figure, there are columns with shear failure that are over that limit it Q_{su}/Q_{mu} index is lower than 1.10.

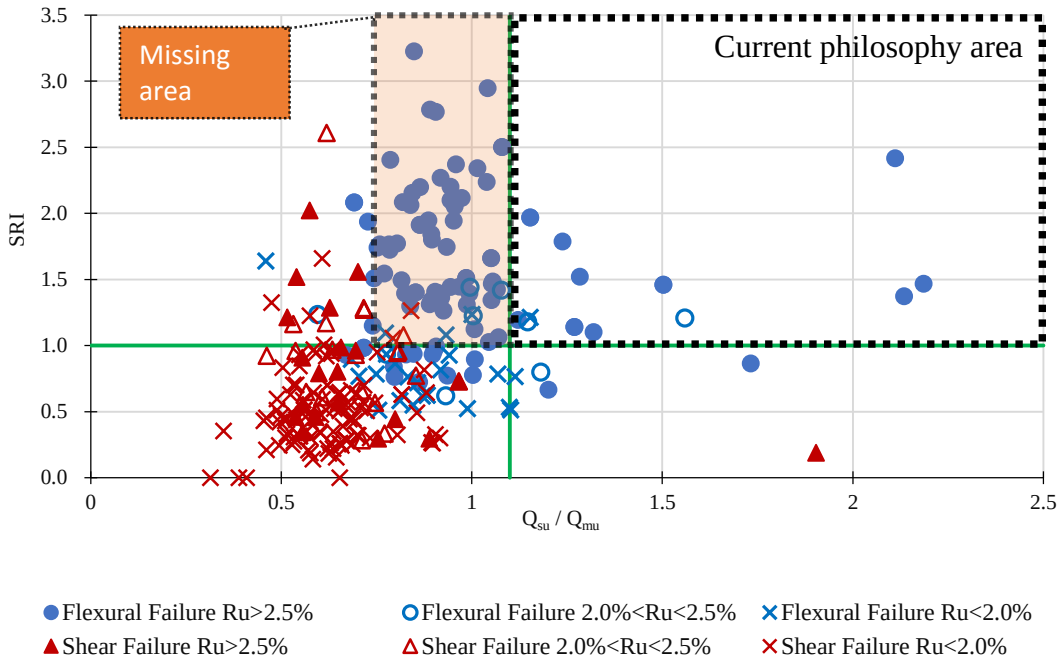

Figure 4-11 Current philosophy of design area

4.4. Conclusions of Chapter 4

At the end of this chapter some conclusions were drown:

For the creation of the database

The Ductility Behavior of RC Columns Database or simply Behavior Database in this document achieved 376 experimental test results. The selected columns are listed at the Appendix 1, the information in this database is the skeleton curve of the shear force - lateral drift relationship. The graphics are plotted in Appendix 2. The results of this research may be influenced by the strength of the concrete, which is dominantly 30MPa.

For the estimation of the actual strength of reinforcement steel

Factors to estimate the actual strength of materials were presented. These factors are exclusively for research purpose and do not have to be used in the structural design. Additionally, its functionality should by confirm by the designer, this information is purely statistically and strongly depends of the source data. The factor are listed in the following table, they depend of the nominal strength and the nominal diameter given the fact that the modulus of elasticity is also uncertain before the design.

It is recommended to increase this information in order to get more accuracy and to cover the current lack of data. At the same time, it is recommended to the authors of papers on this field to publish the nominal and actual strength and modulus of elasticity of materials in order to be available for others researchers.

Factor to get the actual strength

	SD295	SD345	SD390	SD490	SD685
D4		1.06			
D6	1.39	1.11	1.08		
D10	1.20	1.18			
D13	1.17	1.07	1.24	1.09	0.82
D16	1.19	1.11	1.13	1.17	1.05
D19	1.15	1.13	1.22	1.13	1.08
D22		1.13	1.19	1.07	
D25	1.26	1.12			1.01
D29					1.01
D32		1.09			

For the evaluation of the Ductility

The ultimate lateral drift angle, deflection ductility index and the degradation index were calculated for the columns in the Behavior Database according to the criteria of section 4.3. The calculate values were presented and commented in Figure 4-7, Figure 4-8 and Figure 4-9 respectively.

The R_u will be the main parameter to evaluate the performance of the column in the next chapter but the μ_y and the μ_d will be used to explain some particularities about the performance of some columns.

For the current philosophy of design

The standard assumption to avoid shear failure is not accurate in the prediction of the ductility behavior of certain kind of columns, it means, even that the relationship Q_{su}/Q_{mu} is lower than 1.1, the columns developed desirable and satisfactory ductile performance. A missing area, were columns presented a desirable ductile behavior, has been pointed in Figure 4-11 as the “Missing area”.

Bibliography of Chapter 4

[4.1] 佐藤 秀一郎, 池田 昭男, 千葉 正裕, 陣内 浩, 二見 正: 高強度鉄筋の開発に関する研究 : その 20 高強度 RC 柱の繰返し曲げ･せん断実験(II) : 強度性状, 学術講演梗概集. C, 構造 II 1, pp.485-486, 1991 年 8 月 1 日

[4.2] 藤本 利昭, 清水 秀哲: 高強度せん断補強筋を用いた RC 柱部材構造性能に関する実験的研究, 安藤建設技術研究所報 Vol.11, pp.61-70, 2005 年

[4.3] Hassane OUSALEM, Toshimi KABEYASAWA, Akira TASAI and Yasuko OHSUGI: EXPERIMENTAL STUDY ON SEISMIC BEHAVIOR OF REINFORCED CONCRETE COLUMNS UNDER CONSTANT AND VARIABLE AXIAL LOADINGS, コンクリート工学年次論文集, Vol.24, No.2 , pp.229-234, 2002 年 6 月 8 日

[4.4] 福山 洋、岩渕 一徳、諏訪田 晴彦: ピロティ建築物応答低減に関する研究 （その４）変動軸力を受ける鉄筋コンクリート造ピロティ柱の構造実験, 本建築学会大会学術講演梗概集, pp.415-416, 2004 年 8 月

[4.5] 丸田 誠、永井覚、高稲 宜和、山元 雄亮: ステンレス鋼鉄筋を用いたＲＣ柱の構造性能, コンクリート工学年次論文集, Vol.31, No.2, pp.1617-1632, 1905 年 6 月 30 日

[4.6] 木下 拓也、福原 美苗、南 宏: 高強度せん断補強金を用いたＲＣ柱の曲げ破壊性状に関する実験的研究（その２）, 福山大学工学部紀要 弟 30 巻, pp.101-108, 2006 年 12 月

[4.7] 小野 新, 白井 伸明, 安達 洋, 坂槇 義夫: 変動軸力を受ける鉄筋コンクリート柱の弾塑性性状, コンクリート工学年次論文報告集, Vol.11, No.2, pp.495-500, 1989 年 6 月 12 日

[4.8] 岡西 努 , 林 静雄 , 香取 慶一 , 東 健二: 高軸力を受ける鉄筋コンクリート柱の変形性能に関する考察, コンクリート工学年次論文報告集, Vol.14, No.2, pp.297-300, 1992 年 5 月 20 日

[4.9]　小林 努, 山口 輝彰, 日比野 孝一, 今井 弘: せん断力を受ける PCa 柱の力学的性状に関する研究, コンクリート工学年次論文報告集, Vol.14, No.2, pp.475-480, 1992 年 5 月 20 日

[4.10]　加藤 大介 , 菊池 政智: 高強度材料を用いた RC 柱の曲げ性能の評価に関する実験的研究, コンクリート工学年次論文報告集, Vol.14, No.2, pp.541-546, 1992 年 5 月 20 日

[4.11]　岡西 努, 林 静雄, 香取 慶一: 高軸力を受ける鉄筋コンクリート柱の曲げ降伏後の限界変形に関する研究, コンクリート工学年次論文報告集, Vol.15, No.2, pp.519-524, 1993 年 6 月 3 日

[4.12]　松本 智夫, 西原 寛, 近藤 修一, 鈴木 英之: プレキャスト RC 柱部材の変形性能に関する実験的研究, コンクリート工学年次論文報告集 , Vol.15, No.2, pp.659-664, 1993 年 6 月 3 日

[4.13]　岡西努、香取慶一、林静雄、黒正清治: 高軸力を受ける鉄筋コンクリート柱の変形性能に関する実験研究, 日本建築学会構造系論文集　弟 461 号, pp.65-74, 1994 年 7 月 30 日

[4.14]　山川 哲雄, 伊良波 繁雄, 玉城 康哉, 太田 達見: 電食試験により腐食した RC 柱の耐震性能に関する実験的研究, コンクリート工学年次論文報告集, Vol.16, No.1, pp.805-810, 1994 年

[4.15]　細矢博, 安倍勇, 岡田恒男, 北川良和: 鉄筋コンクリート部材の耐力と破壊性状に及ぼすひずみ速度の影響に関する研究―せん断破壊型柱部材の静的および動的水平加力実験―, コンクリート工学論文集 第 5 巻 第 1 号, pp.39-49, 1994 年 1 月

[4.16]　レハノ ベルナルド [他] , 安達 洋, 白井 伸明, 中西 三和: 高軸力及び変動軸力を受ける鉄筋コンクリート造柱の変形性状, 日本建築学会構造系論文集　弟 467 号, pp.93-104, 1995 年 1 月 30 日

[4.17]　中山 耕一, 山川 哲雄, 伊良波 繁雄, 枇杷田 篤: 電食試験により腐食した RC 柱の弾塑性挙動に関する実験的研究, コンクリート工学年次論文報告集, Vol.17, No.1, pp.883-888, 1995 年 6 月 1 日

[4.18] 知念 秀起, 山川 哲雄, 藤崎 忠志: 格子状 FRP 筋を帯筋に用いた RC 柱の弾塑性挙動に関する実験的研究, コンクリート工学年次論文報告集, Vol.17, No.2, pp.995-1000, 1995 年 6 月 1 日

[4.19] 林田 則光、松崎 育弘、石橋 久義、南尚 吾: 鉄筋コンクリート柱の靭性と残存軸耐力に関する実験的研究, 日本建築学会構造工学論文集 Vol.43B, pp.221-226, 1995 年 1 月

[4.20] 村中 圭介、山川 哲雄: 正方形鋼管と帯筋又はプレストレスで高横拘束した短柱の耐震性能, コンクリート工学年次論文報告集, Vol.20, No.3, pp.829-834, 1998 年 6 月 30 日

[4.21] 笠原 美幸、待崎 育弘、中野 克彦、福山 洋: 高靭性型セメント系複合材料を用いた柱部材の構造性能に関する実験研究, コンクリート工学年次論文集, Vol.22, No.3, pp.385-390, 2000 年 6 月 1 日

[4.22] 細矢 博、浅野 芳伸、小河 義郎、今井 弘: 外殻 PCa を用いた鉄筋コンクリート柱の構造特性と最大耐力, 日本建築学会構造系論文集 弟 544 号, pp.117-124, 2001 年 6 月 30 日

[4.23] 渡辺 英義、是永 健好、中野 克彦、松崎 育弘: 曲げ降伏後にせん断破壊する RC 柱の靭性評価に関する実験研究, 日本建築学会構造系論文集 弟 572 号, pp.155-162, 2003 年 10 月 30 日

[4.24] 松本 至 , 中野 克彦 , 熊澤 敬輔 , 松崎 育弘 , 清水 弥一: 高強度コンクリートと高強度せん断補強筋を用いた柱部材の構造性能に関する実験的研究（その 1,2), 学術講演梗概集. C-2, 構造 IV, 鉄筋コンクリート構造, プレストレストコンクリート構造, 壁構造・組積構造, pp.195-196, 2000 年 7 月 31 日

[4.25] 鹿野 仁史 , 前田 博之 , 中野 克彦 , 松崎 育弘 , 太田 勤 , 許斐 光生: 高強度せん断補強筋を用いた RC 柱部材構造性能に関する実験的研究（その 1,2）, 学術講演梗概集. C-2, 構造 IV, 鉄筋コンクリート構造, プレストレストコンクリート構造, 壁構造・組積構造 2002, pp.419-420, 2002 年 8 月 2 日

[4.26] 田中 康介 , 康 大彦 , 西川 和明 [他] , 前田 匡樹: 震災鉄筋コンクリート造建築物の残存耐震性能評価, コンクリート工学年次論文集, Vol.22, No.2, pp.1225-1230, 2003 年 7 月 1 日

[4.27] 杉本 訓祥: 鉄筋コンクリート造柱部材のせん断非線形性状評価手法の実験的検証, 日本建築学会構造系論文集 弟 592 号, pp.137-144, 2005 年 6 月 30 日

[4.28] 花井 伸明 , 梅村 恒 , 市之瀬 敏勝: 曲げ降伏後にせん断破壊する RC 柱の耐力低下に影響する因子, 日本建築学会構造系論文集 弟 593 号, pp.129-136, 2005 年 7 月 30 日

[4.29] 倉本 洋, 宮井 清忠, 南 宏一, 若林 實: 任意方向の曲げ・せん断を受ける二方向 X 形配筋柱の弾塑性挙動, コンクリート工学年次論文報告集, Vol.9, No.2, pp.293-298, 1987 年 6 月 12 日

[4.30] 荒川 卓, 賀 明玄, 荒井 康幸, 溝口 光男: らせん鉄筋補強コンクリート柱の終局せん断強度について, コンクリート工学年次論文報告集, Vol.9, No.2, pp.299-304, 1987 年 6 月 12 日

[4.31] 礒 健一, 柳沢 延房: 高軸力下における鉄筋コンクリート短柱に関する実験的研究, コンクリート工学年次論文報告集, Vol.11, No.2, pp.465-470, 1989 年 6 月 12 日

[4.32] 荒川 卓, 荒井 康幸, 溝口 光男, 吉田 稔: 二軸曲げせん断力を受ける鉄筋コンクリート短柱のせん断抵抗性状, コンクリート工学年次論文報告集, Vol.11, No.2, pp.471-476, 1989 年 6 月 12 日

[4.33] 鈴木 計夫, 中塚 信, 中田 浩之, 山中 昌一: 高強度コンクリート・高強度横補強筋を用いた RC 柱部材, コンクリート工学年次論文報告集, Vol.11, No.2, pp.455-460, 1989 年 6 月 12 日

[4.34] 桑田 裕次, 申山 昭夫, 南 宏一: 600 キロ級の高強度コンクリートを用いた RC 柱のせん断耐力, コンクリート工学年次論文報告集, Vol.15, No.2, pp.473-478, 1993 年 6 月 3 日

[4.35] 井上 章男, 西村 泰志, 倉本 洋: 高強度せん断補強筋と高強度コンクリートを用いた鉄筋コンクリート柱のせん断破壊性状, コンクリート工学年次論文報告集, Vol.15, No.2, pp.467-472, 1993 年 6 月 3 日

[4.36] 中田 浩之, 林 芳尚, 鈴木 計夫, 中塚 佶: 鋼管スリーブによるグラウト充填式継手を有する PCa 柱の力学特性, コンクリート工学年次論文報告集, Vol.17, No.2, pp.261-266, 1995 年 6 月 1 日

[4.37] 小田 稔, 岡本 直, 山中 久幸, 浅倉 晃: アラミド繊維巻付けによる既存 RC 柱のせん断補強, コンクリート工学年次論文報告集, Vol.15, No.2, pp.755-760, 1993 年 6 月 3 日

[4.38] 桑田 裕次, 南 宏一: 480 キロ級の高強度コンクリートを用いた RC 柱のせん断耐力に及ぼす作用軸力比の影響, コンクリート工学年次論文報告集, Vol.17, No.2, pp.857-862, 1995 年 6 月 1 日

[4.39] 瀬尾 正幸, 柏崎 隆志, 野口 博: 高強度材料を用いた RC 短柱のせん断性状に関する解析的研究, コンクリート工学年次論文報告集, Vol.17, No.2, pp.399-404, 1995 年 6 月 1 日

[4.40] 石渡 康弘, 市川 昌和, 中島 英一, 荒川 玄: GFRC と炭素繊維シートによる柱の耐震補強に関する実験的研究, コンクリート工学年次論文報告集, Vol.21, No.3, pp.1405-1410, 1999 年 6 月 21 日

[4.41] 鴨下 直樹, 菊川 和俊, 渡邊 一弘, 新藤 忠徳: 炭素繊維シートを用いた柱の耐震補強に関する実験的研究, コンクリート工学年次論文報告集, Vol.21, No.3, pp.1381-1386, 1981 年 4 月 30 日

[4.42] 若林 實, 南 宏一, 久木 幸雄, 宮内 靖昌: せん断力を受ける鉄筋コンクリート柱に対する X 形配筋の有用性について, 弟 3 回コンクリート工学年次講演会講演論文集, pp.445-448, 1981 年 4 月 30 日

[4.43] 鈴木 英之, 西原 寛, 松崎 育弘: 柱高さの途中まで存在する鉄骨が RC 柱のせん断性状に及ぼす影響, コンクリート工学年次論文報告集, Vol.21, No.3, pp.577-582, 1999 年 6 月 21 日

[4.44] 中澤 淳，山下 祐司，桑田 裕次，南 宏一: 高強度材料を用いた RC 柱のせん断破壊性状, コンクリート工学年次論文報告集, Vol.21, No.3, pp.397-402, 1999 年 6 月 1 日

[4.45] 島崎 和司: RC 造柱の地震後の残存軸力に関する研究(その 2)繰返し載荷とせん断スパン比の影響, 日本建築学会構造系論文集 弟 74 巻 弟 637 号, pp.537-542, 2009 年 3 月

[4.46] 中村 孝也、芳村 学、見波 進: サブストラクチャ疑似動的実験によるせん断破壊型鉄筋コンクリート柱の崩壊実験, 日本建築学会構造系論文集 弟 619 号, pp.141-148, 2007 年 9 月

[4.47] 高稲 宜和、芳村 学、中村 孝也: 鉄筋コンクリート柱の崩壊変形に関する研究, 日本建築学会構造系論文集 弟 573 号, pp.153-160, 2003 年 11 月 30 日

[4.48] 中村 孝也、芳村 学、大和 征良: せん断破壊型鉄筋コンクリート短柱の軸力保持限界に関する研究, 日本建築学会構造系論文集 弟 561 号, pp.193-199, 2002 年 11 月 30 日

[4.49] 山川 哲雄、張愛 暉、佐藤 元: アラミド繊維シートを用いた RC 柱の耐震補強に関する研究, 日本建築学会構造系論文集 弟 545 号, pp.111-117, 2001 年 7 月 30 日

[4.50] 中村 孝也、芳村 学、近藤 隆幸: 擬似動的手法による古い鉄筋コンクリート柱の崩壊実験, 日本建築学会構造工学論文集 Vol.55B, pp.369-376, 2009 年 3 月 27 日

[4.51] 宮内 克之, 秋田 政人, 下枝 博之 [他], 南 宏一: ポリマーセメントモルタルの乾式吹付け工法を用いた既存 RC 造柱の耐震補強, コンクリート工学論文集 弟 22 巻 弟 1 号, pp.43-55, 2011 年 1 月 25 日

[4.52] 金子 慶一、松井 智哉、福池 章平、倉本 洋: CES 付帯柱で補強されたせん断破壊型 RC 柱の挙動, コンクリート工学年次論文集, Vol.32, No.2, pp.1009-1014, 2010 年

[4.53] 田川 利郎, 山川 哲雄, 鴨川 茂義, 飯干 福馬: PC 鋼棒にプレストレスを導入した RC 極短柱の耐震補強実験, コンクリート工学年次論文集, Vol.22, No.3, pp.1639-1644, 2000 年 6 月 1 日

[4.54] 竜 泰之, 中村 孝也, 芳村 学: 鉄筋コンクリート柱の軸力保持限界に関する研究, コンクリート工学年次論文集, Vol.23, No.3, pp.217-222, 2001 年 6 月 8 日

[4.55] 小室 努、渡辺 英義、是永 健好、川端 一三: 150MPa 超高強度コンクリートを用いた RC 柱の耐震性能, コンクリート工学年次論文集, Vol.24, No.2, pp.277-282, 2002 年 6 月 8 日

[4.56] 白石 一郎、宮脇 毅、高木 仁之: 主筋付着の有無が RC 柱のせん断挙動に及ぼす影響, コンクリート工学年次論文集, Vol.24, No.2, pp.871-876, 2002 年 6 月 8 日

[4.57] 山田 和夫、山本 俊彦、岡田 亨: 断面形状の異なる鉄筋コンクリート部材の曲げ・せん断挙動, コンクリート工学年次論文集, Vol.25, No.2, pp.217-222, 2003 年 7 月 1 日

[4.58] Hassane OUSALEM, Toshimio KABEYASAWA, Akira TASAI, Junichi IWAMOTO: Effect of hysteretic reversals on lateral and axial capacities of reinforced concrete columns, コンクリート工学年次論文集, Vol.25, No.2, pp.367-372, 2003 年 7 月 1 日

[4.59] 金子 貴司、田上 淳、丸田 誠、鈴木 紀雄: 鉄筋コンクリート柱部材の挙動に及ぼすひずみ速度の影響に関する実験的研究, コンクリート工学年次論文集, Vol.26, No.2, pp.241-246, 2004 年 6 月 25 日

[4.60] 杉本 訓祥、増田 安彦、津田和明、江戸 宏彰: 超高強度コンクリートを使用した RC 造柱部材の曲げ性状に関する実験的研究, コンクリート工学年次論文集, Vol.27, No.2, pp.667-672, 2005 年 6 月 25 日

[4.61] 近藤 祐輔、今井 弘、細矢 博: 高強度材料を用いたプレキャスト柱の構造性能に関する研究, コンクリート工学年次論文集, Vol.28, No.2, pp.175-180, 2006 年 7 月 30 日

[4.62] 山崎 和宏、田才 晃: 鉄筋コンクリート造柱の軸力支持限界と耐震診断基準値, コンクリート工学年次論文集, Vol.28, No.2, pp.181-186, 2006 年 7 月 30 日

[4.63] 佐藤 幸博、佐々木 仁、高森 直樹、寺岡 勝: 高強度コンクリートを用いた RC 造短柱の耐震性能に関する実験的研究, コンクリート工学年次論文集, Vol.28, No.2, pp.625-630, 2006 年 7 月 30 日

[4.64] 村上 恵都子、増田 安彦、田才 晃、楠 浩一: 低強度コンクリート RC 造柱の破壊性状に関する実験的研究, コンクリート工学年次論文集, Vol.30, No.3, pp.211-216, 2008 年 7 月 30 日

[4.65] 鶴飼 和也、迫田 丈志、前田 匡樹、三橋 博三: 変動軸力を受ける HFRCC 柱の構造性能に関する実験的研究, コンクリート工学年次論文集, Vol.31, No.2, pp.1279-1284, 2009 年

[4.66] 板倉 康久, 安居 功二, 張 富明, 益尾 潔: 高強度コンクリートと高強度せん断補強筋を用いた RC 柱のせん断耐力と変形性能に関する実験的研究, コンクリート工学年次論文集, Vol.14, No.2, pp.291-296, 1992 年 5 月 20 日

[4.67] 日比純一、小谷俊介、青山博之: 高強度コンクリートを用いた RC 柱の変形性能に及ぼす軸力の影響, コンクリート工学年次論文集, Vol.14, No.2, pp.307-312, 1992 年 5 月 20 日

[4.68] 倉本 洋、宮井 清忠、南宏 一、若林 實: 二方向 X 形配筋柱の耐震性能, 日本建築学会構造工学論文集 Vol.32B, pp.171-182, 1986 年 3 月 1 日

[4.69] 村上 雅英、今井 弘: エポキシ樹脂注入工法で補修した RC 柱の弾塑性性状に関する実験的研究, 構造工学シンポジウム講演概要集,, pp.143-152, 1984 年 2 月

[4.70] 岩橋 司, 毛井 崇博、宮内 靖昌、太田 義弘: 鉄筋コンクリート柱の補修・補強に関する実験的研究, コンクリート工学年次論文報告集, Vol. 18, pp.1499-1504, 1996 年 6 月 17 日

[4.71] 片岡 隆広、松崎 育弘、福山 洋、橋本 一郎: シート状連続繊維によりせん断補強された RC 柱の構造性能に関する実験的研究, コンクリート工学年次論文報告集, Vol. 18, pp.1463-1468, 1996 年 6 月 17 日

[4.72] 吉田 格英、北山 和宏、西川 孝: 引張り軸力を受ける鉄筋コンクリート柱のせん断強度に関する研究, コンクリート工学年次論文報告集, Vol. 18, pp.875-880, 1996 年 6 月 17 日

[4.73] 六車 熙, 渡辺 史夫: 鉄筋コンクリート柱のせん断抵抗機構に関する研究 －その２ 付着割裂破壊におけるせん断補強筋の効果－, 日本建築学会論文報告集 第 341 号 昭和 159 年, pp.11-18, 1984 年 7 月 30 日

[4.74] 松崎 育弘 , 別所 佐登志 , 福島 稔 , 畠本 斉: 高強度コンクリートを用いた柱及びはり部材のせん断耐力, 弟 8 回コンクリート工学年次講演会論文集, pp.813-816, 1986 年 6 月 10 日

[4.75] 中江 晃彦, 倉本 洋, 南 宏一: 1200 キロ級のコンクリートを用いた RC 柱部材のせん断破壊性状, コンクリート工学年次論文報告集 , Vol. 12, No. 2, pp.357-362, 1990 年 6 月 12 日

[4.76] 田村 裕之, 南 宏一: 変動圧縮力とくり返し曲げ・せん断を受ける壁柱の弾塑性性状, コンクリート工学年次論文報告集 , Vol. 10, No. 3, pp.589-594, 1988 年 6 月 12 日

[4.77] 城 攻, 後藤 康明, 北野 敦則, 余湖 兼右: CF シートを用いた特殊補強を含む RC 柱の剪断抵抗性能, コンクリート工学年次論文報告集 , Vol. 20, No. 3, pp.1195-1200, 1998 年 6 月 30 日

[4.78] 柴田 拓二, 城 攻: 任意方向の水平力を受ける鉄筋コンクリート短柱のせん断破壊性状, コンクリート工学年次講演会講演論文集 5, pp.377-380, 1983 年 4 月 30 日

[4.79] 大野 義照, 宮本 芳樹: 鉄筋コンクリート柱の力学的性状におよぼす帯筋フック形状の影響, コンクリート工学年次論文報告集 , Vol. 20, No. 3, pp.493-498, 1998 年 6 月 30 日

[4.80] 横尾 一知, 北山 和宏, 小山 明男, 豊田 浩一: 変動軸力が鉄筋コンクリート柱のせん断性状に与える影響, コンクリート工学年次論文報告集 , Vol. 20, No. 3, pp.475-480, 1998 年 6 月 30 日

[4.81] 津村 浩三, 芳村 学: せん断破壊型 RC 柱の 3 方向加力実験, コンクリート工学年次論文報告集 , Vol. 20, No. 3, pp.463-468, 1998 年 6 月 30 日

[4.82] 荒川 卓 , 賀 明玄 , 荒井 康幸 , 溝口 光男: らせん鉄筋柱のせん断抵抗性状について, コンクリート工学年次論文報告集 , Vol. 10, No. 3, pp.577-582, 1988 年 6 月 12 日

[4.83] 桑田 裕次, 中山 昭夫, 南 宏一: 600 キロ級の高強度コンクリートを用いた RC 柱の 2 軸曲げせん断耐力, コンクリート工学年次論文報告集 , Vol. 16, No. 2, pp.521-526, 1994 年 6 月 3 日

[4.84] 浅川 敏雄 [他], 石丸 麟太郎, 吉田 宏, 末永 保美: 高層壁式プレキャスト鉄筋コンクリート造のピロティに用いる鋼管巻き RC 柱の力学的特性に関する研究, 日本建築学会構造系論文集 第 460 号, pp.131-141, 1994 年 6 月 30 日

[4.85] 藤原 敏夫, 狩野 芳一, 寺岡 勝, 佐々木 聡: 高強度コンクリートを用いた RC 短柱の力学性状に関する実験的研究, コンクリート工学年次論文報告集 , Vol. 13, No. 2, pp.433-438,, 1991 年 6 月 10 日

[4.86] 日比 純一, 美原 義徳, 小谷 俊介, 青山 博之: 高強度コンクリートを用いた RC 柱の曲げ降伏後のせん断変形能に関する実験的研究, コンクリート工学年次論文報告集 , Vol. 13, No. 2, pp.427-432, 1991 年 6 月 10 日

[4.87] 香田 伸次, 坂口 昇, 山野辺 宏治, 熊谷 仁志: 高強度鉄筋コンクリート壁柱のせん断特性に関する研究, コンクリート工学年次論文報告集 , Vol. 13, No. 2, pp.439-444, 1991 年 6 月 10 日

[4.88] 溝口 光男, 荒川 卓, 荒井 康幸: 二軸曲げせん断力と変動軸力を受ける高強度 RC 柱の強度性状, コンクリート工学年次論文報告集 , Vol. 13, No. 2, pp.457-462, 1991 年 6 月 10 日

[4.89] 阿満 重幸, 白井 伸明, 安達 洋, 小野 新: 高軸力および変動軸力を受ける鉄筋コンクリート柱の変形性状, コンクリート工学年次論文報告集 , Vol. 13, No. 2, pp.339-344, 1991 年 6 月 10 日

[4.90] Scholarly and Academic Information Navigator: http://ci.nii.ac.jp/

[4.91] Tasai A.: TasaiLab Reinforced Concrete Elements Database (Columns and beams section), Institute of Urban Innovation, Yokohama National University, Japan, 2011, Personal communication.

[4.92] 杉本 訓祥: プレストレスト鉄筋コンクリート梁部材の履歴復元力特性、修士課程論文、東京大学大学院大学系研究科建築学専、平成９年２月３日

[4.93] 石川 裕次, 木村 秀樹:高軸力が作用する高強度 RC 柱部材の最大耐力時変形, 構造工学論文集. B 51B, 441-447, 2005-03-20

[4.94] J. M. Woods, P. D. Kiousis, M. R. Ehsani, H. Saadatmanesh and W. Fritz: Bending ductility of rectangular high strength concrete columns, engineering structures, Vol. 29, pp.1783-1790, 2007.

[4.95] T. Okanishi, K. Katori, S. Hayashi and S. Kokusho: Deformability of reinforced concrete column subjected to high axial force, Journal of Structural and Construction Engineering, AIJ, No. 461, pp.65-74, 1994.7.

[4.96] Architectural Institute of Japan: Calculation standard for horizontal load-carrying of reinforced concrete structure and comments (Public comments), 2014.12. http://www.aij.or.jp/jpn/symposium/2014/public_20141215.html

[4.97] The building center of Japan: The building standard low of Japan, June 2004

CHAPTER 5. PROPOSAL FOR THE DESIGN OF RC COLUMNS

5.1. General view

This chapter presents the proposal requirements for the design of RC columns that can develop large ductility carrying high axial force. The proposal is based in two main aspects:

The first is the equation that provide an adequate way to classify the columns according to the failure behavior, it means flexural or shear mode, it is the called "Index to avoid shear failure" that is the simple principle that the shear strength should be 1.1 times larger than that of the flexural one [5.1]. This principle is shown by equation 5.1

$$\frac{Shear\ strength}{Flexural\ strength} > 1.1 \tag{5-1}$$

The second is about the minimum quantity of shear reinforcement to develop the desirable ultimate lateral drift angle of 2.5% with the here called Shear stress index. This is comparable with that equation proposed by AIJ [5.2] of Chapter 2.

The following sections of this chapter present the Index to avoid shear failure and the Quantity of shear reinforcement equations, these two equations compound the proposed philosophy of design for RC columns that carry high axial force but, additional requirements are set to ensure the proper structural design based in the characteristics of the employed data. The recommended equations are shown in sections 5.2 and 5.3 respectively. At the end of the Chapter, the conclusions is shown.

5.2. Index to avoid shear failure

For the structural design, it is important matter to know if a column will fail in shear or flexural mode, and if columns can develop enough ductility under specific axial force. With regard to the latter, this section is focused on the assumption index to avoid shear failure for RC columns that develop large ductility when axial force is applied on them.

The assumption index to avoid shear failure is defined as the relationship between the analytical value of the ultimate shear strength (Q_{su}) and the ultimate flexural strength

(Q_{mu}). This equation was shown in Chapter 2 by Equation **2-2**. However, as it was shown in the previous chapter, the relationship Q_{su}/Q_{mu} was not completely accurate for the collected data given the fact that columns with low value of Q_{su}/Q_{mu} develop large ductility.

For this reason, more research for the index to avoid shear failure was carried out. The shear strength was calculated with two different approaches. And for the case of the calculation of the flexural strength, five methods were considered. The possible combinations of the ratio Q_{su}/Q_{mu} of all this methods are analyzed and commented in the next section.

5.2.1. Shear strength analysis

For the calculation of the shear strength, the equation 2-5 described in AIJ [5.2] (which is repeated in the next) and the equation 5-2 by AIJ [5.3] were employed.

It is important to mention that the results of this section does not evaluated the equations to obtain the shear strength, this results will employed to find better accuracy of the index to avoid shear failure.

$$Q_{su} = \left\{ \frac{0.068 P_t^{0.23} (F_c + 18)}{\frac{M}{Qd} + 0.12} + 0.85\sqrt{P_w \sigma_{wy}} + 0.1\sigma_0 \right\} bj$$

$$V_u = \mu P_{we} \sigma_{wy} b_e j_e + \left(\upsilon \sigma_B - \frac{5 P_{we} \sigma_{wy}}{\lambda} \right) \frac{bD}{2} \tan\theta$$

$$V_u = \left(\frac{\lambda \upsilon \sigma_B + P_{we} \sigma_{wy}}{3} \right) b_e j_e \qquad (5\text{-}2)$$

$$V_u = \left(\frac{\lambda \upsilon \sigma_B}{2} \right) b_e j_e$$

Where:

$$\lambda = 1 - \frac{S}{2j_e} - \frac{b_s}{4j_e}$$

$$\mu = 2 - 20R_p$$

υ is the effective compressive strength coefficient, $\upsilon = (1 - 20R_p)\upsilon_0$, $\upsilon_0 = 0.7 - \sigma B200$

R_p = Rotation angle, in the analyses, the rotation angle will be consider equal to zero.

These equations were selected because they are well known and their employment is wide spread in Japan. The results of these two method are divided between the experimental shear strength (Q_{exp}) reported during the test by the authors (Q_{exp}/Q_{su} and Q_{exp}/V_u respectively). In this research, the quantity of axial force ratio applied during the tests is significant, for this reason, the results are compared with the value of η in the next figures.

Figure 5-1a shows the relationship Q_{exp}/Q_{su} in function of the axial force ratio. In this figure, it can be seen that the shear strength obtained by the equation 2-5 are safely predicted in most of the experimental testes, few cases are under the limit of Q_{exp}/Q_{su} =1.1. This proves that this equation is adequate to obtain the shear strength for columns failing in shear and flexural failure, for any case of axial force ratio.

In Figure 5-1a, the relationships Q_{exp}/Q_{su} increases as the axial force ratio increase; one reason for this effect could be that the influence of axial force ratio is larger for high values of η and not linear as equation 2-5 describes ($0.1\sigma_0$).

On the other hand, Figure 5-1b shows the relationship Q_{exp}/V_u in function of the axial force ratio. It can be observed that, the shear strength V_u calculated for many of the columns failing in shear mode are over the value of Q_{exp}/V_u = 1.0, and the shear strength calculated for many columns failing in flexural mode are under this limit. This means that, the computed value of V_u is safely predicted for many shear columns and, overestimated for flexural columns.

In this same figure, it can be observed that the relationships Q_{exp}/V_u increases as the axial force ratio increase, this is due that equation 5-2 does not include the effect of axial force ratio. As an effect, the prognostication of the shear strength V_u became more accurate for the columns that were testes with high axial force ratio and wide spread for that columns that were tested with lower axial force.

It is clear that the equation 5-2 by AIJ [5.3] should not be employed to compute the shear strength for columns with expected flexural behavior because this equation gives as a result larger values compared with the experimental ones. In this research, this value will be only employed to determine the index to avoid shear failure.

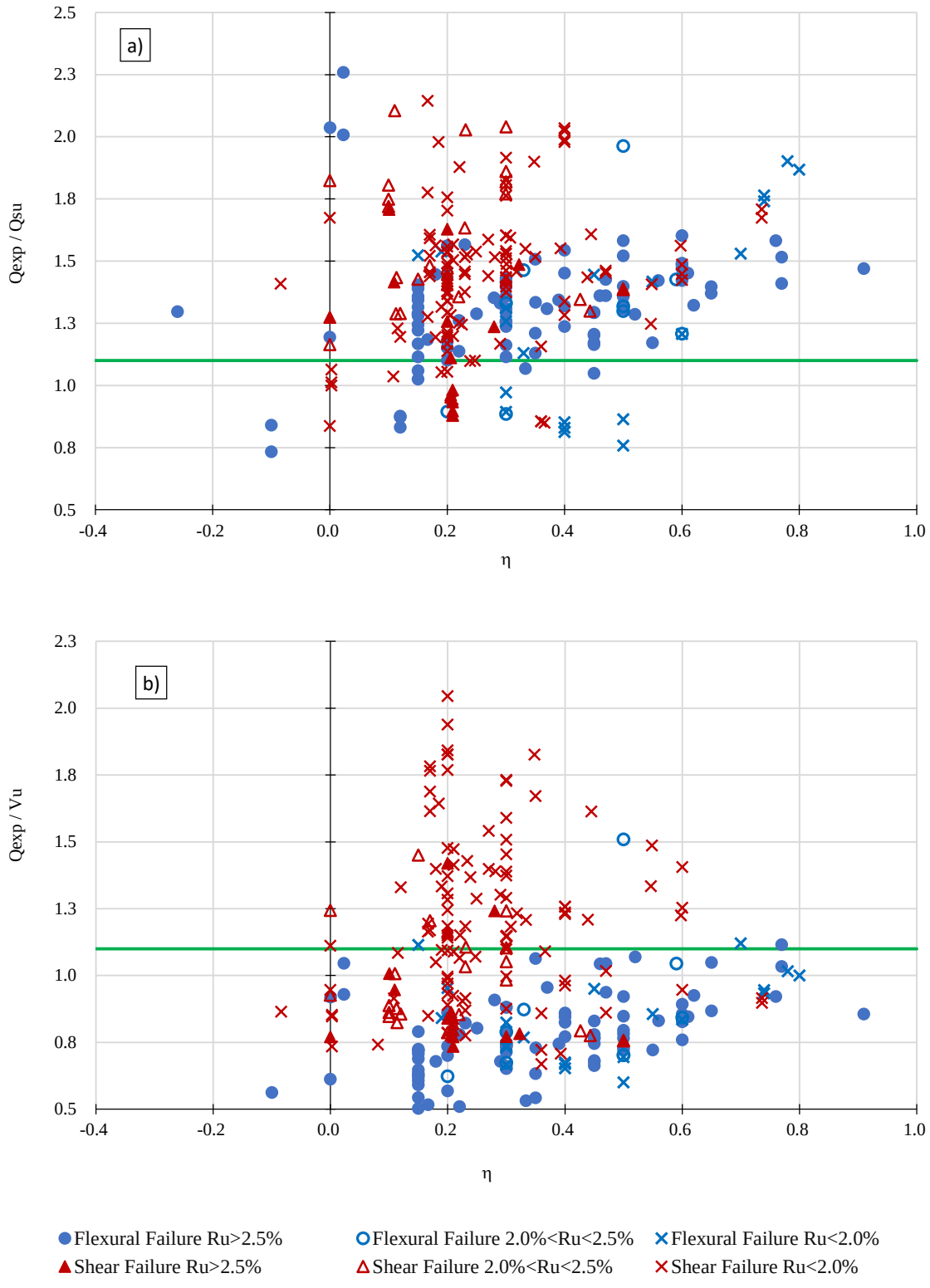

Figure 5-1 V_u/Q_{mu} and Qs_u/Q_{mu} relationship for Q_{mu} method

5.2.2. Flexural strength analysis

Analyses to obtain the flexural moment were carried out with five different models. These are: the moment calculated with equation 2-4 of AIJ [5.1][5.2], and fiber analysis with 4 different combination of confined and unconfined concrete models. The five models are depicted in Figure 5-2.

The Kent and Park confined and unconfined concrete model [5.4] were used for modeling the material behavior of the concrete of the second, third and fourth flexural moment analyses.

The second method employed the Kent and Park confined concrete model disregard of the concrete cover for the full section (*Kent-Park 0C*).

The third method employed the Kent and Park confined concrete model for the core of the transversal section of the columns and the Kent and Park unconfined concrete model for the concrete cover in the direction of the applied moment (*Kent-Park 1C*).

The fourth method employed the Kent and Park confined concrete model for the core of the transversal section of the columns and the Kent and Park unconfined concrete model for the concrete cover in both direction of the cross section (*Kent-Park 2C*).

The last model corresponds to the New RC model (*NewRC 0C*) of The National Land Development Technology Research Center [5.5] for confined concrete. In this case, no cover was considered in the analysis. Figure 5-2 depicts the cross sectional models described in this paragraphs.

Kent-Park model

The stress-strain relations of confined and unconfined concrete of the model are summarized in the next. The confined and non-confined concrete model of Kent-Park are compounded by to lines, the first corresponds to an ascending branch represented by a second degree parabolic curve and the second to a descending straight line. Equation 5-3 represents this model [5.6].

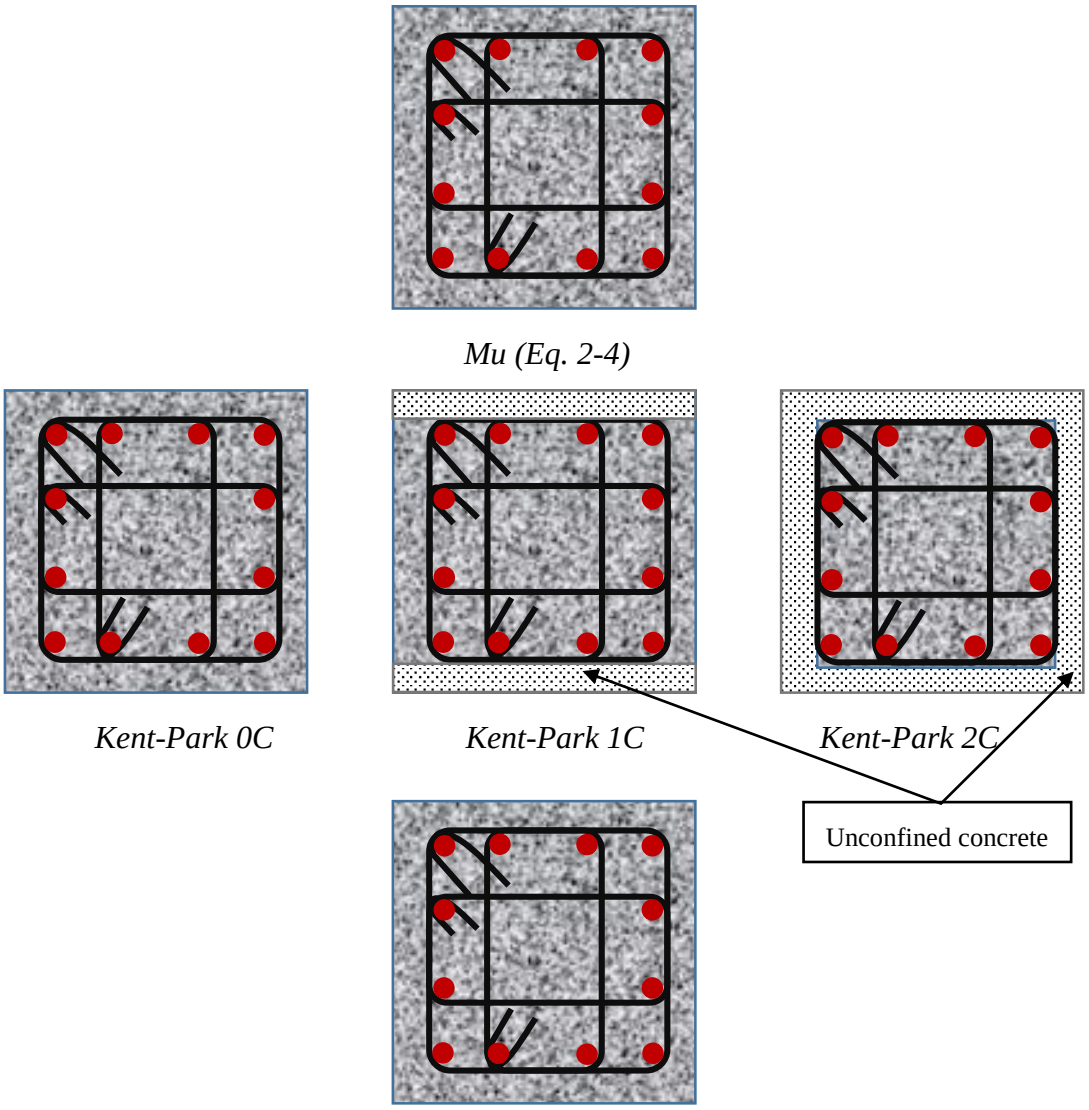

Figure 5-2 Cross sections models for flexural analysis

$$f_c = kf'_c\left(\frac{2\varepsilon_c}{\varepsilon_0 k} - \left(\frac{\varepsilon_c}{\varepsilon_0 k}\right)^2\right) \qquad \varepsilon_c \leq k\varepsilon_0$$

$$f_c = kf'_c\left(1 - Z_m(\varepsilon_c - \varepsilon_0 k)\right) \geq 0.2kf'_c \qquad \varepsilon_c > k\varepsilon_0 \tag{5-3}$$

Where

ε_c is the longitudinal concrete strain

f'_c is the compressive strength of concrete

ε_0 is the strain of unconfined concrete corresponding to f'_c

Commonly accepted ε_0= 0.002 [5.6]

k is a confinement coefficient.

$$k = 1 + \frac{p_g \sigma_y}{f'_c}$$

For unconfined concrete, *E* parameter k is equal to one.

Z_m is the stress declining ratio for the confined concrete after peak stress

$$Z_m = \frac{0.5}{\varepsilon_{50u} + \varepsilon_{50h} - \varepsilon_0 k}$$

$$\varepsilon_{50u} = \frac{3 + \varepsilon_0 f'_c}{f'_c - 1000}$$

$$\varepsilon_{50h} = 0.75 p_g \sqrt{\frac{b_e}{s}}$$

For concrete under confinement, a perfectly plastic residual behavior is assumed at high strain level to account for the load carrying capacity of crushed concrete is still effectively confined by the transverse steel. The confinement effect on the strength of concrete, represented by the coefficient *k*, increases the concrete peak stress from f'_c to kf'_c. It is assumed that confined concrete can sustain a constant stress of $0.2kf'_c$ at strains greater than ε_{20}.

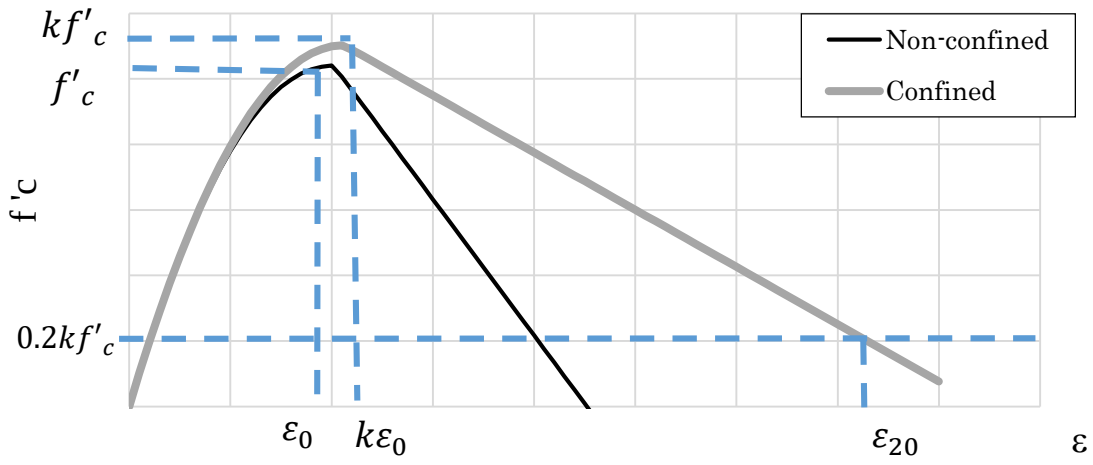

Figure 5-3 Kent and Park model for unconfined and confined concrete

New RC model

Equation 5-4 defines the confined concrete of New RC model [5.5][5.6], and the next paragraphs summarize the concept of the model. Figure 5-4 shows the stress-strain relation of confined concrete of New RC model.

$$\frac{\sigma_c}{{}_C\sigma_{cB}} = \frac{ax + (d-1)x^2}{1 + (a-2)x + dx^2} \tag{5-4}$$

Where:

$${}_C\sigma_{cB} = \sigma_p + k\ \rho_h\ \sigma_{hy}$$

$$\sigma_p = \mu_c\ \sigma_B$$

For rectangular cross sectional columns $1.0\sigma_{cB}$ and for circular cross sectional columns $0.80\sigma_{cB}$

$$k = \begin{cases} k_c\left(1 - \dfrac{s}{2D_c}\right) \\ k_s\left[\dfrac{d''}{C}\right]\left(1 - \dfrac{s}{2D_c}\right) \end{cases}$$

For rectangular cross sectional columns k_c= 2.09 and for circular cross sectional columns k_s= 11.5

$$x = \frac{\varepsilon c}{\varepsilon co}$$

$$a = \frac{E_c\ \varepsilon co}{{}_C\sigma_{cB}}$$

$$\varepsilon co = \varepsilon o \begin{cases} 1 + 4.7(K-1) & K \le 1.5 \\ 3.35 + 20(K-1.5) & K > 1.5 \end{cases}$$

$$\varepsilon o = 0.93({}_C\sigma_{cB})^{0.25}10^{-3}$$

$$K = \frac{{}_C\sigma_{cB}}{\sigma_p}$$

$$E_c = 4.1\lambda\left(\frac{{}_C\sigma_{cB}}{100}\right)^{1/3} 10^4\left(\frac{\gamma}{24}\right)^2$$

λ is defined according to the aggregate that compound the concrete: equal to 1.0. In general, it is equal to 1.2 for high elasticity (limestone aggregate) and equal to 0.9 for low elasticity (quartz schist, andesite, and lightweight aggregate)

$$d = \alpha + \beta\ {}_C\sigma_{cB} + \gamma\sqrt{\frac{(K-1)\ {}_C\sigma_{cB}}{23}}$$

$\alpha = 1.50$

$\beta = -1.71(10^{-2)}$

γ is equal to 2.4 when square pipe section is embedded or equal to 1.6 when stirrups are used.

σ_c axial stress in the concrete

εc axial strain in the concrete

ρ_h confinement reinforcement ratio

σ_{hy} Horizontal reinforcement yielding strength (less than 685 N / mm^2)

σ_{cB} Cylinder strength of concrete

σ_p Strength of plain concrete

${}_C\sigma_{cB}$ Strength of confined concrete

εco Strain when the strength of confined concrete is reached

$d"$ Nominal diameter of the transverse reinforcement

C Effective horizontal support length of the horizontal reinforcement

s Horizontal reinforcement spacing

D_c The distance between the centers of the cross-section to the peripheral transverse reinforcement

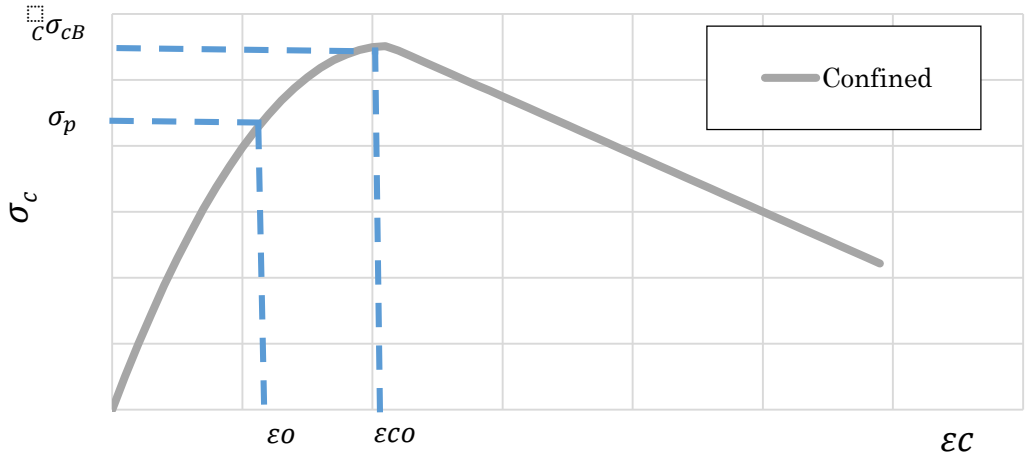

Figure 5-4 New RC model for confined concrete

Results

The flexural strength was calculated from the flexural moment obtained with the previous analysis with the equation 5-5.

$$Q_{mu(i)} = \frac{M_i}{M/Q} \tag{5-5}$$

Where:

M_i is the calculated moment from the above mentioned models (kN•mm)

M/Q is the shear span (mm)

The flexural strength was normalized for each case by the maximum shear strength reported in every test (Q_{exp}). The results of these analyses are presented in the Figure 5-5 for all columns of the Behavior Database.

Figure 5-5a) shows the relationship of Q_{exp}/Q_{mu} and the axial force ratio for Eq. 2-3. The data of columns that develop lateral drift angle larger than 2.5% in flexural failure resemble a parabolic curve where the lower point is located around axial force ratio of 0.3. The nature of this relationship is given by the equations to obtain Q_{mu} (Eq. 2-3). The

minimum value for Q_{exp}/Q_{mu} for columns with flexural failure happened when the balance axial force was applied to the column. This model cannot separate the columns with flexural failure that presented R_u < 2.5% from that with lower R_u in values near to the balance axial force, this can be observed in the figure Figure 5-6 a) where the data for flexural failure is presented.

Figure 5-5b) shows the relationship of Q_{exp}/Q_{mu} and the axial force ratio for the "Kent-Park" model. For the case of columns failing in flexural mode, this model is not accurate in the calculation of the flexural strength, In Figure 5-6b), it can be observed that the flexural strength was overestimated in many cases.

The models "Kent-Park 1C", "Kent-Park 2C" and "New RC" prognosticated the flexural strength safely. This can be observed in the figures Figure 5-6 from c) to e) respectively. However, there are the cases of "Kent-Park 1C" and "New RC" that presented particular results for the columns failing in flexural mode, most for the case of columns that developed R_u lower than 2.5% were overestimated by this two models. It is just "Kent-Park 2C" model that estimated the flexural strength in accurate way; few cases were overestimated as this can be seen in Figure 5-6e).

As conclusion, it can be said that all model overestimated the flexural strength for most of the columns failing in shear failure. The flexural analysis with better results for the columns failing in flexural mode was the Kent and Park model that consider the concrete cover in the two directions (Kent-Park 2C). The model with Q_{mu} from Eq. 2-3 presented a parabolic shape but all the flexural cases were prognosticated safely.

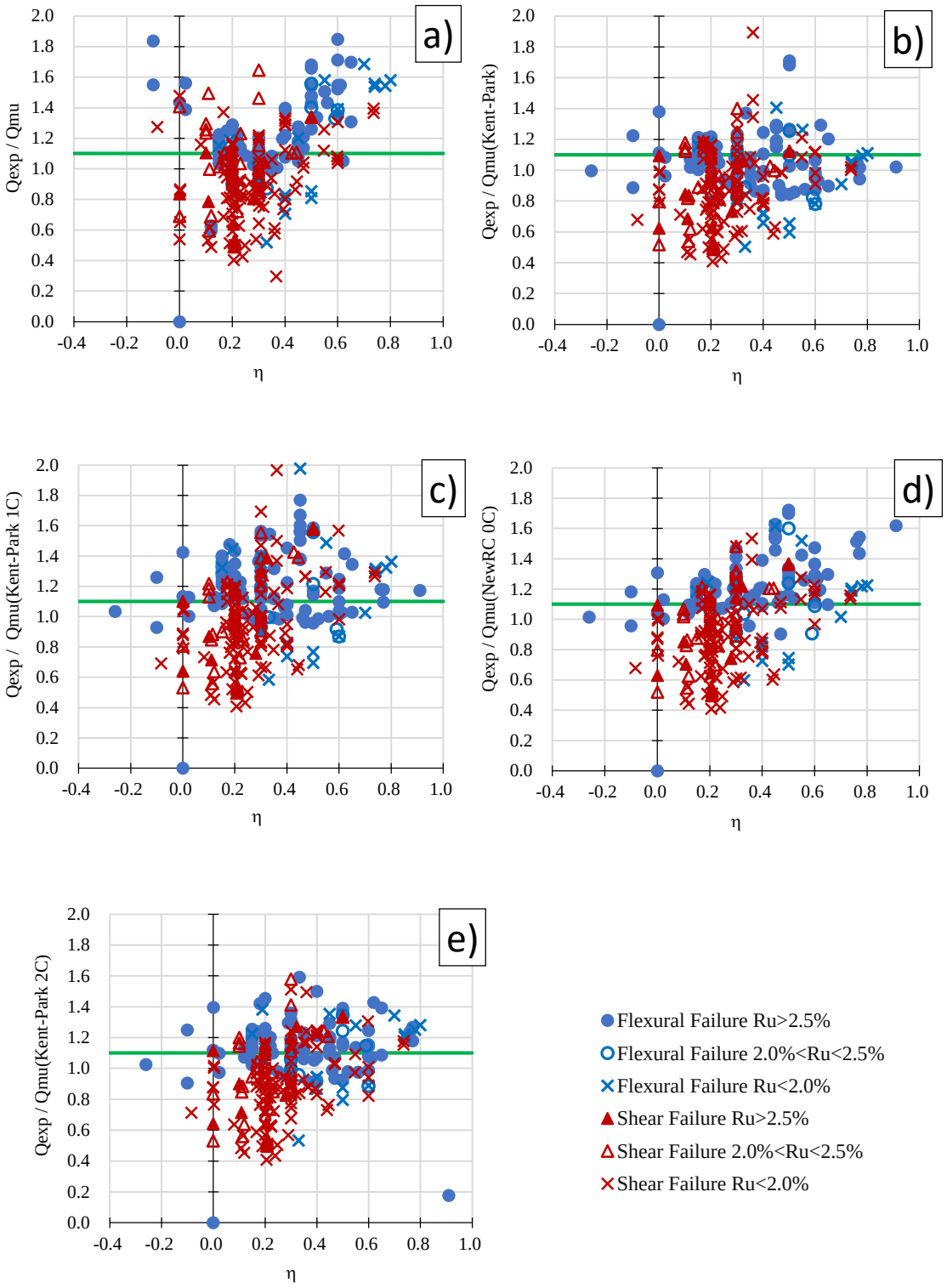

Figure 5-5 Q_{exp}/Q_{mu} relationships

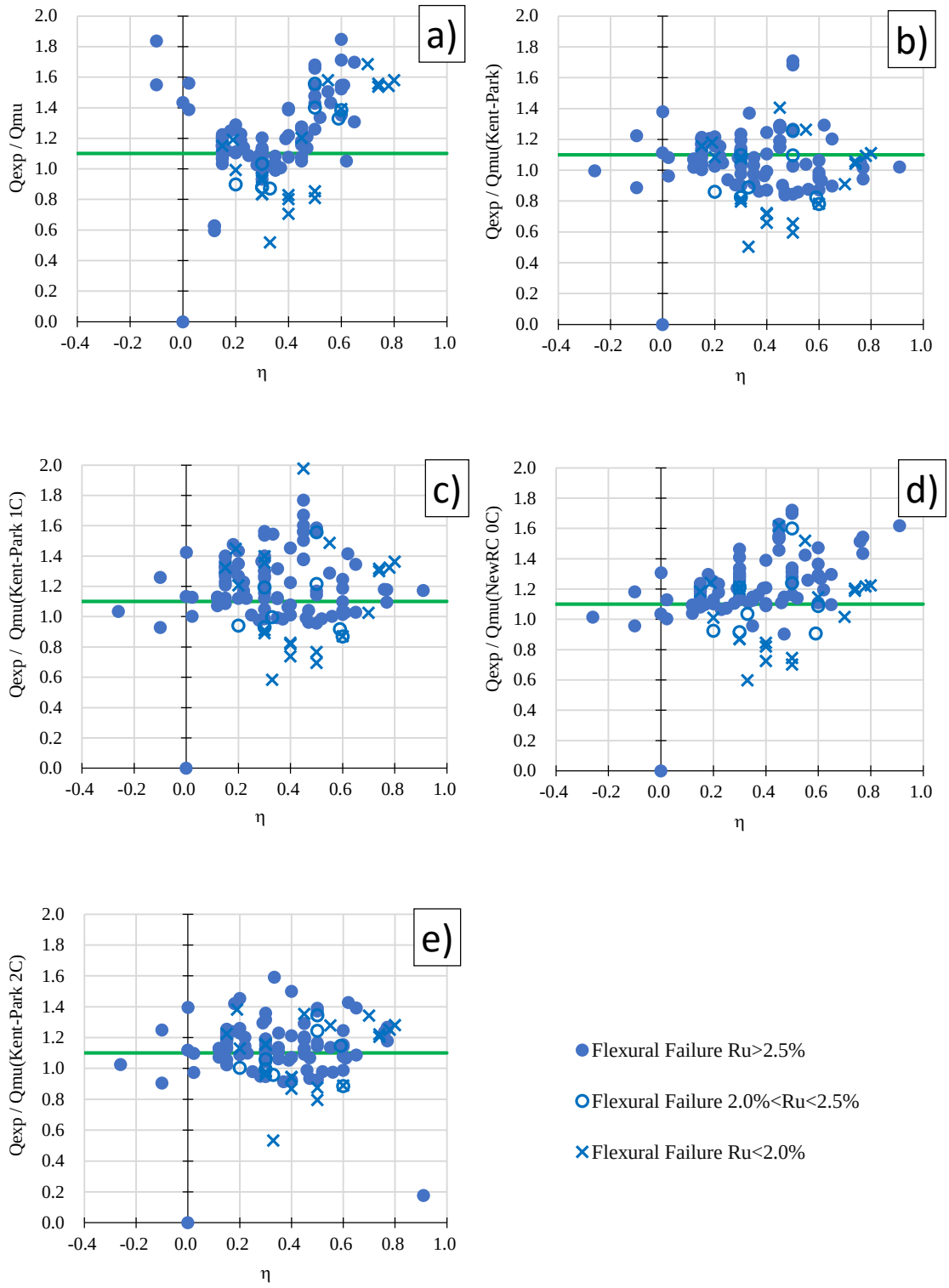

Figure 5-6 Q_{exp}/Q_{mu} relationships for flexural failure columns

Ratio of shear strength to flexural strength

The relationship defined in equation 5-1 is shown in this section, the coefficient of the shear strength calculated in section 5.2.1 and the flexural strength calculated in section 5.2.2 will be presented. The results are presented by flexural model for both cases of flexural strength, first for Q_{su} and second for V_u. The quotient of the shear strength to the flexural strength is shown in the ordinated axis and the axial force ratio in the abscissa axis. The value of 1.1 has been referenced in the ordinated axis to make clear which ratio separated properly columns that develop flexural from shear failure mode.

In each next figures, the data was differenced by failure mode as in the previous figures of this chapter. At the same time, the data is also divided in three ranges of lateral drift angle, these are: columns that developed R_u larger than 2.5%, between 2.5% and 2.0%, and R_u lower than 2.0%. This exact information is shown in the legend of every figure.

Due to the fact that the objective of the coefficient of the shear strength to the flexural strength is to give a criterion to classify the columns as flexural failure, the percentage of columns with shear failure that are the limit of 1.1 and the percentage of columns with flexural failure that are over this same limit will be mentioned. The percentage is given in reference to the population of data for its respective failure mode and not for the whole data population. This percentages will be a criterion to define the index to avoid shear failure.

Figure 5-7 presents the relationship of the Q_{su}/Q_{mu} and V_u/Q_{mu} relationship for Q_{mu} method. As this was mentioned in the section 2.3, the columns that agree the relationship of Q_{su}/Q_{mu} are few. Many columns are not taken in advantage in the structural design due to the reason that they are being considered as non-toughness columns. It is important to recognized that in this case just 0.5% of the columns failing in shear had Q_{su}/Q_{mu} larger than 1.1, columns with flexural failure that have Q_{su}/Q_{mu} larger than 1.1 are 14.7%. On the other hand, the percentage of the relationship V_u/Q_{mu} larger than 1.1 for columns with shear failure is 10.4% and the percentage of the relationship V_u/Q_{mu} larger than 1.1 for columns with flexural failure is 75.9% of the total of columns failing by this mode. This means that V_u/Q_{mu} relationship is a better index to avoid shear failure than Q_{su}/Q_{mu} when Q_{mu} equation is employ.

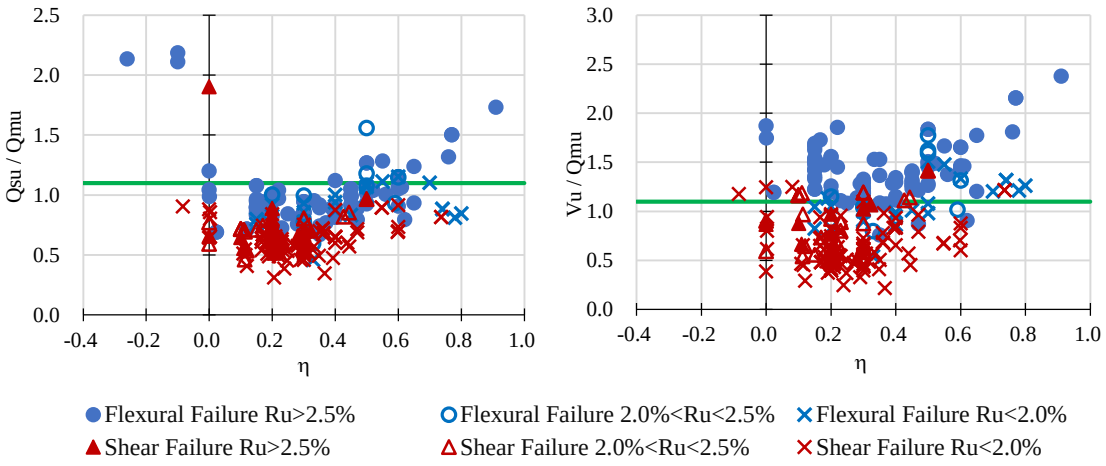

Figure 5-7 Q_{su}/Q_{mu} and V_u/Q_{mu} relationship for Q_{mu} method

Figure 5-8 presents the relationship of the Q_{su}/Q_{mu} and V_u/Q_{mu} relationship for "*Kent-Park 0C*" method disregarding of the concrete cover. In this case, 2.6% of the columns failing in shear mode had $Q_{su}/Q_{mu(Kent\text{-}Park\ 0C)}$ larger than 1.1, and columns with flexural failure mode that had relationship $Q_{su}/Q_{mu(\text{Kent-Park 0C})}$ larger than 1.1 was 9.3%. On the other hand, the percentage of the relationship $V_u/Q_{mu(Kent\text{-}Park\ 0C)}$ larger than 1.1 for columns with shear failure is 5.2% and the percentage of the relationship $V_u/Q_{mu(Kent\text{-}Park\ 0C)}$ larger than 1.1 for columns with flexural failure is 57.4% of the total of columns failing by this mode. This means that, when the "*Kent-Park 0C*" model was employed, the relationship V_u/Q_{mu} is a better index to avoid shear failure because include large number of columns with desirable behavior.

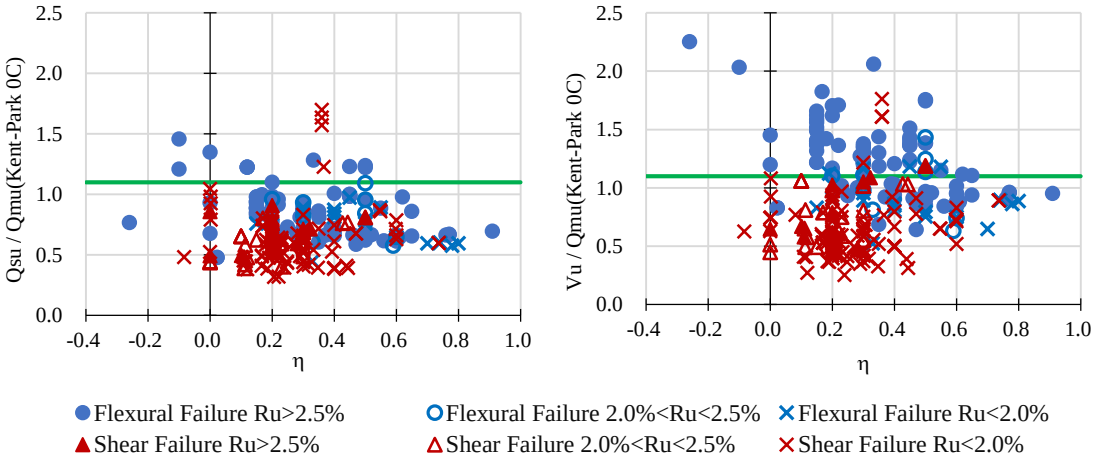

Figure 5-8 Q_{su}/Q_{mu} and V_u/Q_{mu} relationship for Q_{mu} (*Kent-Park 0C*) method

Figure 5-9 presents the relationship of the Q_{su}/Q_{mu} and V_u/Q_{mu} relationship for Kent-Park method considering the concrete cover in the direction of the applied moment (*Kent-Park 1C*). The percentage of the columns failing in shear had $Q_{su}/Q_{mu(Kent\text{-}Park\ 1C)}$ larger than 1.1 was 7.1%; columns with flexural failure that had relationship $Q_{su}/Q_{mu(Kent\text{-}Park\ 1C)}$ larger than 1.1 was 33.3%. The percentage of the relationship $V_u/Q_{mu(Kent\text{-}Park\ 1C)}$ larger than 1.1 for columns with shear failure is 14.8% and the percentage of the relationship $V_u/Q_{mu(Kent\text{-}Park\ 1C)}$ larger than 1.1 for columns in flexural failure was 68.2%. This means that, when the "*Kent-Park 1C*" model was employed, the relationship V_u/Q_{mu} is a better index to avoid shear failure because include large number of columns with desirable behavior.

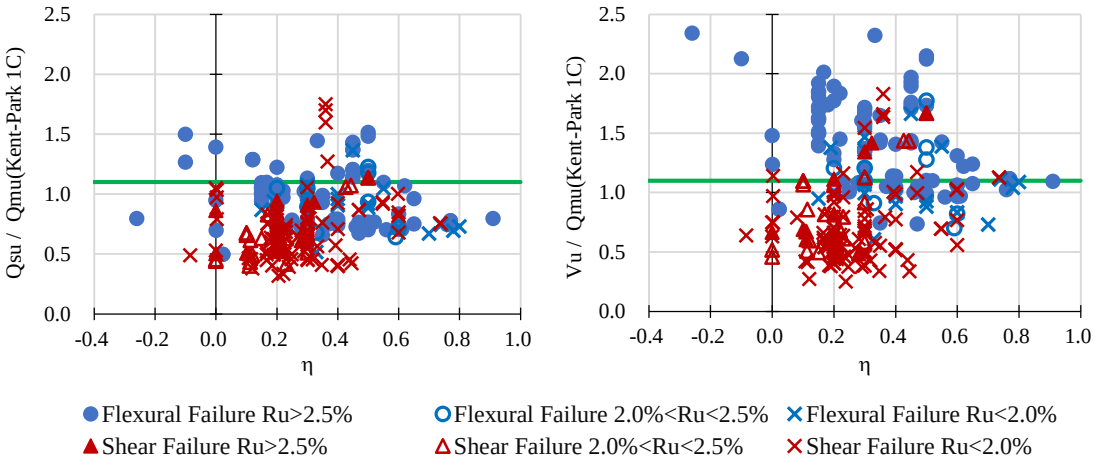

Figure 5-9 Q_{su}/Q_{mu} and V_u/Q_{mu} relationship for Q_{mu} (*Kent-Park 1C*) method

Figure 5-10 presents the relationship of the Q_{su}/Q_{mu} and V_u/Q_{mu} relationship for Kent-Park method the concrete cover in both direction of the cross section (*Kent-Park 2C*). The percentage of the columns failing in shear had $Q_{su}/Q_{mu(Kent\text{-}Park\ 2C)}$ larger than 1.1 was 3.6%; columns with flexural failure that had relationship $Q_{su}/Q_{mu(Kent\text{-}Park\ 2C)}$ larger than 1.1 was 15.5%. The percentage of the relationship $V_u/Q_{mu(Kent\text{-}Park\ 2C)}$ larger than 1.1 for columns with shear failure is 10.4% and the percentage of the relationship $V_u/Q_{mu(Kent\text{-}Park\ 2C)}$ larger than 1.1 for columns in flexural failure was 68.2%. This means that the relationship $V_u/Q_{mu(Kent\text{-}Park\ 2C)}$ is a better index to avoid shear failure because when the Kent-Park method include the concrete cover in both direction of the cross section.

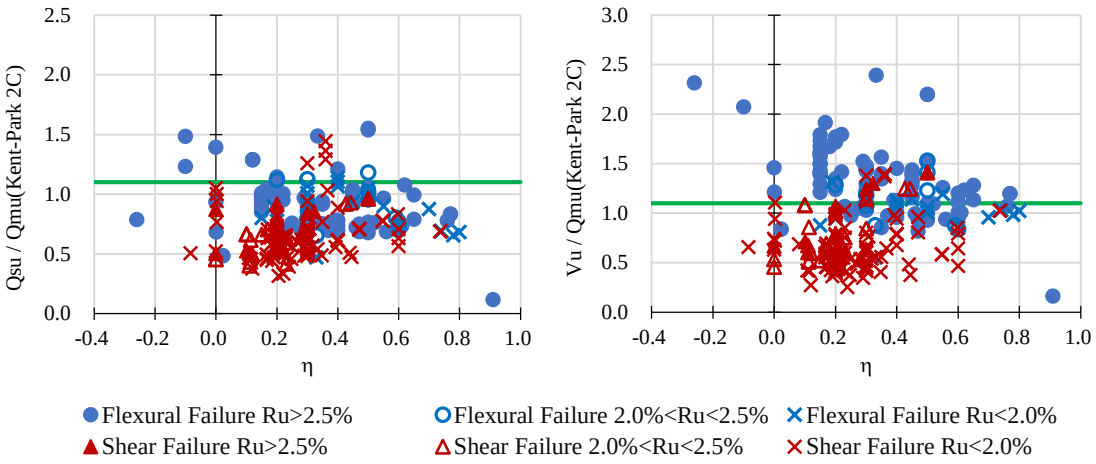

Figure 5-10 Q_{su}/Q_{mu} and V_u/Q_{mu} relationship for Q_{mu} (Kent-Park 2C) method

Figure 5-11 presents the relationship of the Q_{su}/Q_{mu} and V_u/Q_{mu} relationship for New RC disregarding of the concrete cover in the cross section (*NewRC 0C*). The percentage of the columns failing in shear mode had $Q_{su}/Q_{mu(NewRC\ 0C)}$ larger than 1.1 was 3.2%; columns with flexural failure mode that had relationship $Q_{su}/Q_{mu(NewRC\ 0C)}$ larger than 1.1 was 22.4%. The percentage of the relationship $V_u/Q_{mu(NewRC\ 0C)}$ larger than 1.1 for columns with shear failure is 8.4% and the percentage of the relationship $V_u/Q_{mu(NewRC\ 0C)}$ larger than 1.1 for columns in flexural failure was 77.5%. As it was in the previous cases, when the V_u is employed better is the results for index to avoid shear failure.

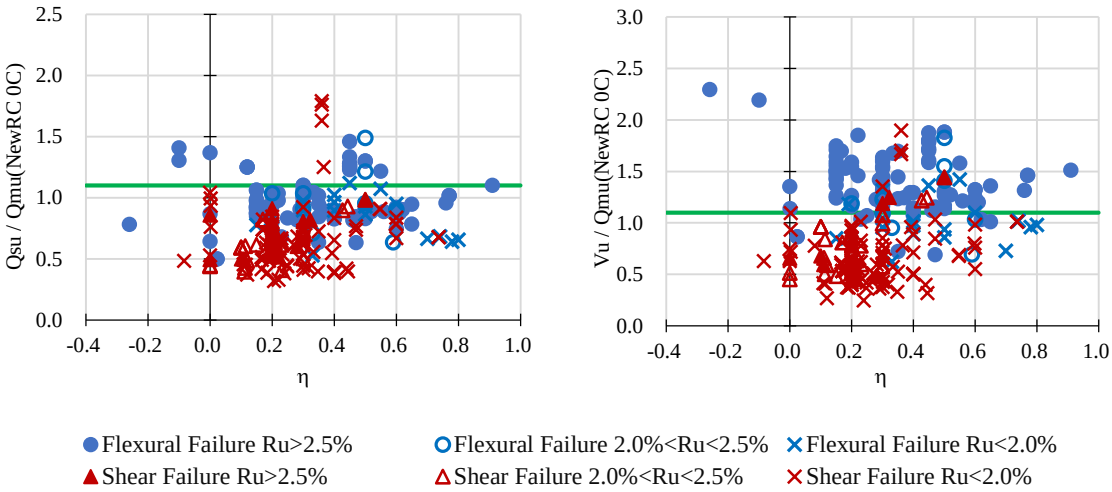

Figure 5-11 Q_{su}/Q_{mu} and V_u/Q_{mu} relationship for Q_{mu} (*New RC 0C*) method

Table 5-1 presents the summary of the results of the index to avoid shear failure calculated in this section. In this table, it is shown the percentages of specimens with shear strength - flexural strength relationship larger than 1.1 for both cases of flexural and shear failure mode. In general, the larger indexes which employed V_u included most of the columns with flexural failure, the indexes which employed Q_{su} included lower quantity of columns with flexural failure.

The best analysis is for the combination of the shear strength V_u obtained by equation 5-2 and the flexural strength obtained by the fiber analysis that employed the "*New RC*" confinement concrete model [5.5] with including 77.5% of the experimental results failing by flexural mode. Not so much difference is found for the index of $V_u/Q_{mu,}$ this index included 75.9% of the columns with flexural behavior, but also it includes 10.4% of the columns failing in shear mode.

One objective of this section is to improve the index to avoid shear failure that include the larger quantity of experiments that have not being taken in account in the structural design and preformed high ductility. From this point of view, the two adobe mentioned methods result are convenience, but in this research, it is proposed as index to avoid shear failure the relationship obtained with equation 5-6 given the fact the components are more common used in the practice than the any fiber analysis.

Table 5-1 Summary of percentage of columns corresponding to each index combination to avoid shear failure

Model			Kent - Park			New RC
	Failure	Q_{mu}	0C	1C	2C	0C
Q_{su}	Shear	0.5%	2.6%	7.1%	3.6%	3.2%
	Flexural	14.7%	9.3%	33.3%	15.5%	22.4%
V_u	Shear	10.4%	5.2%	14.8%	10.4%	8.4%
	Flexural	75.9%	57.4%	68.2%	68.2%	77.5%

$$\frac{V_u}{Q_{mu}} > 1.1 \qquad (5\text{-}6)$$

5.3. Quantity of shear reinforcement

It is well known that columns can develop high ductility if enough lateral reinforcement is provided. AIJ [5.2] suggests the equation 2-1 to delimit a minimum quantity of shear reinforcement in function of the applied axial force ratio (besides other parameters) for columns that should develop large ductility in flexural failure.

$$p_w \, \sigma_{we} \, / \, \upsilon_0 F_c \, \geq 0.30\eta^2 + 0.10 \qquad (2\text{-}1)$$

The first part of this equation is a coefficient of the strength of shear reinforcement ($p_w \, \sigma_{we}$) and the effective strength of concrete ($\upsilon_0 F_c$), this coefficient is compared with a second degree function of the axial force ratio ($0.30\eta^2 + 0.10$) to delimit the minimum reinforced needed for the applied axial force.

The equation 2-1 considers the quantity of shear reinforcement, yielding strength of lateral reinforcement and the compressive strength of concrete but, in this section, a better approximation that includes additional factors will be proposed.

In order to improve the equation 2-1, it was expected to include the effect of axial reinforcement and aspect ratio of the columns in the proposed formulation.

The proposed formulation comes from equation 2-5 Ref. [5.2], where the lateral participation of the axial reinforcement in tension, concrete compressive strength, the aspect relationship, strength of shear reinforcement and axial stress are taking in account as the empirical stress to determine the shear strength.

All these factors compound the stress participation to get the shear strength as the addition of three parts. Equation 2-5 is repeated in the next page.

The first part is the stress participation of the longitudinal characteristics of the column (τ_V), it includes the axial reinforcement in tension (p_t), concrete compressive strength (f_c), and the aspect ratio M/Qd. This relationship is given by equation 5-7. This equation defines the stress participation of the vertical components in the empirical determination of the shear strength, for that reason it was named as τ_V.

The second part of equation 2-5 is the stress participation of the horizontal reinforcement (τ_H), this includes the quantity of lateral reinforcement (p_w) and its effective strength of shear reinforcement (σ_{we}) multiplied by a reduction factor of 0.85. This part is shown in equation 5-8.

Finally, the last part of equation 2-5 is the axial stress participation shown in equation 5-9, this factor is defined as the friction coefficient of the concrete in linear function of the axial stress (σ_0).

The addition of these three stress factors is multiplied by the base of the cross section (b) and distance between centers of stress (j) to determine the empirical shear strength.

$$Q_{su} = \left\{ \frac{0.068 P_t^{0.23}(f_c + 18)}{\frac{M}{Qd} + 0.12} + 0.85\sqrt{P_w \sigma_{wy}} + 0.1\sigma_0 \right\} bj \tag{2-5}$$

$$\tau_V = \frac{[0.068 p_t^{0.23}(f_c + 18)]}{\left(\frac{M}{Qd} + 0.12\right)} \tag{5-7}$$

$$\tau_H = 0.85\sqrt{p_w \sigma_{we}} \tag{5-8}$$

$$0.1\sigma_0 \tag{5-9}$$

In equation 5-8, the strength of shear reinforcement σ_{wy} of equation 2-5 is replaced by the effective strength shear reinforcement $\sigma_{we} = \min(\sigma_{wy}, 85\sqrt{F_C})$ (MPa).

The proposed equation to delimit a minimum quantity of shear reinforcement uses the coefficient of stress participation of the vertical components and the stress participation of the horizontal reinforcement; it means the factor between the equations 5-7 and 5-8 (τ_H / τ_V), this is the Shear stress index.

Comments

The relationship τ_H and τ_V is presented in Figure 5-12. In this figure some comments are drown:

−The columns with shear failure and R_u lower than 2.5% had lower values of the relation $p_w\ \sigma_{we}$ (in in function of τ_V).

−The columns with shear failure and R_u between 2% and 2.5% are in general in the middle values of $p_w\ \sigma_{we}$ for every value of τ_V.

−The columns, with shear failure and R_u larger than 2.5%, are spread between middle and low values of $p_w\ \sigma_{we}$ for every value of τ_V.

−The columns failing in flexural mode which developed R_u lower than 2.5% are placed in the middle of the data for every value of τ_V.

−The high values of this relationship τ_H for every value of τ_V correspond, in general, for the columns with flexural failure and large R_u values.

Summarizing, columns with flexural failure have large values of τ_H but, a minimum value of τ_H in columns to develop flexural behavior deepens on the value of τ_V. The larger is τ_V, the larger is the needed τ_H to develop flexural behavior.

The relationship τ_H / τ_V is useful to classify the columns by failure mode and ductility performance but, in the middle of the plot of Figure 5-12 the transition area between shear and flexural failure is not clear.

On the other hand, the relationship of the strength of shear reinforcement $(p_w\ \sigma_{we})$ and the effective strength of concrete $(\upsilon_0 F_c)$ of the equation 2-1 is shown in Figure 5-13. In this figure, it can be seen that:

-Most of the columns that presented shear failure with R_u lower than 2% had lower relationship of $p_w\sigma_{we}\ /\ \upsilon_0 F_c$ but there are also this type of columns when $\upsilon_0 F_c$ increases.

-The columns with shear failure and R_u larger than 2% are spread all over the figure.

-Columns failing in flexural mode with R_u lower than 2.5% are in the lower values of $p_w\sigma_{we}$ according to every case of $\upsilon_0 F_c$.

-The larger values of the relationship $p_w\sigma_{we}$ in every case of $\upsilon_0 F_c$ correspond to the columns failing in flexural mode that developed R_u larger than 2.5%. In this case, a relationship between failure mode and ultimate lateral drift angle can be observed.

As a synthesis of the comparison of the relationships to define a minimum value of shear reinforcement enough to develop desirable ductility in flexural failure mode, it can be said that both relationships classified satisfactorily the columns. However, in both cases the limit between columns that develop R_u larger than 2.5% is not completely clear, both, it is in the case of the τ_H / τ_V in function that the limit is easier to understand according to the increment of τ_V. In the next, it will be explained how the limit for the relationship τ_H / τ_V in function of the axial force ratio is adapted.

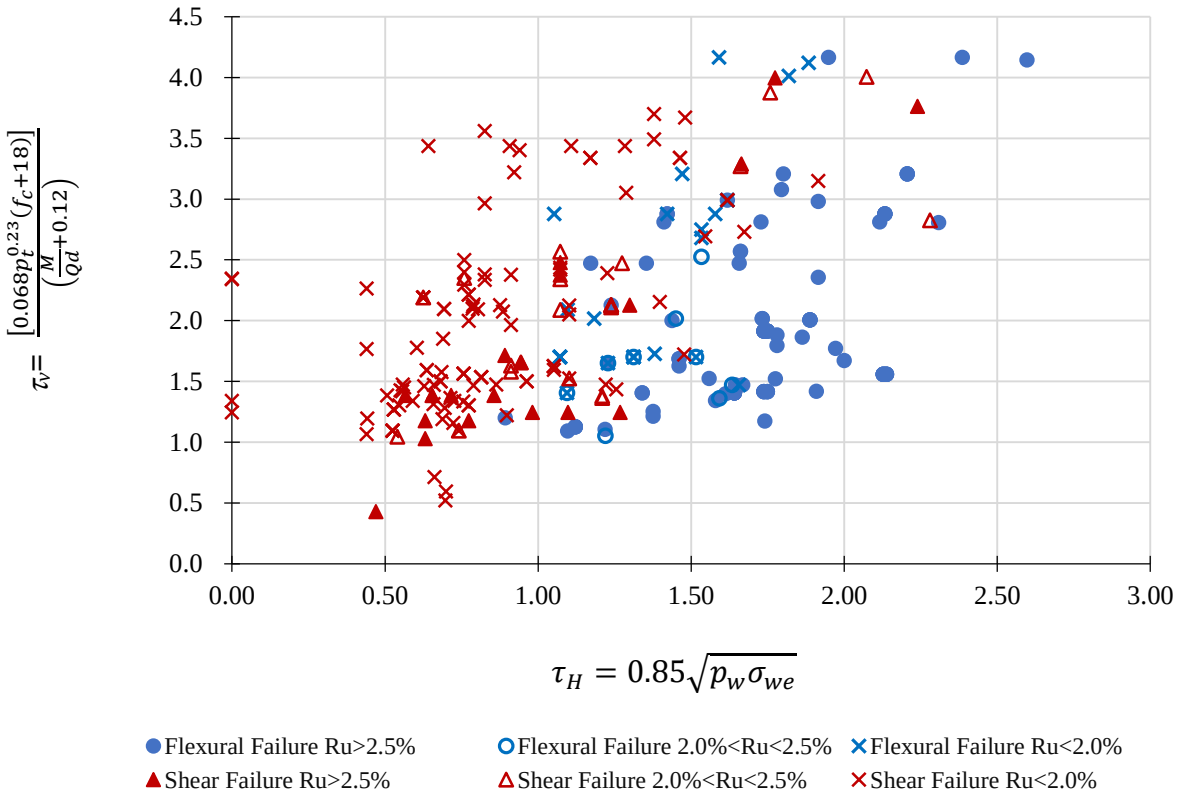

Figure 5-12 τ_v - τ_h relationship

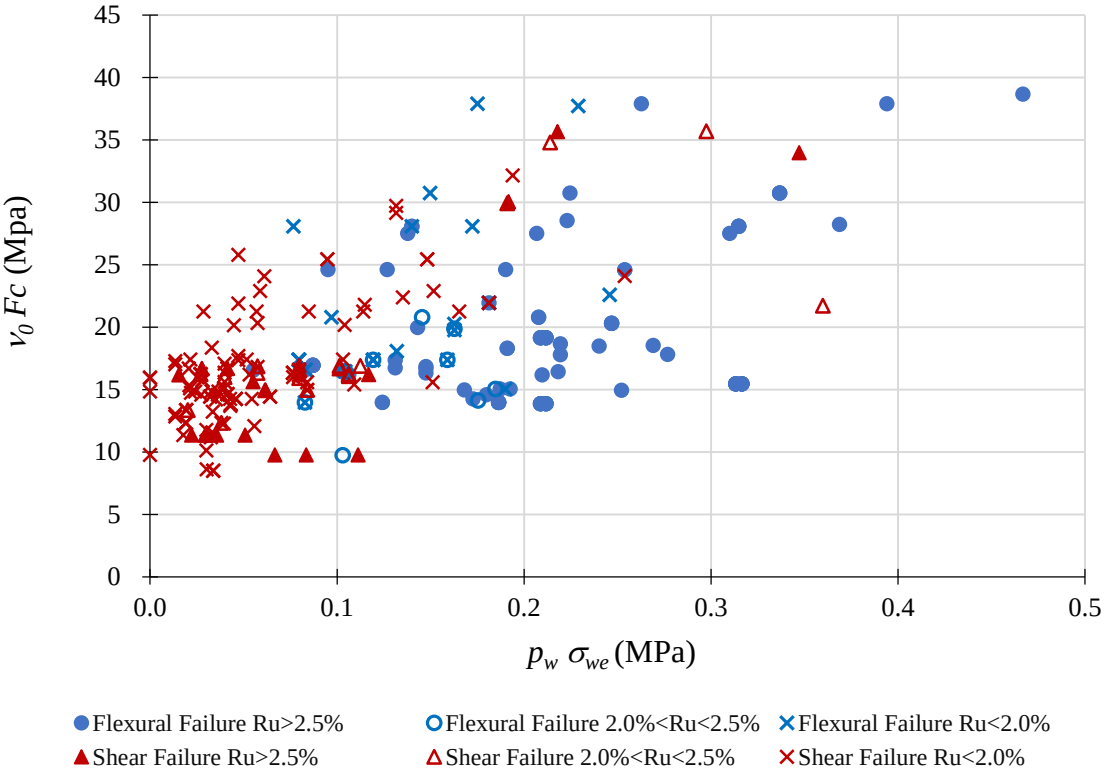

Figure 5-13 Shear reinforcement force – effective concrete strength relationship

Limit for the relationship τ_H / τ_V

The relationship $p_w\ \sigma_{we} / v_0 F_c$ is presented in function of the axial force ratio in Figure 5-14, the continuous line corresponds to the adjustment equation of $0.30\eta^2 + 0.10$. The columns that are over the adjustment are considered as high ductility columns besides other requirements [5.2]. In this figure, it can be observed that some columns failing in shear are over the adjustment, and some values of columns failing by flexural mode with R_u lower than 2.5% are under this limit. The requirement of equation 2-1 by itself cannot classify the columns by failure mode or ductility performance.

Similar phenomenon happens in the τ_H / τ_V relationship, it is presented in function of the axial force ratio in Figure 5-15 where, most of the columns failing by flexural mode with high value of R_u are in the upper part of the figure. At the bottom of the figure, most of the columns failing by shear can be observed. The transition between high and low ductility performance is located between this two areas where, particular cases will be explained in the next paragraph.

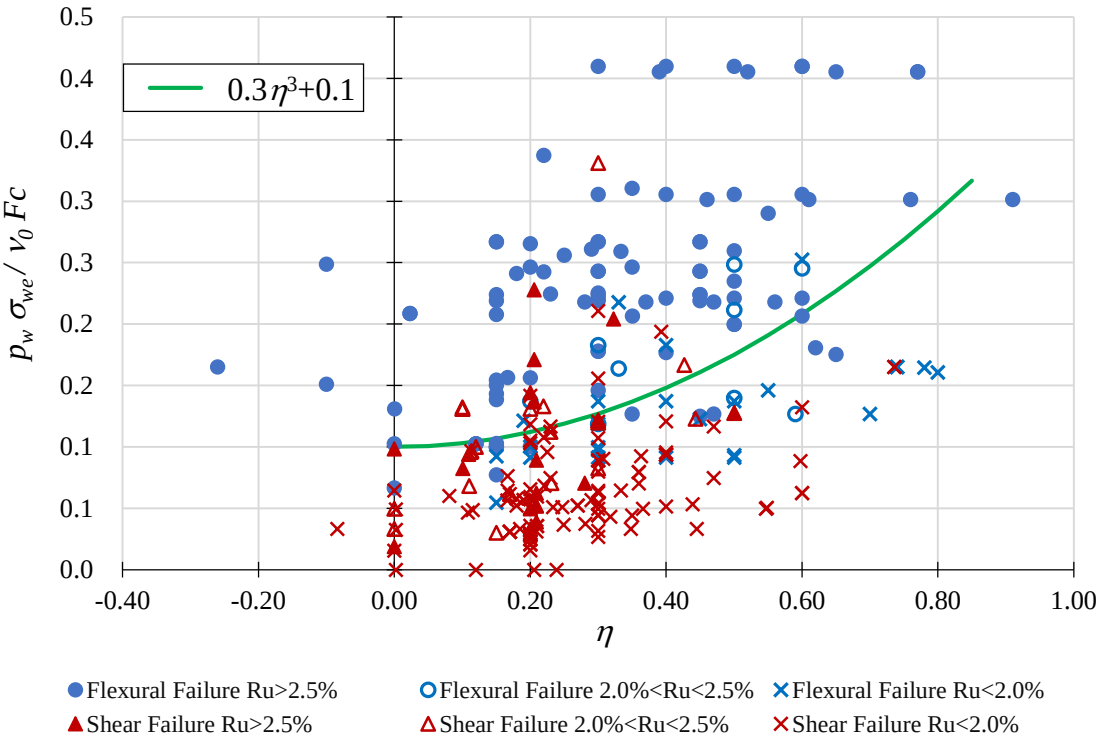

Figure 5-14 Shear reinforcement index –axial force ratio relationship

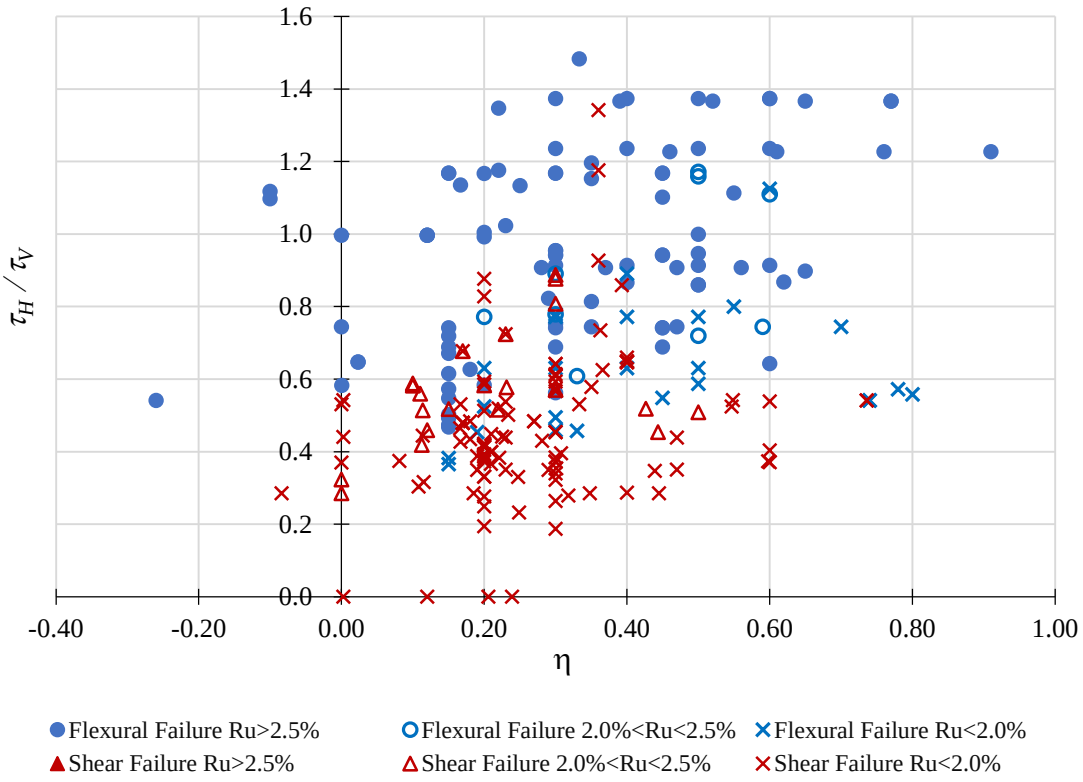

Figure 5-15 Shear stress index – axial force ratio relationship

First, the data presented in Figure 5-15 was filtrated with the proposal equation to classify columns as flexural failure (Eq. 5-6), it means that the columns with relationship $V_u/Q_{mu} < 1.1$ were eliminated from this figure. Then, Figure 5-16 shows the columns that agree the requirement of $V_u/Q_{mu} > 1.1$, the name of particular cases have been written.

For columns failing by shear mode and R_u lower than 2.0%, the numbered case 274 from Appendix 1 is a column with high yielding strength, σ_{wy}= 904MPa, $p_w =$ 0.52%, and $p_g =$ 1.7% (besides other characteristics). This column did not have any problem according to requirement of V_u/Q_{mu} but anyway it developed R_u = 2.1%. This case is important point in the stetting of the limit of minimum quantity of shear reinforcement and cannot be ignored.

For columns failing by shear mode and R_u between 2.0% and 2.5%, the numbered cases 271 and 272 from Appendix 1, named D-3 and S-3 respectively, presented the particularity that the quantity of hoops and ties are lower than 4. Then, the columns that contain less than 4 of total number of hoop bars, ties or crossties are eliminated of the data of Figure 5-15.

No columns failing by shear mode and R_u larger than 2.5% were eliminated due the fact that they did not present any especial characteristics.

For columns failing by flexural mode and R_u lower 2.5%, the numbered case 30 from the Appendix 1, named CA060C, presented physic characteristics that it is similar to all that columns that have flexural failure and desirable ductility. Nevertheless, in this case the developed ultimate drift angle was 1.5%, which is notably so much lower than that expected for high ductility columns. It is difficult to determine the exactly difference, two factor contributed to this result, the first is that the column was tested with 3 time cyclical lateral loading, it is larger than the most of the other cases tested with only 2 cyclical, given this fact, this column reduces its lateral capacity at sooner lateral drift angle than in regular cases. The second reason is the spacing between hoops, this column was tested with axial force ratio of 0.60 quantitatively large axial force where the effect of buckling of the bars is more important. The relationship is S/ϕ = 7.1, where S is the spacing between hoops and ϕ is the diameter of the smallest main reinforcement bar, which is larger than that recommend by the bibliography [5.9]. For the second reason, the columns that presented $S/\phi > 6.0$ where eliminated from the data of Figure 5-15. Column numbered 92 in the Appendix 1, named HDC-3, presented the same problem of this column, both for column 92 the relationship of $S/\phi > 6.0$.

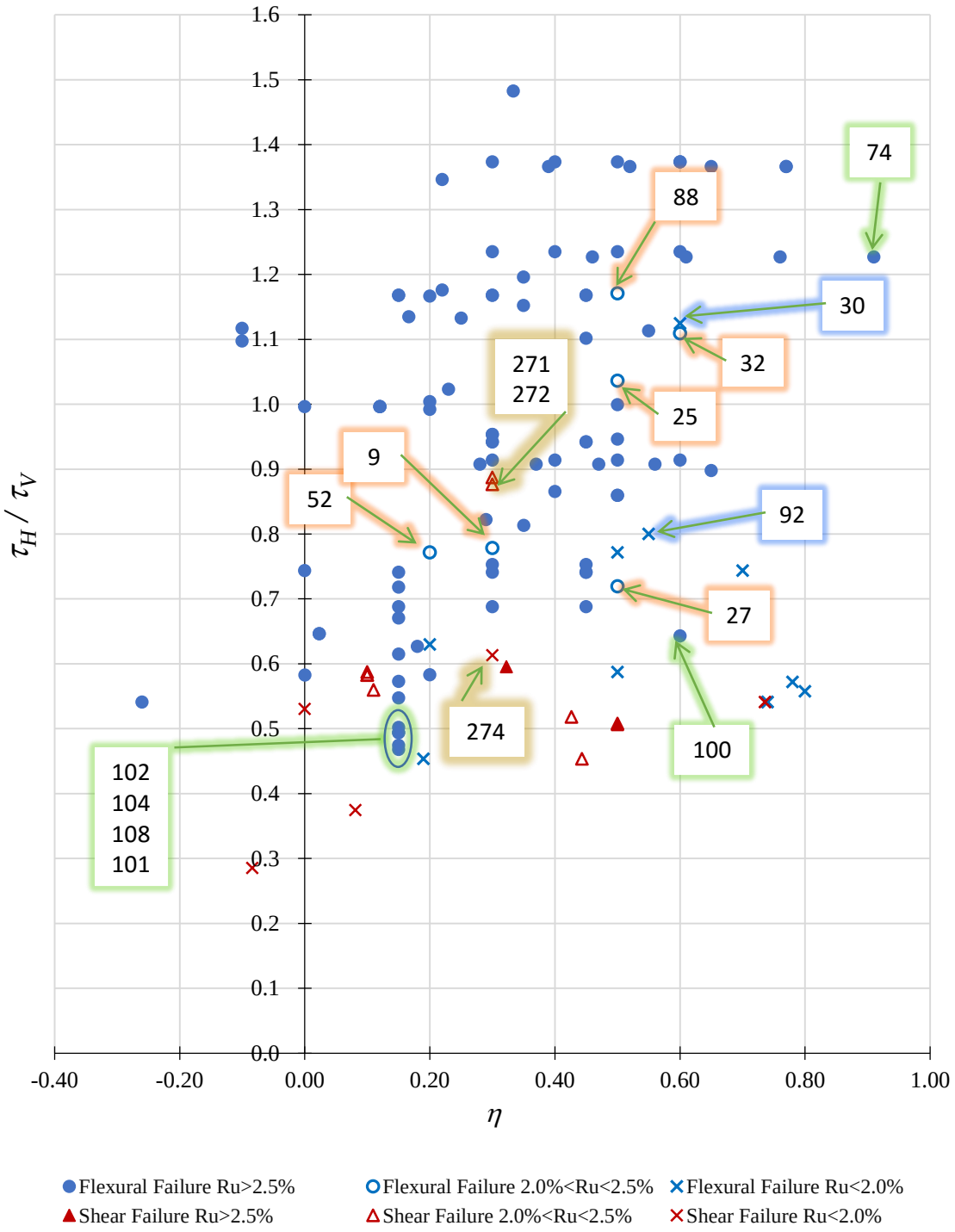

Figure 5-16 Shear stress index –axial force ratio relationship

For columns failing by flexural mode and R_u between 2.0% and 2.5%, the named case 9 of the Appendix 1 developed ultimate lateral drift angle of 2.0%, that can be considered as a minimum from the point of view of the ductility performance. The value of σ_{wy} was 925MPa and low value of p_w= 0.40, in this case the high value of yielding

strength give to the column τ_H / τ_V is larger compared with the columns that use normal strength reinforcement and same p_w. This is an example of why the value of σ_{wy} is limited to σ_{we} as mentioned before.

The numbered case 25 and 27, named F-3 and F-5 respectively in the Appendix 1, presented the same problem than in the previous case, large value of yielding strength in the lateral reinforcement. All the characteristics in the columns are the same, the only difference is the strength of concrete, which in column 27 is 43MPa, three times larger than that in column 25, this gives as a result that the coefficient τ_H / τ_V of column 25 is much larger than that in column 27. This has highlighted that the influence of the strength of concrete in equation 5-7 and the reduction of the yielding strength of the lateral reinforcement in equation 2-1 are not completely accurate when large strength of materials is employed.

The numbered case of 32 in the Appendix 1, named CA01T06C, presented *S/ϕ>= 7.3*. The case was eliminated from the data of Figure 5-15 even the fact that this value developed R_u= 2.2 % which can be considered as acceptable ductility behavior, it is implied that the buckling in the columns had large effect in the behavior of this column.

The numbered case 88 (named RCC-SN-3) from the Appendix 1 is not eliminated from the data of Figure 5-15 because no special characteristics were found. This column, as well as some of the previous ones, has not acceptable value of ultimate drift angle.

For columns failing by flexural mode and R_u larger than 2.5%, the numbered 74 in the Appendix 1 was tested with vary axial force, there is no reason to eliminated this column but, it is important to notice that in this column is applied so much larger axial force ratio, η =0.91.

The named case of 102, 104, 108, and 101 from the Appendix 1 correspond to the cases where high axial strength of materials were used, this values are not eliminated from the data of Figure 5-15 but they are warily considered in the adjustment of the limit for the relationship τ_H / τ_V.

Summarizing the previous paragraphs, the columns with *S/ϕ> 6.0* were eliminated from the useful data due to the influence of the buckling of the rebar. In the same way, the columns that have less than 4 reinforcing lateral bars were eliminated from the data. The columns failing by flexural mode and R_u between 2.0% and 2.5% that have V_u/Q_{mu} larger than 1.1 were kept. The ductility and characteristics of the rest of the columns are considered accepted.

The final useful data for the adjustment for the limit of the relationship τ_H / τ_V is presented in Figure 5-17. So called limit will separate the column between desirable and undesirable performances. In this figure, the marked upper ellipse corresponds to columns that presented the desirable ductility behavior and the lower ellipse corresponds to the undesirable behavior in the structural design of RC columns. The area between these two ellipses represents the looked limit in this section. This limit will be adjusted with and exponential equation as it is explain in the next section.

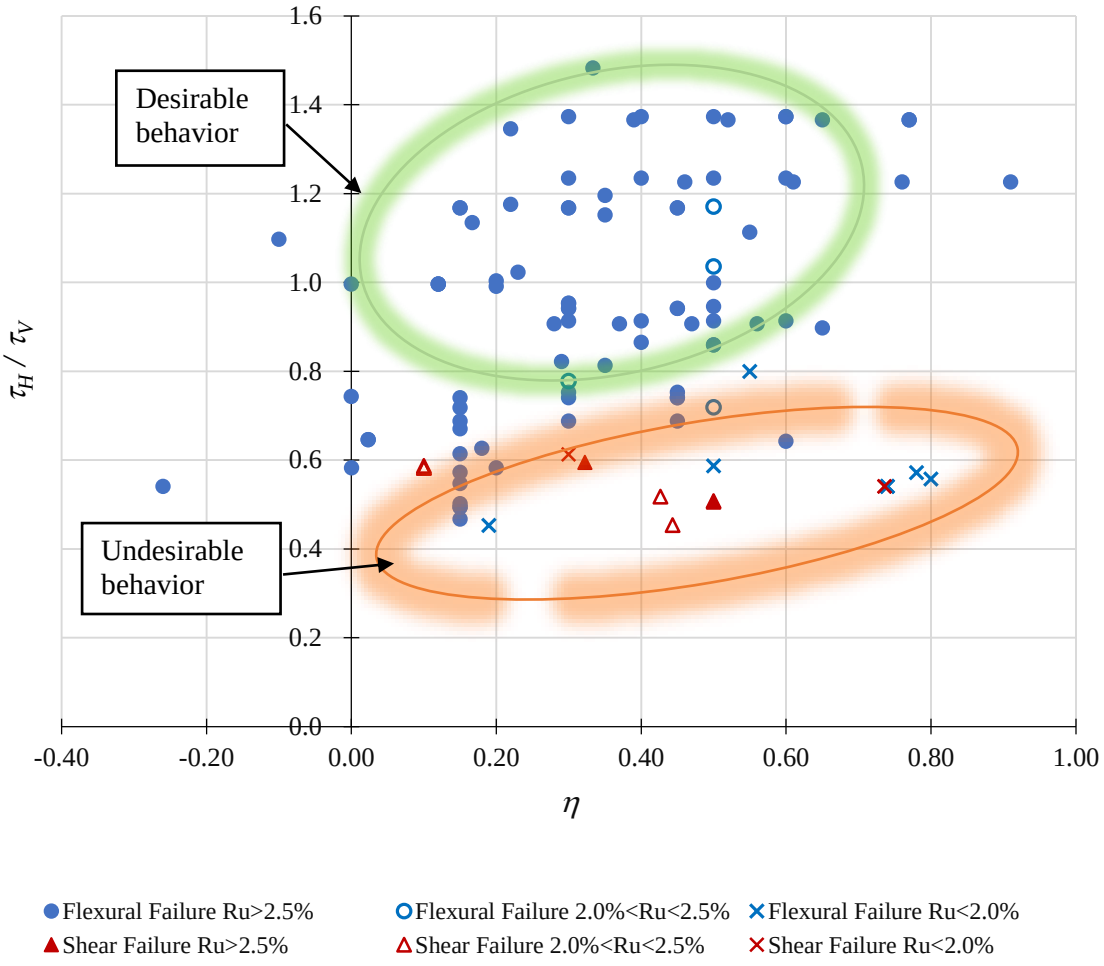

Figure 5-17 Desirable and undesirable behavior cases

Adjustment

In this section, the equation that defines the limit of the ratio τ_H/τ_V in function of η is proposed. This equation delimits the frontier between the desirable values and the no desirable ones.

During the research, many equations were tested in order to fix the frontier but at the end, an equation of third degree in the form $ax^3 + b$ was chosen. As it will be shown, the cubic exponent fixed better than any other to the increment of the ratio τ_H/τ_V when η increases. This equation not only match the tendency of the data but also it is enough simple to be used in the practice of structural design. In this way, the proposal equation is based in equation 5-10. That equation is called here as the Index of Shear Stress (τ_H/τ_V), it should be larger than the relation $a\eta^3 + b$ of the axial force ratio.

$$\frac{\tau_H}{\tau_V} \geq a\eta^3 + b \tag{5-10}$$

The adjustment of equation 5-10 was estimated with the method of least squares [5.10], this method easily generalizes to finding the best fit of the constants to equation 5-10 from the available data. The data correspond to that that is not into any ellipse marked in Figure 5-17, the list can be seen in Table 5-2.

Given the data $\{(x_1, y_1),\dots, (x_n, y_n)\}$ from Table 5-2, the error associated to the equation 5-10 may be defined as:

$$f(a,b) = \sum_i^n \left[\left(\frac{\tau_H}{\tau_V}\right)_i - (a\eta^3 + b)\right]^2 \tag{5-11}$$

The target is to find the value of the constants a and b that minimize the error. This can be found equalizing the first derived $f(a,b)$ with respect to each constant to cero:

$$\frac{df(a,b)}{da} = 0, \qquad \frac{df(a,b)}{db} = 0$$

First, the equation 5-11 is expanded, and the terms are ordered as:

$$f(a,b) = \sum_{i}^{n} \left[\left(\frac{\tau_H}{\tau_V}\right)_i^2 - 2a\eta_i^3 \left(\frac{\tau_H}{\tau_V}\right)_i - 2b\left(\frac{\tau_H}{\tau_V}\right)_i + a^2\eta_i^6 + 2ab\eta_i^3 + b^2 \right]$$

Differentiating $f(a,b)$ with respect to a and equalized to cero as:

$$\frac{d\sum_i^n \left[\left(\frac{\tau_H}{\tau_V}\right)_i^2 - 2a\eta_i^3 \left(\frac{\tau_H}{\tau_V}\right)_i - 2b\left(\frac{\tau_H}{\tau_V}\right)_i + a^2\eta_i^6 + 2ab\eta_i^3 + b^2 \right]}{da} =$$

$$2\mathrm{a}\sum_{i}^{n} \eta_i^6 + 2\mathrm{b}\sum_{i}^{n} \eta_i^3 - 2\sum_{i}^{n} \eta_i^3 \left(\frac{\tau_H}{\tau_V}\right)_i = 0 \qquad (5\text{-}12)$$

Differentiating $f(a,b)$ with respect to b and equalized to cero as:

$$\frac{d\sum_i^n \left[\left(\frac{\tau_H}{\tau_V}\right)_i^2 - 2a\eta_i^3 \left(\frac{\tau_H}{\tau_V}\right)_i - 2b\left(\frac{\tau_H}{\tau_V}\right)_i + a^2\eta_i^6 + 2ab\eta_i^3 + b^2 \right]}{db} =$$

$$2\mathrm{a}\sum_{i}^{n} \eta_i^3 + 2\mathrm{b}n - 2\sum_{i}^{n} \left(\frac{\tau_H}{\tau_V}\right)_i = 0 \qquad (5\text{-}13)$$

Equations 5-12 and 5-13 are the simultaneous equation of two unknown quantities that can be written as:

$$\begin{cases} \mathrm{a}\sum_{i}^{n} \eta_i^6 + \mathrm{b}\sum_{i}^{n} \eta_i^3 = \sum_{i}^{n} \eta_i^3 \left(\frac{\tau_H}{\tau_V}\right)_i \\ \mathrm{a}\sum_{i}^{n} \eta_i^3 + \mathrm{b}n = \sum_{i}^{n} \left(\frac{\tau_H}{\tau_V}\right)_i \end{cases}$$

Where the value of the new constants are calculated in Table 5-2, and presented in the next:

$$\sum_{i}^{n} \eta_i^6 = 1.04$$

$$\sum_{i}^{n} \eta_i^3 = 3.08$$

$$\sum_{i}^{n} \eta_i^3 \left(\frac{\tau_H}{\tau_V}\right)_i = 2.97$$

$$\sum_{i}^{n} \left(\frac{\tau_H}{\tau_V}\right)_i = 26.22$$

$$n = 36$$

Now, the simultaneous equation is reduced to the next form:

$$\begin{cases} 1.04a + 3.08\text{b} = 2.97 \\ 3.08a + 36\text{b} = 26.22 \end{cases}$$

Where the simultaneous equations were solved by the addition method [5.11]. The solution to the constants a and b is:

$f(a, b) = (0.936, 0.648)$

These values correspond to the numerical solution but these are not completely suitable for the practice of structural design, for that reason, the values are rounded to 1 and 0.65 to a and b respectively. Then, equation 5-10 can be defined finally as:

$$\frac{\tau_H}{\tau_V} > \eta^3 + 0.65 \tag{5-14}$$

This equation 5-14 corresponds to the Index of Shear Stress used to delimit the minimum quantity of shear reinforcement in RC columns. This equation can be written in it extended version as:

$$\frac{0.85\sqrt{p_w \sigma_{we}}}{\frac{[0.068 p_t^{0.23}(f_c+18)]}{\left(\frac{M}{Qd}+0.12\right)}} > \eta^3 + 0.65 \tag{5-15}$$

Table 5-2 Summary of specimens in the frontier

Column	η	$(\tau_H/\tau_V)_i$	$\eta^6{}_i$	$\eta^3{}_i$	$\eta^3{}_i(\tau_H/\tau_V)_i$
26	0.50	0.86	0.016	0.125	0.11
28	0.50	0.86	0.016	0.125	0.11
36	0.60	0.91	0.047	0.216	0.20
46	0.00	0.58	0.000	0.000	0.00
47	0.20	0.58	0.000	0.008	0.00
58	0.00	0.74	0.000	0.000	0.00
69	0.56	0.91	0.031	0.176	0.16
73	0.76	1.23	0.193	0.439	0.54
74	0.91	1.23	0.568	0.754	0.92
80	0.02	0.65	0.000	0.000	0.00
81	0.02	0.65	0.000	0.000	0.00
85	-0.26	0.54	0.000	-0.018	-0.01
96	0.18	0.63	0.000	0.006	0.00
103	0.15	0.67	0.000	0.003	0.00
105	0.15	0.61	0.000	0.003	0.00
106	0.45	0.75	0.008	0.091	0.07
109	0.15	0.57	0.000	0.003	0.00
112	0.30	0.75	0.001	0.027	0.02
114	0.15	0.74	0.000	0.003	0.00
115	0.30	0.74	0.001	0.027	0.02
116	0.45	0.74	0.008	0.091	0.07
121	0.45	0.74	0.008	0.091	0.07
130	0.15	0.69	0.000	0.003	0.00
131	0.30	0.69	0.001	0.027	0.02
132	0.45	0.69	0.008	0.091	0.06
137	0.15	0.72	0.000	0.003	0.00
380	0.65	0.90	0.075	0.275	0.25
9	0.30	0.78	0.001	0.027	0.02
27	0.50	0.72	0.016	0.125	0.09
24	0.50	0.59	0.016	0.125	0.07
92	0.55	0.80	0.028	0.166	0.13
360	0.32	0.60	0.001	0.034	0.02
290	0.10	0.59	0.000	0.001	0.00
291	0.1	0.58	0.000	0.001	0.00
292	0.1	0.58	0.000	0.001	0.00
274	0.3	0.61	0.001	0.027	0.02

Summary of specimens in the frontier

(continuation)

Column	η	$(\tau_H/\tau_V)_i$	$\eta^6{}_i$	$\eta^3{}_i$	$\eta^3{}_i(\tau_H/\tau_V)_i$
Σ	-	**26.22**	**1.04**	**3.08**	**2.97**

5.4. Additional requirements

Characteristic of the columns over the adjustment

The equation 5-14 of the Index of Shear Stress is presented in Figure 5-18. In this figure, the characteristics of the columns that are over the adjustment are presented in Table 5-3. This information is presented in 4 groups of axial force ratio: $0 < \eta < 1/6$, $1/6 < \eta < 1/3$, $1/3 < \eta < 1/2$, and $1/2 < \eta < 2/3$.

In this way, the design of columns should not only math the required of the equations Index to avoid shear failure and Shear stress index but also, the requirements of Table 5-3 according to every case of applied axial force ration.

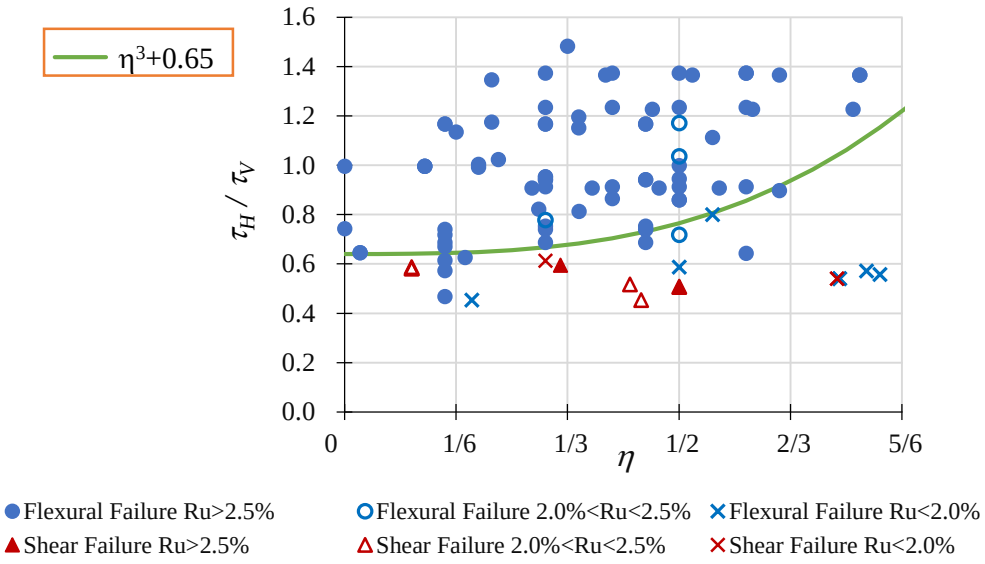

Figure 5-18 Adjustment funtion

For the special cases of $1/3 < \eta < 1/2$ and $1/2 < \eta < 2/3$ which can be considered as high axial force, it is important to mention that the compressive strength of concrete σ_B is limited to a maximum of 67MPa and 38MPa respectively. The yielding strength of longitudinal reinforcement $\sigma_y \leq$ 450MPa and yielding strength of lateral

reinforcement $\sigma_{wy} \leq 600$MPa. The limit of the strength of the materials is due to the ductile behavior. It was intended to avoid materials that present brittle failure even the fact that there are test results that presented large strength of σ_{wy}.

Additionally, the columns should have rectangular cross section, the aspect ratio h_0/D should be larger than 3.0, the ratio S/d should be lower than 0.38. For lateral reinforcement, more than four hoops and ties were arranged in the cross section. For rebar, more than 4 bars should be placed in each face of the cross section, all the reinforcing bars should be deformed bars. For the cases of $1/3 < \eta < 1/2$ the reinforcement ratio should be 1.4% < p_g < 2.3, and for the case of $1/2 < \eta < 2/3$, it should be 1.7% < p_g < 2.3%. The maximum axial force ratio is limited to that maximum axial force allowed by AIJ [5.2] at the final stage of the columns in the hinge region.

Table 5-3 Characteristics per axial force range

η		Fc		σ_y		σ_{wy}		p_g		$Ties$	h_0/D	S/d	R_u	p_w
		MPa		MPa		MPa		%		Pcs.			%	%
min	max	min	max	min	max	min	max	min	max	min	min	max	min	min
0	1/6	24	67	347	485	372	925	1.7	2.5	4	2.4	0.27	2.5	0.30
1/6	1/3	23	77	314	385	367	979	1.2	2.3	4	3.0	0.38	3.0	0.60
1/3	1/2	23	67	314	451	341	1398	1.4	2.3	4	3.0	0.38	2.0	0.75
1/2	2/3	23	38	363	423	341	396	1.7	2.3	4	3.0	0.38	2.5	0.87

5.5. Conclusion of Chapter 5

On this chapter, the proposal for the design of RC columns carrying high axial force was presented. Two equations were proposed:

The first one was the index to avoid shear failure. This equation was the result of the comparison of many other conventions of the coefficient of shear to flexural strength; this equation is thoroughly known and easy to be applied. This equation provided the most convenient way to classify the columns according to its failure mode. It is determinates as the relationship of the :

$$\frac{V_u}{Q_{mu}} \geq 1.1$$

-The second equation is the index of shear stress, this equation came from the empirical equation to get the lateral strength Q_{su}. This was the best result from many other conventions tested during the research.

$$\frac{0.85\sqrt{p_w \sigma_{we}}}{\frac{[0.068 p_t^{0.23}(f_c+18)]}{\left(\frac{M}{Qd}+0.12\right)}} > \eta^3 + 0.65$$

A list of additional requirements was also shown, these complement the requirements for the design of the columns.

Additional requirements

η		Fc		σ_y		σ_{wy}		p_g		*Ties*	h_0/D	S/d	R_u	p_w
		MPa		MPa		MPa		%		Pcs.			%	%
min	max	min	max	min	max	min	max	min	max	min	min	max	min	min
0	1/6	24	67	347	485	372	925	1.7	2.5	4	2.4	0.27	2.5	0.30
1/6	1/3	23	77	314	385	367	979	1.2	2.3	4	3.0	0.38	3.0	0.60
1/3	1/2	23	67	314	451	341	1398	1.4	2.3	4	3.0	0.38	2.0	0.75
1/2	2/3	23	38	363	423	341	396	1.7	2.3	4	3.0	0.38	2.5	0.87

Bibliography of Chapter 5

[5.1] The building center of Japan: The building standard low of Japan, June 2004.

[5.2] Architectural Institute of Japan: Calculation standard for horizontal load-carrying of reinforced concrete structure and comments (Public comments), 2014.12. http://www.aij.or.jp/jpn/symposium/2014/public_20141215.html

[5.3] Architectural Institute of Japan: Design guidelines for earthquake resistant reinforced concrete building based on inelastic displacement concept, 1999.

[5.4] Kent, D.C. and Park, R. “Flexural Members with Confined Concrete,” Journal of Structural Division, Proceedings of the American Society of Civil Engineers, 1971; Vol. 97(ST7): 1969-1990.

[5.5] 建設省総合技術開発プロジェクト鉄筋コンクリート造建築物の超軽量・超高層化技術の開発平成４年度 New RC 研究開発概要報告書, （財）国土開発技術研究センター, pp3-2-76 - 3-2-78, 1993.5

[5.6] CSA A23.3. *Design of Concrete Structures*, Canada Standard Association, Rexdale, Canada, 1994.

[5.7] Assa, B., Nishiyama, M. and Watanabe, F.,“New Approach for Modeling Confined Concrete”, Journal of Structural Engineering, July, pp.743-757, 2001

[5.8] 荒川 卓 : 鉄筋コンクリートはりのせん断抵抗に関する実験結果の綜合 , 日本建築學會研究報告 , 第 54 号 , pp.84-92, 1960

[5.9] Ministry of Land, Infrastructure, Transport, and Tourism: Technical standard manual concerned to the structure of buildings (2007), 2007.8.

[5.10] Harter, H.L.: "Least Squares," Encyclopedia of Statistical Sciences, Kotz, S. and Johnson, N.L., eds., John Wiley & Sons, New York, pp. 593-598, 1983

[5.11] Blyth T.S. and Robertson E.F.: Basic linear algebra, Springer, Berlin Germany, 1998

CHAPTER 6. CONCLUSIONS

6.1. Summary

In Japan, more and more tall buildings are being designed and constructed. For the columns that are located at the corners of lower floors of this kind of buildings, high axial force is demanded during an earthquake. To carry the demanding high axial force, high strength concrete and rebar are mainly used in this type of columns. For the structural design, it is an important matter to know if a column will fail in shear or flexural mode, and if columns can develop enough ductility under specific axial force.

With regard to the latter, this work focused in propose a criteria to design columns that develop large ductility when high axial force is applying during an earthquake. The next paragraphs summarize every of the chapter presented previously.

During Chapter one, General view of the seismicity in Japan and the problematic was presented. The problem was presented through one of the most famous cases ever recorded in the history of the earthquake engineering. This case had the problem that many columns face when an earthquake occurs, an increment of the axial force. At the end of this chapter, it is summarized that the increment of the axial force during the seismic event can lead to the collapse of the complete structure if the columns are not well designed to develop large ductility.

In the second chapter, the study of the current bibliography in this matter was presented. The new proposals of AIJ for the design drastically decremented the requirements for the design of this type of columns. Additionally, no column that meet the minimum requirements of the new proposals of AIJ was found in the bibliography of Japan experimental results. Therefore, the new criteria to design columns with high axial force ratio of AIJ was evaluated.

This evaluation was presented in the Chapter 3, were, the most important results were linked to the failure mode of the columns, all of them develop desirable ductile behavior but the failure mode at the final stage was considered unacceptable. Another problem was the unreliability of the current index to avoid shear failure that underestimate the ductile capacity of many kind of columns.

In the next chapter, Chapter 4, the called “Behavior Database” was presented. This database contains the Skelton curves of 368 experimental tests of RC columns with different characteristics in order to know the developed ductility of each test result. The process of compilation was explained in the chapter, and the evaluation of the ductility of the columns was done by some methods. As a result, it can be said that the current philosophy of design is ignoring large quantity of columns that presented desirable behavior but this are not qualify as potential toughness columns.

Collecting the information from the evaluation of the current design criteria and the experimental results from the databases, the proposal for the design of columns that develop large ductility under high axial force during an earthquake was presented Chapter 5. As a result, two main equations that ensure the flexural failure and large ductility behavior were proposed. These equations are the Index to avoid shear failure and the Index of Shear Stress. Additionally characteristic requirements to ensure a proper design in the columns were attached.

The summary of the proposal for the structural design is presented in the section 6.2 of this Chapter.

6.2. Proposal summary

The design of RC columns that carry high axial force can be done following the next three requirements:

◆Index to Avoid Shear Failure:

$$\frac{V_u}{Q_{mu}} \geq 1.1$$

–*Shear strength* V_u (N)

It is given by the minimum value of the next equations:

$$V_u = \mu P_{we}\sigma_{wy} b_e j_e + \left(\upsilon\sigma_B - \frac{5P_{we}\sigma_{wy}}{\lambda}\right)\frac{bD}{2}\tan\theta$$

$$V_u = \left(\frac{\lambda\upsilon\sigma_B + P_{we}\sigma_{wy}}{3}\right) b_e j_e$$

$$V_u = \left(\frac{\lambda\upsilon\sigma_B}{2}\right) b_e j_e$$

Where:

$\mu = 2 - 20R_p$

R_p*=0,* Rotation angle

υ is the effective compressive strength coefficient, υ*=(1-20*R_p*)*υ_0

υ_0*=0.7-*$\frac{\sigma_B}{200}$

p_{we}: effective shear reinforcement ratio

σ_{wy}: strength of shear reinforcement (MPa)

j_e: effective height of the cross section participating in the truss mechanism (mm), it could be the distance center to center of extern line of the lateral reinforcement in the height of the cross section

b_e: effective width of the cross section participating in the truss mechanism (mm), it could be the distance center to center of extern line of the lateral reinforcement in the width of the cross section

b: width of the cross section (mm)

D: height of the cross section (mm)

σ_B compressive strength of concrete (MPa)

$tan\,\theta = \frac{\sqrt{L^2-D^2}-L}{D}$: angle formed by the truss mechanism (rad)

L: height of the clear span of the column (mm)

$\lambda = 1 - \frac{S}{2j_e} - \frac{b_s}{4j_e}$

S : spacing between hoops (mm)

$b_s = \frac{b_e}{N_s+1}$

N_s: number of tie bars

-Flexural strength Q_{mu} (N)

$$Q_{mu} = \frac{M_u}{M/Q}$$

Where:

M_u: ultimate bending moment (N•mm)

M/Q: shear span (mm)

The ultimate bending moment M_u is determined according to the axial force N as follows:

If $N_{min} \le N \le 0$

$$M_u = \frac{1}{2}a_g\sigma_y g_1 D + \frac{1}{2}NDg_1$$

If $0 \le N \le N_b$

$$M_u = \frac{1}{2}a_g\sigma_y g_1 D + \frac{1}{2}ND\left(1 - \frac{N}{bD\sigma_B}\right)$$

If $N_b \le N \le M_{max}$

$$M_u = \left\{\frac{1}{2}a_g\sigma_y g_1 D + 0.024(1+g_1)(3.6-g_1)bD^2\sigma_B\right\}\left(\frac{N_{max}-N}{N_{max}-N_b}\right)$$

$N_{min} = -a_g \sigma_y$ (N)

a_g: total area of longitudinal reinforcement (mm)

σ_y: yield stress of longitudinal reinforcement (MPa)

g_1: d'' / D

d'' : distance between the center of gravity of longitudinal bars in tension and the center of gravity of longitudinal bars in compression (mm).

$N_{max} = bdF_c + a_g \sigma_y$

$N_b = 0.22(1 + g_1) bD\sigma_B$

◆ Shear Stress Index:

$$\frac{0.85\sqrt{p_w \sigma_{we}}}{\frac{[0.068 p_t^{0.23}(\sigma_B + 18)]}{\left(\frac{M}{Qd} + 0.12\right)}} \geq \eta^3 + 0.65$$

p_w: shear reinforcement ratio (%)

σ_{we}: effective strength of shear reinforcement, $\sigma_{we} = \min(\sigma_{we}, 85\sqrt{\sigma_B})$ (MPa)

p_t: main reinforcement ratio in tension

d: effective height of the cross section (mm)

$\eta = \frac{\sigma_0}{\sigma_B}$ Axial force ratio

σ_0: axial stress in the column $\sigma_0 = N/bD$ (MPa)

N : axial force (N)

p_g: total main reinforcement ratio

◆And also, the design should meet the characteristics of the next table according to the axial force ratio.

Additional requirements

η		σ_B		σ_y		σ_{wy}		p_g		*Ties*	h_0/D	*S/d*	R_u	p_w
		MPa		MPa		MPa		%		Pcs.			%	%
min	max	min	max	min	max	min	max	min	max	min	min	max	min	min
1/3	1/2	23	67	314	451	341	1398	1.4	2.3	4	3.0	0.38	2.0	0.75
1/2	2/3	23	38	363	423	341	396	1.7	2.3	4	3.0	0.38	2.5	0.87

For the special cases of $1/3 < \eta < 1/2$ and $1/2 < \eta < 2/3$ is important to mention that the compressive strength of concrete σ_B is limited to a maximum of 67MPa and 38MPa respectively. The yielding strength of longitudinal reinforcement $\sigma_y \leq$ 450MPa and yielding strength of lateral reinforcement $\sigma_{wy} \leq 600$MPa.

Additionally, the columns should have rectangular cross section, the aspect ratio h_0/D should be larger than 3.0, the ratio *S/d* should be lower than 0.38. For lateral reinforcement, more than four hoops and ties were arranged in the cross section. For rebar, more than 4 bars should be placed in each face of the cross section, all the reinforcing bars should be deformed bars.

For the cases of $1/3 < \eta < 1/2$ the reinforcement ratio should be 1.4% < p_g < 2.3, and for the case of $1/2 < \eta < 2/3$, it should be 1.7% < p_g < 2.3%. The maximum axial force ratio is limited to that maximum axial force allowed by AIJ [5.2] at the final stage of the columns in the hinge region.

APPENDIX 1

Characteristics of the RC columns

Columns's characteristics

Num.	Denomination			Dimentions					Materials		
	Name	Ref.	Digital file	b	D	h_0	h_0/D	d/D	σ_B	σ_y	σ_{wy}
				mm	mm	mm			MPa	MPa	MPa
1	06-1.5-1	[4-1]	柱-1991-AIJ-2	200	200	600	3.0	0.80	44	724	768
2	No.1	[4-2]	柱-2002-梗-2	350	350	1050	3.0	0.80	24	446	925
3	No.2	[4-2]	柱-2002-梗-2	350	350	1050	3.0	0.80	24	446	925
4	No.3	[4-2]	柱-2002-梗-2	350	350	1050	3.0	0.80	24	446	925
5	No.4	[4-2]	柱-2002-梗-2	350	350	1050	3.0	0.80	24	446	925
6	No.5	[4-2]	柱-2002-梗-2	350	350	1050	3.0	0.80	24	446	925
7	No.6	[4-2]	柱-2002-梗-2	350	350	1050	3.0	0.80	41	446	925
8	No.7	[4-2]	柱-2002-梗-2	350	350	1050	3.0	0.80	41	446	925
9	4	[4-3]	柱-2002-年-1	300	300	900	3.0	0.79	14	340	384
10	6	[4-3]	柱-2002-年-1	300	300	900	3.0	0.79	14	340	384
11	8	[4-3]	柱-2002-年-1	300	300	900	3.0	0.79	18	340	384
12	10	[4-3]	柱-2002-年-1	300	300	900	3.0	0.79	18	340	384
13	12	[4-3]	柱-2002-年-1	300	300	900	3.0	0.79	18	340	384
14	No.2-5	[4-4]	柱-2004-梗-3	400	400	1400	3.5	0.79	37	362	360
15	No.2-6	[4-4]	柱-2004-梗-3	400	400	1400	3.5	0.79	37	362	360
16	CSUS1	[4-5]	柱-2008-梗-8	400	400	1200	3.0	0.80	34	314	369
17	CSUS2	[4-5]	柱-2008-梗-8	400	400	1200	3.0	0.80	36	314	369
18	CSUS3	[4-5]	柱-2008-梗-8	400	400	1200	3.0	0.80	36	326	404
19	CSUS4	[4-5]	柱-2008-梗-8	400	400	1200	3.0	0.80	35	314	369
20	F-2	[4-6]	柱-2006-梗-001	300	300	900	3.0	0.81	43	326	1398
21	F-3	[4-6]	柱-2006-梗-001	300	300	900	3.0	0.81	14	326	1398
22	F-4	[4-6]	柱-2006-梗-001	300	300	900	3.0	0.81	43	326	1398
23	F-5	[4-6]	柱-2006-梗-001	300	300	900	3.0	0.81	43	326	1398
24	F-6	[4-6]	柱-2006-梗-001	300	300	900	3.0	0.81	43	326	1398
25	CA025C	[4-7]	柱-1989-年-19	200	200	600	3.0	0.77	26	361	426
26	CA060C	[4-7]	柱-1989-年-19	200	200	600	3.0	0.77	26	361	426
27	CA010T	[4-7]	柱-1989-年-19	200	200	600	3.0	0.77	26	361	426
28	CA01T06C	[4-7]	柱-1989-年-19	200	200	600	3.0	0.77	26	361	426
29	11	[4-8]	柱-1992-年-04	200	200	600	3.0	0.79	38	423	396
30	12	[4-8]	柱-1992-年-04	200	200	600	3.0	0.79	38	423	396
31	13	[4-8]	柱-1992-年-04	200	200	600	3.0	0.79	38	423	396
32	14	[4-8]	柱-1992-年-04	200	200	600	3.0	0.79	38	423	396
33	15	[4-8]	柱-1992-年-04	200	200	600	3.0	0.79	23	423	396
34	16	[4-8]	柱-1992-年-04	200	200	600	3.0	0.79	23	423	396
35	17	[4-8]	柱-1992-年-04	200	200	600	3.0	0.79	23	423	396
36	18	[4-8]	柱-1992-年-04	200	200	600	3.0	0.79	23	423	396
37	19	[4-8]	柱-1992-年-04	200	200	600	3.0	0.79	27	423	396
38	20	[4-8]	柱-1992-年-04	200	200	600	3.0	0.79	27	423	396
39	21	[4-8]	柱-1992-年-04	200	200	600	3.0	0.79	27	423	396
40	22	[4-8]	柱-1992-年-04	200	200	600	3.0	0.79	27	423	396
41	23	[4-8]	柱-1992-年-04	200	200	600	3.0	0.79	27	423	396
42	PC25	[4-9]	柱-1992-年-10	500	500	1200	2.4	0.84	29	389	372
43	7	[4-10]	柱-1992-年-13	250	250	750	3.0	0.80	69	349	760
44	No.1	[4-11]	柱-1993-年-12	200	200	600	3.0	0.78	33	356	1392
45	No.2	[4-11]	柱-1993-年-12	200	200	600	3.0	0.78	33	356	1392
46	No.3	[4-11]	柱-1993-年-12	200	200	600	3.0	0.78	33	356	1392
47	No.4	[4-11]	柱-1993-年-12	200	200	600	3.0	0.78	33	356	1392
48	No.5	[4-11]	柱-1993-年-12	200	200	600	3.0	0.78	33	356	1392

Columns's characteristics

Num.	Denomination			Dimentions					Materials		
	Name	Ref.	Digital file	b	D	h_0	h_0/D	d/D	σ_B	σ_y	σ_{wy}
				mm	mm	mm			MPa	MPa	MPa
49	No.6	[4-11]	柱-1993-年-12	200	200	600	3.0	0.78	33	356	1392
50	No.7	[4-11]	柱-1993-年-12	200	200	600	3.0	0.78	33	356	1392
51	No.8	[4-11]	柱-1993-年-12	200	200	600	3.0	0.78	33	356	1392
52	No.9	[4-11]	柱-1993-年-12	200	200	600	3.0	0.78	33	356	1392
53	No.10	[4-11]	柱-1993-年-12	200	200	600	3.0	0.78	33	356	1392
54	No.1	[4-12]	柱-1993-年-18	450	450	1800	4.0	0.79	30	485	372
55	No.2	[4-12]	柱-1993-年-18	450	450	1800	4.0	0.79	31	485	372
56	No.3	[4-12]	柱-1993-年-18	450	450	1800	4.0	0.79	29	485	372
57	No.4	[4-12]	柱-1993-年-18	450	450	1800	4.0	0.79	33	485	372
58	No.1	[4-13]	柱-1994-黄-163	200	200	600	3.0	0.79	30	423	396
59	No.2	[4-13]	柱-1994-黄-163	200	200	600	3.0	0.79	30	423	396
60	No.3	[4-13]	柱-1994-黄-163	200	200	600	3.0	0.79	30	423	396
61	No.4	[4-13]	柱-1994-黄-163	200	200	600	3.0	0.79	30	423	396
62	No.5	[4-13]	柱-1994-黄-163	200	200	600	3.0	0.79	38	423	396
63	No.6	[4-13]	柱-1994-黄-163	200	200	600	3.0	0.79	38	423	396
64	No.7	[4-13]	柱-1994-黄-163	200	200	600	3.0	0.79	38	423	396
65	No.8	[4-13]	柱-1994-黄-163	200	200	600	3.0	0.79	38	423	396
66	No.9	[4-13]	柱-1994-黄-163	200	200	600	3.0	0.79	27	423	396
67	No.10	[4-13]	柱-1994-黄-163	200	200	600	3.0	0.79	23	423	396
68	No.11	[4-13]	柱-1994-黄-163	200	200	600	3.0	0.79	23	423	396
69	No.12	[4-13]	柱-1994-黄-163	200	200	600	3.0	0.79	23	423	396
70	No.13	[4-13]	柱-1994-黄-163	200	200	600	3.0	0.79	23	423	396
71	No.14	[4-13]	柱-1994-黄-163	200	200	600	3.0	0.79	27	423	396
72	No.15	[4-13]	柱-1994-黄-163	200	200	600	3.0	0.79	27	423	396
73	No.16	[4-13]	柱-1994-黄-163	200	200	600	3.0	0.79	27	423	396
74	No.17	[4-13]	柱-1994-黄-163	200	200	600	3.0	0.79	27	423	396
75	RCC-SN-1	[4-14]	柱-1994-年-4	250	250	750	3.0	0.82	24	398	409
76	SSC-5	[4-15]	柱-1994-コ-177	250	250	650	2.6	0.83	35	359	377
77	SDC-5	[4-15]	柱-1994-コ-177	250	250	650	2.6	0.83	35	359	377
78	C-1	[4-16]	柱-1995-黄-01	278	278	646	2.3	0.81	40	496	371
79	C-2	[4-16]	柱-1995-黄-01	278	278	646	2.3	0.77	40	496	371
80	C-3	[4-16]	柱-1995-黄-01	278	278	646	2.3	0.77	41	496	371
81	CB-1	[4-16]	柱-1995-黄-01	278	278	646	2.3	0.77	46	441	413
82	CB-2	[4-16]	柱-1995-黄-01	278	278	646	2.3	0.77	46	441	413
83	CB-3	[4-16]	柱-1995-黄-01	278	278	646	2.3	0.77	46	441	413
84	RCC-SN-3	[4-17]	柱-1995-年-02	250	250	750	3.0	0.83	24	421	437
85	RCC-SN-4	[4-17]	柱-1995-年-02	250	250	750	3.0	0.83	25	421	437
86	RCC-NN-2	[4-18]	柱-1995-年-25	250	250	750	3.0	0.83	26	409	398
87	RCC-NN-5	[4-18]	柱-1995-年-25	250	250	750	3.0	0.83	34	421	437
88	HDC-3	[4-19]	柱-1997-構-03	300	300	900	3.0	0.75	35	363	979
89	HDC-4	[4-19]	柱-1997-構-03	300	300	900	3.0	0.75	104	363	979
90	HDC-5	[4-19]	柱-1997-構-03	300	300	900	3.0	0.75	36	363	979
91	HDC-6	[4-19]	柱-1997-構-03	300	300	900	3.0	0.75	68	363	979
92	HDC-7	[4-19]	柱-1997-構-03	300	300	900	3.0	0.75	108	363	979
93	CC97H-RS	[4-20]	柱 -1998-年-92	250	250	500	2.0	0.79	48	380	388
94	RC-20-119	[4-21]	柱-2000-年-10	300	300	900	3.0	0.77	30	374	367
95	RC-1A	[4-22]	柱-2001-黄-0002	320	320	1020	3.2	0.77	55	451	449
96	RC-2	[4-22]	柱-2001-黄-0002	280	280	900	3.2	0.88	55	469	449
97	C1シリーズ No.1	[4-23]	柱-2003-黄-0003	350	350	1050	3.0	0.80	55	378	890
98	C1シリーズ No.2	[4-23]	柱-2003-黄-0003	350	350	1050	3.0	0.80	55	378	890
99	C1シリーズ No.3	[4-23]	柱-2003-黄-0003	350	350	1050	3.0	0.80	55	378	890
100	C1シリーズ No.4	[4-23]	柱-2003-黄-0003	350	350	1050	3.0	0.80	65	435	890
101	C1シリーズ No.5	[4-23]	柱-2003-黄-0003	350	350	1050	3.0	0.80	65	435	890

Columns's characteristics

Num.	Denomination			Dimentions					Materials		
	Name	Ref.	Digital file	b	D	h_0	h_0/D	d/D	σ_B	σ_y	σ_{wy}
				mm	mm	mm			MPa	MPa	MPa
102	C1シリーズ No.6	[4-23]	柱-2003-黄-0003	350	350	1050	3.0	0.80	65	435	890
103	C1シリーズ No.7	[4-23]	柱-2003-黄-0003	350	350	1050	3.0	0.80	105	508	890
104	C1シリーズ No.8	[4-23]	柱-2003-黄-0003	350	350	1050	3.0	0.80	105	508	890
105	C1シリーズ No.9	[4-23]	柱-2003-黄-0003	350	350	1050	3.0	0.80	105	508	890
106	C1シリーズ No.10	[4-23]	柱-2003-黄-0003	350	350	1050	3.0	0.80	65	435	890
107	C1シリーズ No.11	[4-23]	柱-2003-黄-0003	350	350	1050	3.0	0.80	65	435	890
108	C1シリーズ No.12	[4-23]	柱-2003-黄-0003	350	350	1050	3.0	0.80	65	435	890
109	C1シリーズ No.13	[4-23]	柱-2003-黄-0003	350	350	1050	3.0	0.80	94	508	890
110	C2シリーズ No.1	[4-24]	柱-2003-黄-0003-2	350	350	1050	3.0	0.80	67	443	797
111	C2シリーズ No.2	[4-24]	柱-2003-黄-0003-2	350	350	1050	3.0	0.80	67	443	797
112	C2シリーズ No.3	[4-24]	柱-2003-黄-0003-2	350	350	1050	3.0	0.80	67	443	797
113	C2シリーズ No.4	[4-24]	柱-2003-黄-0003-2	350	350	1050	3.0	0.80	67	443	381
114	C2シリーズ No.5	[4-24]	柱-2003-黄-0003-2	350	350	1050	3.0	0.80	67	443	797
115	C2シリーズ No.6	[4-24]	柱-2003-黄-0003-2	350	350	1050	3.0	0.80	67	443	1343
116	C2シリーズ No.7	[4-24]	柱-2003-黄-0003-2	350	350	1050	3.0	0.80	67	443	381
117	C2シリーズ No.8	[4-24]	柱-2003-黄-0003-2	350	350	1050	3.0	0.80	67	443	1343
118	C2シリーズ No.9	[4-24]	柱-2003-黄-0003-2	350	350	1050	3.0	0.80	67	443	1343
119	C3シリーズ No.1	[4-25]	柱-2003-黄-0003-3	350	350	1050	3.0	0.80	24	446	925
120	C3シリーズ No.2	[4-25]	柱-2003-黄-0003-3	350	350	1050	3.0	0.80	24	446	925
121	C3シリーズ No.3	[4-25]	柱-2003-黄-0003-3	350	350	1050	3.0	0.80	24	446	925
122	C3シリーズ No.4	[4-25]	柱-2003-黄-0003-3	350	350	1050	3.0	0.80	24	446	925
123	C3シリーズ No.5	[4-25]	柱-2003-黄-0003-3	350	350	1050	3.0	0.80	24	446	925
124	C3シリーズ No.6	[4-25]	柱-2003-黄-0003-3	350	350	1050	3.0	0.80	41	446	925
125	C3シリーズ No.7	[4-25]	柱-2003-黄-0003-3	350	350	1050	3.0	0.80	41	446	925
126	C3シリーズ No.8	[4-25]	柱-2003-黄-0003-3	350	350	1050	3.0	0.80	77	446	925
127	C3シリーズ No.9	[4-25]	柱-2003-黄-0003-3	350	350	1050	3.0	0.80	77	446	925
128	C3シリーズ No.10	[4-25]	柱-2003-黄-0003-3	350	350	1050	3.0	0.80	77	446	925
129	C3シリーズ No.11	[4-25]	柱-2003-黄-0003-3	350	350	1050	3.0	0.80	77	446	925
130	C3シリーズ No.12	[4-25]	柱-2003-黄-0003-3	350	350	1050	3.0	0.80	77	446	925
131	S2-4	[4-26]	柱-2003-年-11	400	400	1600	4.0	0.78	30	390	420
132	S1-4	[4-26]	柱-2003-年-11	400	400	800	2.0	0.78	30	390	420
133	F10-N	[4-27]	柱-2005-黄-0002	470	470	1410	3.0	0.80	40	347	377
134	14	[4-28]	柱-2005-黄-0001	250	250	600	2.4	0.79	31	360	530
135	15	[4-28]	柱-2005-黄-0001	250	250	600	2.4	0.79	31	360	530
136	16	[4-28]	柱-2005-黄-0001	250	250	600	2.4	0.79	31	360	530
137	17	[4-28]	柱-2005-黄-0001	250	250	600	2.4	0.79	31	360	530
138	P01	[4-29]	柱-1987-年-06	200	200	600	3.0	0.84	26	399	308
139	P03	[4-29]	柱-1987-年-06	200	200	600	3.0	0.84	26	399	308
140	1	[4-30]	柱-1987-年-07	250	250	600	2.4	0.83	29	366	368
141	2	[4-30]	柱-1987-年-07	250	250	600	2.4	0.83	29	366	368
142	3	[4-30]	柱-1987-年-07	250	250	600	2.4	0.83	29	366	368
143	4	[4-30]	柱-1987-年-07	250	250	600	2.4	0.83	30	366	368
144	5	[4-30]	柱-1987-年-07	250	250	600	2.4	0.83	32	366	368
145	6	[4-30]	柱-1987-年-07	250	250	600	2.4	0.83	29	366	368
146	7	[4-30]	柱-1987-年-07	250	250	600	2.4	0.83	30	366	368
147	8	[4-30]	柱-1987-年-07	250	250	600	2.4	0.83	31	366	368
148	9	[4-30]	柱-1987-年-07	250	250	600	2.4	0.82	30	366	368
149	10	[4-30]	柱-1987-年-07	250	250	600	2.4	0.78	30	366	368
150	11	[4-30]	柱-1987-年-07	250	250	600	2.4	0.83	29	366	368
151	12	[4-30]	柱-1987-年-07	250	250	600	2.4	0.83	28	366	368
152	13	[4-30]	柱-1987-年-07	250	250	600	2.4	0.83	30	366	368
153	14	[4-30]	柱-1987-年-07	250	250	600	2.4	0.83	31	366	368
154	No.2	[4-31]	柱-1989-年-15	300	300	683	2.3	0.85	53	434	1294
155	No.3	[4-31]	柱-1989-年-15	300	300	683	2.3	0.85	49	434	1294
156	No.4	[4-31]	柱-1989-年-15	300	300	683	2.3	0.85	46	434	1049
157	No.10	[4-31]	柱-1989-年-15	330	330	683	2.1	0.81	49	434	971
158	0A1	[4-32]	柱-1989-年-16	180	180	450	2.5	0.89	29	340	249

Columns's characteristics

Num.	Denomination			Dimentions					Materials		
	Name	Ref.	Digital file	b	D	h_0	h_0/D	d/D	σ_B	σ_y	σ_{wy}
				mm	mm	mm			MPa	MPa	MPa
159	0A0	[4-32]	柱-1989-年-16	180	180	450	2.5	0.89	29	340	249
160	0A2	[4-32]	柱-1989-年-16	180	180	450	2.5	0.89	29	340	249
161	0A4	[4-32]	柱-1989-年-16	180	180	450	2.5	0.89	29	340	249
162	0A5	[4-32]	柱-1989-年-16	180	180	450	2.5	0.89	29	340	249
163	No.7	[4-33]	柱-1989-年-13	220	220	550	2.5	0.79	46	465	487
164	CA06-6-1	[4-34]	柱-1993-年-10	300	300	900	3.0	0.79	72	742	365
165	CA06-6-2	[4-34]	柱-1993-年-10	300	300	900	3.0	0.79	72	742	405
166	CA06-6-3	[4-34]	柱-1993-年-10	300	300	900	3.0	0.79	72	742	873
167	CA06-6-4	[4-34]	柱-1993-年-10	300	300	900	3.0	0.79	72	742	1053
168	CA06-3-1	[4-34]	柱-1993-年-10	300	300	900	3.0	0.79	72	742	365
169	CA06-3-2	[4-34]	柱-1993-年-10	300	300	900	3.0	0.79	72	742	405
170	CA06-3-3	[4-34]	柱-1993-年-10	300	300	900	3.0	0.79	72	742	873
171	CA06-3-4	[4-34]	柱-1993-年-10	300	300	900	3.0	0.79	72	742	1053
172	HT6-4BL	[4-35]	柱-1993-年-09	300	300	900	3.0	0.79	61	919	1428
173	HT6-4CL	[4-35]	柱-1993-年-09	300	300	900	3.0	0.79	61	919	1337
174	HT6-2AH	[4-35]	柱-1993-年-09	300	300	900	3.0	0.79	61	919	1428
175	HT6-2BH	[4-35]	柱-1993-年-09	300	300	900	3.0	0.79	61	919	1428
176	HT6-4BH	[4-35]	柱-1993-年-09	300	300	900	3.0	0.79	61	919	1428
177	HT6-4CH	[4-35]	柱-1993-年-09	300	300	900	3.0	0.79	61	919	1337
178	RC-S3	[4-36]	柱-1995-年-06	400	400	1000	2.5	0.88	41	494	350
179	B-0	[4-37]	柱-1993-年-22	250	250	625	2.5	0.86	32	445	592
180	CA048-T6	[4-38]	柱-1995-年-22	300	300	900	3.0	0.79	48	1025	1382
181	CA048-N0	[4-38]	柱-1995-年-22	300	300	900	3.0	0.79	48	1025	1382
182	CA048-C6	[4-38]	柱-1995-年-22	300	300	900	3.0	0.79	48	1025	1382
183	CA048-C3	[4-38]	柱-1995-年-22	300	300	900	3.0	0.79	48	1025	1382
184	No.1	[4-39]	柱-1995-年-16	200	200	400	2.0	0.79	56	721	846
185	No.8	[4-39]	柱-1995-年-16	200	200	400	2.0	0.79	56	721	846
186	No.9	[4-39]	柱-1995-年-16	200	200	400	2.0	0.79	56	721	846
187	No.10	[4-39]	柱-1995-年-16	200	200	400	2.0	0.79	56	721	846
188	No.12	[4-39]	柱-1995-年-16	200	200	400	2.0	0.79	55	721	846
189	No.13	[4-39]	柱-1995-年-16	200	200	400	2.0	0.79	55	721	846
190	No.14	[4-39]	柱-1995-年-16	200	200	400	2.0	0.79	55	721	846
191	No.15	[4-39]	柱-1995-年-16	200	200	400	2.0	0.79	55	721	846
192	No.16	[4-39]	柱-1995-年-16	200	200	400	2.0	0.79	55	721	846
193	No.17	[4-39]	柱-1995-年-16	200	200	400	2.0	0.79	55	721	846
194	RC-14	[4-40]	柱-1999-年-57	500	500	1500	3.0	0.80	26	390	307
195	A1	[4-41]	柱-1999-年-53	300	300	900	3.0	0.78	26	343	365
196	P-324M	[4-42]	柱-1981-年-08	150	150	450	3.0	0.83	28	341	263
197	S3-00	[4-43]	柱-1999-年-22	400	400	1200	3.0	0.87	26	755	363
198	A-4	[4-44]	柱-1999-年-19	300	300	900	3.0	0.84	40	685	930
199	B-3	[4-44]	柱-1999-年-19	300	300	900	3.0	0.84	21	685	832
200	B-5	[4-44]	柱-1999-年-19	300	300	900	3.0	0.84	60	685	851
201	B-7	[4-44]	柱-1999-年-19	300	300	900	3.0	0.84	64	685	851
202	B-8	[4-44]	柱-1999-年-19	300	300	900	3.0	0.84	64	685	851
203	B-10	[4-44]	柱-1999-年-19	300	300	900	3.0	0.84	64	685	851
204	B-12	[4-44]	柱-1999-年-19	300	300	900	3.0	0.84	116	685	871
205	B-13	[4-44]	柱-1999-年-19	300	300	900	3.0	0.84	116	685	871
206	B-14	[4-44]	柱-1999-年-19	300	300	900	3.0	0.84	116	685	871
207	B-15	[4-44]	柱-1999-年-19	300	300	900	3.0	0.84	116	685	871
208	B-16	[4-44]	柱-1999-年-19	300	300	600	2.0	0.84	116	685	871
209	D-9	[4-44]	柱-1999-年-19	300	300	900	3.0	0.84	102	685	1373
210	8	[4-45]	柱-2009-黄-0001	200	200	800	4.0	0.79	22	375	410
211	C13-J	[4-46]	柱-2007-黄-0001	300	300	900	3.0	0.77	22	371	366
212	C13-T	[4-46]	柱-2007-黄-0001	300	300	900	3.0	0.77	22	371	366
213	C13-H	[4-46]	柱-2007-黄-0001	300	300	900	3.0	0.77	22	371	366
214	S6-N	[4-27]	柱-2005-黄-0002	470	470	1410	3.0	0.80	40	1006	372
215	S6-G	[4-27]	柱-2005-黄-0002	470	470	1410	3.0	0.80	40	1006	372

Columns's characteristics

Num.	Denomination			Dimentions					Materials		
	Name	Ref.	Digital file	b	D	h_0	h_0/D	d/D	σ_B	σ_y	σ_{wy}
				mm	mm	mm			MPa	MPa	MPa
216	S13-N	[4-27]	柱-2005-黄-0002	470	470	1410	3.0	0.82	40	1014	337
217	S13-N-R	[4-27]	柱-2005-黄-0002	700	700	2100	3.0	0.85	42	1014	337
218	No.1	[4-47]	柱-2003-黄-0001	300	300	1200	4.0	0.77	31	402	392
219	No.3	[4-47]	柱-2003-黄-0001	300	300	1200	4.0	0.77	31	402	392
220	No.4	[4-47]	柱-2003-黄-0001	300	300	1200	4.0	0.77	31	402	392
221	No.6	[4-47]	柱-2003-黄-0001	300	300	1200	4.0	0.77	31	409	392
222	No.7	[4-47]	柱-2003-黄-0001	300	300	1200	4.0	0.77	31	409	392
223	No.8	[4-47]	柱-2003-黄-0001	300	300	1200	4.0	0.77	31	388	392
224	2C	[4-48]	柱-2003-黄-0002	300	300	600	2.0	0.77	25	396	392
225	3C	[4-48]	柱-2003-黄-0002	300	300	600	2.0	0.77	25	396	392
226	2C13	[4-48]	柱-2003-黄-0002	300	300	600	2.0	0.77	25	350	392
227	R99L-P0	[4-49]	柱-2001-黄-0001	250	250	1000	4.0	0.80	21	359	333
228	CR96L-S0	[4-49]	柱-2001-黄-0001	250	250	1000	4.0	0.80	26	361	388
229	RC-3	[4-22]	柱-2001-黄-0002	320	320	730	2.3	0.77	53	451	449
230	No.8	[4-22]	柱-2001-黄-0002	300	300	720	2.4	0.77	44	444	470
231	4J11	[4-50]	柱-2009-構-0002	450	450	1500	3.3	0.79	20	403	360
232	4W11	[4-50]	柱-2009-構-0002	450	450	1500	3.3	0.79	20	403	360
233	4H11	[4-50]	柱-2009-構-0002	450	450	1500	3.3	0.79	20	403	360
234	6J11	[4-50]	柱-2009-構-0002	450	450	1500	3.3	0.79	20	403	360
235	4J21	[4-50]	柱-2009-構-0002	450	450	1500	3.3	0.79	20	403	360
236	6J21	[4-50]	柱-2009-構-0002	450	450	1500	3.3	0.79	20	403	360
237	N1	[4-51]	柱-2011-コ-0001	300	300	900	3.0	0.84	19	329	424
238	N6	[4-52]	柱-2011-コ-0001	300	300	900	3.0	0.84	23	329	424
239	N9	[4-53]	柱-2011-コ-0001	300	300	900	3.0	0.84	41	329	424
240	N12	[4-54]	柱-2011-コ-0001	300	300	600	2.0	0.84	23	329	424
241	N18	[4-55]	柱-2011-コ-0001	300	300	600	2.0	0.84	23	329	424
242	No.1	[4-52]	柱-2010-年-14	400	400	1200	3.0	0.86	18	405	337
243	RC-20-013	[4-21]	柱-2000-年-10	300	300	900	3.0	0.77	27	374	318
244	RC-20-060	[4-21]	柱-2000-年-10	300	300	900	3.0	0.77	27	374	367
245	R99S-P0	[4-53]	柱-2000-年-15	250	250	500	2.0	0.80	21	371	333
246	R98S-P0	[4-53]	柱-2000-年-15	250	250	500	2.0	0.80	32	360	333
247	N18M	[4-54]	柱-2001-年-3	300	300	900	3.0	0.77	27	380	375
248	N27M	[4-54]	柱-2001-年-3	300	300	900	3.0	0.77	27	380	375
249	N27C	[4-54]	柱-2001-年-3	300	300	900	3.0	0.77	27	380	375
250	150-4	[4-55]	柱-2002-年-3	300	300	900	3.0	0.81	147	757	1460
251	150-5	[4-55]	柱-2002-年-3	300	300	900	3.0	0.81	147	747	1460
252	S-1	[4-56]	柱-2002-年-6	300	300	1200	4.0	0.87	38	991	446
253	S-2	[4-56]	柱-2002-年-6	300	300	1200	4.0	0.87	38	991	446
254	S-3	[4-56]	柱-2002-年-6	300	300	1200	4.0	0.87	36	991	446
255	S-4	[4-56]	柱-2002-年-6	300	300	1200	4.0	0.87	36	991	446
256	S-5	[4-56]	柱-2002-年-6	300	300	1200	4.0	0.87	38	991	446
257	S-000	[4-57]	柱-2003-年-2	450	266	600	2.3	0.81	26	436	714
258	S-050	[4-57]	柱-2003-年-2	450	266	600	2.3	0.81	26	436	714
259	S-033	[4-57]	柱-2003-年-2	450	266	600	2.3	0.81	26	436	714
260	No.1	[4-58]	柱-2003-年-10	300	300	600	2.0	0.81	28	447	398
261	No.11	[4-58]	柱-2003-年-10	300	300	900	3.0	0.81	28	447	398
262	No.12	[4-58]	柱-2003-年-10	300	300	900	3.0	0.81	28	447	398
263	No.13	[4-58]	柱-2003-年-10	300	300	900	3.0	0.81	26	447	398
264	No.14	[4-58]	柱-2003-年-10	300	300	900	3.0	0.81	26	447	398
265	No.15	[4-58]	柱-2003-年-10	300	300	900	3.0	0.81	26	447	398
266	No.16	[4-58]	柱-2003-年-10	300	300	600	2.0	0.81	26	447	398
267	D-3	[4-59]	柱-2004-年-2	250	250	900	3.6	0.88	31	391	400
268	S-3	[4-59]	柱-2004-年-2	250	250	900	3.6	0.88	31	391	400
269	Ⅰ-No.1	[4-60]	柱-2005-年-2	360	360	720	2.0	0.78	136	710	1082
270	No.11	[4-61]	柱-2006-年-2	300	300	1200	4.0	0.79	82	554	904
271	No.1	[4-62]	柱-2006-年-3	250	250	375	1.5	0.80	18	353	379
272	No.2	[4-62]	柱-2006-年-3	250	250	375	1.5	0.80	18	353	379

Columns's characteristics

Num.	Denomination			Dimentions					Materials		
	Name	Ref.	Digital file	b	D	h_0	h_0/D	d/D	σ_B	σ_y	σ_{wy}
				mm	mm	mm			MPa	MPa	MPa
273	No.3	[4-62]	柱-2006-年-3	250	250	500	2.0	0.80	15	353	379
274	No.4	[4-62]	柱-2006-年-3	250	250	500	2.0	0.80	17	353	379
275	HNO.16	[4-63]	柱-2006-年-4	300	300	700	2.3	0.78	122	721	756
276	LcFS00	[4-64]	柱-2008-年-15	400	400	700	1.8	0.93	11	357	338
277	LcFM00	[4-64]	柱-2008-年-15	400	400	1000	2.5	0.83	11	341	365
278	LcFH00	[4-64]	柱-2008-年-15	400	400	1250	3.1	0.83	11	340	365
279	V-NC3.65	[4-65]	柱-2009-年-085	250	250	800	3.2	0.78	48	355	979
280	C-1	[4-66]	柱-1992-年-03	317	317	700	2.2	0.80	58	433	878
281	C-2	[4-66]	柱-1992-年-03	317	317	700	2.2	0.80	58	433	818
282	C-3	[4-66]	柱-1992-年-03	317	317	700	2.2	0.80	58	433	878
283	C-4	[4-66]	柱-1992-年-03	317	317	700	2.2	0.80	58	433	818
284	S6	[4-67]	柱-1992-年-06	300	300	900	3.0	0.84	74	388	1235
285	S7	[4-67]	柱-1992-年-06	300	300	900	3.0	0.84	74	388	1235
286	RC21	[4-9]	柱-1992-年-10	500	500	1200	2.4	0.84	29	389	372
287	PC22	[4-9]	柱-1992-年-10	500	500	1200	2.4	0.84	29	389	372
288	PC24	[4-9]	柱-1992-年-10	500	500	1200	2.4	0.84	29	389	372
289	PC26	[4-9]	柱-1992-年-10	500	500	1200	2.4	0.84	29	389	372
290	PC27	[4-9]	柱-1992-年-10	500	500	1200	2.4	0.84	29	389	372
291	PC28	[4-9]	柱-1992-年-10	500	500	1200	2.4	0.84	29	389	372
292	AR3	[4-68]	柱-1986-構-01	200	200	600	3.0	0.90	29	414	201
293	48-K12-6	[4-74]	柱-1986-年-08	200	200	400	2.0	0.87	44	727	311
294	48-K12-4	[4-74]	柱-1986-年-08	200	200	400	2.0	0.87	44	727	311
295	48-K12-2	[4-74]	柱-1986-年-08	200	200	400	2.0	0.87	44	727	311
296	48-K12-0	[4-74]	柱-1986-年-08	200	200	400	2.0	0.87	44	727	311
297	C3	[4-69]	柱-1984-構-02	500	500	1000	2.0	0.82	24	318	336
298	No.1	[4-70]	柱-1996-年-20	350	350	900	2.6	0.84	25	372	301
299	No.1	[4-71]	柱-1996-年-19	300	300	1100	3.7	0.77	33	363	326
300	No.2	[4-71]	柱-1996-年-19	300	300	1100	3.7	0.77	33	363	347
301	No.3	[4-71]	柱-1996-年-19	300	300	1100	3.7	0.77	33	363	347
302	A1	[4-72]	柱-1996-年-06	300	300	600	2.0	0.83	24	867	395
303	A2	[4-72]	柱-1996-年-06	300	300	600	2.0	0.83	24	867	395
304	A3	[4-72]	柱-1996-年-06	300	300	600	2.0	0.83	22	867	395
305	A4	[4-72]	柱-1996-年-06	300	300	600	2.0	0.83	23	867	395
306	A231	[4-72]	柱-1996-年-06	400	400	800	2.0	0.82	44	425	1402
307	A232	[4-72]	柱-1996-年-06	400	400	800	2.0	0.82	44	425	1402
308	A233	[4-72]	柱-1996-年-06	400	400	800	2.0	0.82	44	425	1402
309	A234	[4-72]	柱-1996-年-06	400	400	800	2.0	0.82	44	425	1402
310	CN-M1	[4-73]	柱-1984-黄-03	250	250	750	3.0	0.86	14	441	0
311	13H-100M	[4-73]	柱-1984-黄-03	250	250	750	3.0	0.86	17	441	1362
312	13H-80M	[4-73]	柱-1984-黄-03	250	250	750	3.0	0.86	17	441	1362
313	13H-60M	[4-73]	柱-1984-黄-03	250	250	750	3.0	0.86	17	441	1362
314	8H-60M	[4-73]	柱-1984-黄-03	250	250	750	3.0	0.86	17	441	855
315	8H-50M	[4-73]	柱-1984-黄-03	250	250	750	3.0	0.86	17	441	855
316	8H-35M	[4-73]	柱-1984-黄-03	250	250	750	3.0	0.86	17	441	855
317	3N-50M	[4-73]	柱-1984-黄-03	250	250	750	3.0	0.86	14	441	295
318	3N-40M	[4-73]	柱-1984-黄-03	250	250	750	3.0	0.86	14	441	295
319	3N-30M	[4-73]	柱-1984-黄-03	250	250	750	3.0	0.86	14	441	295
320	CA12-6-1	[4-75]	柱－1990－年-02	300	300	900	3.0	0.79	114	736	406
321	CA12-6-2	[4-75]	柱－1990－年-02	300	300	900	3.0	0.79	114	736	765
322	CA12-6-3	[4-75]	柱－1990－年-02	300	300	900	3.0	0.79	114	736	765
323	CA12-3-1	[4-75]	柱－1990－年-02	300	300	900	3.0	0.79	114	736	406
324	CA12-3-2	[4-75]	柱－1990－年-02	300	300	900	3.0	0.79	114	736	765
325	CA12-3-3	[4-75]	柱－1990－年-02	300	300	900	3.0	0.79	114	736	765
326	SA0	[4-76]	柱 -1988-年-43	120	600	1200	2.0	0.73	29	501	329
327	SA4	[4-76]	柱 -1988-年-43	120	600	1200	2.0	0.73	30	501	329
328	SB4	[4-76]	柱 -1988-年-43	120	600	1200	2.0	0.73	30	501	329
329	SC4	[4-76]	柱 -1988-年-43	120	600	1200	2.0	0.73	30	501	329

Columns's characteristics

Num.	Denomination			Dimentions					Materials		
	Name	Ref.	Digital file	b	D	h_0	h_0/D	d/D	σ_B	σ_y	σ_{wy}
				mm	mm	mm			MPa	MPa	MPa
330	SD4	[4-76]	柱 -1988-年-43	120	600	1200	2.0	0.73	29	501	329
331	19	[4-82]	柱 -1988-年-42	250	250	900	3.6	0.80	31	363	381
332	24	[4-82]	柱 -1988-年-42	250	250	600	2.4	0.80	31	363	381
333	25	[4-82]	柱 -1988-年-42	250	250	900	3.6	0.80	30	363	381
334	27	[4-82]	柱 -1988-年-42	250	250	900	3.6	0.80	19	363	381
335	28	[4-82]	柱 -1988-年-42	250	250	900	3.6	0.80	41	363	381
336	BS	[4-77]	柱 -1998-年-119	300	300	600	2.0	0.79	19	767	367
337	ＳＳ-0-Ｎ0	[4-78]	柱-1983-年-35	300	300	900	3.0	0.87	24	390	307
338	ＳＳ-0-Ｎ1	[4-78]	柱-1983-年-35	300	300	900	3.0	0.87	24	390	307
339	ＳＳ-0-Ｎ2	[4-78]	柱-1983-年-35	300	300	900	3.0	0.87	24	390	307
340	ＳＲ-0-Ｎ1	[4-78]	柱-1983-年-35	225	400	900	2.3	0.90	24	390	307
341	S-1	[4-79]	柱-1998-年-59	300	300	900	3.0	0.77	25	366	304
342	S-2	[4-79]	柱-1998-年-59	300	300	900	3.0	0.77	25	366	304
343	S-3	[4-79]	柱-1998-年-59	300	300	900	3.0	0.77	25	366	304
344	S-4	[4-79]	柱-1998-年-59	300	300	900	3.0	0.77	25	366	304
345	K1	[4-80]	柱-1998-年-57	250	250	500	2.0	0.81	27	829	346
346	K2	[4-80]	柱-1998-年-57	250	250	500	2.0	0.81	29	829	346
347	K3	[4-80]	柱-1998-年-57	250	250	500	2.0	0.81	29	829	346
348	K4	[4-80]	柱-1998-年-57	250	250	500	2.0	0.81	29	829	346
349	S00	[4-81]	柱-1998-年-55	400	400	600	1.5	0.82	25	392	365
350	CC06-6-1	[4-83]	柱-1994-年-53	300	300	900	3.0	0.79	67	744	369
351	CC06-3-1	[4-83]	柱-1994-年-53	300	300	900	3.0	0.79	67	744	369
352	TC-1A	[4-84]	柱-1994-黄-161	300	300	1000	3.3	0.71	28	376	358
353	HNO.1	[4-85]	柱-1991-年-42	300	300	800	2.7	0.77	71	611	312
354	HNO.4	[4-85]	柱-1991-年-42	300	300	800	2.7	0.73	73	611	312
355	S1	[4-86]	柱-1991-年-41	300	300	900	3.0	0.83	96	423	1250
356	S2	[4-86]	柱-1991-年-41	300	300	900	3.0	0.83	89	423	795
357	S3	[4-86]	柱-1991-年-41	300	300	900	3.0	0.83	92	423	1250
358	S4	[4-86]	柱-1991-年-41	300	300	900	3.0	0.83	96	423	795
359	S5	[4-86]	柱-1991-年-41	300	300	900	3.0	0.80	99	711	1250
360	S1	[4-87]	柱-1991-年-43	200	800	1600	2.0	0.81	92	1002	1294
361	S2	[4-87]	柱-1991-年-43	200	800	3200	4.0	0.81	83	1002	1294
362	S3	[4-87]	柱-1991-年-43	200	800	3200	4.0	0.81	95	1002	1294
363	S4	[4-87]	柱-1991-年-43	200	800	3200	4.0	0.81	95	1002	1294
364	S5	[4-87]	柱-1991-年-43	200	800	3200	4.0	0.81	85	1002	1294
365	OV25ă	[4-88]	柱-1991-年-46	180	180	450	2.5	0.89	34	343	203
366	OV13ă	[4-88]	柱-1991-年-46	180	180	450	2.5	0.89	33	343	203
367	OV13m	[4-88]	柱-1991-年-46	180	180	450	2.5	0.89	46	343	203
368	OV12h	[4-88]	柱-1991-年-46	180	180	450	2.5	0.89	59	343	203
369	CB060C	[4-89]	柱-1991-年-29	278	278	646	2.3	0.77	46	441	413
370	CB07T06C	[4-89]	柱-1991-年-29	278	278	646	2.3	0.77	46	441	413
371	HDC-1	[4-19]	柱-1997-構-03	300	300	900	3.0	0.79	22	363	439
372	HDC-2	[4-19]	柱-1997-構-03	300	300	900	3.0	0.79	24	363	439
373	1		This document	350	350	1100	3.1	0.89	30	420	341
374	2-A		This document	325	325	975	3.0	0.81	31	420	341
375	2-B		This document	325	325	1100	3.4	0.79	30	537	341
376	3		This document	325	325	975	3.0	0.81	31	420	341

Reinforcement

Num.	***Rebar***		***Stirrups***				***Characteristics***						
	Bars	*Denomination*	*Bars*		*S*	*Denomination*	p_g	p_t	p_w	*S/D*	*S/d*	S/ϕ	*a/d*
	pz mm			*mm*	*mm*		*%*	*%*	*%*				
1	4 D13		2	ű9.3	75		1.27	0.63	0.91	0.38	0.47	5.8	1.50
2	12 D16	SD 390	4	D6	40	785	1.95	0.97	0.90	0.11	0.14	2.5	1.50
3	12 D16	SD 390	4	D6	40	785	1.95	0.97	0.90	0.11	0.14	2.5	1.50
4	12 D16	SD 390	4	D6	40	785	1.95	0.97	0.90	0.11	0.14	2.5	1.50
5	12 D16	SD 390	4	D6	90	785	1.95	0.97	0.40	0.26	0.32	5.6	1.50
6	12 D16	SD 390	4	D6	60	785	1.95	0.97	0.60	0.17	0.21	3.8	1.50
7	12 D16	SD 390	4	D6	40	785	1.95	0.97	0.90	0.11	0.14	2.5	1.50
8	12 D16	SD 390	4	D6	40	785	1.95	0.97	0.90	0.11	0.14	2.5	1.50
9	12 D13		2	D6	75		1.69	0.84	0.28	0.25	0.32	5.8	1.50
10	12 D13		2	D6	75		1.69	0.84	0.28	0.25	0.32	5.8	1.50
11	12 D13		2	D6	75		1.69	0.84	0.28	0.25	0.32	5.8	1.50
12	12 D13		2	D6	75		1.69	0.84	0.28	0.25	0.32	5.8	1.50
13	12 D13		2	D6	75		1.69	0.84	0.28	0.25	0.32	5.8	1.50
14	20 D13	SD 345	4	D6	40	SD 345	1.58	0.79	0.79	0.10	0.13	3.1	1.75
15	20 D13	SD 345	4	D6	40	SD 345	1.58	0.79	0.79	0.10	0.13	3.1	1.75
16	12 D19		4	D10	60		2.15	1.07	1.19	0.15	0.19	3.2	1.50
17	12 D19		4	D10	60		2.15	1.07	1.19	0.15	0.19	3.2	1.50
18	12 D19		4	D10	60		2.15	1.07	1.19	0.15	0.19	3.2	1.50
19	12 D19		2	D10	200		2.15	1.07	0.18	0.50	0.63	10.5	1.50
20	12 D13		4	U5.1	75		1.69	0.84	0.35	0.25	0.31	5.8	1.50
21	12 D13		4	U5.1	40		1.69	0.84	0.65	0.13	0.16	3.1	1.50
22	12 D13		4	U5.1	35		1.69	0.84	0.75	0.12	0.14	2.7	1.50
23	12 D13		4	U5.1	50		1.69	0.84	0.52	0.17	0.21	3.8	1.50
24	12 D13		4	U5.1	35		1.69	0.84	0.75	0.12	0.14	2.7	1.50
25	12 D10		4	D6	70		2.14	1.07	0.90	0.35	0.46	7.0	1.50
26	12 D10		4	D6	71		2.14	1.07	0.89	0.36	0.46	7.1	1.50
27	12 D10		4	D6	72		2.14	1.07	0.88	0.36	0.47	7.2	1.50
28	12 D10		4	D6	73		2.14	1.07	0.87	0.37	0.48	7.3	1.50
29	12 D10		4	D6	60		2.14	1.07	1.07	0.30	0.38	6.0	1.50
30	12 D10		4	D6	60		2.14	1.07	1.07	0.30	0.38	6.0	1.50
31	12 D10		4	D6	60		2.14	1.07	1.07	0.30	0.38	6.0	1.50
32	12 D10		4	D6	60		2.14	1.07	1.07	0.30	0.38	6.0	1.50
33	12 D10		4	D6	60		2.14	1.07	1.07	0.30	0.38	6.0	1.50
34	12 D10		4	D6	60		2.14	1.07	1.07	0.30	0.38	6.0	1.50
35	12 D10		4	D6	60		2.14	1.07	1.07	0.30	0.38	6.0	1.50
36	12 D10		4	D6	60		2.14	1.07	1.07	0.30	0.38	6.0	1.50
37	12 D10		4	D6	40		2.14	1.07	1.60	0.20	0.25	4.0	1.50
38	12 D10		4	D6	40		2.14	1.07	1.60	0.20	0.25	4.0	1.50
39	12 D10		4	D6	40		2.14	1.07	1.60	0.20	0.25	4.0	1.50
40	12 D10		4	D6	40		2.14	1.07	1.60	0.20	0.25	4.0	1.50
41	12 D10		4	D6	40		2.14	1.07	1.60	0.20	0.25	4.0	1.50
42	16 D22	SD 345	4	D10	100		2.48	1.08	0.57	0.20	0.24	4.5	1.20
43	12 D13		4	D6	80		2.43	1.22	0.63	0.32	0.40	6.2	1.50
44	12 D10		2	U5.1	60		2.14	1.07	0.33	0.30	0.39	6.0	1.50
45	12 D10		2	U5.1	60		2.14	1.07	0.33	0.30	0.39	6.0	1.50
46	12 D10		2	U5.1	60		2.14	1.07	0.33	0.30	0.39	6.0	1.50
47	12 D10		2	U5.1	60		2.14	1.07	0.33	0.30	0.39	6.0	1.50
48	12 D10		2	U5.1	40		2.14	1.07	0.49	0.20	0.26	4.0	1.50

Reinforcement

Num.	Rebar		Stirrups					Characteristics						
	Bars	Denomination	Bars		S	Denomination		p_g	p_t	p_w	S/D	S/d	S/ϕ	a/d
	pz mm			mm	mm			%	%	%				
49	12 D10		2	U5.1	40			2.14	1.07	0.49	0.20	0.26	4.0	1.50
50	12 D10		2	U5.1	40			2.14	1.07	0.49	0.20	0.26	4.0	1.50
51	12 D10		2	U5.1	40			2.14	1.07	0.49	0.20	0.26	4.0	1.50
52	12 D10		2	U5.1	30			2.14	1.07	0.65	0.15	0.19	3.0	1.50
53	12 D10		2	U5.1	30			2.14	1.07	0.65	0.15	0.19	3.0	1.50
54	12 D19	SD 390	4	D6	95	SD	295	1.70	0.85	0.30	0.21	0.27	5.0	2.00
55	12 D19	SD 390	4	D6	40	SD	295	1.70	0.85	0.70	0.09	0.11	2.1	2.00
56	12 D19	SD 390	4	D6	25	SD	295	1.70	0.85	1.13	0.06	0.07	1.3	2.00
57	12 D19	SD 390	4	D6	40	SD	295	1.70	0.85	0.70	0.09	0.11	2.1	2.00
58	12 D10		2	D6	60			2.14	1.07	0.53	0.30	0.38	6.0	1.50
59	12 D10		2	D6	60			2.14	1.07	0.53	0.30	0.38	6.0	1.50
60	12 D10		2	D6	60			2.14	1.07	0.53	0.30	0.38	6.0	1.50
61	12 D10		2	D6	60			2.14	1.07	0.53	0.30	0.38	6.0	1.50
62	12 D10		4	D6	60			2.14	1.07	1.06	0.30	0.38	6.0	1.50
63	12 D10		4	D6	60			2.14	1.07	1.06	0.30	0.38	6.0	1.50
64	12 D10		4	D6	60			2.14	1.07	1.06	0.30	0.38	6.0	1.50
65	12 D10		4	D6	60			2.14	1.07	1.06	0.30	0.38	6.0	1.50
66	12 D10		4	D6	40			2.14	1.07	1.58	0.20	0.25	4.0	1.50
67	12 D10		4	D6	60			2.14	1.07	1.06	0.30	0.38	6.0	1.50
68	12 D10		4	D6	60			2.14	1.07	1.06	0.30	0.38	6.0	1.50
69	12 D10		4	D6	60			2.14	1.07	1.06	0.30	0.38	6.0	1.50
70	12 D10		4	D6	60			2.14	1.07	1.06	0.30	0.38	6.0	1.50
71	12 D10		4	D6	40			2.14	1.07	1.58	0.20	0.25	4.0	1.50
72	12 D10		4	D6	40			2.14	1.07	1.58	0.20	0.25	4.0	1.50
73	12 D10		4	D6	40			2.14	1.07	1.58	0.20	0.25	4.0	1.50
74	12 D10		4	D6	40			2.14	1.07	1.58	0.20	0.25	4.0	1.50
75	12 D10	SD 295	4	D6	60	SD	345	1.37	0.68	0.84	0.24	0.29	6.0	1.50
76	16 D16	SD 345	4	D6	50			5.08	2.22	1.01	0.20	0.24	3.1	1.30
77	16 D16	SD 345	4	D6	50			5.08	2.22	1.01	0.20	0.24	3.1	1.30
78	12 D13		4	D6	52			1.97	0.98	0.88	0.19	0.23	4.0	1.16
79	24 D13		4	D6	52			3.93	1.64	0.88	0.19	0.24	4.0	1.16
80	24 D13		4	D6	52			3.93	1.64	0.88	0.19	0.24	4.0	1.16
81	24 D13		4	D6	52			3.93	1.64	0.88	0.19	0.24	4.0	1.16
82	24 D13		4	D6	52			3.93	1.64	0.88	0.19	0.24	4.0	1.16
83	24 D13		4	D6	52			3.93	1.64	0.88	0.19	0.24	4.0	1.16
84	12 D10	SD 345	4	D6	60	SD	295	1.37	0.68	0.84	0.24	0.29	6.0	1.50
85	12 D10	SD 345	4	D6	60	SD	295	1.37	0.68	0.84	0.24	0.29	6.0	1.50
86	12 D10	SD 345	4	D6	40	SD	295	1.37	0.68	1.27	0.16	0.19	4.0	1.50
87	12 D10	SD 345	4	D6	40	SD	295	1.37	0.68	1.27	0.16	0.19	4.0	1.50
88	16 D13	SD 345	4	D6	80	SD	785	2.25	1.13	0.53	0.27	0.36	6.2	1.50
89	16 D13	SD 345	4	D6	80	SD	785	2.25	1.13	0.53	0.27	0.36	6.2	1.50
90	16 D13	SD 345	4	D6	40	SD	785	2.25	1.13	1.06	0.13	0.18	3.1	1.50
91	16 D13	SD 345	4	D6	40	SD	785	2.25	1.13	1.06	0.13	0.18	3.1	1.50
92	16 D13	SD 345	4	D6	40	SD	785	2.25	1.13	1.06	0.13	0.18	3.1	1.50
93	12 D19	SD 345	4	D6	40			5.50	2.75	1.27	0.16	0.20	2.1	1.00
94	12 D13		2	D10	40			1.69	0.84	1.19	0.13	0.17	3.1	1.50
95	12 D16	SD 390	4	D6	35	SD	390	2.33	1.16	1.13	0.11	0.14	2.2	1.59
96	24 D13	SD 390	4	D6	40	SD	390	3.88	1.94	1.13	0.14	0.16	3.1	1.61
97	12 D16	SD 345	4	D6	120		785	1.95	0.97	0.30	0.34	0.43	7.5	1.50
98	12 D16	SD 345	4	D6	90		785	1.95	0.97	0.40	0.26	0.32	5.6	1.50
99	12 D16	SD 345	4	D6	60		785	1.95	0.97	0.60	0.17	0.21	3.8	1.50
100	12 D16	SD 390	4	D6	90		785	1.95	0.97	0.40	0.26	0.32	5.6	1.50
101	12 D16	SD 390	4	D6	60		785	1.95	0.97	0.60	0.17	0.21	3.8	1.50

Reinforcement

Num.	***Rebar***		***Stirrups***				***Characteristics***						
	Bars	*Denomination*	*Bars*		*S*	*Denomination*	p_g	p_t	p_w	*S/D*	*S/d*	S/ϕ	*a/d*
	pz *mm*			*mm*	*mm*		*%*	*%*	*%*				
102	12 D16	SD 390	4	D6	40	785	1.95	0.97	0.90	0.11	0.14	2.5	1.50
103	12 D16	SD 49	4	D6	90	785	1.95	0.97	0.40	0.26	0.32	5.6	1.50
104	12 D16	SD 49	4	D6	60	785	1.95	0.97	0.60	0.17	0.21	3.8	1.50
105	12 D16	SD 49	4	D6	40	785	1.95	0.97	0.90	0.11	0.14	2.5	1.50
106	12 D16	SD 390	4	D6	90	785	1.95	0.97	0.40	0.26	0.32	5.6	1.50
107	12 D16	SD 390	4	D6	60	785	1.95	0.97	0.60	0.17	0.21	3.8	1.50
108	12 D16	SD 390	4	D6	40	785	1.95	0.97	0.90	0.11	0.14	2.5	1.50
109	12 D16	SD 49	4	D6	40	785	1.95	0.97	0.90	0.11	0.14	2.5	1.50
110	12 D16	SD 390	4	D6	40		1.95	0.97	0.90	0.11	0.14	2.5	1.50
111	12 D16	SD 390	4	D6	40		1.95	0.97	0.90	0.11	0.14	2.5	1.50
112	12 D16	SD 390	4	D6	40		1.95	0.97	0.90	0.11	0.14	2.5	1.50
113	12 D16	SD 390	4	D6	90		1.95	0.97	0.40	0.26	0.32	5.6	1.50
114	12 D16	SD 390	4	D6	90		1.95	0.97	0.40	0.26	0.32	5.6	1.50
115	12 D16	SD 390	4	D6	90		1.95	0.97	0.40	0.26	0.32	5.6	1.50
116	12 D16	SD 390	4	D6	40		1.95	0.97	0.90	0.11	0.14	2.5	1.50
117	12 D16	SD 390	4	D6	40		1.95	0.97	0.90	0.11	0.14	2.5	1.50
118	12 D16	SD 390	4	D6	90		1.95	0.97	0.40	0.26	0.32	5.6	1.50
119	12 D16	SD 390	4	D6	40	785	1.95	0.97	0.90	0.11	0.14	2.5	1.50
120	12 D16	SD 390	4	D6	40	785	1.95	0.97	0.90	0.11	0.14	2.5	1.50
121	12 D16	SD 390	4	D6	40	785	1.95	0.97	0.90	0.11	0.14	2.5	1.50
122	12 D16	SD 390	4	D6	90	785	1.95	0.97	0.40	0.26	0.32	5.6	1.50
123	12 D16	SD 390	4	D6	60	785	1.95	0.97	0.60	0.17	0.21	3.8	1.50
124	12 D16	SD 390	4	D6	40	785	1.95	0.97	0.90	0.11	0.14	2.5	1.50
125	12 D16	SD 390	4	D6	40	785	1.95	0.97	0.90	0.11	0.14	2.5	1.50
126	12 D16	SD 390	4	D6	40	785	1.95	0.97	0.90	0.11	0.14	2.5	1.50
127	12 D16	SD 390	4	D6	40	785	1.95	0.97	0.90	0.11	0.14	2.5	1.50
128	12 D16	SD 390	4	D6	40	785	1.95	0.97	0.90	0.11	0.14	2.5	1.50
129	12 D16	SD 390	4	D6	90	785	1.95	0.97	0.40	0.26	0.32	5.6	1.50
130	12 D16	SD 390	4	D6	60	785	1.95	0.97	0.60	0.17	0.21	3.8	1.50
131	10 D16		4	D6	80		1.24	0.62	0.40	0.20	0.26	5.0	2.00
132	10 D16		4	D6	80		1.24	0.62	0.40	0.20	0.26	5.0	1.00
133	12 D22		4	D10	80		2.10	1.05	0.76	0.17	0.21	3.6	1.50
134	8 D16		4	D3	33.7		2.54	1.27	0.37	0.13	0.17	2.1	2.40
135	8 D16		4	D3	33.7		2.54	1.27	0.37	0.13	0.17	2.1	2.40
136	8 D16		4	D3	33.7		2.54	1.27	0.37	0.13	0.17	2.1	2.40
137	8 D16		4	D3	33.7		2.54	1.27	0.37	0.13	0.17	2.1	2.40
138	16 D10		2	ű4	31.4		2.85	1.25	0.40	0.16	0.19	3.1	1.50
139	16 D10		2	ű4	31.4		2.85	1.25	0.40	0.16	0.19	3.1	1.5
140	12 D16	SD 345	2	ű6	105		3.81	1.91	0.22	0.42	0.51	6.5	1.20
141	12 D16	SD 345	2	ű6	52.2		3.81	1.91	0.43	0.21	0.25	3.3	1.20
142	12 D16	SD 345	0	ű6	0		3.81	1.91	0.00	0.00	0.00	0.0	1.20
143	12 D16	SD 345	2	ű6	105		3.81	1.91	0.22	0.42	0.51	6.5	1.20
144	12 D16	SD 345	2	ű6	105		3.81	1.91	0.22	0.42	0.51	6.5	1.20
145	12 D16	SD 345	2	ű6	52.2		3.81	1.91	0.43	0.21	0.25	3.3	1.20
146	12 D16	SD 345	2	ű6	52.2		3.81	1.91	0.43	0.21	0.25	3.3	1.20
147	12 D16	SD 345	2	ű6	52.2		3.81	1.91	0.43	0.21	0.25	3.3	1.20
148	16 D16	SD 345	2	ű6	52.2		5.08	2.54	0.43	0.21	0.26	3.3	1.20
149	8 D16	SD 345	2	ű6	52.2		2.54	1.27	0.43	0.21	0.27	3.3	1.20
150	12 D16	SD 345	0	ű6	0		3.81	1.91	0.00	0.00	0.00	0.0	1.20
151	12 D16	SD 345	2	ű6	105		3.81	1.91	0.22	0.42	0.51	6.5	1.20
152	12 D16	SD 345	2	ű6	52.2		3.81	1.91	0.43	0.21	0.25	3.3	1.20
153	12 D16	SD 345	2	ű6	37		3.81	1.91	0.61	0.15	0.18	2.3	1.20
154	18 D13		4	ű4	85		2.53	1.13	0.20	0.28	0.33	6.5	1.14
155	18 D13		4	ű4	85		2.53	1.13	0.20	0.28	0.33	6.5	1.14
156	18 D13		4	ű4	42		2.53	1.13	0.40	0.14	0.16	3.2	1.14
157	32 D13		4	ű4	30		3.72	1.69	0.51	0.09	0.11	2.3	1.04
158	8 D13		2	ű4	64.3		3.13	1.17	0.22	0.36	0.40	4.9	1.25

Reinforcement

Num.	***Rebar***		***Stirrups***					***Characteristics***						
	Bars	*Denomination*	*Bars*	*S*	*Denomination*			p_g	p_t	p_w	*S/D*	*S/d*	S/ϕ	*a/d*
	pz mm		*mm*	*mm*				*%*	*%*	*%*				
159	8 D13		2	ű4	64.3			3.13	1.17	0.22	0.36	0.40	4.9	1.25
160	8 D13		2	ű4	64.3			3.13	1.17	0.22	0.36	0.40	4.9	1.25
161	8 D13		2	ű4	64.3			3.13	1.17	0.22	0.36	0.40	4.9	1.25
162	8 D13		2	ű4	64.3			3.13	1.17	0.22	0.36	0.40	4.9	1.25
163	12 D13		4	D6	39			3.14	1.57	1.48	0.18	0.22	3.0	1.25
164	12 D19		4	D6	80			3.82	1.91	0.53	0.27	0.34	4.2	1.50
165	12 D19		4	D10	80			3.82	1.91	1.19	0.27	0.34	4.2	1.50
166	12 D19		4	D6	80			3.82	1.91	0.53	0.27	0.34	4.2	1.50
167	12 D19		4	D10	80			3.82	1.91	1.19	0.27	0.34	4.2	1.50
168	12 D19		4	D6	80			3.82	1.91	0.53	0.27	0.34	4.2	1.50
169	12 D19		4	D10	80			3.82	1.91	1.19	0.27	0.34	4.2	1.50
170	12 D19		4	D6	80			3.82	1.91	0.53	0.27	0.34	4.2	1.50
171	12 D19		4	D10	80			3.82	1.91	1.19	0.27	0.34	4.2	1.50
172	12 D19		4	ű5	80			3.82	1.91	0.33	0.27	0.34	4.2	1.50
173	12 D19		4	ű7	76			3.82	1.91	0.68	0.25	0.32	4.0	1.50
174	12 D19		2	ű5	60			3.82	1.91	0.22	0.20	0.25	3.2	1.50
175	12 D19		2	ű5	40			3.82	1.91	0.33	0.13	0.17	2.1	1.50
176	12 D19		4	ű5	80			3.82	1.91	0.33	0.27	0.34	4.2	1.50
177	12 D19		4	ű7	76			3.82	1.91	0.68	0.25	0.32	4.0	1.50
178	10 D19	SD 390	2	D10	60	SD	295	1.79	0.72	0.59	0.15	0.17	3.2	1.25
179	8 D16		2	ű4	180			2.54	1.27	0.06	0.72	0.84	11.3	2.50
180	12 D16		4	D4	50			2.65	1.32	0.33	0.17	0.21	3.1	1.50
181	12 D16		4	D4	50			2.65	1.32	0.33	0.17	0.21	3.1	1.50
182	12 D16		4	D4	50			2.65	1.32	0.33	0.17	0.21	3.1	1.50
183	12 D16		4	D4	50			2.65	1.32	0.33	0.17	0.21	3.1	1.50
184	12 D13	SD 685	4	D6	106	SD	785	3.80	1.90	0.60	0.53	0.67	8.2	1.00
185	12 D13	SD 685	4	D6	106	SD	785	3.80	1.90	0.60	0.53	0.67	8.2	1.00
186	12 D13	SD 685	4	D6	106	SD	785	3.80	1.90	0.60	0.53	0.67	8.2	1.00
187	12 D13	SD 685	4	D6	106	SD	785	3.80	1.90	0.60	0.53	0.67	8.2	1.00
188	12 D13	SD 685	2	D6	106	SD	785	3.80	1.90	0.30	0.53	0.67	8.2	1.00
189	12 D13	SD 685	2	D6	106	SD	785	3.80	1.90	0.30	0.53	0.67	8.2	1.00
190	12 D13	SD 685	2	D6	106	SD	785	3.80	1.90	0.30	0.53	0.67	8.2	1.00
191	12 D13	SD 685	2	D6	106	SD	785	3.80	1.90	0.30	0.53	0.67	8.2	1.00
192	12 D13	SD 685	4	D6	53	SD	785	3.80	1.90	1.20	0.27	0.33	4.1	1.00
193	12 D13	SD 685	4	D6	53	SD	785	3.80	1.90	1.20	0.27	0.33	4.1	1.00
194	12 D22		2	D10	200			1.86	0.93	0.14	0.40	0.50	9.1	1.50
195	12 D13		2	D6	180			1.69	0.84	0.12	0.60	0.77	13.8	1.50
196	8 D10		2	ű4	40			2.54	1.27	0.42	0.27	0.32	4.0	1.50
197	8 D19	SD 685	2	D10	120	SD	295	1.43	0.72	0.30	0.30	0.34	6.3	1.50
198	16 D16	SD 685	2	ű6.2	50			3.53	1.54	0.40	0.17	0.20	3.1	1.50
199	16 D16	SD 685	2	ű6.2	50			3.53	1.54	0.40	0.17	0.20	3.1	1.50
200	16 D16	SD 685	2	ű6.2	50			3.53	1.54	0.40	0.17	0.20	3.1	1.50
201	16 D16	SD 685	2	ű6.2	50			3.53	1.54	0.40	0.17	0.20	3.1	1.50
202	16 D16	SD 685	2	ű6.2	50			3.53	1.54	0.40	0.17	0.20	3.1	1.50
203	16 D16	SD 685	4	ű6.2	35			3.53	1.54	1.15	0.12	0.14	2.2	1.50
204	16 D16	SD 685	2	ű6.2	100			3.53	1.54	0.20	0.33	0.40	6.3	1.50
205	16 D16	SD 685	2	ű6.2	50			3.53	1.54	0.40	0.17	0.20	3.1	1.50
206	16 D16	SD 685	2	ű6.2	50			3.53	1.54	0.40	0.17	0.20	3.1	1.50
207	16 D16	SD 685	2	ű6.2	35			3.53	1.54	0.58	0.12	0.14	2.2	1.50
208	16 D16	SD 685	2	ű6.2	50			3.53	1.54	0.40	0.17	0.20	3.1	1.00
209	16 D16	SD 685	4	ű6.2	35			3.53	1.54	1.15	0.12	0.14	2.2	1.50
210	12 D10	SD 295	2	D4	124	SD	295	2.14	1.07	0.10	0.62	0.78	12.4	2.00
211	12 D13		2	D6	200			1.69	0.84	0.11	0.67	0.86	15.4	1.50
212	12 D13		2	D6	200			1.69	0.84	0.11	0.67	0.86	15.4	1.50
213	12 D13		2	D6	200			1.69	0.84	0.11	0.67	0.86	15.4	1.50
214	12 D25		4	D6	80			2.75	1.38	0.34	0.17	0.21	3.2	1.50
215	12 D25		2	D6	40			2.75	1.38	0.34	0.09	0.11	1.6	1.50

Reinforcement

Num.	***Rebar***		***Stirrups***				***Characteristics***						
	Bars	*Denomination*	*Bars*	*S*	*Denomination*		p_g	p_t	p_w	*S/D*	*S/d*	S/ϕ	*a/d*
	pz mm			*mm*	*mm*		*%*	*%*	*%*				
216	16 D32		4	D13	140		5.75	2.16	0.77	0.30	0.36	4.4	1.50
217	16 D32		4	D13	100		2.59	0.97	0.72	0.14	0.17	3.1	1.50
218	12 D16	SD 345	2	D6	100	SD 345	2.65	1.32	0.21	0.33	0.43	6.3	2.00
219	12 D16	SD 345	2	D6	200	SD 345	2.65	1.32	0.11	0.67	0.86	12.5	2.00
220	12 D16	SD 345	2	D6	100	SD 345	2.65	1.32	0.21	0.33	0.43	6.3	2.00
221	12 D13	SD 345	2	D6	100	SD 345	1.69	0.84	0.21	0.33	0.43	7.7	2.00
222	12 D13	SD 345	2	D6	150	SD 345	1.69	0.84	0.14	0.50	0.65	11.5	2.00
223	12 D10	SD 295	2	D6	150	SD 345	0.95	0.48	0.14	0.50	0.65	15.0	2.00
224	12 D16	SD 345	2	D6	100	SD 345	2.65	1.32	0.21	0.33	0.43	6.3	1.00
225	12 D16	SD 345	2	D6	100	SD 345	2.65	1.32	0.21	0.33	0.43	6.3	1.00
226	12 D13	SD 295	2	D6	100	SD 345	1.69	0.84	0.21	0.33	0.43	7.7	1.00
227	12 D13	SD 345	2	ű4	125		2.43	1.22	0.08	0.50	0.62	9.6	2.00
228	12 D13	SD 345	2	D6	150		2.43	1.22	0.17	0.60	0.75	11.5	2.00
229	20 D16	SD 390	4	D6	35	SD 390	3.88	1.16	1.13	0.11	0.14	2.2	1.14
230	12 D16	SD 390	4	D6	60	SD 390	2.65	1.32	0.70	0.20	0.26	3.8	1.20
231	12 D19	SD 345	2	D10	300	SD 295	1.70	0.85	0.11	0.67	0.85	15.8	1.67
232	12 D19	SD 345	2	D10	300	SD 295	1.70	0.85	0.11	0.67	0.85	15.8	1.67
233	12 D19	SD 345	2	D10	300	SD 295	1.70	0.85	0.11	0.67	0.85	15.8	1.67
234	12 D19	SD 345	2	D10	300	SD 295	1.70	0.85	0.11	0.67	0.85	15.8	1.67
235	12 D19	SD 345	2	D10	150	SD 295	1.70	0.85	0.21	0.33	0.42	7.9	1.67
236	12 D19	SD 345	2	D10	150	SD 295	1.70	0.85	0.21	0.33	0.42	7.9	1.67
237	16 D13	SD 295	2	D6	100	SD 295	2.25	0.99	0.21	0.33	0.40	7.7	1.50
238	16 D13	SD 295	2	D6	100	SD 295	2.25	0.99	0.21	0.33	0.40	7.7	1.50
239	16 D13	SD 295	2	D6	100	SD 295	2.25	0.99	0.21	0.33	0.40	7.7	1.50
240	16 D13	SD 295	2	D6	100	SD 295	2.25	0.99	0.21	0.33	0.40	7.7	1.00
241	16 D13	SD 295	2	D6	100	SD 295	2.25	0.99	0.21	0.33	0.40	7.7	1.00
242	10 D22	SD 345	2	D10	200	SD 295	2.42	0.97	0.18	0.50	0.58	9.1	1.50
243	12 D13		2	D6	160		1.69	0.84	0.13	0.53	0.69	12.3	1.50
244	12 D13		2	D10	80		1.69	0.84	0.59	0.27	0.35	6.2	1.50
245	12 D10		2	ű4	125		1.37	0.68	0.08	0.50	0.62	12.5	1.00
246	12 D10		2	ű4	125		1.37	0.68	0.08	0.50	0.62	12.5	1.00
247	12 D16	SD 345	2	D6	100	SD 345	2.65	1.32	0.21	0.33	0.43	6.3	1.50
248	12 D16	SD 345	2	D6	100	SD 345	2.65	1.32	0.21	0.33	0.43	6.3	1.50
249	12 D16	SD 345	2	D6	100	SD 345	2.65	1.32	0.21	0.33	0.43	6.3	1.50
250	12 D16	SD 685	4	ű6	75		2.65	1.32	0.50	0.25	0.31	4.7	1.50
251	12 D16	SD 685	4	ű6	75		2.65	1.32	0.50	0.25	0.31	4.7	1.50
252	8 D22		2	D6	110		3.44	1.72	0.19	0.37	0.42	5.0	2.00
253	8 D22		2	D6	55		3.44	1.72	0.38	0.18	0.21	2.5	2.00
254	8 D22		2	D6	55		3.44	1.72	0.38	0.18	0.21	2.5	2.00
255	8 D22		2	D6	55		3.44	1.72	0.38	0.18	0.21	2.5	2.00
256	8 D22		2	D6	55		3.44	1.72	0.38	0.18	0.21	2.5	2.00
257	12 D16	SD 390	0	ű4	0		1.99	1.00	0.00	0.00	0.00	0.0	1.69
258	12 D16	SD 390	2	ű4	50		1.99	1.00	0.11	0.19	0.23	3.1	1.69
259	12 D16	SD 390	2	ű4	33		1.99	1.00	0.17	0.12	0.15	2.1	1.69
260	12 D13		2	D6	50		1.69	0.70	0.42	0.17	0.20	3.8	1.00
261	16 D13		2	D6	150		2.25	0.99	0.14	0.50	0.61	11.5	1.50
262	16 D13		2	D6	150		2.25	0.99	0.14	0.50	0.61	11.5	1.50
263	16 D13		2	D6	50		2.25	0.99	0.42	0.17	0.20	3.8	1.50
264	16 D13		2	D6	50		2.25	0.99	0.42	0.17	0.20	3.8	1.50
265	16 D13		4	D6	50		2.25	0.99	0.84	0.17	0.20	3.8	1.50
266	12 D13		2	D6	50		1.69	0.70	0.42	0.17	0.20	3.8	1.00
267	8 D13		2	D6	50		1.62	0.61	0.51	0.20	0.23	3.8	1.80
268	8 D13		2	D6	50		1.62	0.61	0.51	0.20	0.23	3.8	1.80
269	12 D19	SD 685	4	D10	134		2.65	1.33	0.59	0.37	0.48	7.1	1.00
270	12 D16	SD 49	4	ű5	52		2.65	1.32	0.50	0.17	0.22	3.3	2.00
271	12 D10		2	D4	54		1.37	0.68	0.19	0.22	0.27	5.4	0.75
272	12 D10		2	D4	54		1.37	0.68	0.19	0.22	0.27	5.4	0.75

Reinforcement

Num.	***Rebar***		***Stirrups***					***Characteristics***						
	Bars	*Denomination*	*Bars*	*S*	*Denomination*			p_g	p_t	p_w	*S/D*	*S/d*	*S/ϕ*	*a/d*
	pz mm			*mm*	*mm*			*%*	*%*	*%*				
273	12 D10		2	D4	54			1.37	0.68	0.19	0.22	0.27	5.4	1.00
274	12 D10		2	D4	54			1.37	0.68	0.19	0.22	0.27	5.4	1.00
275	21 D13	685	4	D6	55			2.93	1.32	0.77	0.18	0.24	4.2	1.17
276	8 D13	SD 295	2	D6	75			0.63	0.24	0.21	0.19	0.20	5.8	1.75
277	12 D16	SD 295	2	D10	150			1.49	0.74	0.24	0.38	0.45	9.4	2.50
278	12 D19	SD 295	2	D10	150			2.15	1.07	0.24	0.38	0.45	7.9	3.13
279	12 D13	SD 345	2	D6	55	SD	785	2.43	1.22	0.46	0.22	0.28	4.2	1.60
280	16 D13	SD 390	4	ű4	54			2.02	0.88	0.29	0.17	0.21	4.2	1.11
281	16 D13	SD 390	4	ű5	54			2.02	0.88	0.46	0.17	0.21	4.2	1.11
282	16 D13	SD 390	4	ű4	54			2.02	0.88	0.29	0.17	0.21	4.2	1.11
283	16 D13	SD 390	4	ű5	54			2.02	0.88	0.46	0.17	0.21	4.2	1.11
284	16 D13		4	ű5	50			2.25	0.99	0.52	0.17	0.20	3.8	1.50
285	16 D13		4	ű5	50			2.25	0.99	0.52	0.17	0.20	3.8	1.50
286	16 D22	SD 345	4	D10	100			2.48	1.08	0.57	0.20	0.24	4.5	1.20
287	16 D22	SD 345	4	D10	100			2.48	1.08	0.57	0.20	0.24	4.5	1.20
288	16 D22	SD 345	4	D10	100			2.48	1.08	0.57	0.20	0.24	4.5	1.20
289	16 D22	SD 345	2	D10	100			2.48	1.08	0.29	0.20	0.24	4.5	1.20
290	16 D22	SD 345	4	D10	100			2.48	1.08	0.57	0.20	0.24	4.5	1.20
291	16 D22	SD 345	4.4	D10	100			2.48	1.08	0.63	0.20	0.24	4.5	1.20
292	13 D10	SD 35	2	ű4	50			2.35	1.00	0.25	0.25	0.28	5.0	1.50
293	12 D13		4	ű6	47			3.80	1.27	1.20	0.24	0.27	3.6	1.00
294	12 D13		4	ű6	47			3.80	1.27	1.20	0.24	0.27	3.6	1.00
295	12 D13		4	ű6	47			3.80	1.27	1.20	0.24	0.27	3.6	1.00
296	12 D13		4	ű6	47			3.80	1.27	1.20	0.24	0.27	3.6	1.00
297	12 D22		2	ű9	100			1.86	0.93	0.25	0.20	0.24	4.5	1.00
298	10 D16	SD 345	2	D6	100	SD	295	1.62	0.65	0.18	0.29	0.34	6.3	1.43
299	12 D16	SD 295	2	D6	160			2.65	1.32	0.13	0.53	0.69	10.0	1.83
300	12 D16	SD 295	2	D10	160			2.65	1.32	0.30	0.53	0.69	10.0	1.83
301	12 D16	SD 295	2	D10	80			2.65	1.32	0.59	0.27	0.35	5.0	1.83
302	16 D13	SD 8	2	D6	50	SD	295	2.25	0.99	0.42	0.17	0.20	3.8	1.00
303	16 D13	SD 8	2	D6	50	SD	295	2.25	0.99	0.42	0.17	0.20	3.8	1.00
304	16 D13	SD 8	2	D6	50	SD	295	2.25	0.99	0.42	0.17	0.20	3.8	1.00
305	16 D13	SD 8	2	D6	100	SD	295	2.25	0.99	0.21	0.33	0.40	7.7	1.00
306	16 D19		2	ű6	140			2.87	1.43	0.10	0.35	0.43	7.4	1.00
307	16 D19		2	ű6	70			2.87	1.43	0.20	0.18	0.21	3.7	1.00
308	16 D19		2	ű6	47			2.87	1.43	0.30	0.12	0.14	2.5	1.00
309	16 D19		2	ű6	35			2.87	1.43	0.40	0.09	0.11	1.8	1.00
310	6 D19		0	0	0			2.75	1.38	0.00	0.00	0.00	0.0	1.50
311	6 D19		2	ű4	100			2.75	1.38	0.10	0.40	0.47	5.3	1.50
312	6 D19		2	ű4	80			2.75	1.38	0.13	0.32	0.37	4.2	1.50
313	6 D19		2	ű4	60			2.75	1.38	0.17	0.24	0.28	3.2	1.50
314	6 D19		2	ű4	60			2.75	1.38	0.17	0.24	0.28	3.2	1.50
315	6 D19		2	ű4	50			2.75	1.38	0.20	0.20	0.23	2.6	1.50
316	6 D19		2	ű4	35			2.75	1.38	0.29	0.14	0.16	1.8	1.50
317	6 D19		2	ű6	50			2.75	1.38	0.45	0.20	0.23	2.6	1.50
318	6 D19		2	ű6	40			2.75	1.38	0.57	0.16	0.19	2.1	1.50
319	6 D19		2	ű6	30			2.75	1.38	0.75	0.12	0.14	1.6	1.50
320	12 D19	SD 7	4	D10	80	SD	35	3.82	1.91	1.19	0.27	0.34	4.2	1.50
321	12 D19	SD 7	4	D10	180	SD	8	3.82	1.91	0.53	0.60	0.76	9.5	1.50
322	12 D19	SD 7	4	D10	80	SD	8	3.82	1.91	1.19	0.27	0.34	4.2	1.50
323	12 D19	SD 7	4	D10	80	SD	35	3.82	1.91	1.19	0.27	0.34	4.2	1.50
324	12 D19	SD 7	4	D10	180	SD	8	3.82	1.91	0.53	0.60	0.76	9.5	1.50
325	12 D19	SD 7	4	D10	80	SD	8	3.82	1.91	1.19	0.27	0.34	4.2	1.50
326	12 D8	SD	2	ű4	45			0.83	0.28	0.47	0.08	0.10	5.6	1.00
327	12 D8	SD	2	ű4	45			0.83	0.28	0.47	0.08	0.10	5.6	1.00
328	12 D8	SD	2	ű4	45			0.83	0.28	0.47	0.08	0.10	5.6	1.00
329	12 D8	SD	2	ű4	45			0.83	0.28	0.47	0.08	0.10	5.6	1.00

Reinforcement

Num.	***Rebar***		***Stirrups***					***Characteristics***						
	Bars	*Denomination*	*Bars*		*S*	*Denomination*		p_g	p_t	p_w	*S/D*	*S/d*	S/ϕ	*a/d*
	pz *mm*			*mm*	*mm*			*%*	*%*	*%*				
330	12 D8	SD	2	ű4	45			0.83	0.28	0.47	0.08	0.10	5.6	1.00
331	12 D16		2	ű6	75			3.81	1.91	0.30	0.30	0.38	4.7	1.80
332	12 D16		2	ű6	75			3.81	1.91	0.30	0.30	0.38	4.7	1.20
333	12 D16		2	ű6	75			3.81	1.91	0.30	0.30	0.38	4.7	1.80
334	12 D16		2	ű6	75			3.81	1.91	0.30	0.30	0.38	4.7	1.80
335	12 D16		2	ű6	75			3.81	1.91	0.30	0.30	0.38	4.7	1.80
336	12 D16	SD 685	2	ű6	150	SR	295	2.65	1.10	0.13	0.50	0.64	9.4	1.00
337	8 D19		2	ű6	63			2.55	0.96	0.30	0.21	0.24	3.3	1.50
338	8 D19		2	ű6	63			2.55	0.96	0.30	0.21	0.24	3.3	1.50
339	8 D19		2	ű6	63			2.55	0.96	0.30	0.21	0.24	3.3	1.50
340	8 D19		2	ű6	71			2.55	0.96	0.35	0.18	0.20	3.7	1.13
341	12 D16		2	D6	100			2.65	1.32	0.21	0.33	0.43	6.3	1.50
342	12 D16		2	D6	100			2.65	1.32	0.21	0.33	0.43	6.3	1.50
343	12 D16		2	D6	50			2.65	1.32	0.42	0.17	0.22	3.1	1.50
344	12 D16		2	D6	50			2.65	1.32	0.42	0.17	0.22	3.1	1.50
345	16 D13		2	D6	65			3.24	1.42	0.39	0.26	0.32	5.0	1.00
346	16 D13		2	D6	65			3.24	1.42	0.39	0.26	0.32	5.0	1.00
347	16 D13		2	D6	65			3.24	1.42	0.39	0.26	0.32	5.0	1.00
348	16 D13		2	D6	65			3.24	1.42	0.39	0.26	0.32	5.0	1.00
349	16 D22		2	D10	180			3.87	1.69	0.20	0.45	0.55	8.2	2.25
350	12 D19	SD 685	4	D10	80	SD	345	3.82	1.91	1.19	0.27	0.34	4.2	1.50
351	12 D19	SD 685	4	D10	80	SD	345	3.82	1.91	1.19	0.27	0.34	4.2	1.50
352	38 D16	SD 345	4	D6	50	SD	345	8.38	3.97	0.84	0.17	0.24	3.1	1.67
353	12 D16		4	D6	50			2.65	1.32	0.84	0.17	0.22	3.1	1.33
354	16 D16		4	D6	50			3.53	1.99	0.84	0.17	0.23	3.1	1.33
355	16 D13		4	ű5	50			2.25	0.99	0.52	0.17	0.20	3.8	1.50
356	16 D13		4	ű5	30			2.25	0.99	0.87	0.10	0.12	2.3	1.50
357	16 D13		4	ű5	50			2.25	0.99	0.52	0.17	0.20	3.8	1.50
358	16 D13		4	ű5	35			2.25	0.99	0.75	0.12	0.14	2.7	1.50
359	12 D13		4	ű5	50			1.69	0.84	0.52	0.17	0.21	3.8	1.50
360	12 D22		2	ű6	95			2.90	1.45	0.30	0.12	0.15	4.3	1.00
361	12 D22		2	ű6	95			2.90	1.45	0.30	0.12	0.15	4.3	2.00
362	12 D22		2	ű6	47			2.90	1.45	0.60	0.06	0.07	2.1	2.00
363	12 D22		2	ű6	47			2.90	1.45	0.60	0.06	0.07	2.1	2.00
364	12 D22		2	ű6	47			2.90	1.45	0.60	0.06	0.07	2.1	2.00
365	8 D13	SD 3	3	ű4	45			3.13	1.17	0.47	0.25	0.28	3.5	1.25
366	8 D13	SD 3	3	ű4	45			3.13	1.17	0.47	0.25	0.28	3.5	1.25
367	8 D13	SD 3	3	ű4	45			3.13	1.17	0.47	0.25	0.28	3.5	1.25
368	8 D13	SD 3	3	ű4	45			3.13	1.17	0.47	0.25	0.28	3.5	1.25
369	24 D13		4	D6	52			3.93	1.64	0.88	0.19	0.24	4.0	1.16
370	24 D13		4	D6	52			3.93	1.64	0.88	0.19	0.24	4.0	1.16
371	12 D13	SD 345	2	D6	125	SD	295	1.69	0.84	0.17	0.42	0.53	9.6	1.50
372	12 D13	SD 345	2	D6	125	SD	295	1.69	0.84	0.17	0.42	0.53	9.6	1.50
373	8 D13	SD 390	2	D6	30	SD	295	0.83	0.31	0.60	0.09	0.10	2.3	1.57
374	14 D13	SD 390	4	D6	45	SD	295	1.71	0.86	0.87	0.14	0.17	3.5	1.50
375	12 D16	SD 49	4	D6	45	SD	295	2.26	1.13	0.87	0.14	0.17	2.8	1.70
376	14 D13	SD 390	4	D6	45	SD	295	1.71	0.86	0.87	0.14	0.17	3.5	1.50

Behavior Database

Num.	*Failure mode*	Q_0	Q_y	Q_{max}	Q_u	R_0	R_y	R_{max}	R_μ	μ_y	μ_d	*he / Qmax*
			kN	*kN*	*kN*		*%*	*%*	*%*			
1		0	105	140	112	0	0.8	2.0	3.4	4.0	1.7	3.0
2	Flexural	0	287	383	373	0	0.4	1.2	6.1	14.1	5.2	6.3
3	Flexural	0	341	455	456	0	0.4	0.9	5.9	15.8	6.8	6.2
4	Flexural	0	373	497	398	0	0.3	1.0	6.6	23.2	6.9	5.3
5	Flexural-with Shear Collapse	0	338	451	361	0	0.3	1.0	1.9	5.6	1.9	2.0
6	Flexural-with Shear Collapse	0	347	462	370	0	0.3	1.2	6.1	18.2	5.1	1.6
7	Flexural	0	461	614	491	0		1.0	6.7		6.7	
8	Flexural	0	509	678	575	0	0.3	1.1	6.7	21.2	5.9	5.7
9		0	129	173	138	0	0.2	0.5	1.1	6.1	2.3	1.2
10		0	153	204	164	0	0.2	0.3	1.1	7.3	3.2	1.0
11		0	175	234	187	0	0.3	0.6	1.0	4.0	1.7	0.9
12		0	197	263	210	0	0.2	0.4	0.9	5.2	2.2	1.0
13		0	163	218	174	0	0.3	0.7	1.6	5.9	2.3	1.6
14		0	446	595	476	0	0.3	0.9	3.2	9.6	3.5	2.9
15		0	443	591	473	0	0.3	0.6	3.1	11.6	4.9	2.9
16	Flexural	0	420	560	577	0	0.3	0.8	4.0	11.9	4.8	3.9
17	Flexural	0	584	778	622	0	0.3	3.0	5.3	16.3	1.7	3.7
18	Flexural	0	606	808	646	0	0.4	2.8	4.3	11.2	1.5	3.8
19	Shear	0	365	487	390	0	0.3	0.6	0.7	2.4	1.1	0.5
20	Flexural	0	380	506	405	0	0.2	0.9	1.9	8.8	2.2	1.6
21	Flexural	0	392	523	418	0	0.4	0.9	2.1	6.0	2.5	2.0
22	Flexural	0	405	541	432	0	0.3	0.9	2.6	8.1	3.0	2.2
23	Flexural	0	381	507	406	0	0.3	0.9	2.4	8.3	2.7	2.3
24	Flexural	0	411	548	438	0	0.4	1.5	2.9	6.7	1.9	2.6
25	Flexural	0	98	131	105	0	0.5	1.5	2.7	5.7	1.9	2.4
26	Flexural	0	102	135	108	0	0.3	0.8	1.5	5.7	2.0	1.3
27	Flexural	0	48	56	72	0	0.5	0.8	6.5	13.3	8.2	7.2
28	Flexural	0	101	135	108	0	0.4	0.9	2.2	5.9	2.3	1.9
29	Flexural	0	135	180	144	0			4.9			
30	Flexural	0	142	189	151	0			5.0			
31	Flexural	0	146	195	156	0			4.8			
32	Flexural	0	153	204	163	0			3.4			
33	Flexural	0	115	153	122	0			4.8			
34	Flexural	0	123	165	132	0			2.5			
35	Flexural	0	135	179	143	0			2.6			
36	Flexural	0	125	167	133	0			2.5			
37	Flexural	0	133	177	142	0			5.0			
38	Flexural	0	154	205	164	0			4.9			
39	Flexural	0	151	202	162	0			5.3			
40	Flexural	0	148	197	158	0			5.0			
41	Flexural	0	159	213	170	0			5.0			
42	Flexural	0	826	1102	881	0	0.6	1.5	4.1	7.0	2.6	3.7
43	Flexural	0	323	430	344	0	0.4	1.5	3.0	7.2	2.0	2.7
44	Flexural	0	94	125	100	0		0.5	1.9		3.7	
45	Flexural	0	104	139	111	0		0.5	1.7		3.3	
46	Flexural	0	93	124	100	0		0.5	1.2		2.4	
47	Flexural	0	99	132	106	0		0.5	1.1		2.1	
48	Flexural	0	98	130	104	0	0.4	1.4	2.3	6.5	1.7	1.8

Behavior Database

Num.	*Failure mode*	Q_0	Q_y	Q_{max}	Q_u	R_0	R_y	R_{max}	R_μ	μ_y	μ_d	*he / Qmax*
			kN	*kN*	*kN*		*%*	*%*	*%*			
49	Flexural	0	104	139	111	0	0.3	0.7	1.8	5.6	2.7	1.6
50	Flexural	0	106	141	113	0	0.3	0.8	1.5	5.7	1.8	0.9
51	Flexural	0	94	125	100	0	0.2	0.5	1.1	5.1	2.2	0.9
52	Flexural	0	110	147	118	0		0.5	2.4		4.7	
53	Flexural	0	110	146	117	0		0.5	1.7		3.4	
54	Flexural	0	264	352	281	0	0.5	1.0	3.9	7.2	4.1	3.8
55	Flexural	0	388	517	414	0	0.5	1.1	4.0	8.1	3.7	3.6
56	Flexural	0	439	585	468	0	0.3	1.1	3.9	11.4	3.5	3.7
57	Flexural	0	204	272	218	0	0.4	1.0	4.0	9.8	4.0	3.9
58	Flexural	0	123	165	132	0	0.5	1.7	4.0	8.4	2.4	3.7
59	Flexural	0	121	162	129	0	0.4	1.2	2.9	7.3	2.5	2.3
60	Flexural	0	121	162	129	0	0.4	1.3	2.3	5.5	1.8	1.9
61	Flexural	0	130	173	139	0	0.4	1.3	1.5	3.4	1.2	1.3
62	Flexural	0	133	177	178	0	0.6	1.5	3.1	5.1	2.1	4.4
63	Flexural	0	138	183	187	0	0.6	1.2	3.3	5.9	2.8	4.7
64	Flexural	0	146	195	184	0	0.6	1.9	4.2	7.4	2.2	4.4
65	Flexural	0	153	204	163	0	0.5	2.0	3.5	6.7	1.7	3.2
66	Flexural	0	151	201	212	0	0.6	2.1	6.2	10.4	3.0	6.0
67	Flexural	0	116	154	162	0	0.6	1.9	4.7	7.6	2.5	4.4
68	Flexural	0	123	165	132	0	0.5	1.6	2.8	6.0	1.8	2.5
69	Flexural	0	135	179	143	0	0.4	1.5	3.4	7.9	2.2	3.4
70	Flexural	0	125	167	133	0	0.3	1.5	2.7	7.9	1.8	2.3
71	Flexural	0	133	177	142	0	0.4	1.5	2.7	7.1	1.8	2.4
72	Flexural	0	128	171	204	0	0.4	1.2	4.9	12.0	4.2	5.1
73	Flexural	0	136	182	200	0	0.5	1.1	5.0	11.0	4.4	5.4
74	Flexural	0	140	187	197	0	0.5	1.5	4.9	9.9	3.3	4.9
75	Flexural	0	146	195	179	0	0.3	1.1	3.0	9.9	2.7	2.7
76	Flexural	0	259	345	276	0	0.7	1.7	3.6	4.9	2.1	3.1
77	Flexural	0	291	388	310	0	0.5	1.3	3.5	6.5	2.7	3.0
78	Flexural	0	323	431	345	0	0.4	1.6	2.0	5.7	1.2	1.7
79	Flexural	0	375	500	400	0	0.3	0.8	1.2	3.5	1.4	1.4
80	Flexural	0	376	502	401	0	0.4	0.8	1.6	4.5	2.0	0.7
81	Flexural	0	145	193	193	0	0.7	2.8	3.0	4.5	1.1	2.5
82	Flexural	0	387	516	413	0	0.3	0.7	1.0	2.9	1.3	0.7
83	Flexural	0	382	510	408	0	0.4	0.8	1.5	4.2	1.9	1.0
84	Flexural	0	175	234	187	0	0.3	0.9	2.3	6.9	2.5	0.9
85	Flexural	0	162	216	173	0	0.2	1.0	2.9	12.8	2.9	1.5
86	Flexural	0	150	200	160	0	0.3	1.0	3.0	10.5	2.9	1.4
87	Flexural	0	186	248	199	0	0.3	0.9	2.8	10.3	3.1	1.4
88	Flexural	0	315	420	336	0	0.4	0.8	1.3	3.4	1.6	1.2
89	Flexural-with Shear Collapse	0	538	717	574	0	0.39	1.02	1.51	3.9	1.5	1.3
90	Flexural	0	307	410	328	0	0.41	0.71	4.20	10.1	5.9	3.5
91	Flexural	0	440	587	470	0	0.34	0.74	5.01	14.6	6.8	4.3
92	Flexural	0	563	751	601	0	0.36	1.04	3.69	10.3	3.5	3.5
93	Flexural	0	279	373	298	0	0.39	0.95	0.97	2.5	1.0	0.4
94	Flexural	0	205	273	218	0	0.40	0.97	3.22	8.0	3.3	2.8
95	Flexural	0	430	573	458	0	0.34	0.96	5.12	15.2	5.4	4.8
96	Flexural	0	374	498	398	0			3.00			
97	Flexural-with Shear Collapse	0	424	565	452	0	0.47	0.99	2.94	6.2	3.0	2.8
98	Flexural-with Shear Collapse	0	428	571	457	0	0.34	3.04	5.88	17.2	1.9	5.6
99	Flexural	0	422	562	450	0	0.33	4.24	6.67	20.1	1.6	6.3
100	Flexural-with Shear Collapse	0	482	643	514	0	0.36	1.43	4.00	11.1	2.8	3.3
101	Flexural	0	487	649	519	0		1.50	6.67		4.5	

Behavior Database

Num.	*Failure mode*	Q_0	Q_y	Q_{max}	Q_u	R_0	R_y	R_{max}	R_μ	μ_y	μ_d	*he / Qmax*
			kN	*kN*	*kN*		*%*	*%*	*%*			
102	Other	0	647	863	690	0	0.26	1.00	5.26	20.6	5.2	4.7
103	Flexural-with Shear Collapse	0	593	790	632	0		0.86	1.92		2.2	
104	Flexural-with Shear Collapse	0	635	847	678	0	0.31	0.99	4.35	13.9	4.4	3.2
105	Flexural	0	612	816	653	0		1.00	6.67		6.7	
106	Other	0	551	734	587	0		1.00	1.59		1.6	
107	Other	0	559	745	596	0	0.19	1.00	2.38	12.4	2.4	2.2
108	Flexural	0	653	870	696	0		3.04	6.67		2.2	
109	Other	0	770	1027	822	0		1.44	4.55		3.2	
110	Flexural	0	485	646	566	0	0.31	0.93	6.67	21.6	7.1	6.2
111	Flexural-with Shear Collapse	0	644	859	687	0	0.28	1.43	5.26	18.7	3.7	4.8
112	Flexural-with Shear Collapse	0	652	869	695	0	0.28	0.94	2.50	8.8	2.6	2.3
113	Flexural-with Shear Collapse	0	484	645	516	0	0.51	0.77	0.99	1.9	1.3	0.9
114	Flexural-with Shear Collapse	0	467	623	498	0	0.37	0.76	4.17	11.4	5.5	3.8
115	Flexural-with Shear Collapse	0	486	648	518	0	0.26	0.93	5.00	18.9	5.4	5.0
116	Flexural-with Shear Collapse	0	664	885	708	0	0.22	0.46	1.30	6.0	2.8	1.1
117	Flexural	0	638	851	681	0	0.20	0.96	6.67	33.7	7.0	6.2
118	Flexural-with Shear Collapse	0	556	741	593	0		0.81	1.47		1.8	
119	Flexural	0	278	371	367	0	0.43	0.88	6.67	15.4	7.6	6.5
120	Flexural	0	328	437	450	0	0.36	0.82	6.67	18.3	8.2	6.3
121	Flexural	0	371	495	424	0	0.28	0.86	6.67	23.8	7.7	6.1
122	Flexural-with Shear Collapse	0	321	428	342	0	0.26	1.29	2.00	7.7	1.5	2.0
123	Flexural-with Shear Collapse	0	343	457	366	0	0.30	0.99	5.56	18.5	5.6	6.3
124	Flexural	0	461	614	491	0		0.91	6.67		7.3	
125	Flexural	0	509	678	578	0	0.23	0.86	6.67	29.1	7.8	6.0
126	Flexural	0	489	652	522	0		0.71	6.67		9.4	
127	Flexural	0	634	845	676	0		0.68	6.67		9.8	
128	Flexural	0	659	878	702	0	0.25	0.49	4.00	16.0	8.2	3.5
129	Flexural-with Shear Collapse	0	603	804	643	0		0.89	1.00		1.1	
130	Flexural-with Shear Collapse	0	609	812	650	0		0.69	3.45		5.0	
131	Flexural	0	251	334	267	0	0.38	1.18	4.00	6.7	2.7	
132	Flexural	0	449	598	478	0		0.80	1.20		1.5	
133	Flexural	0	602	803	642	0	0.27	0.55	3.47	12.7	6.3	3.7
134	Flexural-with Shear Collapse	0	0	0	0	0			6.50			
135	Flexural-with Shear Collapse	0	106	141	113	0			3.30			
136	Flexural-with Shear Collapse	0	101	134	107	0			3.30			
137	Flexural-with Shear Collapse	0	106	141	113	0			2.50			
138	Shear	0	95	126	101	0	0.52	1.45	2.91	5.7	2.0	2.6
139	Shear	0	117	155.6	124	0	0.53	1.123	2.24	4.2	2	1.9
140	Shear	0	123	164	131	0	0.33	1.07	2.31	7.0	2.2	2.0
141	Shear	0	149	199	159	0	0.46	1.17	3.00	6.6	2.6	2.7
142	Shear	0	116	155	124	0	0.13	0.26	0.84	6.4	3.3	0.7
143	Shear	0	146	195	156	0	0.20	0.76	1.60	8.1	2.1	1.4
144	Shear	0	127	169	135	0	0.13	0.36	1.17	9.0	3.2	1.1
145	Shear	0	164	219	175	0	0.27	0.98	2.12	7.9	2.2	1.9
146	Shear	0	157	210	168	0	0.25	1.05	1.88	7.4	1.8	1.7
147	Shear	0	187	249	199	0	0.41	1.25	2.79	6.8	2.2	2.5
148	Shear	0	172	229	183	0	0.32	1.08	2.31	7.2	2.1	2.0
149	Shear	0	161	214	171	0	0.32	1.22	2.35	7.3	1.9	2.1
150	Shear	0	120	159	128	0	0.07	0.18	0.49	7.4	2.7	0.5
151	Shear	0	140	186	149	0	0.11	0.59	1.25	11.3	2.1	1.2
152	Shear	0	177	236	189	0	0.23	0.86	1.79	7.9	2.1	1.6
153	Shear	0	204	272	218	0	0.29	1.10	2.26	7.9	2.1	2.0
154	Shear	0	364	486	389	0	0.36	1.08	1.80	5.0	1.7	1.5
155	Shear	0	392	523	418	0	0.27	0.49	1.37	5.0	2.8	1.2
156	Shear	0	380	506	405	0	0.49	1.05	1.78	3.6	1.7	1.4
157	Shear	0	589	785	628	0	0.29	0.60	1.58	5.5	2.6	1.3
158	Shear	0	50	67	54	0	0.38	0.84	1.50	4.0	1.8	1.2

Behavior Database

Num.	*Failure mode*	Q_0	Q_y	Q_{max}	Q_u	R_0	R_y	R_{max}	R_μ	μ_y	μ_d	*he / Qmax*
			kN	*kN*	*kN*		*%*	*%*	*%*			
159	Shear	0	72	97	77	0	0.44	0.96	2.25	5.1	2.3	1.9
160	Shear	0	96	128	102	0	0.30	0.78	1.25	4.2	1.6	1.1
161	Shear	0	106	142	114	0	0.21	0.47	0.59	2.9	1.2	0.4
162	Shear	0	94	125	100	0	0.15	0.30	0.57	3.7	1.9	0.5
163	Shear	0	303	404	323	0	0.22	0.84	2.06	9.2	2.4	1.9
164	Shear	0	342	456	365	0	0.36	0.99	1.74	4.8	1.8	1.5
165	Shear	0	489	652	522	0	0.86	2.01	4.09	4.8	2.0	3.5
166	Shear	0	419	559	447	0	0.48	1.73	3.11	6.4	1.8	2.6
167	Shear	0	518	690	552	0	0.85	2.58	4.82	5.7	1.9	4.2
168	Shear	0	391	521	417	0	0.37	0.78	1.63	4.4	2.1	1.4
169	Shear	0	519	692	554	0	0.57	1.88	2.84	5.0	1.5	2.4
170	Shear	0	430	573	459	0	0.37	1.19	2.69	7.3	2.3	2.5
171	Shear	0	549	732	586	0	0.66	2.65	4.48	6.8	1.7	3.9
172	Shear	0	420	560	448	0	0.65	1.73	3.53	5.4	2.0	3.0
173	Shear	0	492	656	524	0	0.66	1.79	3.64	5.5	2.0	3.1
174	Shear	0	402	536	429	0	0.29	0.89	1.06	3.7	1.2	0.8
175	Shear	0	417	557	445	0	0.31	0.89	1.17	3.8	1.3	1.0
176	Shear	0	467	623	499	0	0.40	0.90	2.10	5.2	2.3	1.9
177	Shear	0	474	632	506	0	0.36	1.06	3.61	10.1	3.4	3.3
178	Shear	0	507	676	541	0	0.29	0.97	1.49	5.1	1.5	1.3
179	Shear	0	82	110	88	0	0.45	1.05	1.71	3.8	1.6	1.4
180	Shear	0	308	411	328	0	1.24	1.84	4.96	4.0	2.7	3.9
181	Shear	0	324	432	346	0	1.11	2.47	4.50	4.0	1.8	3.6
182	Shear	0	328	437	350	0	0.50	1.57	3.58	7.1	2.3	3.0
183	Shear	0	375	500	400	0	0.40	0.99	1.61	4.0	1.6	1.3
184	Shear	0	234	313	250	0	0.40	0.89	2.09	5.3	2.3	1.8
185	Shear	0	201	269	215	0	0.89	1.78	3.47	3.9	2.0	3.1
186	Shear	0	245	327	262	0	0.87	1.95	1.90	2.2	1.0	1.3
187	Shear	0	259	346	277	0	0.48	0.85	1.04	2.2	1.2	0.7
188	Shear	0	135	180	144	0	0.62	1.65	3.87	6.2	2.3	3.2
189	Shear	0	161	215	172	0	0.18	0.93	1.92	10.8	2.1	1.7
190	Shear	0	184	246	197	0	0.15	0.44	0.91	6.2	2.0	0.8
191	Shear	0	198	265	212	0	0.14	0.38	0.92	6.4	2.4	0.8
192	Shear	0	289	385	308	0	0.41	1.82	7.42	17.9	4.1	6.9
193	Shear	0	296	395	316	0	0.15	0.49	3.87	25.6	7.9	3.6
194	Shear	0	468	624	499	0	0.22	0.51	1.01	4.7	2.0	0.9
195	Shear	0	196	261	209	0	0.32	0.77	0.93	2.9	1.2	0.7
196	Shear	0	52	69	55	0	0.23	0.93	3.23	13.8	3.5	2.9
197	Shear	0	323	431	345	0	0.41	0.94	2.26	5.5	2.4	1.9
198	Shear	0	320	427	342	0	0.32	0.98	1.66	5.2	1.7	1.4
199	Shear	0	298	397	318	0	0.66	2.04	3.26	4.9	1.6	2.8
200	Shear	0	331	441	353	0	0.28	1.29	1.92	7.0	1.5	1.7
201	Shear	0	413	550	440	0	0.43	0.97	1.25	2.9	1.3	1.0
202	Shear	0	460	613	490	0	0.63	1.50	2.51	4.0	1.7	2.1
203	Shear	0	401	535	428	0	0.26	0.50	1.11	4.2	2.2	0.9
204	Shear	0	504	672	538	0	0.25	0.44	1.09	4.3	2.5	0.9
205	Shear	0	573	764	611	0	0.36	0.52	0.77	2.1	1.5	0.6
206	Shear	0	683	911	729	0	0.42	1.10	2.15	5.1	2.0	1.9
207	Shear	0	745	993	794	0	0.30	1.41	2.61	8.7	1.9	2.3
208	Shear	0	687	916	733	0	0.18	0.50	1.22	6.7	2.4	1.1
209	Shear	0	793	1057	846	0	0.56	1.91	3.19	5.7	1.7	2.8
210	Shear	0	57	76	61	0	0.67	1.79	1.97	3.0	1.1	1.6
211	Shear	0	143	191	153	0	0.24	0.63	0.88	3.6	1.4	0.7
212	Shear	0	151	201	161	0	0.34	0.63	0.81	2.3	1.3	0.6
213	Shear	0	159	212	170	0	0.40	0.88	1.15	2.9	1.3	0.9
214	Shear	0	524	699	559	0	0.26	0.75	2.85	10.8	3.8	1.3
215	Shear	0	568	757	606	0	0.29	1.07	1.89	6.4	1.8	1.6

Behavior Database

Num.	*Failure mode*	Q_0	Q_y	Q_{max}	Q_u	R_0	R_y	R_{max}	R_μ	μ_y	μ_d	*he / Qmax*
			kN	*kN*	*kN*		*%*	*%*	*%*			
216	Shear	0	750	1000	800	0	0.61	1.36	2.23	3.7	1.6	1.7
217	Shear	0	1721	2295	1922	0	0.67	1.56	2.35	3.5	1.5	1.5
218	Shear	0	176	234	187	0	0.39	0.94	1.38	3.5	1.5	1.6
219	Shear	0	173	230	184	0	0.36	0.94	1.24	3.4	1.3	1.0
220	Shear	0	196	261	209	0	0.40	0.95	1.17	2.9	1.2	0.9
221	Shear	0	164	219	175	0	0.36	1.18	7.41	20.3	6.3	4.8
222	Shear	0	160	213	170	0	0.40	1.46	2.57	6.5	1.8	2.3
223	Shear	0	131	174	139	0	0.31	1.43	7.64	24.8	5.4	7.2
224	Shear	0	167	222	178	0	0.07	0.30	0.76	10.7	2.6	0.7
225	Shear	0	198	264	211	0	0.09	0.53	1.01	10.9	1.9	0.9
226	Shear	0	195	260	208	0	0.24	0.72	1.38	5.8	1.9	1.2
227	Shear	0	76	101	81	0	0.23	0.56	1.09	4.8	1.9	0.9
228	Shear	0	139	185	148	0	0.43	0.95	1.23	2.9	1.3	0.9
229	Shear	0	611	815	652	0	0.38	0.93	1.54	4.1	1.7	1.3
230	Shear	0	459	612	490	0	0.32	0.93	1.27	4.0	1.4	1.1
231	Shear	0	310	413	330	0	0.44	0.75	0.84	1.9	1.1	0.5
232	Shear	0	324	432	346	0	0.47	0.60	0.67	1.4	1.1	0.4
233	Shear	0	296	395	316	0	0.53	0.75	0.81	1.5	1.1	0.5
234	Shear	0	327	436	349	0	0.52	0.76	0.91	1.7	1.2	0.6
235	Shear	0	335	447	358	0	0.88	1.56	2.29	2.6	1.5	1.7
236	Shear	0	326	434	347	0	0.44	0.74	1.28	2.9	1.7	1.0
237	Shear	0	218	290	232	0	0.28	0.63	1.78	6.4	2.8	1.6
238	Shear	0	200	266	213	0	0.35	0.65	1.79	5.1	2.8	0.8
239	Shear	0	345	460	368	0	0.33	0.91	1.49	4.4	1.6	1.2
240	Shear	0	237	316	253	0	0.23	0.39	0.70	3.1	1.8	0.6
241	Shear	0	244	326	260	0	0.19	0.56	0.95	5.1	1.7	0.6
242	Shear	0	270	360	288	0	0.19	0.42	0.79	4.2	1.9	0.7
243	Shear	0	202	269	215	0	0.40	0.90	1.27	3.2	1.4	1.0
244	Shear	0	203	271	217	0	0.42	0.90	1.93	4.6	2.1	1.7
245	Shear	0	98	131	105	0	0.10	0.26	0.48	4.7	1.8	0.4
246	Shear	0	134	178	142	0	0.23	0.51	0.82	3.5	1.6	0.7
247	Shear	0	200	266	213	0	0.35	0.78	1.09	3.1	1.4	0.9
248	Shear	0	220	293	234	0	0.21	0.75	1.29	6.2	1.7	1.1
249	Shear	0	200	266	213	0	0.30	0.56	0.81	2.7	1.4	0.6
250	Shear	0	649	865	692	0	0.33	0.55	1.64	5.0	3.0	1.4
251	Shear	0	656	875	700	0	0.32	0.96	1.98	6.2	2.1	1.7
252	Shear	0	118	157	126	0	0.46	1.37	1.50	3.3	1.1	1.2
253	Shear	0	180	240	192	0	0.61	1.13	1.32	2.1	1.2	0.9
254	Shear	0	204	272	218	0	0.42	1.06	1.87	4.4	1.8	1.5
255	Shear	0	188	250	200	0	0.80	1.33	1.63	2.0	1.2	1.1
256	Shear	0	167	222	178	0	0.86	1.41	1.81	2.1	1.3	1.3
257	Shear	0	140	187	150	0	0.09	0.17	0.67	7.3	3.9	0.6
258	Shear	0	184	245	196	0	0.14	0.41	0.85	6.1	2.1	0.7
259	Shear	0	186	248	198	0	0.16	0.50	1.34	8.5	2.7	1.2
260	Shear	0	240	320	256	0	0.18	0.76	1.29	7.0	1.7	1.1
261	Shear	0	180	240	192	0	0.17	0.50	0.89	5.2	1.8	0.8
262	Shear	0	188	250	200	0	0.20	0.48	0.95	4.7	2.0	0.8
263	Shear	0	200	266	213	0	0.24	0.80	1.32	5.5	1.6	1.2
264	Shear	0	225	300	240	0	0.33	1.06	2.10	6.3	2.0	1.9
265	Flexural	0	248	330	264	0	0.44	1.63	4.97	11.4	3.0	4.7
266	Shear	0	258	344	275	0	0.25	0.93	1.28	5.1	1.4	1.1
267	Shear	0	203	271	217	0	0.35	1.02	2.37	6.9	2.3	2.1
268	Shear	0	183	244	195	0	0.34	1.02	2.13	6.3	2.1	1.9
269	Shear	0	975	1300	1040	0	0.28	0.63	1.53	5.4	2.4	1.3
270	Shear	0	523	697	558	0	0.35	0.96	1.61	4.6	1.7	1.3
271	Shear	0	116	155	124	0	0.07	0.73	1.27	18.0	1.7	1.2
272	Shear	0	105	140	112	0	0.05	0.24	0.77	14.1	3.1	0.7

Behavior Database

Num.	*Failure mode*	Q_0	Q_y	Q_{max}	Q_u	R_0	R_y	R_{max}	R_μ	μ_y	μ_d	*he / Qmax*
			kN	*kN*	*kN*		*%*	*%*	*%*			
273	Shear	0	97	130	104	0	0.09	0.54	1.51	16.9	2.8	1.4
274	Shear	0	101	135	108	0	0.19	0.52	0.86	4.6	1.7	0.7
275	Shear	0	670	894	715	0	0.19	0.59	1.05	5.7	1.8	0.9
276	Shear	0	209	279	223	0	0.05	0.30	0.64	13.6	2.1	0.6
277	Shear	0	176	234	187	0	0.10	0.32	1.11	11.7	3.5	1.0
278	Shear	0	165	220	176	0	0.13	0.33	1.25	10.0	3.8	1.1
279	Shear	0	241	321	257	0	0.43	0.95	1.56	3.7	1.7	1.2
280	Shear	0	430	573	459	0	0.23	0.80	1.77	7.8	2.2	1.6
281	Shear	0	468	624	499	0	0.25	1.02	1.71	6.7	1.7	1.5
282	Shear	0	503	670	536	0	0.21	0.49	0.94	4.5	1.9	0.8
283	Shear	0	520	694	555	0	0.18	0.48	1.31	7.1	2.7	1.2
284	Shear	0	513	684	547	0	0.26	0.62	2.24	8.7	3.6	2.0
285	Shear	0	517	689	551	0	0.25	0.58	2.85	11.5	4.9	2.6
286	Shear	0	795	1060	848	0	0.51	1.53	2.07	4.0	1.4	2.0
287	Shear	0	774	1033	826	0	0.55	1.79	2.14	3.9	1.2	2.6
288	Shear	0	761	1015	812	0	0.51	1.74	2.13	4.2	1.2	1.8
289	Shear	0	582	776	621	0	0.13	0.48	0.93	6.9	1.9	0.8
290	Shear	0	707	942	754	0	0.45	1.25	2.16	4.9	1.7	2.6
291	Shear	0	794	1059	847	0	0.40	1.28	4.16	10.4	3.3	3.4
292	Shear	0	112	150	120	0	0.24	1.05	1.50	6.2	1.4	1.3
293	Shear	0	250	333	267	0	0.27	0.90	2.47	9.1	2.8	2.2
294	Shear	0	244	325	260	0	0.38	1.38	2.49	6.6	1.8	2.2
295	Shear	0	231	308	246	0	0.42	1.58	3.67	8.8	2.3	3.2
296	Shear	0	215	287	230	0	0.84	1.64	4.17	5.0	2.5	3.5
297	Shear	0	388	517	414	0	0.19	0.37	0.90	4.9	2.4	0.8
298	Shear	0	248	330	264	0	0.20	0.40	1.06	5.4	2.6	0.9
299	Shear	0	168	224	179	0	0.47	1.02	1.33	2.8	1.3	1.0
300	Shear	0	177	235	188	0	0.48	1.01	1.55	3.2	1.5	1.2
301	Shear	0	184	245	196	0	0.49	0.97	1.58	3.2	1.6	1.3
302	Shear	0	196	262	209	0	0.47	1.48	3.47	7.3	2.3	4.1
303	Shear	0	188	250	200	0	0.60	1.45	4.36	7.2	3.0	3.8
304	Shear	0	180	240	192	0	0.76	1.66	4.49	5.9	2.7	5.0
305	Shear	0	140	186	149	0	0.68	1.25	2.34	3.5	1.9	1.9
306	Shear	0	594	792	633	0	0.09	0.25	0.63	6.7	2.6	0.6
307	Shear	0	568	758	606	0	0.16	0.71	1.07	6.5	1.5	0.9
308	Shear	0	774	1032	826	0	0.17	0.58	1.11	6.5	1.9	1.0
309	Shear	0	772	1029	823	0	0.28	0.68	1.11	4.0	1.6	1.0
310	Shear	0	69	92	74	0	0.09	0.23	0.38	4.1	1.6	0.4
311	Shear	0	91	122	97	0	0.14	0.33	1.02	7.1	3.1	1.1
312	Shear	0	89	118	95	0	0.12	0.28	2.49	20.5	9.0	2.3
313	Shear	0	94	125	100	0	0.14	0.38	3.44	24.0	8.9	2.7
314	Shear	0	96	127	102	0	0.15	0.44	2.56	16.5	5.9	2.3
315	Shear	0	94	126	100	0	0.15	0.39	4.41	28.6	11.2	2.8
316	Shear	0	117	130	122	0	0.26	1.00	3.26	12.5	3.3	3.1
317	Shear	0	84	112	90	0	0.15	0.94	3.53	24.2	3.8	2.9
318	Shear	0	89	119	95	0	0.16	0.71	3.76	23.2	5.3	2.9
319	Shear	0	110	146	117	0	0.28	1.36	3.78	13.5	2.8	3.0
320	Shear	0	700	934	747	0	1.06	2.50	3.37	3.2	1.3	2.7
321	Shear	0	598	798	638	0	0.81	1.98	2.95	3.7	1.5	2.4
322	Shear	0	684	912	730	0	1.09	2.81	4.96	4.6	1.8	4.2
323	Shear	0	707	943	754	0	0.54	1.32	1.89	3.5	1.4	1.5
324	Shear	0	627	836	669	0	0.51	1.10	2.04	4.0	1.9	1.7
325	Shear	0	759	1011	809	0	0.57	1.84	4.27	7.4	2.3	3.8
326	Shear	0	110	147	147	0	0.38	1.81	3.02	8.0	1.7	2.7
327	Shear	0	251	334	268	0	0.22	0.48	1.05	4.8	2.2	0.9
328	Shear	0	256	341	273	0	0.21	0.59	1.23	6.0	2.1	1.1
329	Shear	0	252	335	268	0	0.21	0.55	1.27	6.0	2.3	1.1

Behavior Database

Num.	*Failure mode*	Q_0	Q_y	Q_{max}	Q_u	R_0	R_y	R_{max}	R_μ	μ_y	μ_d	*he / Qmax*
			kN	*kN*	*kN*		*%*	*%*	*%*			
330	Shear	0	253	337	270	0	0.22	0.61	1.29	5.8	2.1	1.1
331	Shear	0	137	183	147	0	0.46	1.18	2.38	5.1	2.0	2.0
332	Shear	0	168	224	179	0	0.22	0.98	1.75	7.8	1.8	1.6
333	Shear	0	149	199	159	0	0.36	1.13	2.18	6.0	1.9	1.9
334	Shear	0	131	175	140	0	0.37	1.13	1.95	5.2	1.7	1.7
335	Shear	0	174	232	185	0	0.41	1.08	1.89	4.6	1.7	1.6
336	Shear	0	162	216	173	0	0.34	1.38	2.23	6.5	1.6	2.0
337	Shear	0	154	206	165	0	0.31	0.72	0.82	2.7	1.1	0.6
338	Shear	0	195	260	208	0	0.22	0.61	1.24	5.7	2.0	1.1
339	Shear	0	197	263	210	0	0.18	0.61	1.07	6.0	1.8	0.9
340	Shear	0	172	229	184	0	0.16	0.48	1.31	8.1	2.7	1.2
341	Shear	0	195	260	208	0	0.19	0.49	0.55	3.0	1.1	0.4
342	Shear	0	206	274	219	0	0.27	0.67	0.93	3.4	1.4	0.7
343	Shear	0	201	268	214	0	0.29	0.85	1.27	4.4	1.5	1.1
344	Shear	0	210	280	224	0	0.22	0.67	0.96	4.4	1.4	0.8
345	Shear	0	131	175	140	0	1.49	2.66	6.99	4.7	2.6	5.8
346	Shear	0	185	247	198	0	0.33	1.13	1.80	5.4	1.6	1.5
347	Shear	0	164	219	175	0	0.54	1.24	2.64	4.9	2.1	2.3
348	Shear	0	159	212	169	0	0.40	0.65	1.41	3.6	2.2	1.1
349	Shear	0	311	414	331	0	0.30	0.72	1.59	5.3	2.2	1.4
350	Shear	0	473	631	505	0	0.86	2.05	3.53	4.1	1.7	3.0
351	Shear	0	437	583	466	0	0.46	1.27	2.30	5.0	1.8	2.0
352	Shear	0	272	363	290	0	0.42	1.16	1.90	4.5	1.6	1.6
353	Shear	0	513	684	547	0	0.41	0.94	1.28	3.1	1.4	1.0
354	Shear	0	535	714	571	0	0.25	0.48	0.84	3.3	1.8	0.7
355	Shear	0	559	745	596	0	0.39	1.03	4.53	11.5	4.4	4.0
356	Shear	0	574	765	612	0	0.43	1.64	5.52	12.9	3.4	5.1
357	Shear	0	552	735	588	0	0.49	1.05	2.04	4.2	1.9	1.6
358	Shear	0	581	775	620	0	0.34	0.77	2.30	6.8	3.0	2.0
359	Shear	0	633	843	675	0	0.32	0.76	2.00	6.2	2.6	1.7
360	Shear	0	1020	1360	1088	0	0.52	1.02	0.97	1.8	0.9	0.3
361	Shear	0	648	864	691	0	0.37	1.33	2.26	6.1	1.7	1.7
362	Shear	0	740	987	789	0	0.34	1.28	1.95	5.7	1.5	1.7
363	Shear	0	695	927	741	0	0.30	1.47	2.60	8.6	1.8	1.8
364	Shear	0	714	952	762	0	0.55	1.83	3.10	5.7	1.7	2.7
365	Shear	0	96	128	102	0	0.22	0.65	1.39	6.4	2.1	1.2
366	Shear	0	90	120	96	0	0.19	0.44	1.55	8.4	3.6	1.4
367	Shear	0	112	149	119	0	0.17	0.46	1.59	9.3	3.4	1.4
368	Shear	0	131	174	139	0	0.17	0.35	0.86	5.0	2.5	0.7
369	Shear	0	375	500	400	0	0.31	0.78	0.93	3.0	1.2	0.7
370	Shear	0	368	490	392	0	0.37	0.80	1.44	3.9	1.8	1.2
371	Shear	0	189	252	201	0	0.19	0.51	0.82	4.2	1.6	0.7
372	Shear	0	178	237	190	0	0.20	0.50	0.78	3.9	1.6	0.6
373	Flexural	0	279	372	298	0	0.34	0.97	2.85	8.5	2.9	4.5
374	Flexural	0	299	399	319	0	0.51	1.01	3.40	6.7	3.4	3.1
375	Flexural	0	318	424	339	0	0.64	2.01	6.16	9.7	3.1	5.9
376	Flexural	0	317	423	338	0	0.76	2.00	4.39	5.8	2.2	3.7

Analysis

Num.	*Shear*			*Moment*					*Factors*			
	Qsu	*Qmu*	*Vu*	*Mu*	*Kent-Park*	*Kent-Park 1C*	*Kent-Park 2C*	*NewRC 0C*	*Qsu / Qmu*	*SRI*	*Vu/ Qmu*	*SSI*
	kN	*kN*	*kN*	*kN*m*	*kN*m*	*kN*m*	*kN*m*	*kN*m*				
1	129	127	104	38	38	38		41	1.02	2.33	0.82	1.54
2	362	335	496	176	194	179	190	179	1.08	2.50	1.48	1.79
3	392	414	496	217	221	198	219	187	0.95	2.10	1.20	1.72
4	412	392	496	206	219	189	231	169	1.05	1.66	1.27	1.58
5	322	414	424	217	205	188	212	185	0.78	0.93	1.02	1.15
6	353	414	476	217	212	191	215	186	0.85	1.40	1.15	1.41
7	489	566	737	297	286	247	271	241	0.86	1.91	1.30	1.39
8	524	532	737	279	275	228	296	219	0.99	1.51	1.39	1.27
9	143	183	122	83	81	78	83	76	0.78	0.72	0.67	1.16
10	151	102	122	46	59	54	68	48	1.48	0.29	1.20	0.62
11	160	212	150	95	92	88	94	88	0.75	0.68	0.71	1.09
12	171	107	150	48	0	0	73	0	1.60	0.27	1.40	0.58
13	149	185	150	83	86	83	87	83	0.80	0.78	0.81	1.12
14	482	454	669	318	357	209	215	344	1.06	0.93	1.47	1.28
15	482	454	669	318	250	209	215	344	1.06	0.93	1.47	1.28
16	476	504	766	303	290	265	273	305	0.94	2.20	1.52	1.51
17	573	544	794	327	277	227	221	376	1.05	1.34	1.46	1.22
18	578	548	807	329	284	233	225	378	1.06	1.48	1.47	1.29
19	364	518	298	311	281	257	304	279	0.70	0.32	0.58	0.57
20	358	326	481	147	171	140	165	142	1.10	0.53	1.48	0.76
21	267	171	241	77	110	98	101	81	1.56	1.21	1.41	1.50
22	413	326	586	147	194	155	177	143	1.27	1.14	1.80	1.11
23	385	326	566	147	181	147	170	143	1.18	0.80	1.74	0.93
24	413	326	586	147	194	155	177	143	1.27	1.14	1.80	1.11
25	102	121	124	36	42	39	40	37	0.84	2.16	1.03	1.70
26	112	97	123	29	52	47	46	35	1.15	1.21	1.26	1.30
27	77	36	122	11	19	18	19	18	2.11	2.42	3.36	1.72
28	112	97	121	29	52	47	46	37	1.15	1.18	1.24	1.28
29	133	176	189	53	60	55	57	48	0.75	1.74	1.07	1.35
30	143	176	189	53	65	56	61	52	0.82	1.49	1.08	1.28
31	143	155	189	46	69	61	63	50	0.93	1.26	1.22	1.18
32	143	134	189	40	70	60	62	47	1.07	1.06	1.41	1.05
33	107	136	147	41	47	44	44	40	0.79	2.41	1.08	1.82
34	113	135	147	40	50	46	46	41	0.84	2.06	1.09	1.73
35	113	121	147	36	52	47	47	41	0.93	1.75	1.21	1.59
36	113	108	147	32	53	48	46	39	1.05	1.47	1.36	1.43
37	125	147	182	44	52	47	48	43	0.85	3.23	1.24	2.03
38	133	147	182	44	56	50	51	44	0.91	2.77	1.24	1.92
39	133	131	182	39	59	52	52	45	1.01	2.34	1.39	1.77
40	133	115	182	35	60	54	51	43	1.15	1.97	1.58	1.59
41	133	115	182	35	60	54	51	43	1.15	1.97	1.58	1.59
42	541	548	938	329	479	464	473	505	0.99	1.31	1.71	0.90
43	275	334	343	125	133	112	111	129	0.82	1.40	1.03	0.89
44	133	145	146	44	45	41	38	42	0.92	0.82	1.01	0.96
45	143	167	146	50	51	46	43	48	0.86	0.72	0.88	0.93
46	153	176	146	53	57	51	43	51	0.87	0.62	0.83	0.88
47	153	155	146	46	61	52	45	53	0.99	0.52	0.95	0.81
48	146	145	161	44	45	42	39	42	1.00	1.22	1.11	1.17

Analysis

Num.	*Shear*			*Moment*					*Factors*			
	Qsu	*Qmu*	*Vu*	*Mu*	*Kent-Park*	*Kent-Park 1C*	*Kent-Park 2C*	*NewRC 0C*	*Qsu / Qmu*	*SRI*	*Vu/ Qmu*	*SSI*
	kN	*kN*	*kN*	*kN*m*	*kN*m*	*kN*m*	*kN*m*	*kN*m*				
49	156	167	161	50	52	47	44	48	0.93	1.08	0.97	1.14
50	166	176	161	53	59	52	45	52	0.94	0.93	0.92	1.08
51	166	155	161	46	63	54	47	54	1.07	0.78	1.04	1.00
52	166	167	169	50	53	47	44	48	1.00	1.44	1.01	1.32
53	176	176	169	53	61	53	46	52	1.00	1.24	0.96	1.25
54	295	245	454	221	285	279	283	306	1.20	0.67	1.85	1.14
55	437	462	790	416	394	357	375	424	0.94	1.44	1.71	1.73
56	548	575	867	517	384	341	331	473	0.95	1.94	1.51	2.16
57	324	148	814	134	200	195	196	207	2.19	1.47	5.49	1.69
58	109	163	118	49	54	50	43	52	0.67	0.93	0.72	1.07
59	113	142	118	43	58	50	45	54	0.80	0.76	0.83	0.99
60	113	122	118	37	59	53	42	53	0.93	0.62	0.97	0.87
61	113	103	118	31	57	51	39	51	1.10	0.51	1.14	0.75
62	131	172	189	52	59	54	56	48	0.76	1.77	1.10	1.35
63	140	182	189	55	64	56	60	47	0.77	1.55	1.04	1.30
64	143	161	189	48	68	56	63	51	0.89	1.31	1.17	1.20
65	143	142	189	43	70	61	63	49	1.01	1.12	1.33	1.10
66	133	88	182	26	59	51	48	39	1.50	1.46	2.06	1.23
67	113	127	147	38	51	47	47	42	0.89	1.84	1.16	1.64
68	113	106	147	32	53	48	46	39	1.07	1.42	1.38	1.40
69	113	86	147	26	51	46	44	36	1.32	1.10	1.71	1.13
70	113	65	147	20	49	43	283	31	1.73	0.87	2.25	0.87
71	132	148	182	44	55	50	50	44	0.89	2.79	1.23	1.93
72	133	128	182	38	60	52	52	45	1.04	2.24	1.43	1.73
73	133	107	182	32	61	53	50	42	1.24	1.79	1.70	1.48
74	133	88	182	26	59	51	48	39	1.50	1.46	2.06	1.23
75	154	158	220	59	63	59	61	59	0.97	2.12	1.39	1.78
76	172	249	289	81	116	112	115	112	0.69	2.08	1.16	0.99
77	172	249	289	81	116	112	115	112	0.69	2.08	1.16	0.99
78	295	495	385	160	157	140	145	134	0.60	1.23	0.78	0.89
79	263	324	384	105	147	122	129	133	0.81	0.58	1.19	0.51
80	269	317	391	102	146	119	127	132	0.85	0.55	1.23	0.48
81	149	70	421	23	63	60	61	61	2.14	1.37	6.03	0.86
82	293	331	421	107	158	127	137	138	0.88	0.63	1.27	0.51
83	293	331	421	107	158	127	137	138	0.88	0.63	1.27	0.51
84	180	167	254	63	80	72	70	71	1.08	1.42	1.52	1.51
85	178	199	262	75	78	72	73	71	0.90	1.80	1.31	1.66
86	176	169	304	63	69	64	66	64	1.04	2.95	1.79	2.04
87	220	239	357	90	95	83	88	81	0.92	2.27	1.49	1.73
88	296	266	384	120	150	127	148	124	1.11	0.77	1.44	0.98
89	466	602	389	271	273	223	234	260	0.77	1.10	0.65	0.69
90	349	272	445	122	177	143	162	129	1.28	1.52	1.64	1.36
91	441	538	582	242	244	194	204	219	0.82	2.09	1.08	1.22
92	519	600	409	270	280	229	238	260	0.86	2.20	0.68	0.96
93	330	717	371	179	184	159	174	156	0.46	1.64	0.52	0.67
94	237	247	295	111	120	110	113	111	0.96	2.37	1.20	1.77
95	430	578	589	295	270	222	238	260	0.74	1.51	1.02	1.17
96	334	368	492	166	232	180	196	202	0.91	0.99	1.34	0.74
97	402	466	556	245	246	213	248	242	0.86	0.72	1.19	0.73
98	421	466	630	245	248	214	248	242	0.90	0.96	1.35	0.84
99	452	466	725	245	251	216	249	242	0.97	1.45	1.55	1.03
100	463	546	651	286	289	254	274	279	0.85	0.94	1.19	0.77
101	494	546	748	286	292	257	275	279	0.90	1.41	1.37	0.94

Analysis

Num.	*Shear*			*Moment*					*Factors*			
	Qsu	*Qmu*	*Vu*	*Mu*	*Kent-Park*	*Kent-Park 1C*	*Kent-Park 2C*	*NewRC 0C*	*Qsu / Qmu*	*SRI*	*Vu/ Qmu*	*SSI*
	kN	*kN*	*kN*	*kN*m*	*kN*m*	*kN*m*	*kN*m*	*kN*m*				
102	671	716	863	376	354	255	353	280	0.94	1.40	1.21	1.02
103	630	789	521	414	407	345	373	396	0.80	0.87	0.66	0.58
104	661	789	609	414	411	346	374	396	0.84	1.30	0.77	0.72
105	699	789	666	414	415	348	376	396	0.89	1.95	0.84	0.88
106	546	765	651	401	345	275	325	317	0.71	0.79	0.85	0.74
107	577	765	748	401	352	283	330	317	0.75	1.18	0.98	0.91
108	615	765	863	401	370	292	336	312	0.80	1.77	1.13	1.11
109	774	1048	783	550	480	360	445	405	0.74	1.67	0.75	0.90
110	529	560	836	294	301	264	282	286	0.94	2.10	1.49	1.13
111	615	786	836	412	377	293	342	320	0.78	1.77	1.06	1.09
112	672	735	836	386	358	258	353	287	0.91	1.39	1.14	1.00
113	423	560	428	294	293	256	277	286	0.76	0.51	0.76	0.56
114	464	560	640	294	296	259	279	286	0.83	0.93	1.14	0.76
115	502	560	715	294	298	262	281	286	0.90	0.93	1.28	0.76
116	612	735	706	386	330	235	343	287	0.83	0.76	0.96	0.74
117	731	735	886	386	389	279	375	288	0.99	1.39	1.20	1.00
118	589	786	715	412	361	287	337	320	0.75	0.78	0.91	0.73
119	362	335	496	176	194	179	190	179	1.08	2.50	1.48	1.79
120	392	414	496	217	221	198	219	187	0.95	2.10	1.20	1.72
121	412	392	496	206	219	189	231	169	1.05	1.66	1.27	1.58
122	322	414	424	217	205	188	212	185	0.78	0.93	1.02	1.15
123	353	414	476	217	212	191	215	186	0.85	1.40	1.15	1.41
124	489	566	737	297	286	247	271	241	0.86	1.91	1.30	1.39
125	524	532	737	279	275	228	296	219	0.99	1.51	1.39	1.27
126	585	612	872	321	328	283	303	311	0.96	2.05	1.42	1.05
127	683	870	872	457	417	316	377	352	0.79	1.73	1.00	1.02
128	749	814	872	427	399	276	388	316	0.92	1.36	1.07	0.93
129	613	870	654	457	389	301	364	352	0.70	0.77	0.75	0.68
130	645	870	753	457	398	309	370	352	0.74	1.15	0.87	0.83
131	303	301	462	241	220	198	212	237	1.01	0.90	1.53	1.53
132	412	602	494	241	220	198	212	237	0.68	0.90	0.82	0.80
133	623	697	1011	492	466	423	451	486	0.89	1.34	1.45	1.10
134	145	139	#N/A	42	64	62	62	64	1.05	1.03	#N/A	1.53
135	161	225	#N/A	67	79	75	75	77	0.72	0.98	#N/A	1.53
136	161	225	#N/A	67	79	75	75	77	0.72	0.98	#N/A	1.53
137	161	225	#N/A	67	79	75	75	77	0.72	0.98	#N/A	1.53
138	74	114	98	34	45	44	42	44	0.65	0.80	0.86	0.87
139	88	155	98	47	54	51	48	52	0.57	0.65	0.63	0.84
140	141	237	138	71	95	92	92	94	0.59	0.50	0.58	0.50
141	156	237	201	71	95	93	93	95	0.66	0.98	0.85	0.70
142	129	316	93	95	102	102	102	105	0.41	0.00	0.30	0.00
143	158	316	141	95	106	103	103	105	0.50	0.47	0.44	0.49
144	163	317	145	95	108	105	104	107	0.51	0.45	0.46	0.47
145	170	316	199	95	106	103	103	105	0.54	0.96	0.63	0.70
146	173	316	203	95	108	104	104	106	0.55	0.93	0.64	0.68
147	176	317	206	95	109	105	104	106	0.56	0.91	0.65	0.66
148	178	384	204	115	127	123	123	125	0.46	0.92	0.53	0.64
149	149	215	203	64	77	73	73	74	0.70	0.93	0.94	0.79
150	145	373	94	112	110	110	110	114	0.39	0.00	0.25	0.00
151	169	372	136	112	114	111	110	113	0.45	0.43	0.36	0.50
152	190	376	204	113	119	114	113	116	0.50	0.83	0.54	0.67
153	200	377	248	113	120	112	111	116	0.53	1.16	0.66	0.78
154	345	584	422	199	209	186	189	205	0.59	0.45	0.72	0.42
155	391	650	415	222	219	188	215	205	0.60	0.35	0.64	0.40
156	339	537	503	184	199	180	180	190	0.63	0.94	0.94	0.64
157	528	755	642	258	273	220	285	230	0.70	0.64	0.85	0.46
158	48	53	61	12	22	22	21	22	0.91	0.33	1.16	0.44

Analysis

Num.	*Shear*			*Moment*					*Factors*			
	Qsu	*Qmu*	*Vu*	*Mu*	*Kent-Park*	*Kent-Park 1C*	*Kent-Park 2C*	*NewRC 0C*	*Qsu / Qmu*	*SRI*	*Vu/ Qmu*	*SSI*
	kN	*kN*	*kN*	*kN*m*	*kN*m*	*kN*m*	*kN*m*	*kN*m*				
159	53	69	61	15	27	27	26	27	0.77	0.33	0.89	0.44
160	65	126	61	28	38	36	33	37	0.51	0.30	0.49	0.43
161	75	151	61	34	43	41	34	42	0.49	0.24	0.41	0.41
162	78	137	61	31	45	41	37	44	0.57	0.21	0.45	0.39
163	217	350	294	96	105	92	100	85	0.62	2.61	0.84	1.19
164	367	792	343	356	328	278		305	0.46	0.60	0.43	0.51
165	409	792	501	356	333	283		304	0.52	1.51	0.63	0.81
166	407	792	484	356	332	282		304	0.51	1.19	0.61	0.72
167	480	792	572	356	369	296		304	0.61	2.69	0.72	1.08
168	426	945	343	425	321	264		300	0.45	0.51	0.36	0.50
169	469	945	501	425	329	270		300	0.50	1.29	0.53	0.78
170	466	945	484	425	328	269		300	0.49	1.02	0.51	0.70
171	540	945	572	425	357	282		300	0.57	2.29	0.60	1.05
172	369	864	474	389	312	268		286	0.43	0.76	0.55	0.62
173	414	864	556	389	333	274		286	0.48	1.57	0.64	0.89
174	399	994	376	447	298	253		273	0.40	0.43	0.38	0.49
175	420	994	434	447	315	257		273	0.42	0.65	0.44	0.60
176	420	994	474	447	300	254		273	0.42	0.65	0.48	0.60
177	464	994	556	447	322	265		273	0.47	1.34	0.56	0.86
178	439	711	562	355	362	314	375	340	0.62	0.92	0.79	0.78
179	131	203	75	64	79	78	78	79	0.64	0.16	0.37	0.57
180	210	333	454	150	193	181		190	0.63	0.81	1.36	0.78
181	260	471	454	212	250	216		223	0.55	0.88	0.96	0.78
182	310	671	454	302	232	205		212	0.46	0.81	0.68	0.77
183	359	789	454	355	228	195		206	0.46	0.66	0.57	0.74
184	218	557	193	111	110	96		101	0.39	1.20	0.35	0.58
185	171	320	193	64	84	77		83	0.53	1.52	0.60	0.60
186	194	464	193	93	102	91		99	0.42	1.43	0.42	0.60
187	233	450	193	90	108	90		98	0.52	0.73	0.43	0.45
188	153	320	122	64	83	77		83	0.48	0.76	0.38	0.43
189	177	461	122	92	100	90		99	0.38	0.72	0.27	0.43
190	200	553	122	111	108	94		100	0.36	0.60	0.22	0.41
191	215	448	122	90	104	87		97	0.48	0.37	0.27	0.32
192	214	461	255	92	103	92		99	0.46	2.86	0.55	0.85
193	252	448	255	90	116	94		97	0.56	1.47	0.57	0.64
194	439	697	356	523	433	420	520	431	0.63	0.27	0.51	0.59
195	153	223	114	100	101	98	101	101	0.69	0.25	0.51	0.60
196	56	85	42	19	21	20	19	21	0.65	0.57	0.50	0.77
197	337	603	316	362	306	296		300	0.56	0.68	0.52	0.90
198	301	647	397	291	261	233		237	0.47	0.86	0.61	0.81
199	219	527	273	237	211	194		190	0.41	0.96	0.52	1.02
200	307	560	450	252	289	265		283	0.55	0.99	0.80	0.69
201	396	802	455	361	321	265		287	0.49	0.79	0.57	0.64
202	396	802	455	361	321	265		287	0.49	0.79	0.57	0.64
203	501	705	710	317	323	250		268	0.71	1.64	1.01	0.94
204	577	1126	225	507	433	339		393	0.51	0.34	0.20	0.31
205	606	1126	302	507	451	343		393	0.54	0.68	0.27	0.44
206	606	1126	302	507	451	343		393	0.54	0.68	0.27	0.44
207	625	1126	329	507	457	355		393	0.55	0.97	0.29	0.53
208	742	1689	302	507	451	343		393	0.44	0.68	0.18	0.31
209	660	1040	564	468	452	343		362	0.63	2.09	0.54	0.83
210	53	75	41	30	34	34	32	35	0.71	0.28	0.55	0.79
211	136	208	80	94	94	92	95	94	0.65	0.26	0.38	0.63
212	136	208	80	94	94	92	95	94	0.65	0.26	0.38	0.63
213	136	208	80	94	94	92	95	94	0.65	0.26	0.38	0.63
214	568	1592	641	1122	662	625		650	0.36	0.59	0.40	0.68
215	568	1592	616	1122	666	627		650	0.36	0.59	0.39	0.68

Analysis

Num.	*Shear*			*Moment*					*Factors*			
	Qsu	*Qmu*	*Vu*	*Mu*	*Kent-Park*	*Kent-Park 1C*	*Kent-Park 2C*	*NewRC 0C*	*Qsu / Qmu*	*SRI*	*Vu/ Qmu*	*SSI*
	kN	*kN*	*kN*	*kN*m*	*kN*m*	*kN*m*	*kN*m*	*kN*m*				
216	608	2249	978	1585	953	866		881	0.27	1.22	0.43	0.87
217	1293	2891	2337	3036	1731	1622		1680	0.45	1.10	0.81	0.94
218	164	241	150	145	147	138	147	145	0.68	0.44	0.62	0.90
219	150	241	100	145	144	137	146	145	0.62	0.22	0.42	0.64
220	182	275	150	165	154	136	149	150	0.66	0.39	0.54	0.88
221	156	195	147	117	118	111	118	116	0.80	0.44	0.75	1.00
222	147	195	117	117	117	110	117	116	0.75	0.30	0.60	0.82
223	138	156	115	93	91	88	90	91	0.89	0.30	0.74	0.93
224	211	431	158	129	133	128	134	131	0.49	0.51	0.37	0.53
225	226	490	158	147	139	129	139	135	0.46	0.45	0.32	0.52
226	198	319	153	96	98	95	98	96	0.62	0.51	0.48	0.59
227	85	135	60	68	70	70	70	71	0.63	0.18	0.44	0.63
228	122	174	88	87	85	80	79	84	0.70	0.32	0.50	0.83
229	462	761	584	278	264	224	239	234	0.61	1.66	0.77	0.90
230	339	588	415	212	204	182	191	181	0.58	1.23	0.70	0.85
231	271	404	185	303	276	269	320	276	0.67	0.28	0.46	0.73
232	271	404	185	303	276	269	320	276	0.67	0.28	0.46	0.73
233	271	404	185	303	276	269	320	276	0.67	0.28	0.46	0.73
234	271	404	185	303	276	269	320	276	0.67	0.28	0.46	0.73
235	302	404	286	303	283	272	321	276	0.75	0.57	0.71	1.03
236	302	404	286	303	283	272	321	276	0.75	0.57	0.71	1.03
237	159	243	155	109	112	108	114	109	0.65	0.51	0.64	0.84
238	187	204	167	92	107	99	119	101	0.92	0.30	0.82	0.62
239	240	377	213	170	164	141	86	162	0.64	0.35	0.56	0.57
240	209	397	180	119	120	115	122	117	0.53	0.49	0.45	0.55
241	225	306	182	92	107	99	119	101	0.73	0.30	0.59	0.43
242	236	437	186	262	269	262	299	264	0.54	0.44	0.42	0.76
243	153	233	114	105	104	101	104	104	0.66	0.24	0.49	0.59
244	197	234	210	105	110	103	106	105	0.84	1.27	0.90	1.33
245	115	200	85	50	52	51	51	52	0.58	0.19	0.43	0.38
246	147	251	116	63	65	62	61	65	0.58	0.14	0.46	0.30
247	170	282	147	127	131	127	132	130	0.60	0.48	0.52	0.74
248	185	321	147	144	138	129	139	135	0.58	0.43	0.46	0.72
249	185	321	147	144	138	129	139	135	0.58	0.43	0.46	0.72
250	837	1342	-115	604	492	371		409	0.62	0.82	-0.09	0.47
251	837	1338	-115	602	492	371		420	0.63	0.82	-0.09	0.47
252	123	437	176	262	274	270		272	0.28	0.40	0.40	0.69
253	209	599	272	359	312	288		293	0.35	0.88	0.45	0.96
254	240	686	269	412	280	267		273	0.35	0.83	0.39	0.98
255	169	504	269	302	309	301		304	0.34	0.89	0.53	1.00
256	134	409	272	245	259	255		258	0.33	0.75	0.66	0.98
257	187	286	176	86	106	106	110	111	0.65	0.00	0.61	0.00
258	230	286	223	86	112	106	110	111	0.80	0.32	0.78	0.89
259	245	286	262	86	112	106	110	111	0.86	0.49	0.91	1.10
260	256	433	231	130	119	111	118	115	0.59	0.94	0.53	0.79
261	160	291	132	131	137	131	139	137	0.55	0.31	0.45	0.61
262	160	291	132	131	137	131	139	137	0.55	0.31	0.45	0.61
263	184	289	223	130	140	131	138	134	0.63	0.97	0.77	1.09
264	184	289	223	130	140	131	138	134	0.63	0.97	0.77	1.09
265	211	289	310	130	142	132	135	139	0.73	1.94	1.07	1.55
266	250	427	223	128	117	109	116	112	0.59	0.97	0.52	0.81
267	133	165	189	74	87	78	77	82	0.81	0.96	1.15	1.31
268	134	167	192	75	88	79	78	83	0.80	0.94	1.15	1.29
269	1195	2316	76	834	676	519		584	0.52	1.10	0.03	0.39
270	435	578	489	347	314	247	277	282	0.75	0.95	0.85	0.91
271	133	237	104	44	48	46	46	47	0.56	0.51	0.44	0.50
272	133	237	104	44	48	46	46	47	0.56	0.51	0.44	0.50

Analysis

Num.	*Shear*			*Moment*					*Factors*			
	Qsu	*Qmu*	*Vu*	*Mu*	*Kent-Park*	*Kent-Park 1C*	*Kent-Park 2C*	*NewRC 0C*	*Qsu / Qmu*	*SRI*	*Vu/ Qmu*	*SSI*
	kN	*kN*	*kN*	*kN*m*	*kN*m*	*kN*m*	*kN*m*	*kN*m*				
273	108	165	86	41	44	43	43	43	0.66	0.53	0.52	0.68
274	113	167	95	42	45	44	44	45	0.68	0.53	0.57	0.66
275	649	1358	251	475	411	307		357	0.48	1.09	0.19	0.48
276	241	333	229	117	103	99	131	96	0.72	0.51	0.69	1.33
277	273	382	217	191	161	156	189	152	0.72	0.57	0.57	1.69
278	257	380	220	238	204	201	235	197	0.67	0.57	0.58	1.93
279	250	286	253	114	134	108	113	120	0.88	0.82	0.88	0.91
280	393	672	504	235	230	192	217	223	0.58	0.64	0.75	0.53
281	412	672	598	235	233	194	219	223	0.61	1.01	0.89	0.66
282	459	666	504	233	238	185	229	218	0.69	0.45	0.76	0.46
283	477	666	598	233	247	192	235	218	0.72	0.70	0.90	0.58
284	494	511	610	230	274	195	231	226	0.97	0.73	1.19	0.66
285	496	513	610	231	275	196	232	227	0.97	0.73	1.19	0.65
286	587	819	935	491	540	522	530	596	0.72	1.28	1.14	0.90
287	590	822	938	493	542	524	532	598	0.72	1.27	1.14	0.89
288	590	822	938	493	542	538	532	598	0.72	1.27	1.14	0.89
289	579	1037	612	622	580	535	658	562	0.56	0.59	0.59	0.63
290	640	1037	938	622	589	541	564	662	0.62	1.17	0.91	0.89
291	650	1037	987	622	590	542	564	663	0.63	1.29	0.95	0.93
292	82	155	69	47	56	54	49	55	0.53	0.25	0.44	0.50
293	154	322	211	64	91	78		83	0.48	0.85	0.66	0.54
294	154	384	211	77	93	82		86	0.40	1.20	0.55	0.66
295	132	364	211	73	93	83		91	0.36	1.58	0.58	0.72
296	111	224	211	45	84	73		76	0.50	1.77	0.94	0.72
297	#N/A	447	543	223	363	353	406	358	#N/A	0.59	1.22	0.58
298	218	378	185	170	161	156	176	160	0.58	0.30	0.49	0.58
299	163	257	119	141	141	134	144	141	0.64	0.22	0.46	0.57
300	182	257	154	141	143	135	136	141	0.71	0.53	0.60	0.89
301	204	257	237	141	146	137	138	141	0.79	1.06	0.92	1.26
302	186	462	230	138	175	156		172	0.40	1.17	0.50	0.78
303	171	404	230	121	159	154		156	0.42	1.14	0.57	0.78
304	150	346	214	104	139	137		138	0.43	1.09	0.62	0.84
305	133	346	167	104	139	137		138	0.38	0.54	0.48	0.58
306	566	1228	479	491	434	392	469	420	0.46	0.21	0.39	0.28
307	610	1228	638	491	461	405	483	420	0.50	0.42	0.52	0.39
308	644	1228	727	491	475	415	492	420	0.52	0.63	0.59	0.48
309	673	1228	805	491	488	423	499	421	0.55	0.84	0.66	0.55
310	72	229	#N/A	86	85	85	85	84	0.31	0.00	#N/A	0.00
311	129	241	97	91	91	89	89	89	0.53	0.28	0.40	0.56
312	134	241	109	91	91	89	89	89	0.56	0.35	0.45	0.62
313	142	241	126	91	92	89	89	89	0.59	0.46	0.52	0.72
314	130	241	112	91	91	89	89	89	0.54	0.46	0.46	0.72
315	134	241	120	91	92	89	89	89	0.56	0.55	0.50	0.79
316	145	241	138	91	92	89	89	89	0.60	0.79	0.57	0.94
317	118	229	99	86	86	85	85	85	0.52	1.21	0.43	1.20
318	123	229	108	86	87	85	85	85	0.54	1.52	0.47	1.34
319	131	229	120	86	87	85	85	85	0.57	2.02	0.53	1.55
320	554	963	349	434	435	346		375	0.57	1.12	0.36	0.56
321	544	963	256	434	430	345		387	0.56	0.93	0.27	0.51
322	597	963	349	434	441	351		375	0.62	2.10	0.36	0.76
323	672	1248	349	561	433	330		382	0.54	0.90	0.28	0.53
324	662	1248	256	561	428	329		382	0.53	0.76	0.21	0.48
325	716	1248	349	561	454	347		382	0.57	1.70	0.28	0.73
326	115	61	-341	36	81	80	79	81	1.90	0.95	-5.63	1.00
327	169	260	217	156	260	249	166	258	0.65	0.63	0.83	0.90
328	169	259	216	156	260	249	165	258	0.65	0.63	0.83	0.91
329	169	259	216	156	260	249	165	258	0.65	0.63	0.83	0.91

Analysis

Num.	*Shear*			*Moment*					*Factors*			
	Qsu	*Qmu*	*Vu*	*Mu*	*Kent-Park*	*Kent-Park 1C*	*Kent-Park 2C*	*NewRC 0C*	*Qsu / Qmu*	*SRI*	*Vu/ Qmu*	*SSI*
	kN	*kN*	*kN*	*kN*m*	*kN*m*	*kN*m*	*kN*m*	*kN*m*				
330	166	254	214	152	260	249	162	258	0.65	0.65	0.84	0.92
331	87	123	142	55	101	97	97	100	0.71	0.66	1.16	0.86
332	119	244	152	73	111	106	106	109	0.49	0.60	0.62	0.58
333	98	161	140	73	110	105	105	108	0.61	0.61	0.87	0.87
334	89	129	119	58	98	94	93	94	0.68	0.66	0.92	1.05
335	108	169	155	76	118	108	107	117	0.64	0.52	0.92	0.71
336	150	437	128	131	146	144		146	0.34	0.38	0.29	0.48
337	123	139	169	63	106	104	106	105	0.88	0.64	1.21	0.82
338	146	240	169	108	133	126	132	128	0.61	0.59	0.70	0.81
339	170	297	169	134	141	135	141	137	0.57	0.48	0.57	0.77
340	180	334	211	150	166	163	176	165	0.54	0.70	0.63	0.65
341	178	314	133	141	132	123	133	129	0.57	0.35	0.42	0.67
342	178	314	133	141	132	123	133	129	0.57	0.35	0.42	0.67
343	195	314	188	141	136	125	135	129	0.62	0.70	0.60	0.95
344	195	314	188	141	136	125	135	129	0.62	0.70	0.60	0.95
345	119	360	140	90	119	115		118	0.33	0.84	0.39	0.62
346	183	549	144	137	110	103		105	0.33	0.49	0.26	0.51
347	136	414	144	103	133	118		119	0.33	0.85	0.35	0.60
348	138	414	146	103	133	118		120	0.33	0.84	0.35	0.59
349	487	1395	285	419	357	345	424	351	0.35	0.35	0.20	0.61
350	382	758	490	341	319	279		303	0.50	1.45	0.65	0.82
351	451	932	490	419	318	258		282	0.48	1.19	0.53	0.79
352	234	493	400	246	222	204	209	214	0.47	1.32	0.81	1.21
353	429	806	416	323	271	215	241	247	0.53	0.70	0.52	0.58
354	457	660	416	264	256	182	219	233	0.69	0.43	0.63	0.43
355	524	753	515	339	331	259	279	293	0.70	0.96	0.68	0.66
356	515	734	569	330	324	248	271	283	0.70	1.56	0.78	0.87
357	566	663	529	298	332	238	274	275	0.85	0.77	0.80	0.62
358	576	701	513	315	340	244	281	289	0.82	1.08	0.73	0.71
359	624	820	503	369	341	247		292	0.76	0.80	0.61	0.65
360	984	2150	802	1720	1378	1328		1381	0.46	0.68	0.37	0.34
361	1134	1251	843	2001	1091	975		1027	0.91	0.64	0.67	0.68
362	1304	1271	926	2034	1334	1274		1126	1.03	1.29	0.73	0.90
363	1302	1267	926	2027	1336	1277		1129	1.03	1.29	0.73	0.90
364	1231	1254	1007	2006	1297	1054		1042	0.98	1.29	0.80	0.95
365	89	148	84	33	49	44	39	48	0.60	0.34	0.57	0.47
366	81	158	83	36	45	40	36	44	0.51	0.43	0.52	0.52
367	102	199	95	45	55	51	40	54	0.51	0.33	0.48	0.41
368	113	212	101	48	59	51	45	58	0.53	0.31	0.48	0.35
369	293	358	421	116	158	125	137	140	0.82	0.63	1.17	0.52
370	293	358	421	116	158	125	137	140	0.82	0.63	1.17	0.52
371	179	200	129	90	94	88	104	89	0.89	0.27	0.64	0.66
372	190	212	136	95	98	92	110	94	0.90	0.26	0.64	0.64
373	355	354	410	194	158	136	187	134	1.00	0.78	1.16	1.25
374	323	288	390	140	156	134	130	176	1.12	1.19	1.36	1.27
375	321	403	411	196	180	165	163	195	0.80	0.84	1.02	1.11
376	303	323	406	178	171	153	148	188	0.94	0.77	1.26	0.97

APPENDIX 2

Lateral Force- Lateral Drift Angle Relationship

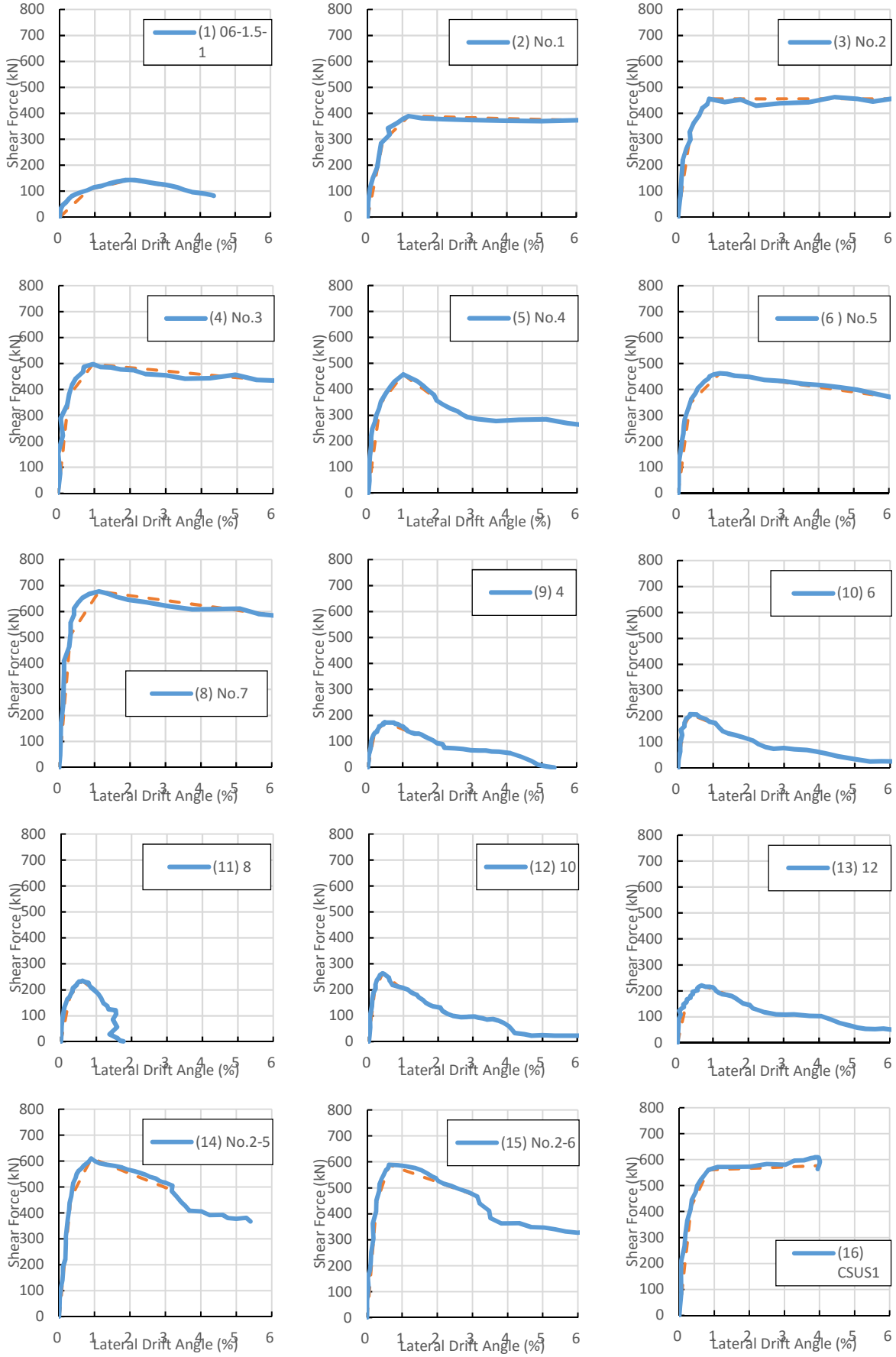
(1) 06-1.5-1
(2) No.1
(3) No.2
(4) No.3
(5) No.4
(6) No.5
(8) No.7
(9) 4
(10) 6
(11) 8
(12) 10
(13) 12
(14) No.2-5
(15) No.2-6
(16) CSUS1
Shear Force (kN)
Lateral Drift Angle (%)

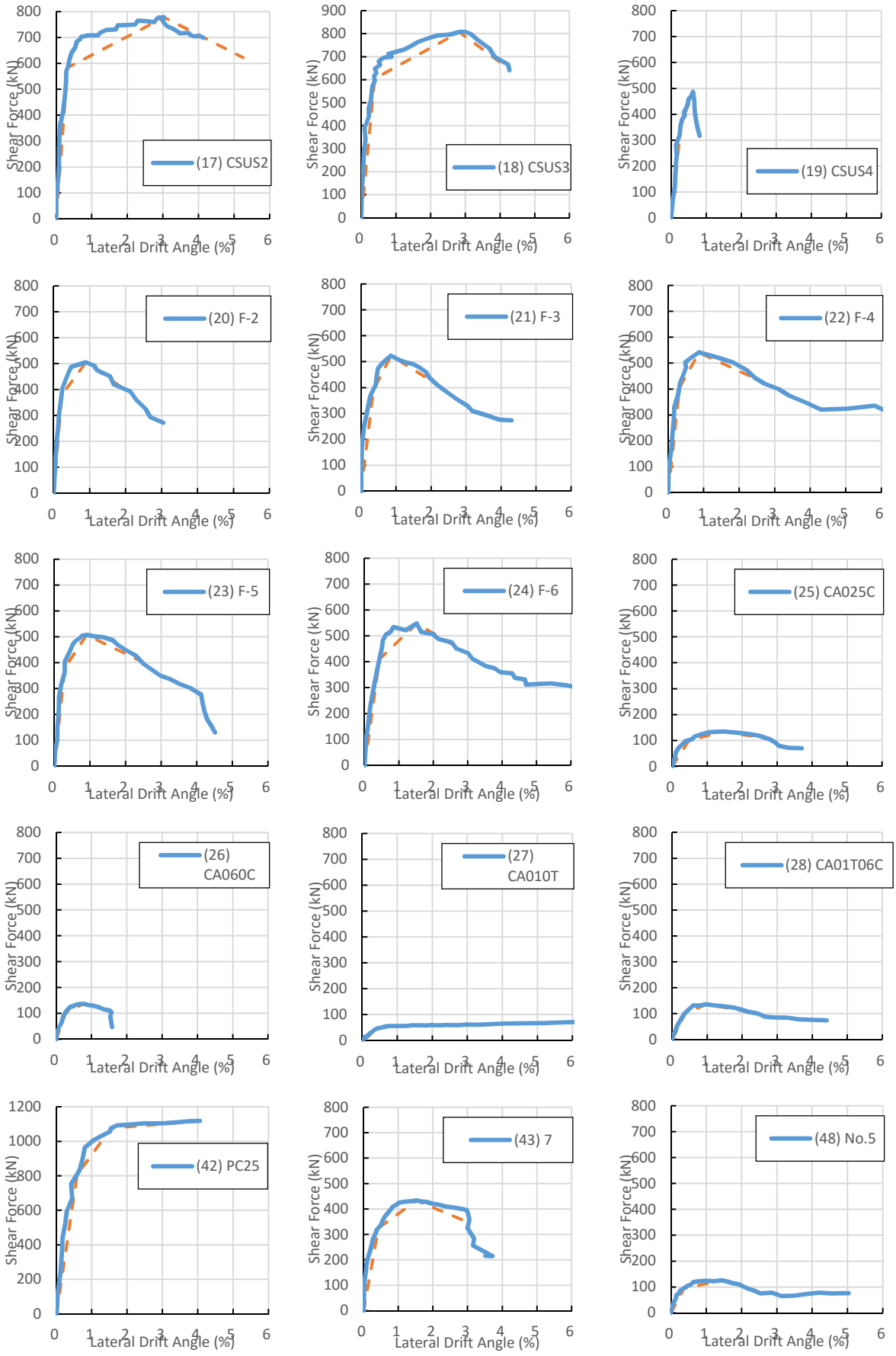
Shear Force (kN)
Lateral Drift Angle (%)
(17) CSUS2
(18) CSUS3
(19) CSUS4
(20) F-2
(21) F-3
(22) F-4
(23) F-5
(24) F-6
(25) CA025C
(26) CA060C
(27) CA010T
(28) CA01T06C
(42) PC25
(43) 7
(48) No.5

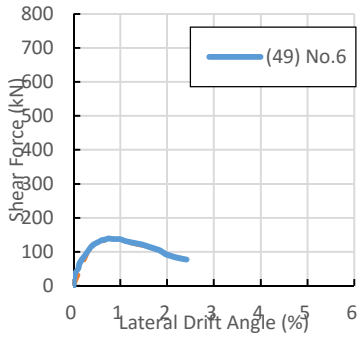
(49) No.6
Shear Force (kN)
Lateral Drift Angle (%)

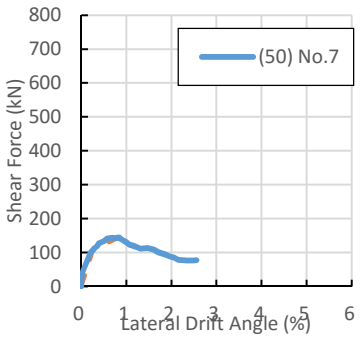
(50) No.7
Shear Force (kN)
Lateral Drift Angle (%)

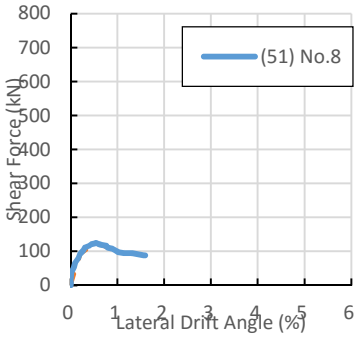
(51) No.8
Shear Force (kN)
Lateral Drift Angle (%)

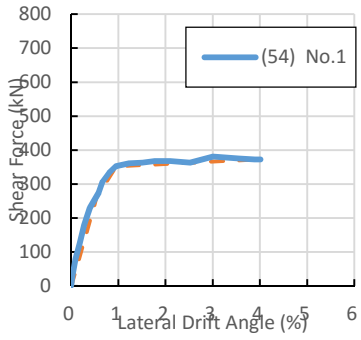
(54) No.1
Shear Force (kN)
Lateral Drift Angle (%)

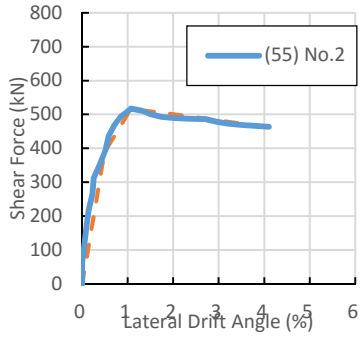
(55) No.2
Shear Force (kN)
Lateral Drift Angle (%)

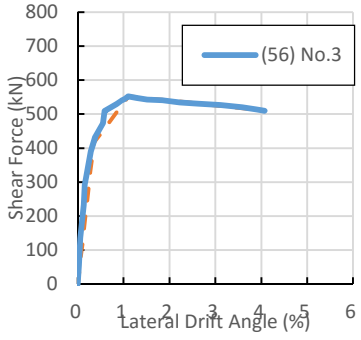
(56) No.3
Shear Force (kN)
Lateral Drift Angle (%)

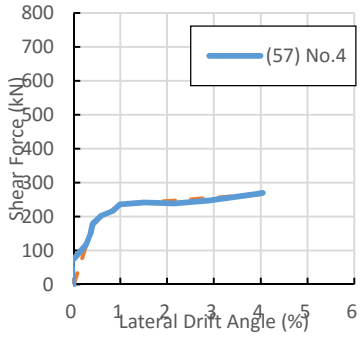
(57) No.4
Shear Force (kN)
Lateral Drift Angle (%)

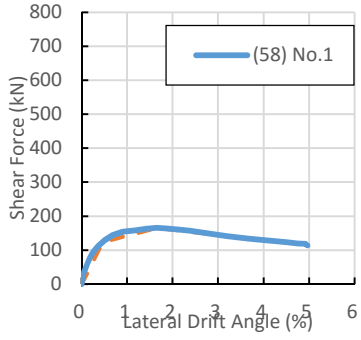
(58) No.1
Shear Force (kN)
Lateral Drift Angle (%)

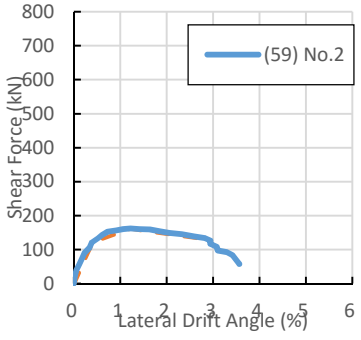
(59) No.2
Shear Force (kN)
Lateral Drift Angle (%)

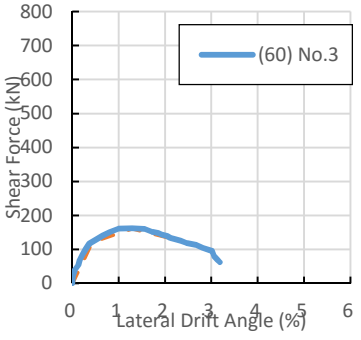
(60) No.3
Shear Force (kN)
Lateral Drift Angle (%)

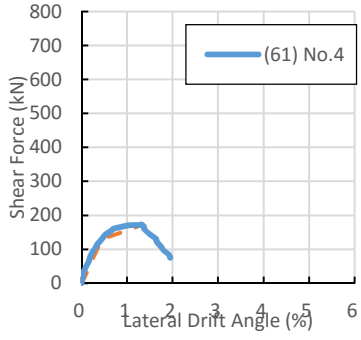
(61) No.4
Shear Force (kN)
Lateral Drift Angle (%)

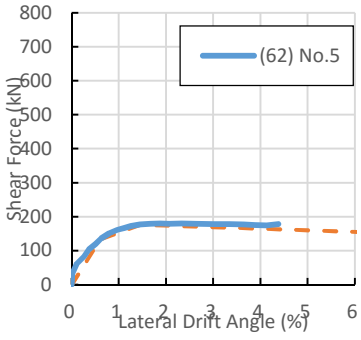
(62) No.5
Shear Force (kN)
Lateral Drift Angle (%)

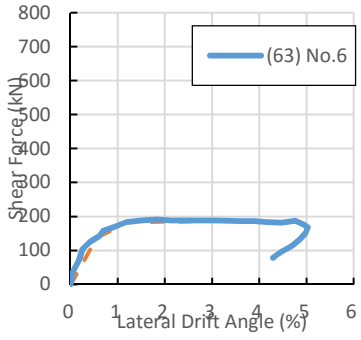
(63) No.6
Shear Force (kN)
Lateral Drift Angle (%)

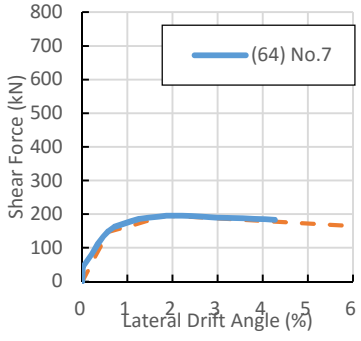
(64) No.7
Shear Force (kN)
Lateral Drift Angle (%)

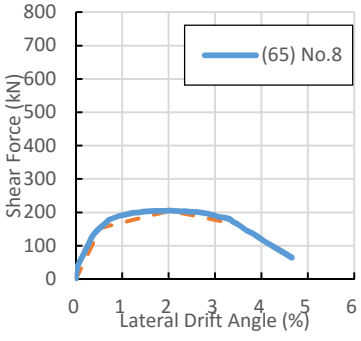
(65) No.8
Shear Force (kN)
Lateral Drift Angle (%)

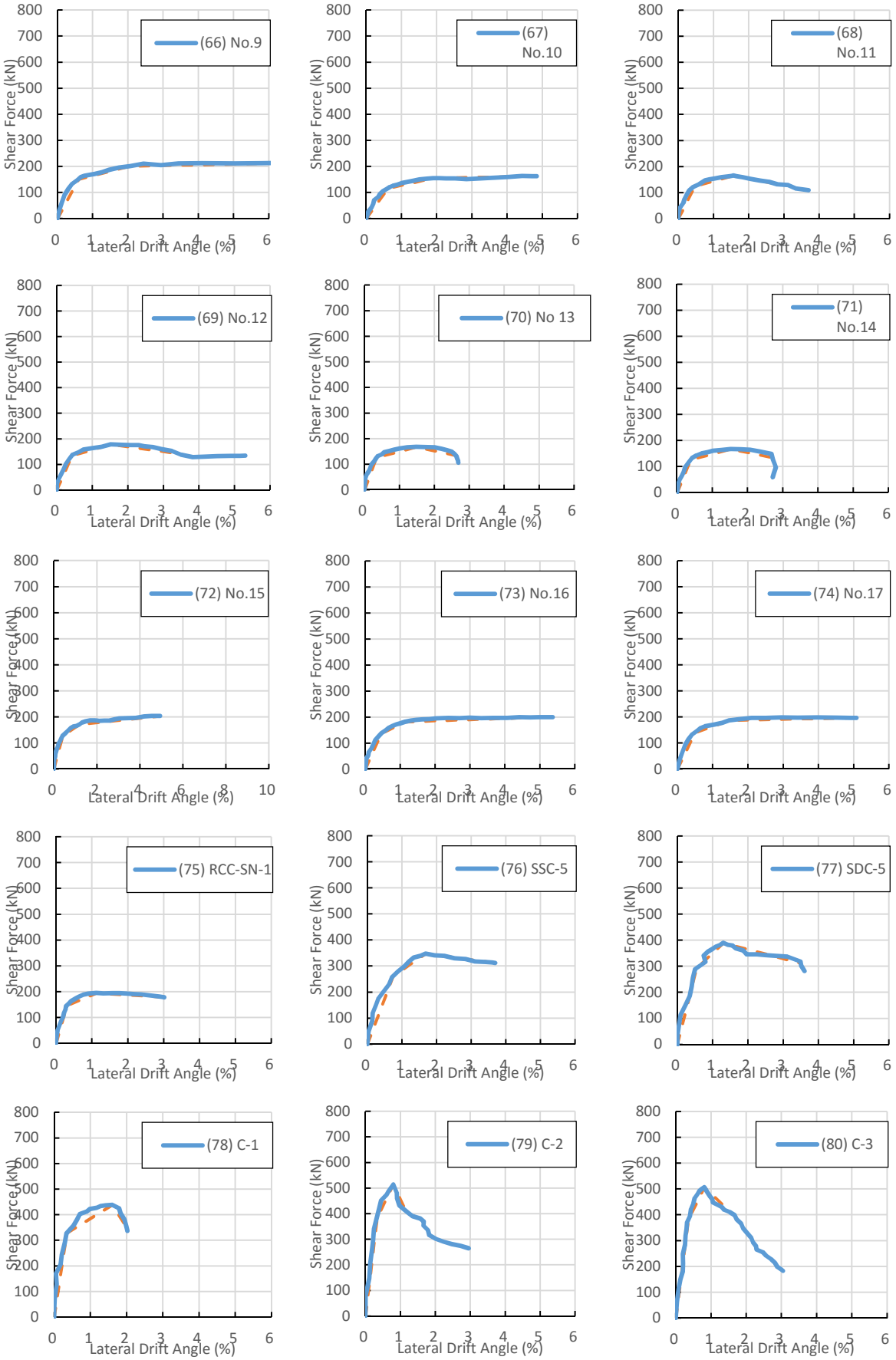
(66) No.9
(67) No.10
(68) No.11
(69) No.12
(70) No 13
(71) No.14
(72) No.15
(73) No.16
(74) No.17
(75) RCC-SN-1
(76) SSC-5
(77) SDC-5
(78) C-1
(79) C-2
(80) C-3
Shear Force (kN)
Lateral Drift Angle (%)

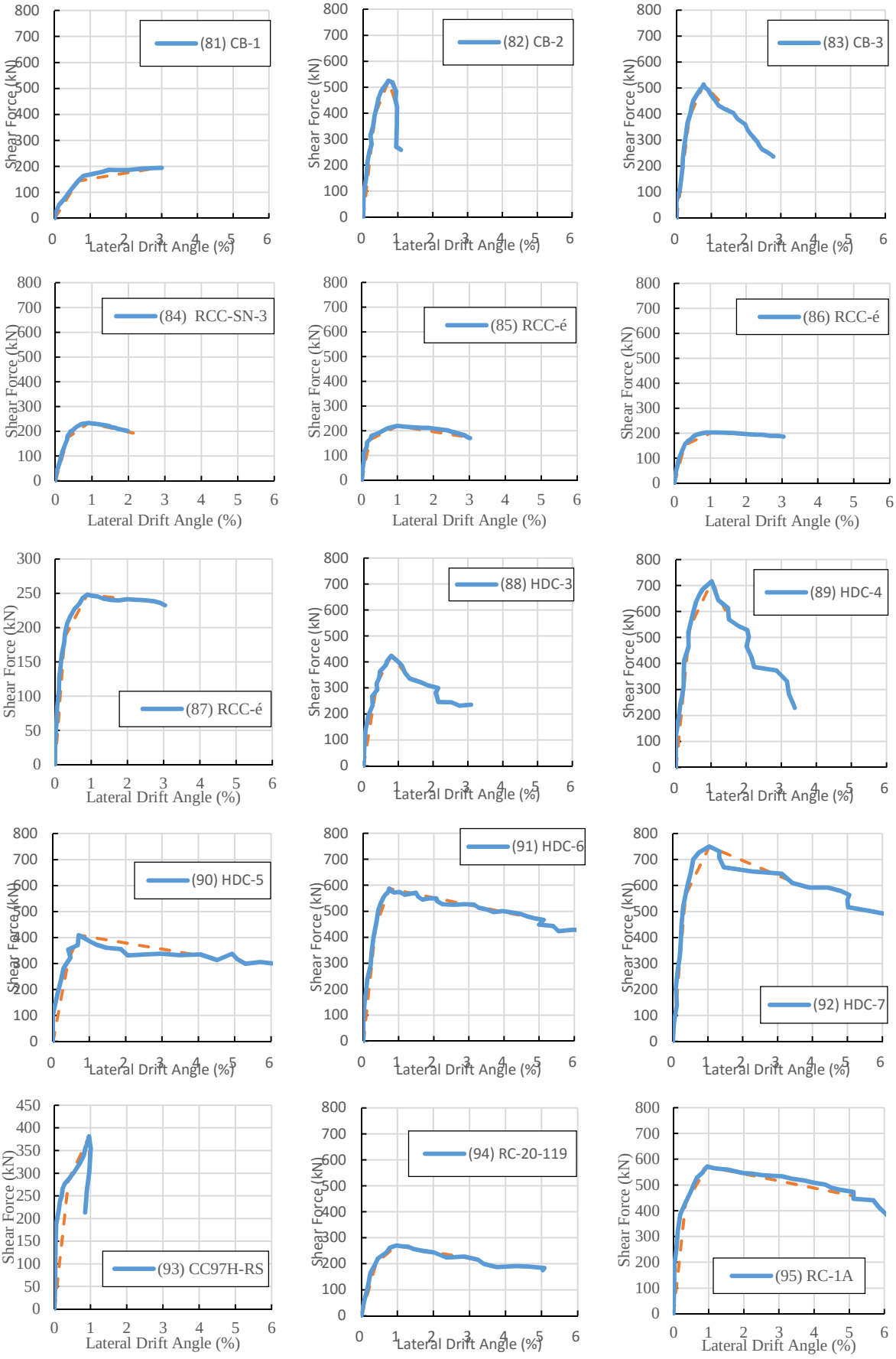
(81) CB-1
(82) CB-2
(83) CB-3
(84) RCC-SN-3
(85) RCC-é
(86) RCC-é
(87) RCC-é
(88) HDC-3
(89) HDC-4
(90) HDC-5
(91) HDC-6
(92) HDC-7
(93) CC97H-RS
(94) RC-20-119
(95) RC-1A
Shear Force (kN)
Lateral Drift Angle (%)

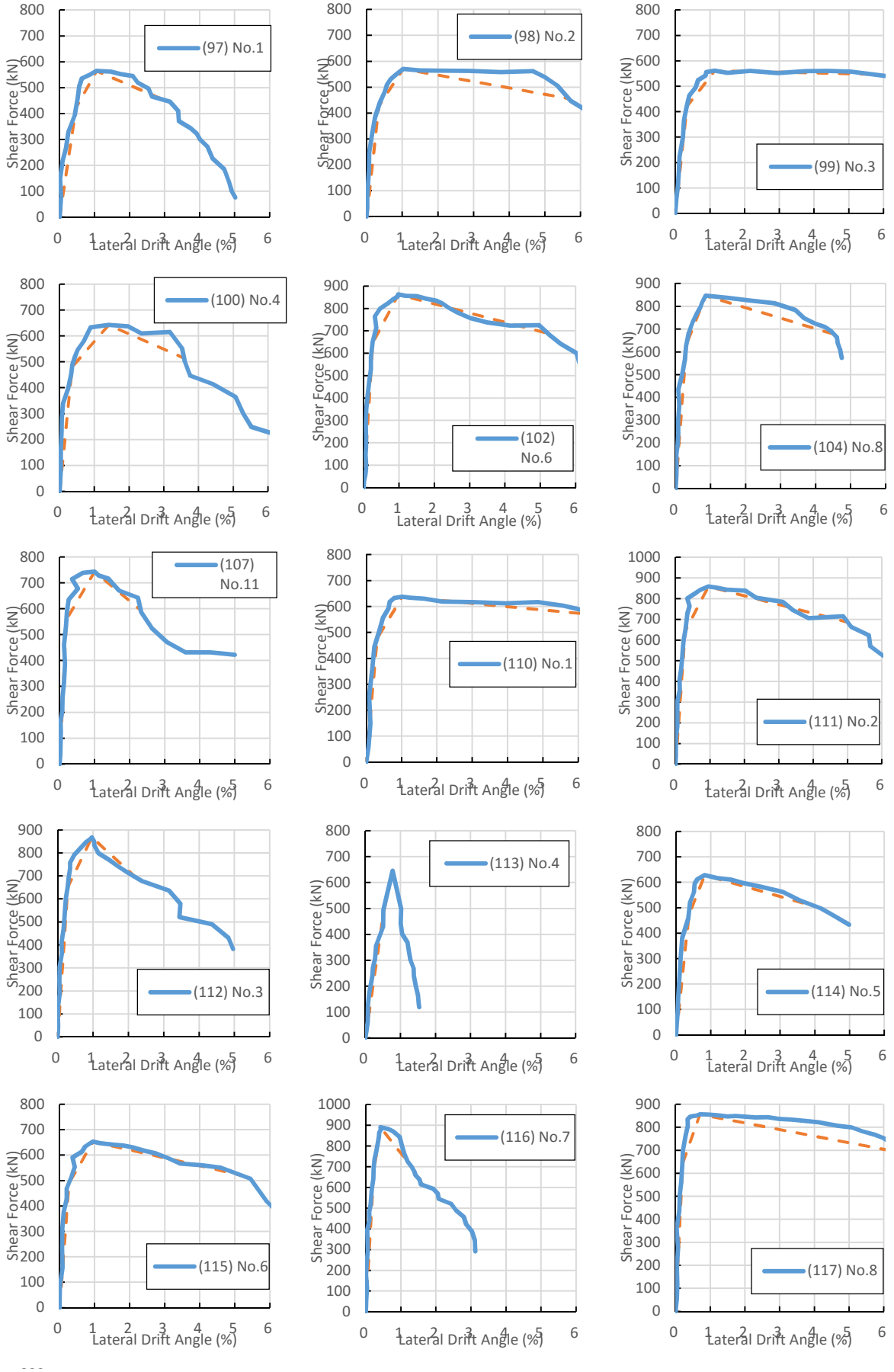
(97) No.1
(98) No.2
(99) No.3
(100) No.4
(102) No.6
(104) No.8
(107) No.11
(110) No.1
(111) No.2
(112) No.3
(113) No.4
(114) No.5
(115) No.6
(116) No.7
(117) No.8
Shear Force (kN)
Lateral Drift Angle (%)

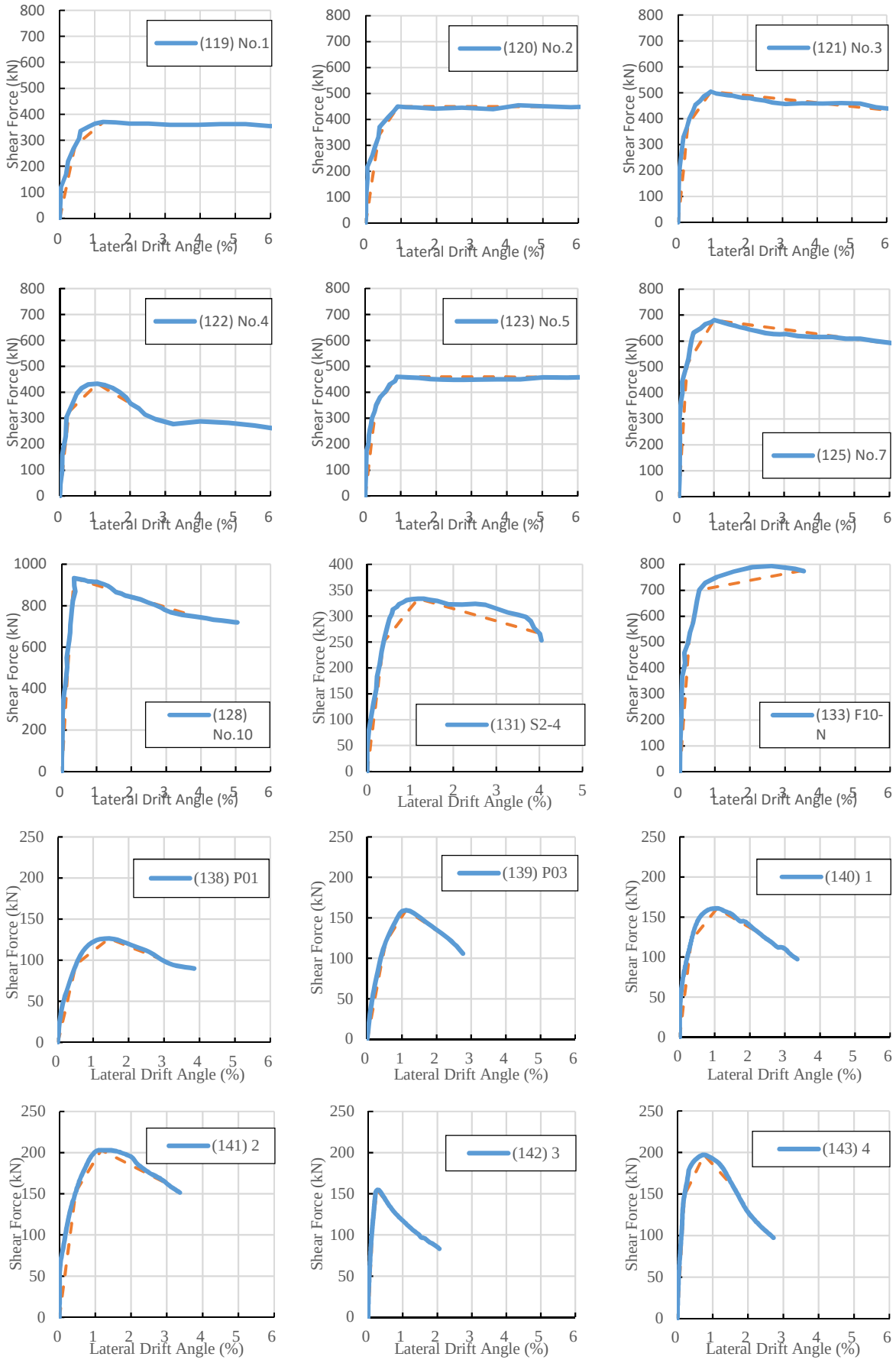
(119) No.1
(120) No.2
(121) No.3
(122) No.4
(123) No.5
(125) No.7
(128) No.10
(131) S2-4
(133) F10-N
(138) P01
(139) P03
(140) 1
(141) 2
(142) 3
(143) 4
Shear Force (kN)
Lateral Drift Angle (%)

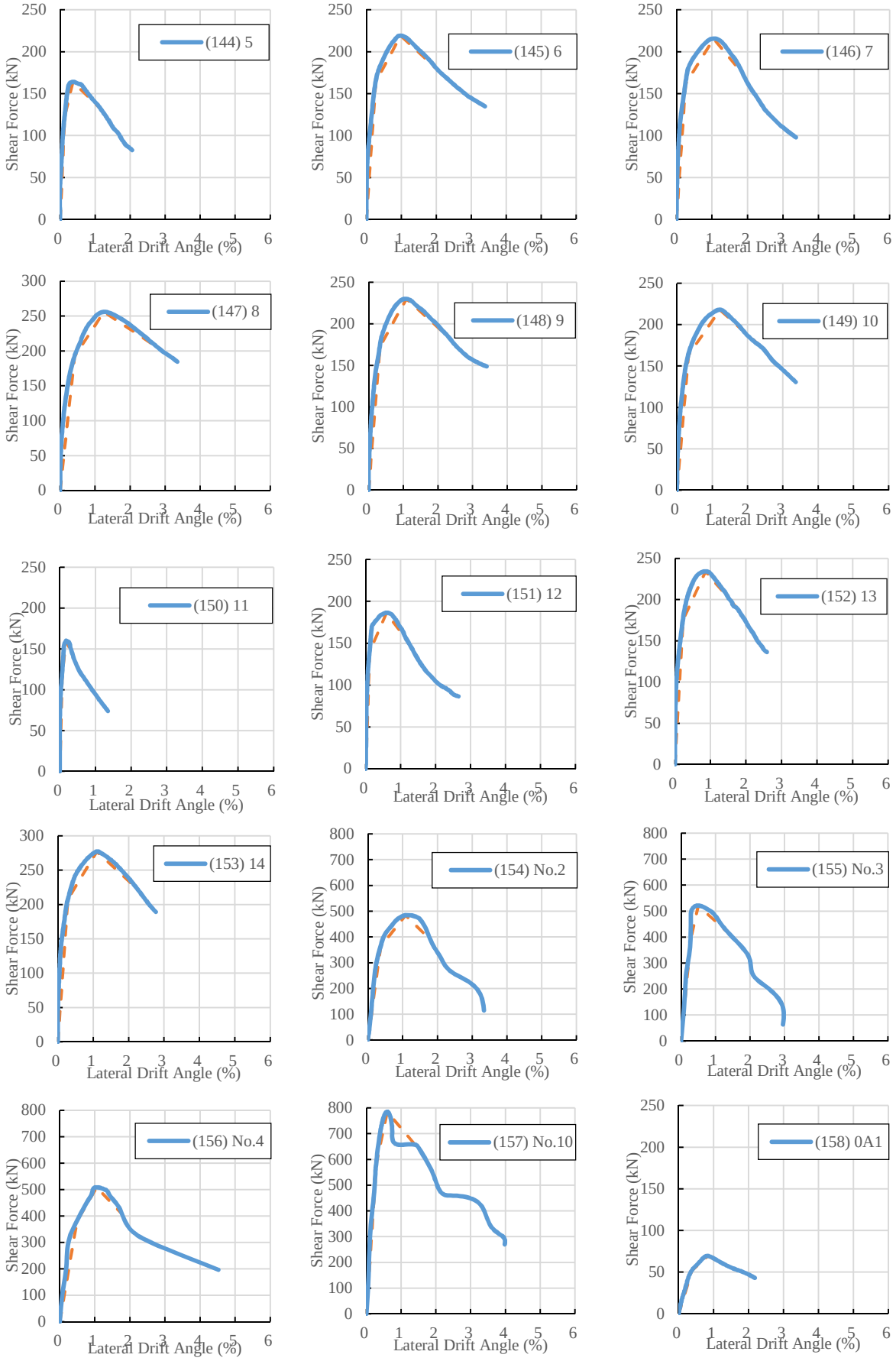
(144) 5
(145) 6
(146) 7
(147) 8
(148) 9
(149) 10
(150) 11
(151) 12
(152) 13
(153) 14
(154) No.2
(155) No.3
(156) No.4
(157) No.10
(158) 0A1
Shear Force (kN)
Lateral Drift Angle (%)

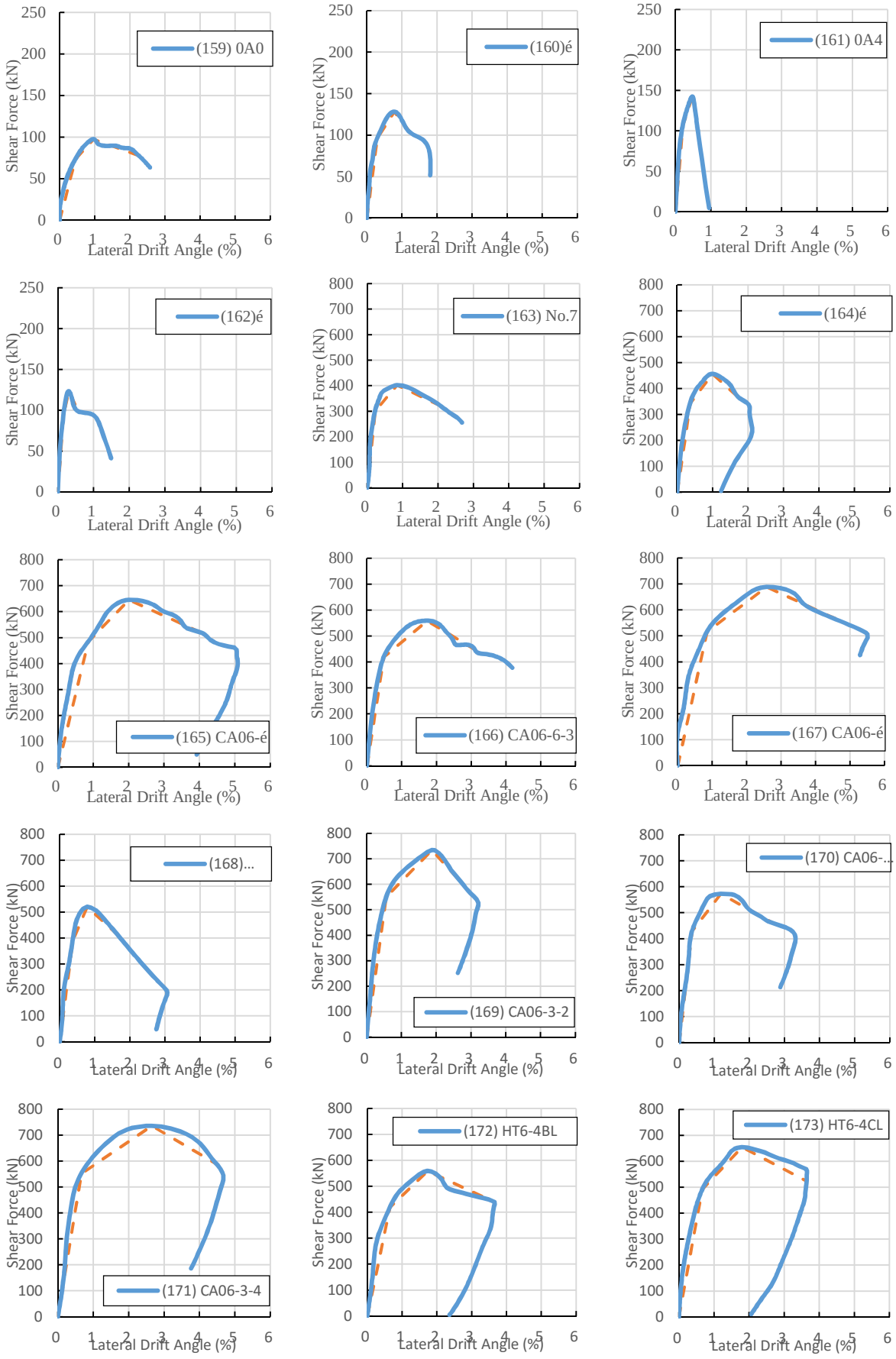
(159) 0A0
(160)é
(161) 0A4
(162)é
(163) No.7
(164)é
(165) CA06-é
(166) CA06-6-3
(167) CA06-é
(168)...
(169) CA06-3-2
(170) CA06-...
(171) CA06-3-4
(172) HT6-4BL
(173) HT6-4CL
Shear Force (kN)
Lateral Drift Angle (%)

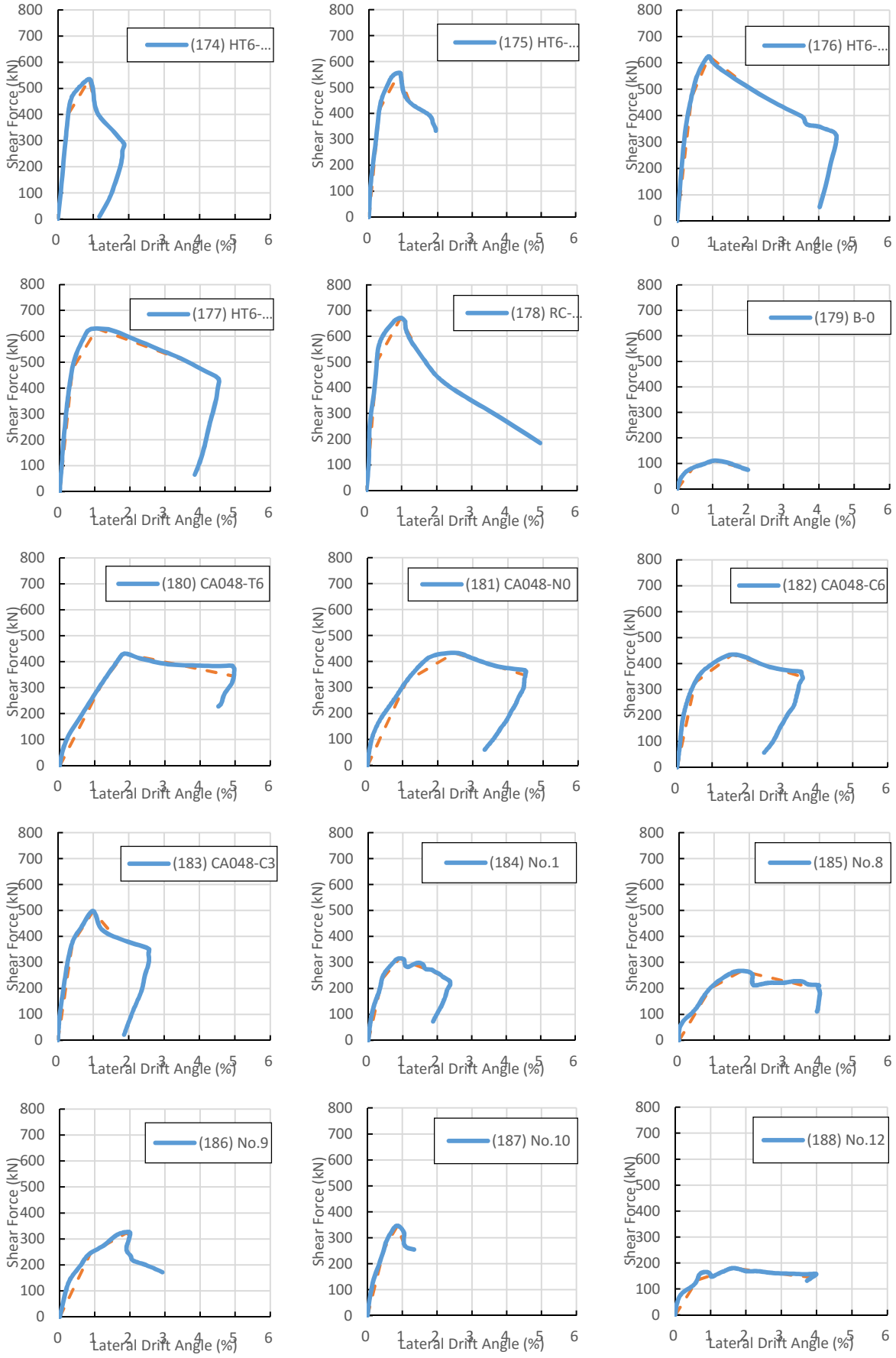
(174) HT6-...
(175) HT6-...
(176) HT6-...
(177) HT6-...
(178) RC-...
(179) B-0
(180) CA048-T6
(181) CA048-N0
(182) CA048-C6
(183) CA048-C3
(184) No.1
(185) No.8
(186) No.9
(187) No.10
(188) No.12
Shear Force (kN)
Lateral Drift Angle (%)

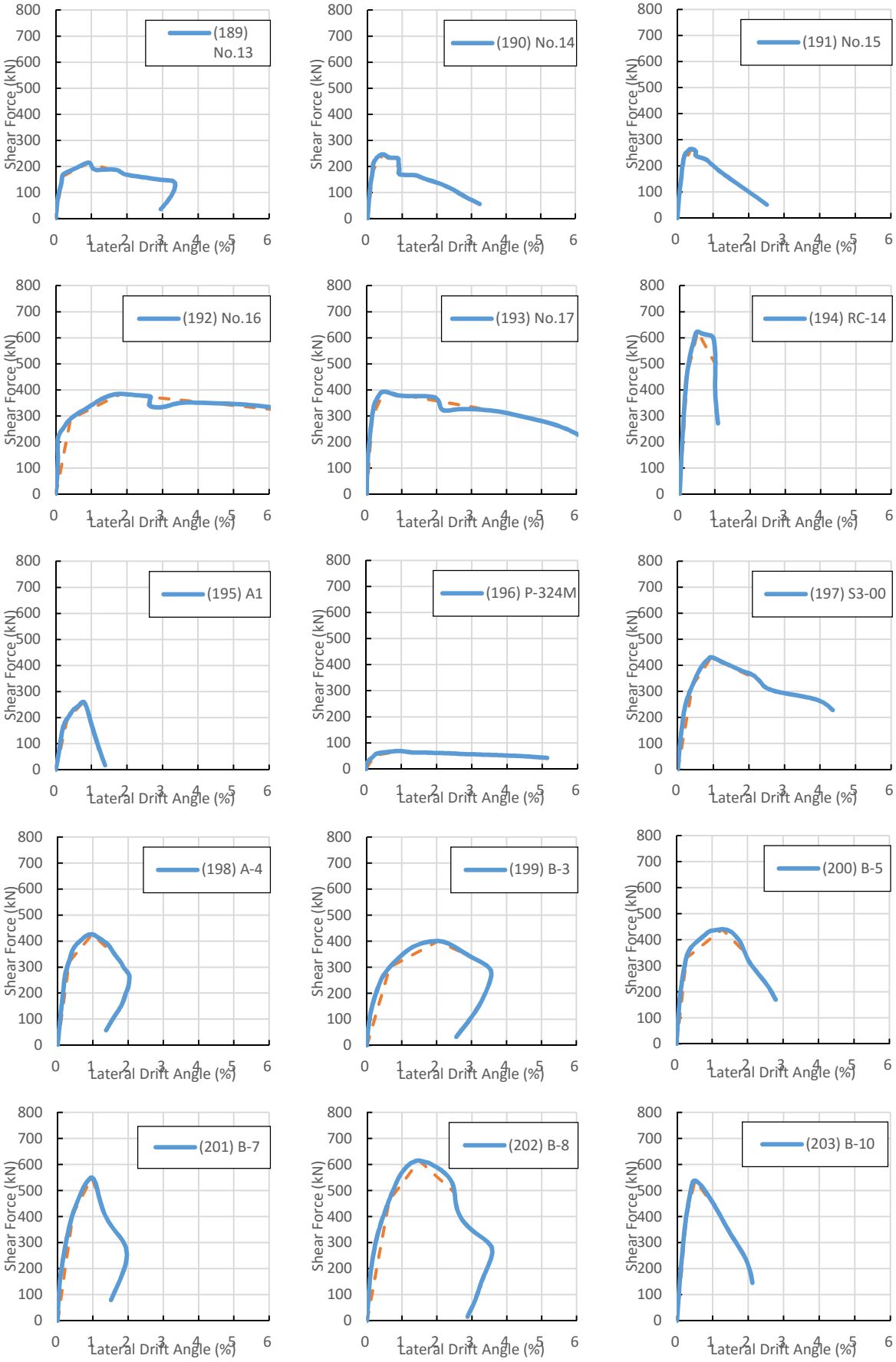
(189) No.13
(190) No.14
(191) No.15
(192) No.16
(193) No.17
(194) RC-14
(195) A1
(196) P-324M
(197) S3-00
(198) A-4
(199) B-3
(200) B-5
(201) B-7
(202) B-8
(203) B-10
Shear Force (kN)
Lateral Drift Angle (%)

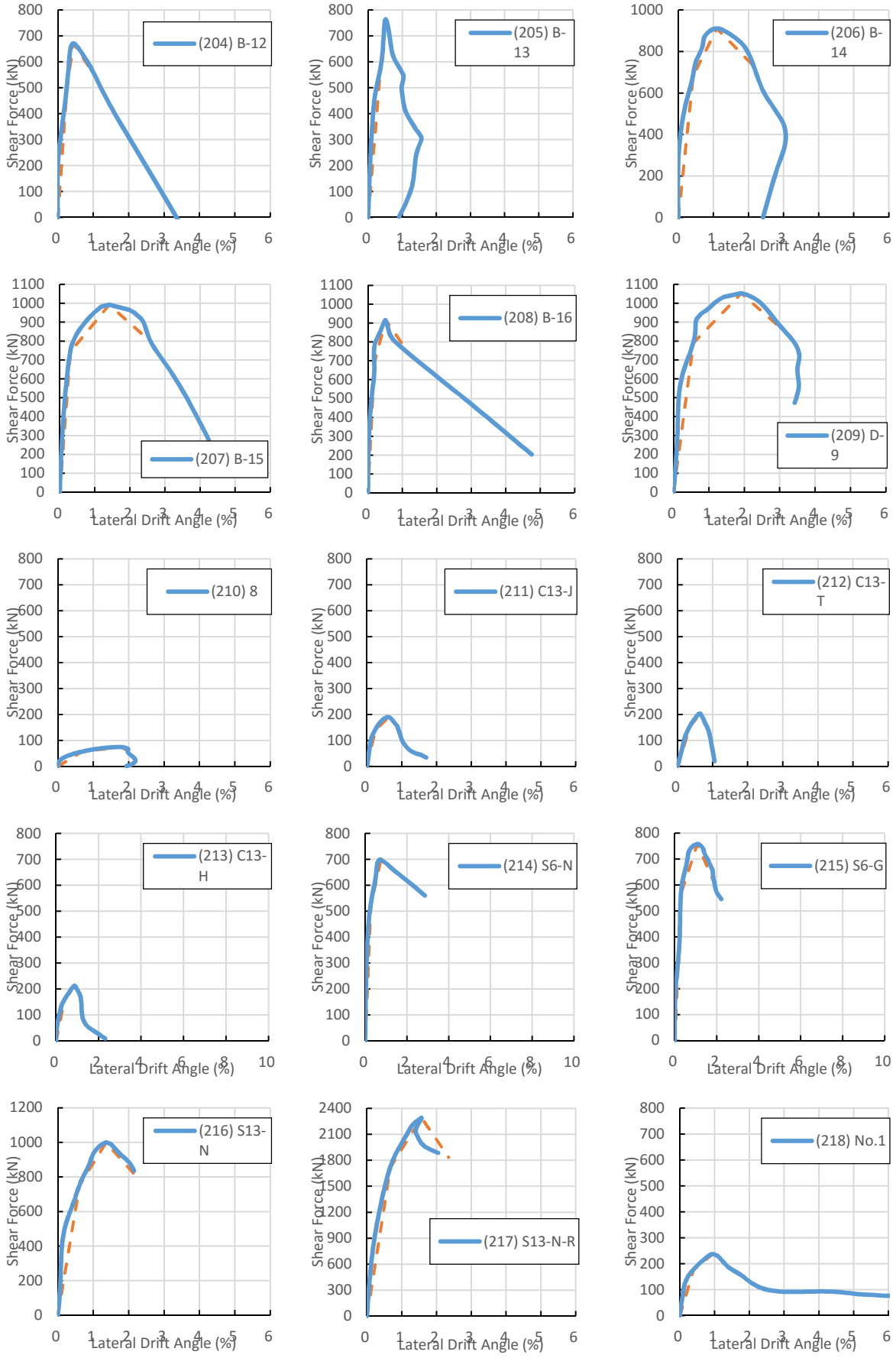
(204) B-12
(205) B-13
(206) B-14
(207) B-15
(208) B-16
(209) D-9
(210) 8
(211) C13-J
(212) C13-T
(213) C13-H
(214) S6-N
(215) S6-G
(216) S13-N
(217) S13-N-R
(218) No.1
Shear Force (kN)
Lateral Drift Angle (%)

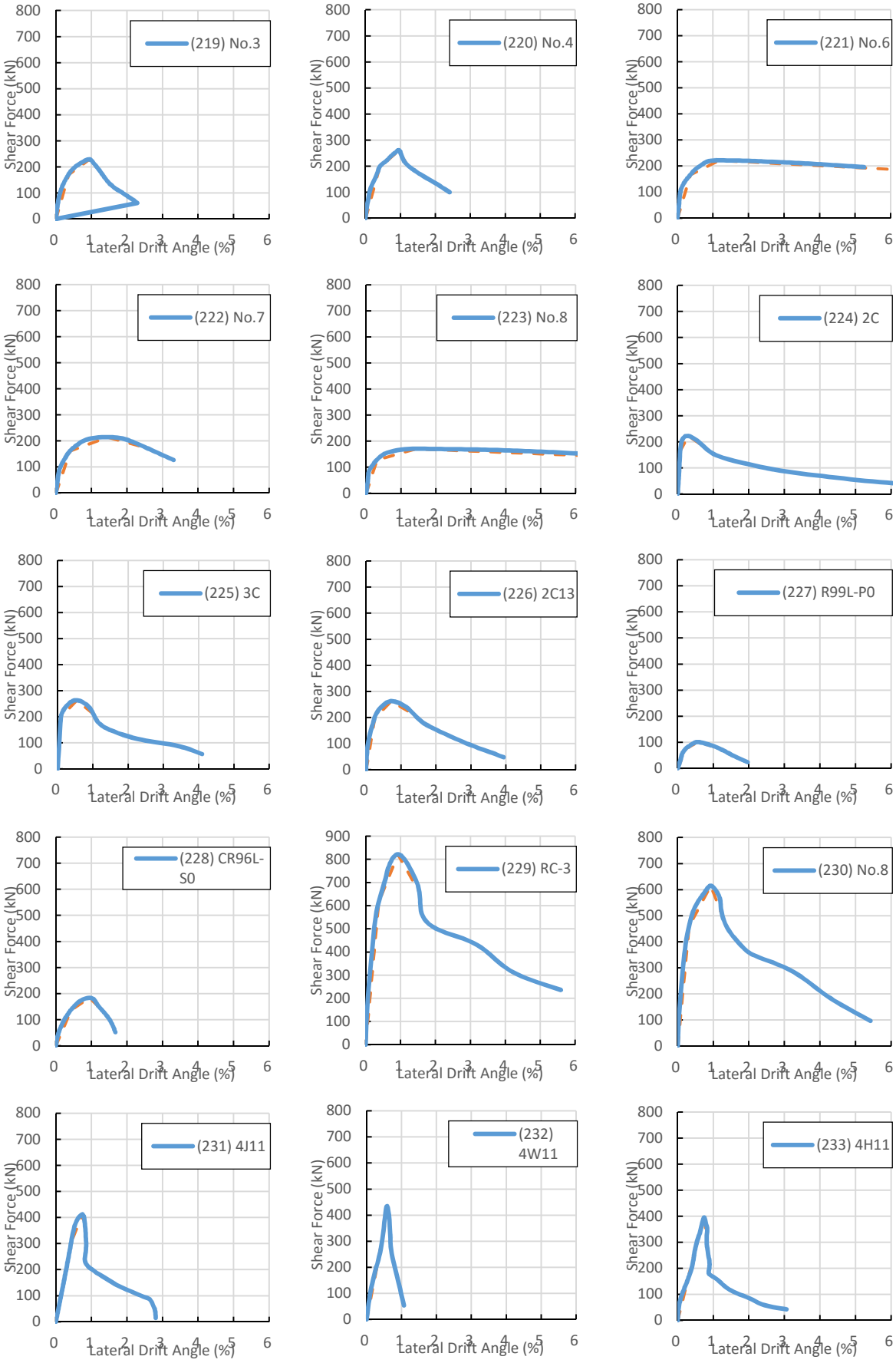
(219) No.3
(220) No.4
(221) No.6
(222) No.7
(223) No.8
(224) 2C
(225) 3C
(226) 2C13
(227) R99L-P0
(228) CR96L-S0
(229) RC-3
(230) No.8
(231) 4J11
(232) 4W11
(233) 4H11
Shear Force (kN)
Lateral Drift Angle (%)

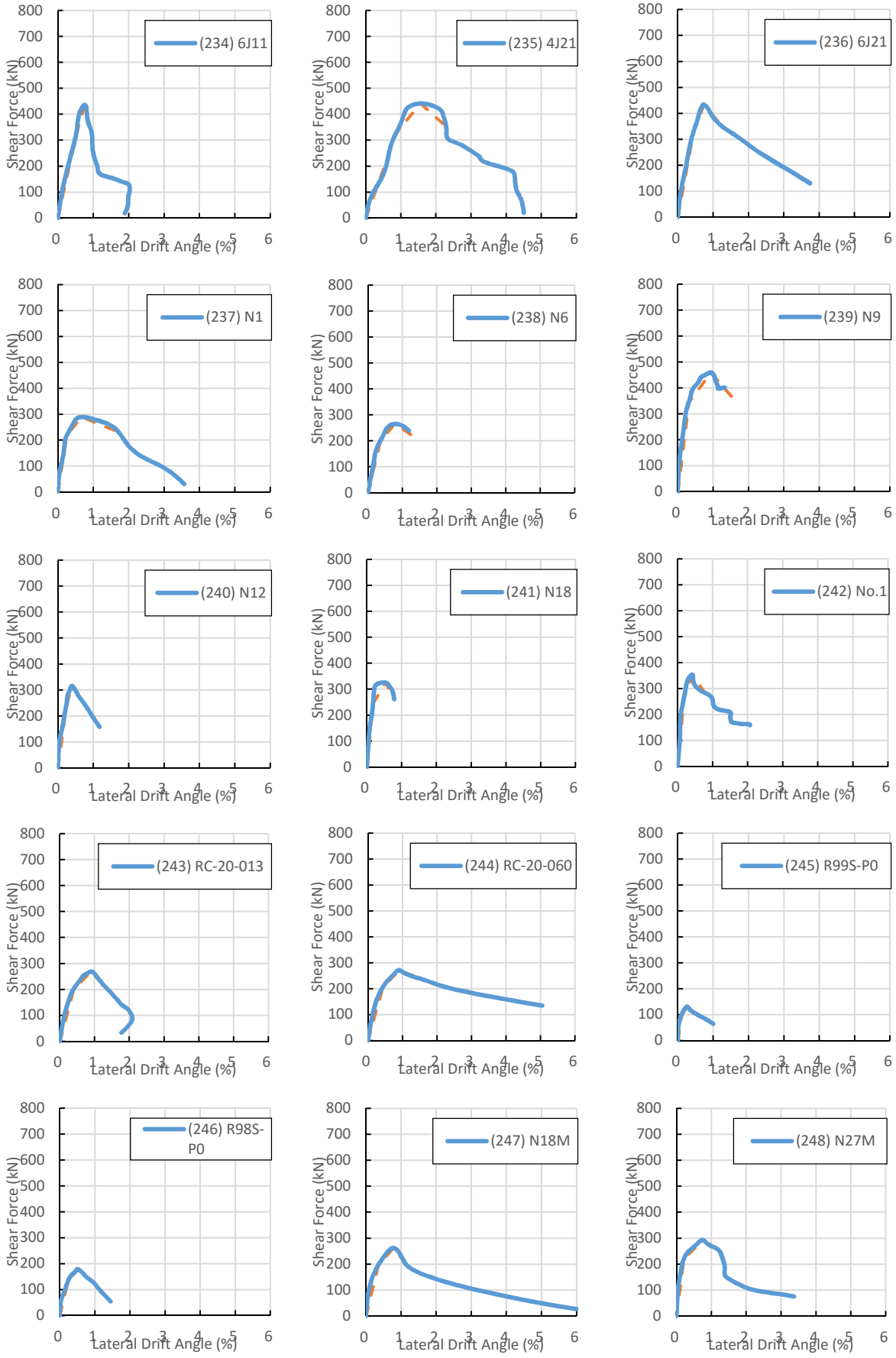
(234) 6J11
(235) 4J21
(236) 6J21
(237) N1
(238) N6
(239) N9
(240) N12
(241) N18
(242) No.1
(243) RC-20-013
(244) RC-20-060
(245) R99S-P0
(246) R98S-P0
(247) N18M
(248) N27M
Shear Force (kN)
Lateral Drift Angle (%)
0
100
200
300
400
500
600
700
800
1
2
3
4
5
6

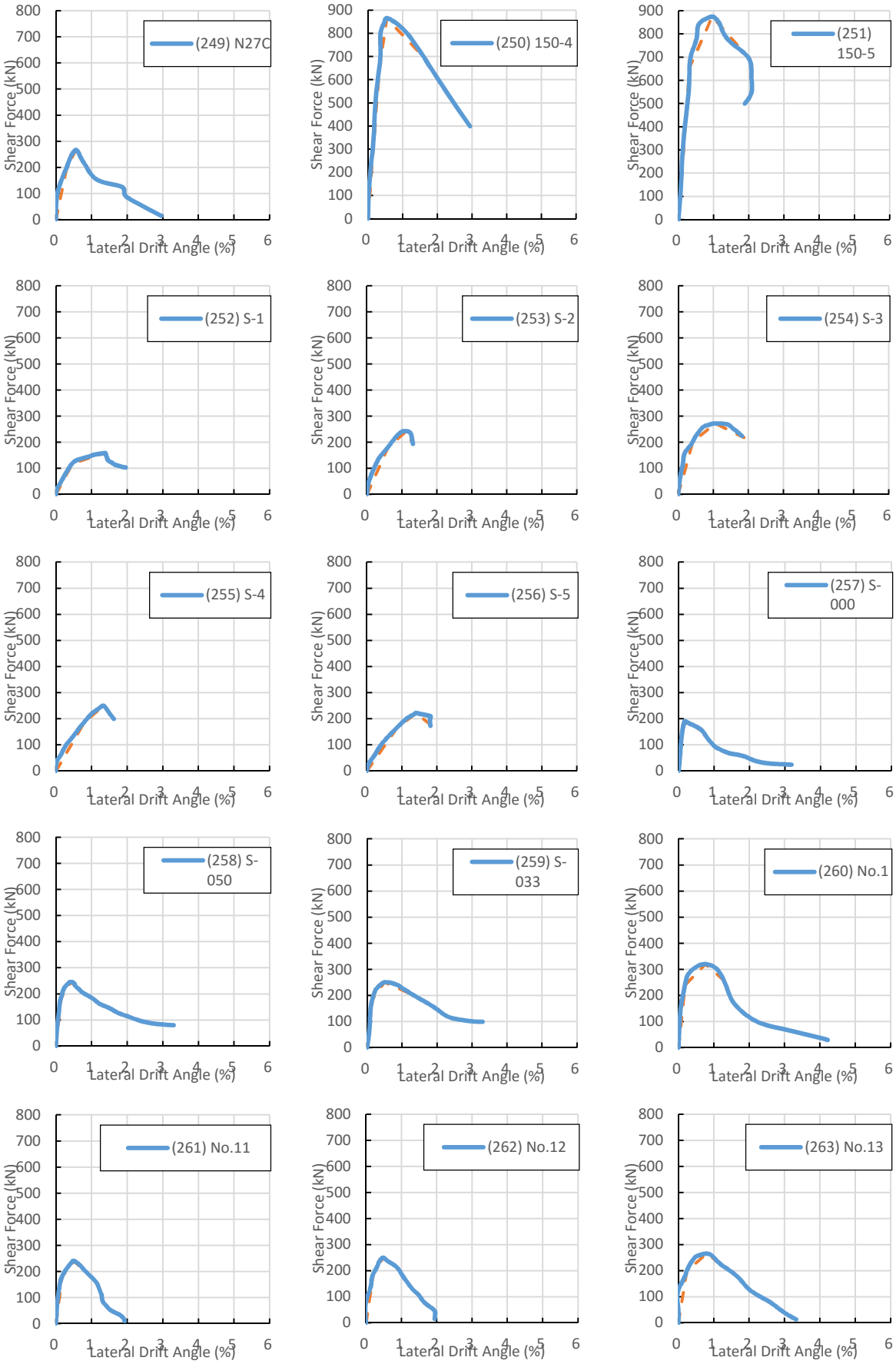
(249) N27C
(250) 150-4
(251) 150-5
(252) S-1
(253) S-2
(254) S-3
(255) S-4
(256) S-5
(257) S-000
(258) S-050
(259) S-033
(260) No.1
(261) No.11
(262) No.12
(263) No.13
Shear Force (kN)
Lateral Drift Angle (%)

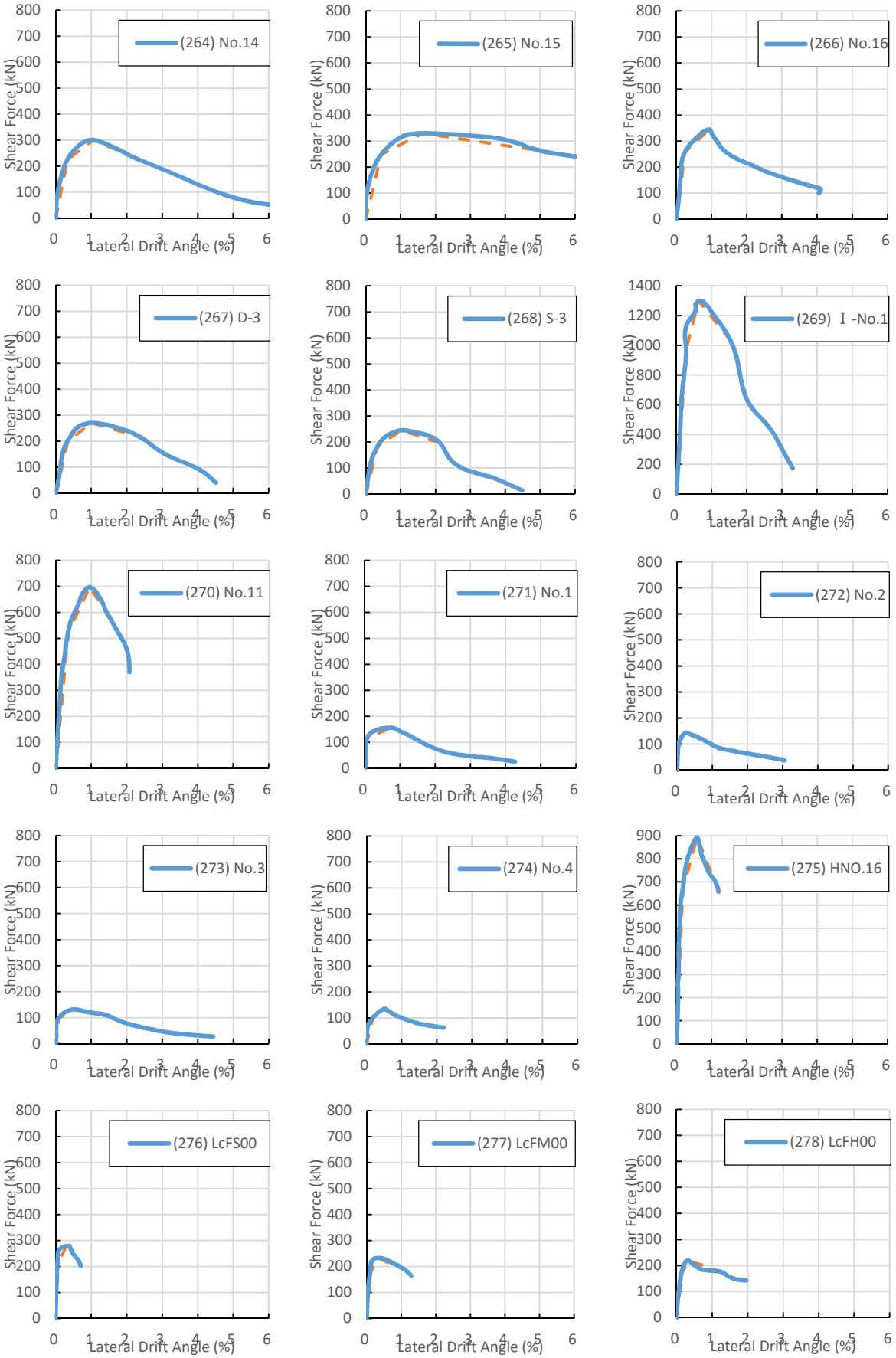
(264) No.14
(265) No.15
(266) No.16
(267) D-3
(268) S-3
(269) Ⅰ-No.1
(270) No.11
(271) No.1
(272) No.2
(273) No.3
(274) No.4
(275) HNO.16
(276) LcFS00
(277) LcFM00
(278) LcFH00
Shear Force (kN)
Lateral Drift Angle (%)

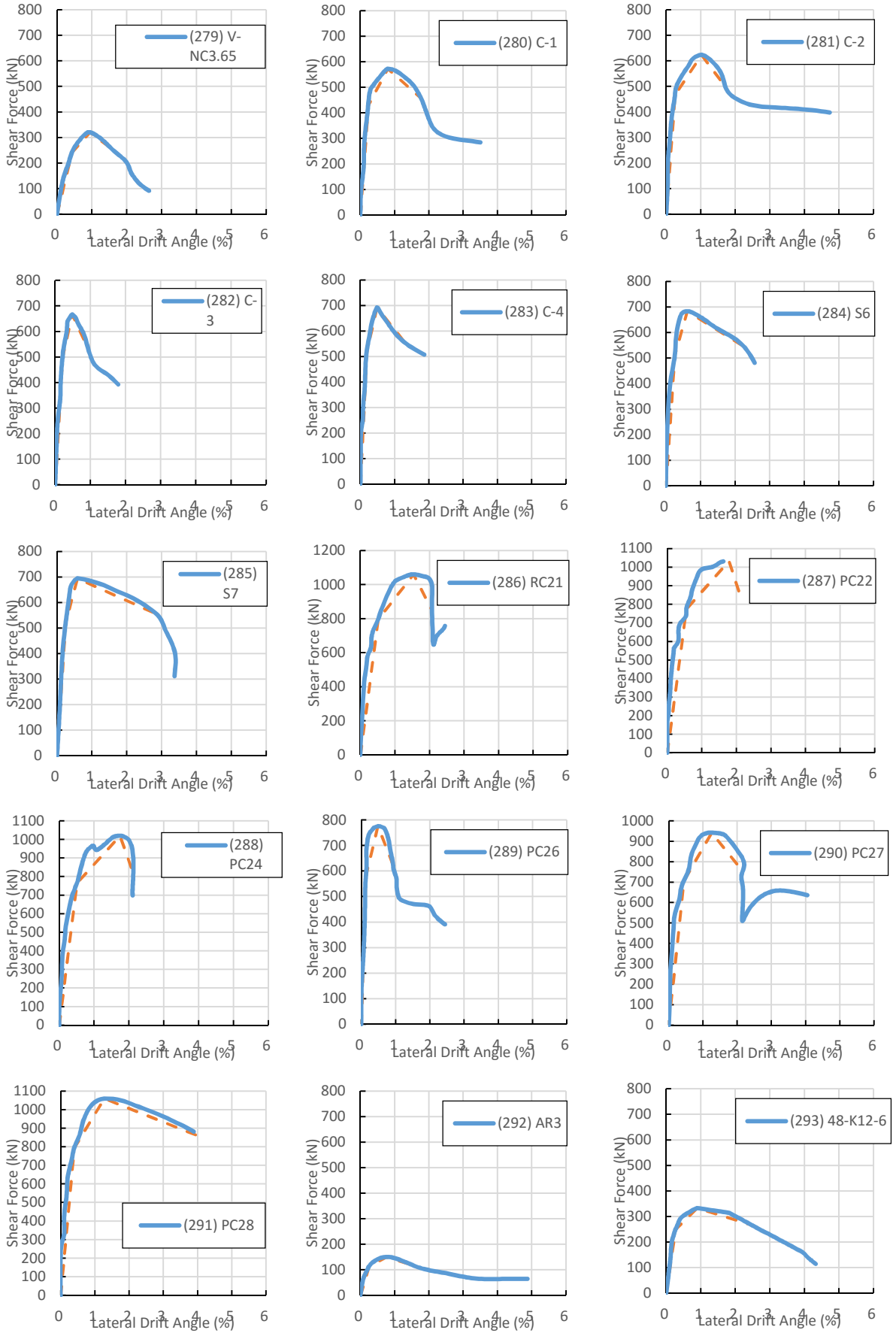
(279) V-NC3.65
(280) C-1
(281) C-2
(282) C-3
(283) C-4
(284) S6
(285) S7
(286) RC21
(287) PC22
(288) PC24
(289) PC26
(290) PC27
(291) PC28
(292) AR3
(293) 48-K12-6
Shear Force (kN)
Lateral Drift Angle (%)

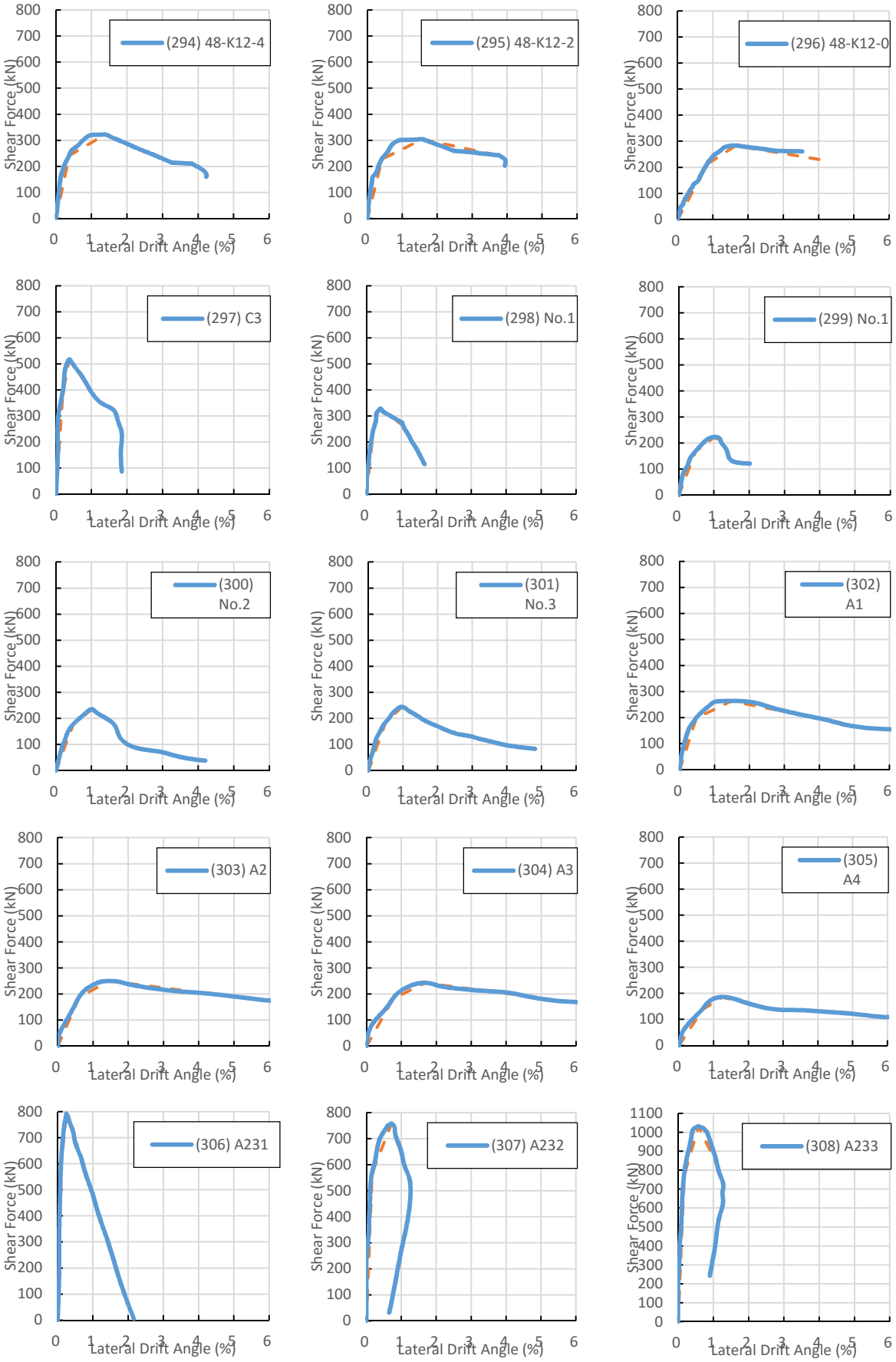
(294) 48-K12-4
(295) 48-K12-2
(296) 48-K12-0
(297) C3
(298) No.1
(299) No.1
(300) No.2
(301) No.3
(302) A1
(303) A2
(304) A3
(305) A4
(306) A231
(307) A232
(308) A233
Shear Force (kN)
Lateral Drift Angle (%)

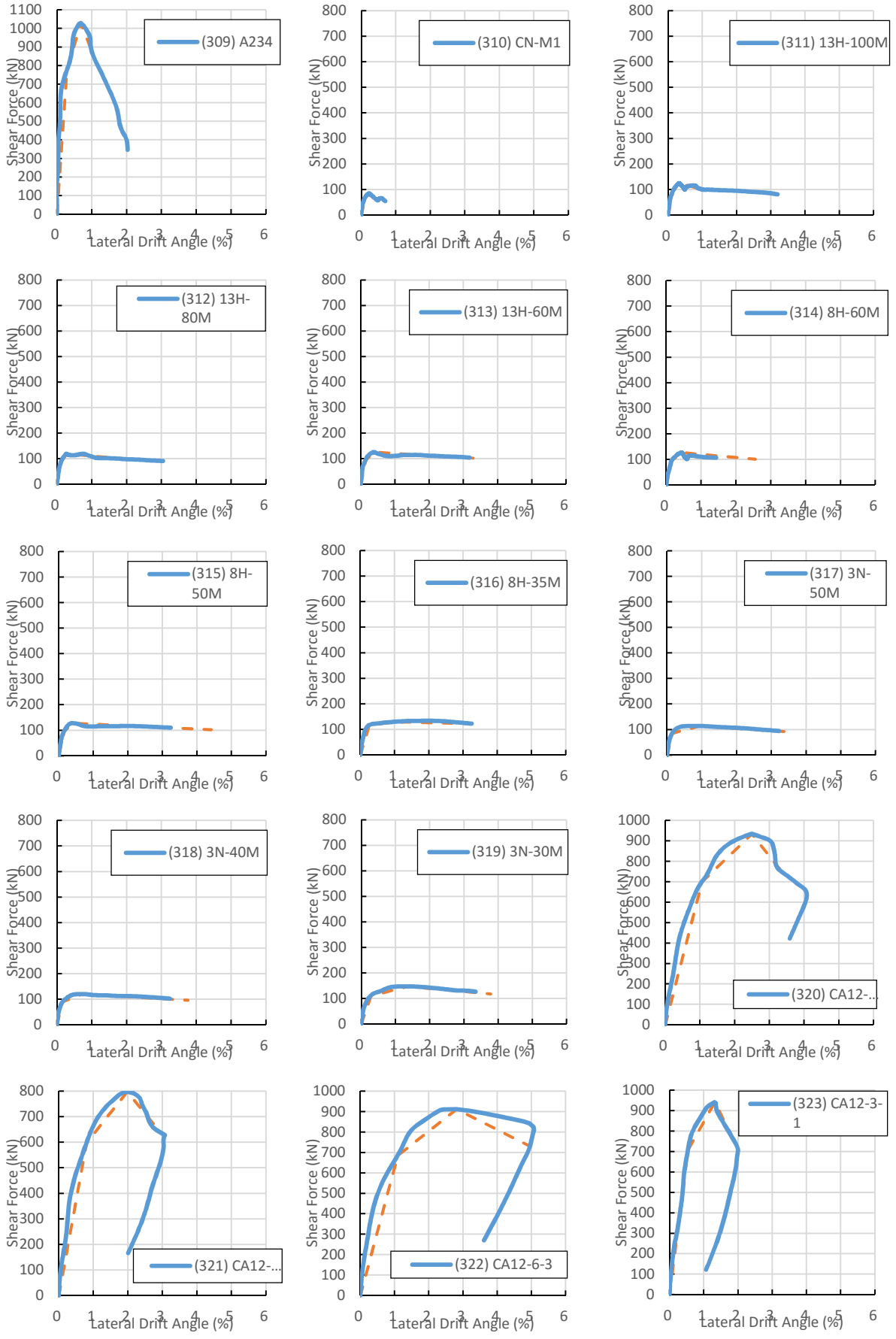
(309) A234
(310) CN-M1
(311) 13H-100M
(312) 13H-80M
(313) 13H-60M
(314) 8H-60M
(315) 8H-50M
(316) 8H-35M
(317) 3N-50M
(318) 3N-40M
(319) 3N-30M
(320) CA12-...
(321) CA12-...
(322) CA12-6-3
(323) CA12-3-1
Shear Force (kN)
Lateral Drift Angle (%)

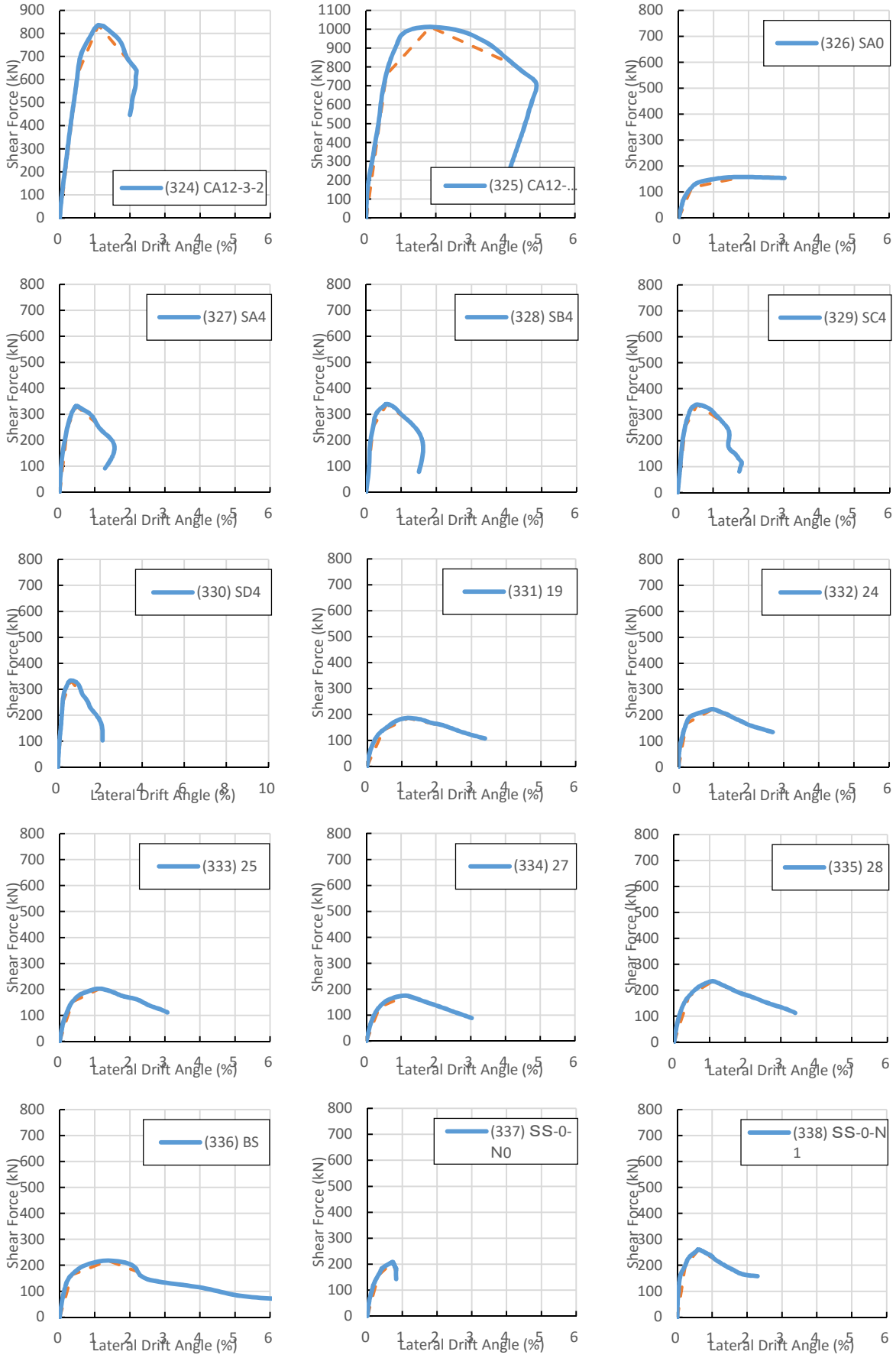
Shear Force (kN)
Lateral Drift Angle (%)
(324) CA12-3-2
(325) CA12-...
(326) SA0
(327) SA4
(328) SB4
(329) SC4
(330) SD4
(331) 19
(332) 24
(333) 25
(334) 27
(335) 28
(336) BS
(337) SS-0-N0
(338) SS-0-N1

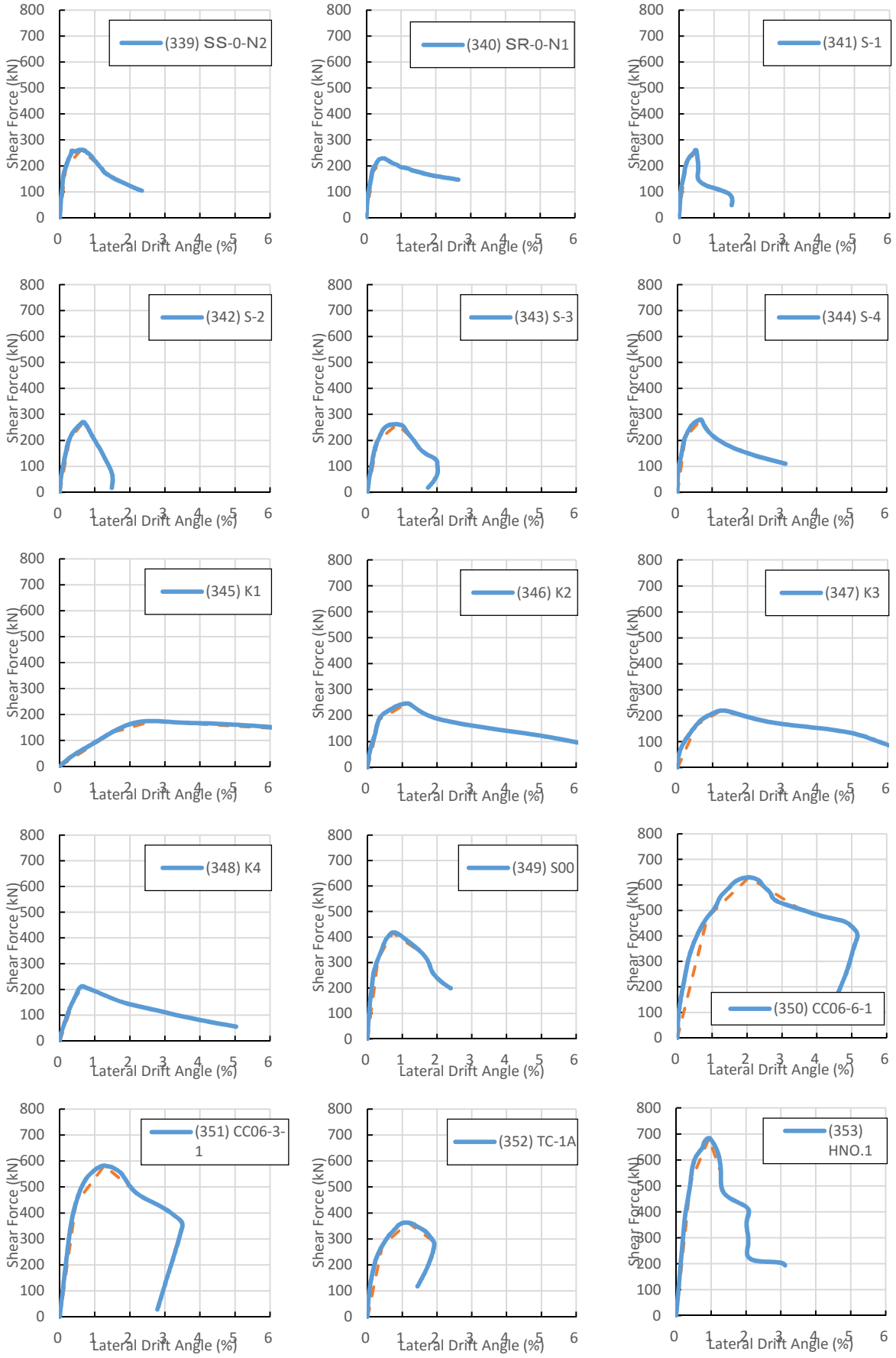
(339) SS-0-N2
(340) SR-0-N1
(341) S-1
(342) S-2
(343) S-3
(344) S-4
(345) K1
(346) K2
(347) K3
(348) K4
(349) S00
(350) CC06-6-1
(351) CC06-3-1
(352) TC-1A
(353) HNO.1
Shear Force (kN)
Lateral Drift Angle (%)

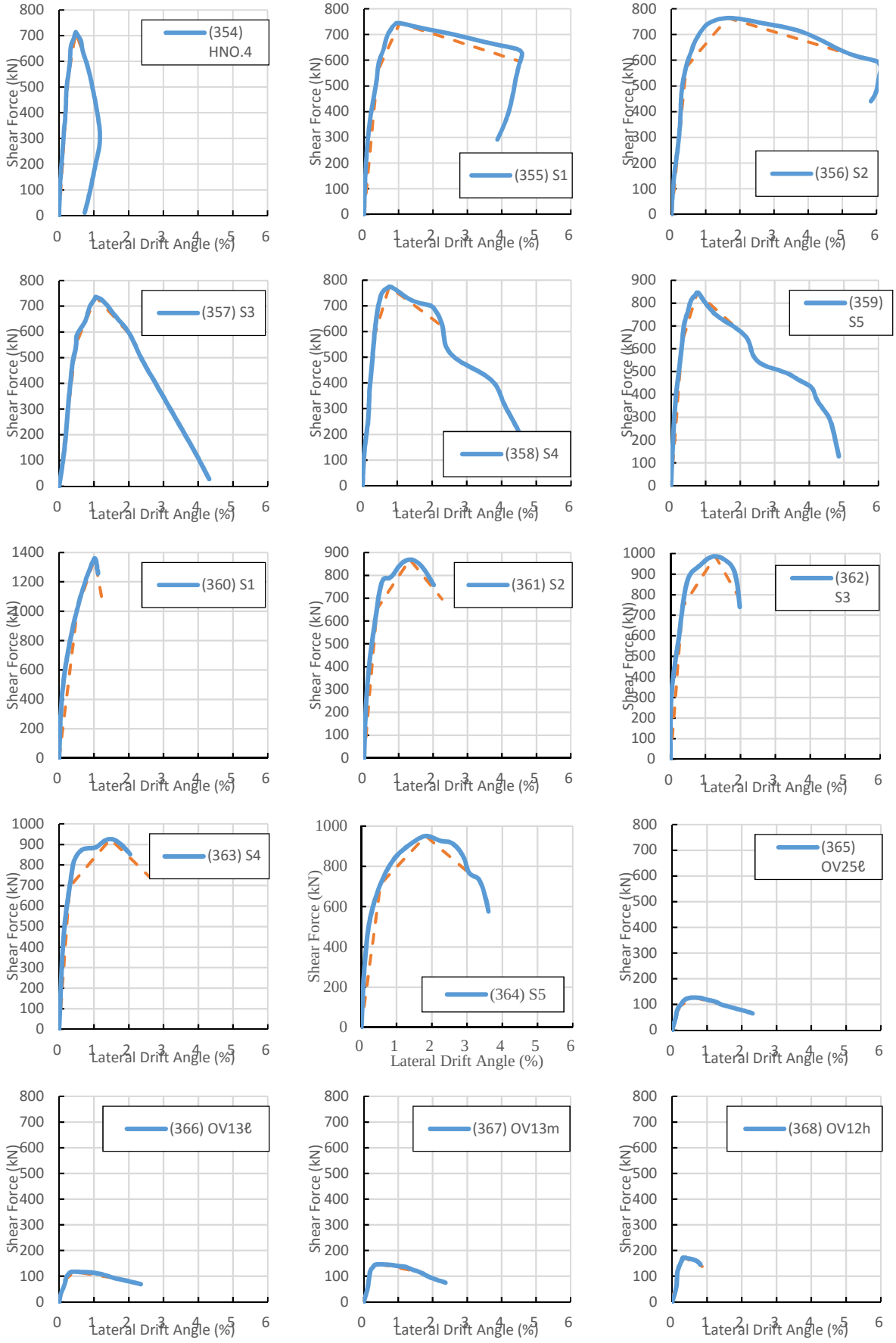
(354) HNO.4
(355) S1
(356) S2
(357) S3
(358) S4
(359) S5
(360) S1
(361) S2
(362) S3
(363) S4
(364) S5
(365) OV25ℓ
(366) OV13ℓ
(367) OV13m
(368) OV12h
Shear Force (kN)
Lateral Drift Angle (%)

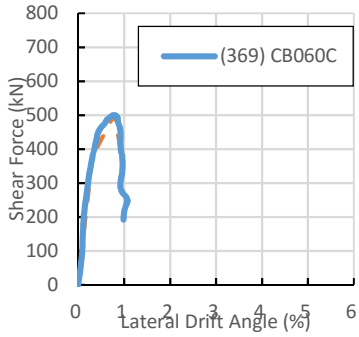
(369) CB060C
Shear Force (kN)
Lateral Drift Angle (%)

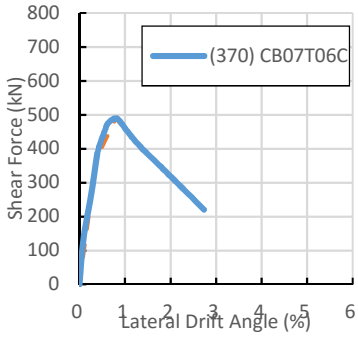
(370) CB07T06C
Shear Force (kN)
Lateral Drift Angle (%)

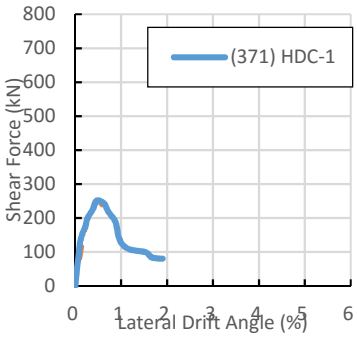
(371) HDC-1
Shear Force (kN)
Lateral Drift Angle (%)

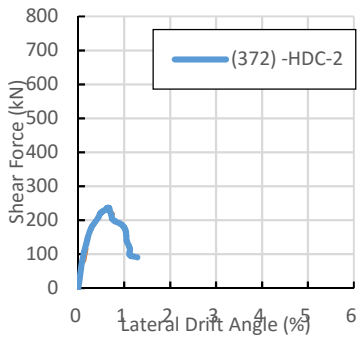
(372) -HDC-2
Shear Force (kN)
Lateral Drift Angle (%)

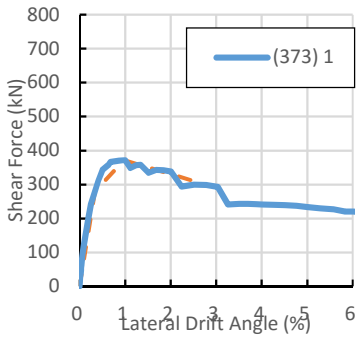
(373) 1
Shear Force (kN)
Lateral Drift Angle (%)

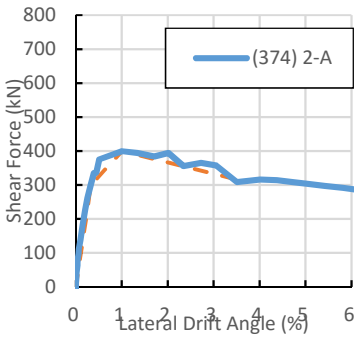
(374) 2-A
Shear Force (kN)
Lateral Drift Angle (%)

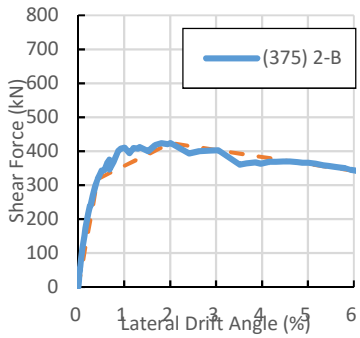
(375) 2-B
Shear Force (kN)
Lateral Drift Angle (%)

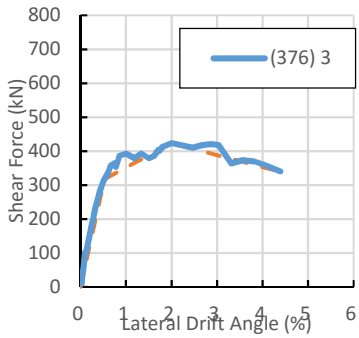
(376) 3
Shear Force (kN)
Lateral Drift Angle (%)

LIST OF FIGURES

LIST OF TABLES